Lecture note on "Modern Physics and Machine Learning"

Please note that this lecture note is constantly updated.

last update: 2024/9/24

contact: Yuto Ashida (The University of Tokyo)

Contents

CHAPTER 1

Introduction

In this course, we aim to learn some of the fundamental topics in modern quantum science, at the intersection of quantum optics, quantum information, and many-body physics. We will also try to cover elements of machine learning methods related to those topics, especially reinforcement learning that is gaining importance in the context of quantum control and other related fields. As I am theorist, the lectures will be given from a theoretical perspective, while I shall try to connect them with actual quantum experiments in laboratory when appropriate. Below let me provide a brief overview and background of this course.

It is a wonderful time for studying quantum science; one can now routinely perform microscopic observations and manipulations of genuine quantum systems in the laboratory. This has allowed us to study and understand quantum physics in a highly controlled and clean/coherent manner, paving the way toward realizing future quantum devices, such as quantum computers or quantum simulators. At the same time, such development necessarily requires us to understand physics of *open* systems as no physical systems can be completely isolated from their environments.

The system-environment interaction, or said differently, measurement backaction in general causes wavefunction collapse and is often detrimental to performing operations in quantum devices that are supposed to be coherent. Besides the role as the main obstacle for quantum technologies, however, such coupling to external degrees of freedom has often offered a new possibility of realizing some unique and exotic phenomena that are otherwise very difficult to realize in isolated systems. It is thus of fundamental importance to understand basics of open quantum systems, and it is this topic we aim to cover in Chapters 2 and 3.

We will also cover foundations of quantum optics and quantum light-matter interactions in Chapters 4 and 5. These topics will not only serve as a perfect example for a rather abstract theory of open quantum systems presented in the previous Chapters, but also play central roles in the modern quantum technologies. For example, superconducting qubits and circuit/cavity QED systems discussed there are currently one of the most promising building blocks toward realizing quantum computers. Moreover, theoretical methods we introduce there, including variational principles and bosonic/fermionic Gaussian states, are in fact useful theoretical tools to understand quantum many-body physics in condensed matter systems.

On another front, recent years have witnessed the emergence of a new powerful computational technique, that is, machine learning. In particular, deep artificial neural networks are now routinely used to classify images, translate languages, control robots, and even play video games at superhuman levels. In the context of physics, machine learning has found applications to predicting certain material properties,

classifying phases of matter, and controlling quantum or classical physical systems. This is a rapidly growing area of research and it is of course impossible to cover all the topics in the emerging field of "machine learning and physics" in the present course. Rather we here try to especially focus on one important branch of machine learning, namely, *reinforcement learning*.

Compared to a more elementary topic like supervised learning, reinforcement learning can be considered as advanced concept since it requires neither teacher training a student nor a priori knowledge about a problem at hand. In this sense, reinforcement learning can potentially find a novel solution to the problem beyond human abilities; said differently, machine can have kind of creativity. Indeed, when combined with deep neural networks, it has achieved superhuman performance in the game of Go. We will also see an illustrative example which indicates that the reinforcement learning holds great promise for controlling open quantum systems. We will learn about some basic concepts of machine learning methods including reinforcement learning in Chapters 6 and 7. Nevertheless, I would *not* pretend to teach specific techniques for numerical implementations, such as how to use existing libraries etc., but rather the main goal of this part is to help you to gain intuition/key ideas behind the machine learning algorithms. I believe that the proper understanding of those algorithms is more important than learning about specific numerical techniques, as you should then be able to straightforwardly generalize/apply existing codes to problems at your hand.

Summary of Chapter 1

This course attempts to cover the following topics:

- Review of (mostly) undergrad quantum mechanics (Chap. 2)
- General theory of quantum measurement and Markovian open quantum systems (Chap. 3)
- Brief introduction to non-Hermitian physics (Chap. 3)
- Quantization of the electromagnetic field (Chap. 4)
- General theory of bosonic and fermionic Gaussian states (Chap. 4)
- Basics of time-dependent variational principles (Chap. 4)
- Introduction to circuit/cavity/waveguide quantum electrodynamics (Chap. 4 and 5)
- General theory of quantum light-matter interaction (Chap. 5)
- Brief review of basic concepts in machine learning (Chap. 6)
- Basics of (deep) reinforcement learning (Chap. 7)
- Black-box optimization and its application to deep reinforcement learning (Chap. 6 and 7)
- Deep reinforcement learning of a simple quantum control task (Chap. 7)

What is *not* included in this course:

- Non-Markovian or nonperturbative open quantum systems
- Theory of non-Gaussian many-body states
- Details about supervised/unsupervised learning
- Model-based reinforcement learning algorithms
- Details about policy-based reinforcement learning algorithms
- Details about implementations for machine learning practitioners
- and many other important topics...

CHAPTER 2

Quantum mechanics review

2.1. Fundamental concepts

2.1.1. Quantum states. Mathematically, a quantum state $|\psi\rangle$ is described as a vector in a Hilbert space $\mathcal{H}$:

Hilbert space. Hilbert space $\mathcal{H}$ is a vector space over the complex numbers $\mathbb{C}$. It associates with an inner product $\langle\psi|\phi\rangle$ of an ordered pair of vectors $|\psi\rangle, |\phi\rangle$, which satisfies

- Conjugate symmetry: $\langle\phi|\psi\rangle = \langle\psi|\phi\rangle^*$.
- Linearity: $\langle\psi|(a|\phi\rangle + b|\varphi\rangle) = a\langle\psi|\phi\rangle + b\langle\psi|\varphi\rangle$.
- Positivity: $\||\psi\rangle\| \equiv \sqrt{\langle\psi|\psi\rangle} > 0$ for $|\psi\rangle \neq 0$.

It is also a complete metric space with respect to the distance defined by the norm $d(|\psi_1\rangle, |\psi_2\rangle) = \||\psi_1\rangle - |\psi_2\rangle\|$.

Precisely speaking, we should consider a quantum state as a *ray*, which is an equivalent class of vectors that differ only by a nonzero complex constant factor. Since we are interested in a vector that has the unit norm, $\langle\psi|\psi\rangle = 1$, this just means that its overall phase factor is physically irrelevant, i.e., it does not affect an expectation value of a physical observable as we see below.

2.1.2. Observables. An observable is a physical quantity that can be measured and mathematically described as a self-adjoint operator. To see this, let us first introduce the notion of a Hermitian operator.

Hermiticity. A linear map $\hat{O}$ is a Hermitian operator if and only if $\langle\phi|\hat{O}|\psi\rangle = \langle\psi|\hat{O}|\phi\rangle^*$ for $\forall|\psi\rangle, |\phi\rangle \in \mathcal{H}$.

We can also express this condition as the self-adjoint condition $\hat{O} = \hat{O}^\dagger$, where we define the adjoint $\hat{O}^\dagger$ of $\hat{O}$ by[1]

$$\langle\phi|\hat{O}\psi\rangle = \langle\hat{O}^\dagger\phi|\psi\rangle. \tag{2.1.1}$$

It is known that a self-adjoint operator has a spectral decomposition, i.e., its eigenstates form a complete orthonormal basis in $\mathcal{H}$:

[1] Strictly speaking, for infinite-dimensional case, the self-adjointness not only requires the Hermiticity, but also the condition that the domains of $\hat{O}$ and $\hat{O}^\dagger$ are the same. Yet, this subtle difference does not cause problems at least in this course, so we shall use the terms Hermitian or self-adjoint operators interchangeably.

$$\hat{O} = \sum_n \lambda_n \hat{P}_n, \tag{2.1.2}$$

where λ_n is an eigenvalue and $\hat{P}_n$ is the projection operator onto the corresponding eigenspace satisfying

$$\hat{P}_n \hat{P}_m = \delta_{nm} \hat{P}_n \tag{2.1.3}$$

$$\hat{P}_n = \hat{P}_n^\dagger. \tag{2.1.4}$$

These projectors form a complete set such that they span the entire Hilbert space

$$\sum_n \hat{P}_n = \hat{I}, \tag{2.1.5}$$

where $\hat{I}$ is the identity operator.

2.1.3. Time evolution. Time evolution of a quantum state is given by the Schrödinger equation (we set $\hbar = 1$):

$$i\frac{d}{dt}|\psi(t)\rangle = \hat{H}|\psi(t)\rangle, \tag{2.1.6}$$

where $\hat{H}$ is a self-adjoint operator called the Hamiltonian. Its solution is easily obtained as

$$|\psi(t)\rangle = \hat{U}(t)|\psi(0)\rangle, \tag{2.1.7}$$

$$\hat{U}(t) = e^{-i\hat{H}t}. \tag{2.1.8}$$

Here $\hat{U}(t)$ is the unitary operator, i.e., $\hat{U}(t)\hat{U}^\dagger(t) = 1$. As a result, the norm of a quantum state is preserved:

$$\langle\psi(0)|\psi(0)\rangle = \langle\psi(t)|\psi(t)\rangle = 1. \tag{2.1.9}$$

2.1.4. Measurement. A measurement of an observable $\hat{O}$ for a state $|\psi\rangle$ gives one of the eigenvalues λ_n with probability

$$p_n = \langle\psi|\hat{P}_n|\psi\rangle \tag{2.1.10}$$

and prepares the corresponding eigenstate:

$$\frac{\hat{P}_n|\psi\rangle}{\sqrt{p_n}}. \tag{2.1.11}$$

Suppose that we perform the same measurement processes for the same state many times; then the expectation value $\langle\hat{O}\rangle$ of the measurement outcomes is given by

$$\langle \hat{O} \rangle \equiv \sum_n \lambda_n p_n = \sum_n \lambda_n \langle \psi | \hat{P}_n | \psi \rangle = \langle \psi | \hat{O} | \psi \rangle, \tag{2.1.12}$$

where we used the spectral decomposition of $\hat{O}$. Note that the phase factor of a vector $|\psi\rangle$ is irrelevant to the expectation value as we mentioned above.

2.1.5. Tensor product. Consider two systems, A and B, whose Hilbert space is denoted by $\mathcal{H}_A$ and $\mathcal{H}_B$, respectively. Then the composite system $A + B$ is given by the tensor product $\mathcal{H}_A \otimes \mathcal{H}_B$, i.e., it is now spanned by a quantum state $|\psi\rangle_A \otimes |\phi\rangle_B$ with $|\psi\rangle_A \in \mathcal{H}_A$ and $|\phi\rangle_B \in \mathcal{H}_B$.

To understand the notion of tensor product, it is useful to consider a simple example of a pair of two-level systems. Let us describe a quantum state $|\psi\rangle$ of a two-level system spanned by $\{|0\rangle, |1\rangle\}$ as a vector representation

$$|\psi\rangle = a|0\rangle + b|1\rangle \iff |\psi\rangle = \begin{pmatrix} a \\ b \end{pmatrix}. \tag{2.1.13}$$

Then suppose that we have the following states in each of the two-level systems

$$|\psi\rangle_A = \begin{pmatrix} u \\ v \end{pmatrix}, \quad |\phi\rangle_B = \begin{pmatrix} x \\ y \end{pmatrix}. \tag{2.1.14}$$

The resulting composite state is a four-dimensional vector given by

$$|\psi\rangle_A \otimes |\phi\rangle_B = \begin{pmatrix} ux \\ uy \\ vx \\ vy \end{pmatrix}. \tag{2.1.15}$$

Similarly, if we have the operators

$$\hat{A} = \begin{pmatrix} a & b \\ c & d \end{pmatrix}, \quad \hat{B} = \begin{pmatrix} e & f \\ g & h \end{pmatrix}, \tag{2.1.16}$$

the composite operator is a 4×4 matrix given by

$$\hat{A} \otimes \hat{B} = \begin{pmatrix} ae & af & be & bf \\ ag & ah & bg & bh \\ ce & cf & de & df \\ cg & ch & dg & dh \end{pmatrix}. \tag{2.1.17}$$

2.2. Ensembles

The formulation of quantum mechanics in the previous section is provided for an ideal situation, in which all the microscopic quantum degrees of freedom in a system of interest are accessible to an

observer; in other words, this formulation is supposed to deal with a completely isolated (or closed) quantum system. However, in real world, what we can observe is only a small part of an entire quantum system and this small quantum system interacts with external degrees of freedom that one cannot handle, i.e., a real quantum system necessarily behaves as an open system.

To motivate this, consider the following quantum state in the composite space of a pair of two-level systems:

$$|\psi\rangle_{AB} = \frac{1}{\sqrt{2}} \left(|0\rangle_A |0\rangle_B + |1\rangle_A |1\rangle_B \right). \tag{2.2.1}$$

Suppose that we have access to a two-level system A, but not for B and thus we know nothing about a state of B. In this case, only an observable acting on A is of interest and we expect that there exists a self-consistent theoretical description within A. To see this, consider the expectation value of an observable $\hat{O}_A$ that (nontrivially) acts only on A:

$$\langle \hat{O}_A \rangle \equiv_{AB} \langle \psi | \hat{O}_A \otimes \hat{I}_B | \psi \rangle_{AB} \tag{2.2.2}$$

$$= \frac{1}{2} \left({}_A\langle 0 | \hat{O}_A | 0 \rangle_A + {}_A\langle 1 | \hat{O}_A | 1 \rangle_A \right). \tag{2.2.3}$$

We now see that the expectation value can be obtained by solely dealing with a quantum state in A. However, this value is different from the usual expression for the expectation value with respect to a pure state, but can be represented as the trace over the following *density operator* $\hat{\rho}_A$:

$$\langle \hat{O}_A \rangle = \mathrm{Tr}_A [\hat{\rho}_A \hat{O}_A] \equiv \sum_{i=0,1} {}_A\langle i | \hat{\rho}_A \hat{O}_A | i \rangle_A \tag{2.2.4}$$

with

$$\hat{\rho}_A \equiv \mathrm{Tr}_B [|\psi\rangle_{AB\,AB} \langle \psi|] = \frac{1}{2} \left(|0\rangle_{A\,A} \langle 0| + |1\rangle_{A\,A} \langle 1| \right). \tag{2.2.5}$$

We should interpret $\hat{\rho}_A$ as an *ensemble* of possible quantum states occurring with the equal probability. This means that the expectation value is equal to the ensemble average (or incoherent mixture) over the corresponding expectation values with respect to two states:

$$\langle \hat{O}_A \rangle = \frac{1}{2} \sum_{i=0,1} {}_A\langle i | \hat{O}_A | i \rangle_A. \tag{2.2.6}$$

In other words, an initially pure quantum state should in general be described as an incoherent mixture of different pure states after it interacts with unknown external degrees of freedom. For instance, the relative phase in the original pure state $|\psi\rangle_{AB}$ is no longer accessible and there will be no interference effects in $\hat{\rho}_A$. The partial trace over B above corresponds to such procedure of discarding knowledge about external degrees of freedom; since an observer cannot access to environment degrees of freedom, the best one can

do is to take the unbiased summation over quantum states in B. As we see later, this process lies at the heart of important phenomenon called *decoherence*.

2.2.1. Density operators. In general, an operator $\hat{\rho}$ acting on a Hilbert space $\mathcal{H}$ is called a density operator if it satisfies the following properties:

- $\hat{\rho} = \hat{\rho}^\dagger$
- $\hat{\rho} \geq 0 \iff \langle\psi|\hat{\rho}|\psi\rangle \geq 0 \ \ \forall|\psi\rangle \in \mathcal{H}$
- $\mathrm{Tr}(\hat{\rho}) = 1$

If a quantum state is a pure state $|\psi\rangle$, the corresponding density operator is given by

$$\hat{\rho} = |\psi\rangle\langle\psi| \tag{2.2.7}$$

and satisfies the following condition

$$\hat{\rho}^2 = \hat{\rho}. \tag{2.2.8}$$

It is often useful to note the fact that there is an orthonormal basis that diagonalizes $\hat{\rho}$ with nonnegative and real eigenvalues whose summation gives one:

$$\hat{\rho} = \sum_i p_i |i\rangle\langle i|, \ \ \langle i|j\rangle = \delta_{ij}, \ \ \sum_i p_i = 1. \tag{2.2.9}$$

The coefficients p_i can naturally be interpreted as the probability weight associated with $\hat{\rho}$, which is the incoherent mixture of pure states $\{|i\rangle\}$.

It is also worthwhile to note that a density operator satisfies the convexity; using two density matrices $\hat{\rho}_{1,2}$, one can construct another density matrix by a linear combination:

$$\hat{\rho}(\lambda) = \lambda\hat{\rho}_1 + (1-\lambda)\hat{\rho}_2, \ \ 0 \leq \lambda \leq 1. \tag{2.2.10}$$

Indeed, it obviously satisfies the self-adjoint condition $\hat{\rho}(\lambda) = \hat{\rho}^\dagger(\lambda)$ and the normalization $\mathrm{Tr}[\hat{\rho}(\lambda)] = 1$. The positivity is also satisfied because

$$\langle\psi|\hat{\rho}(\lambda)|\psi\rangle = \lambda\langle\psi|\hat{\rho}_1|\psi\rangle + (1-\lambda)\langle\psi|\hat{\rho}_2|\psi\rangle \geq 0, \ \ \forall|\psi\rangle \in \mathcal{H} \tag{2.2.11}$$

We note that for any density operator $\hat{\rho}_A$ one can perform its purification, that is, one can construct a composite pure state $|\Psi\rangle_{AB}$ that gives $\hat{\rho}_A$ upon doing a partial trace over degrees of freedom in B. Using the expression (2.2.9), one possible purification is given by

$$|\Psi\rangle_{AB} = \sum_i \sqrt{p_i}|i\rangle_A \otimes |\phi_i\rangle_B \tag{2.2.12}$$

with orthonormal states in B

$$ {}_B\langle\phi_i|\phi_j\rangle_B = \delta_{ij}. \tag{2.2.13}$$

Indeed, it leads to the required relation

$$ \hat{\rho}_A = \mathrm{Tr}_B[|\Psi\rangle_{AB\,AB}\langle\Psi|]. \tag{2.2.14}$$

2.3. Distance measures

Suppose that we have two density operators $\hat{\rho}$ and $\hat{\sigma}$. Since a density operator satisfies the positivity, there exists the square-root operator $\sqrt{\hat{\rho}}$ following from the condition $(\sqrt{\hat{\rho}})^2 = \hat{\rho}$. For instance, in the diagonal basis, it is given by

$$ \sqrt{\hat{\rho}} = \sum_i \sqrt{p_i}|i\rangle\langle i|. \tag{2.3.1}$$

Building on this, one can quantify the distinguishability of two ensembles via the following measure known as the *fidelity*:

$$ F(\hat{\rho},\hat{\sigma}) \equiv \left(\mathrm{Tr}\left[\sqrt{\sqrt{\hat{\rho}}\hat{\sigma}\sqrt{\hat{\rho}}}\right]\right)^2. \tag{2.3.2}$$

Alternatively, one can represent the fidelity as the L^1 norm as follows:

$$ F(\hat{\rho},\hat{\sigma}) = \left|\sqrt{\hat{\sigma}}\sqrt{\hat{\rho}}\right|_1^2 \tag{2.3.3}$$

where we define the L^1 norm by

$$ \left|\hat{A}\right|_1 \equiv \mathrm{Tr}\left[\sqrt{\hat{A}^\dagger\hat{A}}\right]. \tag{2.3.4}$$

A useful expression of the L^1 norm is

$$ \left|\hat{A}\right|_1 = \max_{\hat{U}}\left|\mathrm{Tr}\left[\hat{U}^\dagger\hat{A}\right]\right|, \tag{2.3.5}$$

where $\hat{U}$ is unitary. One can check this expression by using the singular value decomposition of $\hat{A}$.

It satisfies the following properties

- $F(\hat{\rho},\hat{\sigma}) = F(\hat{\sigma},\hat{\rho})$
- $0 \leq F(\hat{\rho},\hat{\sigma}) \leq 1$, $F(\hat{\rho},\hat{\rho}) = 1$
- $F(\hat{\rho},\hat{\sigma}) = \left(\sum_i \sqrt{p_i q_i}\right)^2$ if $[\hat{\rho},\hat{\sigma}] = 0$

where p_i and q_i are eigenvalues of $\hat{\rho}$ and $\hat{\sigma}$, respectively, and we define the commutator by

$$ [\hat{A},\hat{B}] \equiv \hat{A}\hat{B} - \hat{B}\hat{A}. \tag{2.3.6}$$

Note that the last relation for commuting density operators is nothing but the usual fidelity between (classical) probability distributions. The upper bound in the second relation $F \leq 1$ follows from the relation

$$F(\hat{\rho}, \hat{\sigma}) \leq \mathrm{Tr}(\hat{\rho})\mathrm{Tr}(\hat{\sigma}) = 1, \tag{2.3.7}$$

which can be shown by using the relation (2.3.5) and the Cauchy-Schwarz inequality:

$$F(\hat{\rho}, \hat{\sigma}) = \left| \mathrm{Tr}\left[\left(\sqrt{\hat{\rho}}\hat{U}\right)^{\dagger} \sqrt{\hat{\sigma}} \right] \right|^2 \leq \mathrm{Tr}\left(\left(\sqrt{\hat{\rho}}\hat{U}\right)^{\dagger} \left(\sqrt{\hat{\rho}}\hat{U}\right) \right) \mathrm{Tr}\left(\sqrt{\hat{\sigma}}\sqrt{\hat{\sigma}}\right) = \mathrm{Tr}(\hat{\rho})\mathrm{Tr}(\hat{\sigma}). \tag{2.3.8}$$

If one of the density operators is pure $\hat{\rho} = |\psi\rangle\langle\psi|$, then the fidelity reduces to

$$F(\hat{\rho}, \hat{\sigma}) = \langle\psi|\hat{\sigma}|\psi\rangle. \tag{2.3.9}$$

In particular, when the other one is also pure $\hat{\sigma} = |\phi\rangle\langle\phi|$, it simplifies to the overlap

$$F(\hat{\rho}, \hat{\sigma}) = |\langle\psi|\phi\rangle|^2. \tag{2.3.10}$$

Finally, there exists a useful general relation between the fidelity and the trace norm:

$$F(\hat{\rho}, \hat{\sigma}) \leq 1 - \frac{1}{4} |\hat{\rho} - \hat{\sigma}|_1^2 . \tag{2.3.11}$$

It will be a good exercise for you to check this inequality (hint: you may use the triangle inequality for the trace norm, the Cauchy-Schwarz inequality, and the relation (2.3.5)).

2.4. Example: Qubit

Let us illustrate the fundamental notions introduced above by discussing the minimal example: a two-dimensional Hilbert space spanned by orthonormal quantum states $\{|0\rangle, |1\rangle\}$. Since an overall phase factor is irrelevant, a generic normalized state in this space is described as

$$|\psi(\theta, \phi)\rangle = \cos\left(\frac{\theta}{2}\right)|0\rangle + e^{i\phi}\sin\left(\frac{\theta}{2}\right)|1\rangle = \begin{pmatrix} \cos\left(\frac{\theta}{2}\right) \\ e^{i\phi}\sin\left(\frac{\theta}{2}\right) \end{pmatrix}. \tag{2.4.1}$$

The angles θ and ϕ characterize the probability weights for each state and the relative phase between two states, respectively.

This represents a quantum counterpart of classical bit, namely, *qubit*. For instance, the spin-1/2 degree of freedom of electron or two internal states in photon polarizations exactly behave as the qubit. However, as we will see in later Chapters, qubits in many of state-of-the-art quantum computers, such as superconducting qubits, actually use two lowest levels in a larger Hilbert space. Thus, it is important to keep in mind that they do not perfectly operate as two-level systems in strict sense, but rather effectively play the role of qubits with a certain (usually high) fidelity.

2.4.1. Bloch sphere. It is useful to consider the basis $|0\rangle, |1\rangle$ as the spin-up and down states along the z axis, $|0\rangle = |\uparrow\rangle, |1\rangle = |\downarrow\rangle$. A general qubit state $|\psi(\theta,\phi)\rangle$ can then be interpreted as a spin vector on the Bloch sphere pointing in the direction corresponding to the angle

$$\mathbf{n} = (\sin\theta\cos\phi, \sin\theta\sin\phi, \cos\theta)^{\mathrm{T}}. \tag{2.4.2}$$

To see this, let us introduce the Pauli operators

$$\hat{\sigma}_1 = \begin{pmatrix} 0 & 1 \\ 1 & 0 \end{pmatrix}, \quad \hat{\sigma}_2 = \begin{pmatrix} 0 & -i \\ i & 0 \end{pmatrix}, \quad \hat{\sigma}_3 = \begin{pmatrix} 1 & 0 \\ 0 & -1 \end{pmatrix}. \tag{2.4.3}$$

(We also often interchangeably use the notation $\hat{\sigma}_{1,2,3} = \hat{\sigma}^{x,y,z}$ later.) These operators satisfy the commutation and anticommutation relations

$$[\hat{\sigma}_i, \hat{\sigma}_j] = \hat{\sigma}_i\hat{\sigma}_j - \hat{\sigma}_j\hat{\sigma}_i = 2i\sum_{k=1}^{3}\epsilon_{ijk}\hat{\sigma}_k \tag{2.4.4}$$

$$\{\hat{\sigma}_i, \hat{\sigma}_j\} = \hat{\sigma}_i\hat{\sigma}_j + \hat{\sigma}_j\hat{\sigma}_i = 2\delta_{ij}\hat{I} \tag{2.4.5}$$

where ϵ_{ijk} is the completely antisymmetric tensor. One can check that a state $|\psi(\theta,\phi)\rangle$ is an eigenstate of

$$\mathbf{n}\cdot\hat{\boldsymbol{\sigma}} = \begin{pmatrix} \cos\theta & e^{-i\phi}\sin\theta \\ e^{i\phi}\sin\theta & -\cos\theta \end{pmatrix} \tag{2.4.6}$$

and has an eigenvalue $+1$.

2.4.2. Unitary operator. The most general unitary operator acting on the two-dimensional Hilbert space is expressed by

$$\hat{U}(\theta,\phi) = \begin{pmatrix} \cos\left(\frac{\theta}{2}\right) & -e^{-i\phi}\sin\left(\frac{\theta}{2}\right) \\ e^{i\phi}\sin\left(\frac{\theta}{2}\right) & \cos\left(\frac{\theta}{2}\right) \end{pmatrix}. \tag{2.4.7}$$

In the language of the Bloch sphere, this corresponds to the counterclockwise rotation by angle θ around the axis $\mathbf{n}_0$:

$$\hat{U}(\theta,\phi) = \exp\left(-\frac{i\theta}{2}\mathbf{n}_0\cdot\hat{\boldsymbol{\sigma}}\right), \quad \mathbf{n}_0 = (-\sin\phi, \cos\phi, 0)^{\mathrm{T}}. \tag{2.4.8}$$

A generic qubit state $|\psi(\theta,\phi)\rangle$ can be obtained by acting this unitary operator on $|0\rangle = (1,0)^{\mathrm{T}}$:

$$|\psi(\theta,\phi)\rangle = \hat{U}(\theta,\phi)|0\rangle. \tag{2.4.9}$$

This is as it should be, since $|0\rangle$ corresponds to spin pointing in positive z direction and $\hat{U}(\theta,\phi)$ rotates this into the direction $\mathbf{n} = (\sin\theta\cos\phi, \sin\theta\sin\phi, \cos\theta)^{\mathrm{T}}$ that corresponds to a state $|\psi(\theta,\phi)\rangle$ as mentioned earlier.

2.4.3. Density operator. We next discuss a density operator of a qubit. The general 2×2 Hermitian matrix is parameterized by 4 real parameters. Since a density operator satisfies the normalization condition $\mathrm{Tr}[\hat{\rho}] = 1$, it is characterized by 3 real parameters. As Pauli operators are linearly independent and traceless, we conclude that the most general form of a density matrix is given by

$$\hat{\rho}(\mathbf{v}) = \frac{1}{2}(\hat{I} + \mathbf{v}\cdot\hat{\boldsymbol{\sigma}}) = \frac{1}{2}\begin{pmatrix} 1+v_3 & v_1 - iv_2 \\ v_1 + iv_2 & 1 - v_3 \end{pmatrix}, \quad \mathbf{v}\in\mathbb{R}^3, \quad |\mathbf{v}| \le 1. \tag{2.4.10}$$

Its determinant is

$$\det\hat{\rho} = \frac{1}{4}\left(1 - \mathbf{v}^2\right). \tag{2.4.11}$$

Thus, the condition $|\mathbf{v}| \le 1$ ensures that $\hat{\rho}$ only has nonnegative eigenvalues.

The condition for a pure state $\hat{\rho}^2 = \hat{\rho}$ can be read as

$$(\mathbf{v}\cdot\hat{\boldsymbol{\sigma}})^2 = \hat{I} \iff |\mathbf{v}| = 1. \tag{2.4.12}$$

Thus, using a unit-norm vector $\mathbf{n}$, we can represent a density operator for a generic pure state as

$$\hat{\rho}(\mathbf{n}) = \frac{1}{2}(\hat{I} + \mathbf{n}\cdot\hat{\boldsymbol{\sigma}}). \tag{2.4.13}$$

It is easy to check that this density operator with $\mathbf{n} = (\sin\theta\cos\phi, \sin\theta\sin\phi, \cos\theta)^{\mathrm{T}}$ in fact corresponds to the above pure state $|\psi(\theta,\phi)\rangle$:

$$\hat{\rho}(\mathbf{n}) = |\psi(\theta,\phi)\rangle\langle\psi(\theta,\phi)|. \tag{2.4.14}$$

2.5. Example: Harmonic oscillator

2.5.1. Fock state. We next consider another elementary example - a harmonic oscillator[2]:

$$\hat{H} = \frac{\omega}{4}\left(\hat{p}^2 + \hat{x}^2\right) = \omega\left(\hat{a}^\dagger\hat{a} + \frac{1}{2}\right) \tag{2.5.1}$$

$$\hat{x} = \hat{a} + \hat{a}^\dagger, \quad \hat{p} = i(\hat{a}^\dagger - \hat{a}), \quad [\hat{x},\hat{p}] = 2i. \tag{2.5.2}$$

Its spectrum is obtained by noting the fact that the annihilation $\hat{a}$ and creation $\hat{a}^\dagger$ operators satisfy the commutation relation

$$[\hat{a},\hat{a}^\dagger] = 1, \tag{2.5.3}$$

and introducing the Fock states $\{|n\rangle\}$ with $n = 0, 1, 2\ldots$ as

[2]There are several possible choices for position/momentum operators; another common convention is $\hat{x} = (\hat{a} + \hat{a}^\dagger)/\sqrt{2}$, $\hat{p} = i(\hat{a}^\dagger - \hat{a})/\sqrt{2}$. The choice (2.5.2) is often used in quantum optics, so we shall follow this notation.

$$\hat{a}|n\rangle = \sqrt{n}|n-1\rangle, \;\; \hat{a}^\dagger|n\rangle = \sqrt{n+1}|n+1\rangle, \tag{2.5.4}$$

$$\hat{a}^\dagger\hat{a}|n\rangle = n|n\rangle. \tag{2.5.5}$$

In particular, for the ground state with $n = 0$, also called as vacuum state, we get

$$\hat{a}|0\rangle = 0. \tag{2.5.6}$$

The corresponding eigenvalue is

$$E_n = \omega\left(n + \frac{1}{2}\right). \tag{2.5.7}$$

2.5.2. Coherent state. Fock states are eigenstates of the number operator $\hat{n} \equiv \hat{a}^\dagger\hat{a}$, while one can also construct an eigenstate of the annihilation operator $\hat{a}$, the coherent state:

$$|\alpha\rangle \equiv \sum_{n=0}^{\infty} \frac{\alpha^n}{\sqrt{n!}} e^{-|\alpha|^2/2}|n\rangle, \;\; \alpha \in \mathbb{C} \tag{2.5.8}$$

$$\hat{a}|\alpha\rangle = \alpha|\alpha\rangle. \tag{2.5.9}$$

The occupation probabilities in the Fock basis obey the Poisson distribution with mean $\bar{n} \equiv |\alpha|^2$:

$$P(n) = \frac{\bar{n}^n}{n!} e^{-\bar{n}}. \tag{2.5.10}$$

Note that $|\alpha\rangle$ is not an eigenstate of the creation operator $\hat{a}^\dagger$, which acts as

$$\hat{a}^\dagger|\alpha\rangle = \left(\frac{\partial}{\partial\alpha} + \alpha^*\right)|\alpha\rangle. \tag{2.5.11}$$

The vacuum state $|0\rangle$ is a special example of a coherent state with $\alpha = 0$. In fact, a general coherent state can be obtained by acting the following displacement operator on the vacuum:

$$\hat{D}(\alpha) = e^{\alpha\hat{a}^\dagger - \alpha^*\hat{a}} = e^{-|\alpha|^2/2} e^{\alpha\hat{a}^\dagger} e^{-\alpha^*\hat{a}} = e^{|\alpha|^2/2} e^{-\alpha^*\hat{a}} e^{\alpha\hat{a}^\dagger}, \tag{2.5.12}$$

$$\hat{D}(\alpha)|0\rangle = |\alpha\rangle. \tag{2.5.13}$$

The displacement operator satisfies the following properties

- $\hat{D}^\dagger(\alpha) = D^{-1}(\alpha) = D(-\alpha)$
- $\hat{D}^\dagger(\alpha)\hat{a}\hat{D}(\alpha) = \hat{a} + \alpha$
- $\hat{D}^\dagger(\alpha)\hat{a}^\dagger\hat{D}(\alpha) = \hat{a}^\dagger + \alpha^*$
- $\hat{D}(\alpha+\beta) = e^{-(\alpha\beta^* - \alpha^*\beta)/2}\hat{D}(\alpha)\hat{D}(\beta) = e^{(\alpha\beta^* - \alpha^*\beta)/2}\hat{D}(\beta)\hat{D}(\alpha)$

The last relation follows from the Baker-Campbell-Hausdorff (BCH) formula:

$$e^{\hat{A}+\hat{B}} = e^{\hat{A}}e^{\hat{B}}e^{-\frac{1}{2}[\hat{A},\hat{B}]} = e^{\hat{B}}e^{\hat{A}}e^{\frac{1}{2}[\hat{A},\hat{B}]} \text{ if } [\hat{A},[\hat{A},\hat{B}]] = [\hat{B},[\hat{A},\hat{B}]] = 0. \tag{2.5.14}$$

In particular, note that two different coherent states are not orthogonal:

$$|\langle\beta|\alpha\rangle| = e^{-|\alpha-\beta|^2/2}. \tag{2.5.15}$$

2.5.3. Squeezed state. To motivate the notion of a squeezed state, consider the following Hamiltonian that includes the so-called $\hat{A}^2$ term on top of the usual harmonic oscillator[3]:

$$\hat{H} = \omega\hat{a}^\dagger\hat{a} + \frac{g^2}{2\omega}\hat{A}^2, \quad \hat{A} \equiv \hat{a}^\dagger + \hat{a}. \tag{2.5.16}$$

Since this Hamiltonian is still quadratic in terms of creation or annihilation operators, one can diagonalize it by using the unitary transformation often called as the Bogoliubov transformation:

$$\hat{b} = \cosh r\hat{a} + \sinh r\hat{a}^\dagger \equiv \hat{U}_r^\dagger\hat{a}\hat{U}_r, \tag{2.5.17}$$

$$e^r = \sqrt{\frac{\Omega}{\omega}}, \quad \Omega = \sqrt{\omega^2 + 2g^2}, \quad \hat{U}_r = e^{\frac{r}{2}\left(\hat{a}^{\dagger 2} - \hat{a}^2\right)}. \tag{2.5.18}$$

Note that the new annihilation/creation operators $\hat{b}$, $\hat{b}^\dagger$ satisfy the canonical commutation relation

$$[\hat{b}, \hat{b}^\dagger] = 1. \tag{2.5.19}$$

Thus, the above Hamiltonian is diagonalized as

$$\hat{H} = \Omega\hat{b}^\dagger\hat{b} + \text{const.}, \tag{2.5.20}$$

where we use $\hat{a} = \cosh r\hat{b} - \sinh r\hat{b}^\dagger$. The unitary operator $\hat{U}$ is an example of the *squeezing* operator, and the transformed ground state is given by the squeezed vacuum

$$|0\rangle_b \equiv \hat{U}_r^\dagger|0\rangle = e^{\frac{r}{2}\left(\hat{a}^2 - \hat{a}^{\dagger 2}\right)}|0\rangle = e^{\frac{ir}{4}(\hat{x}\hat{p}+\hat{p}\hat{x})}|0\rangle. \tag{2.5.21}$$

To see the reason why it represents "squeezing", it is useful to rewrite the Hamiltonian in terms of position and momentum operators as (aside constant)

$$\hat{H} = \frac{\omega}{4}\left(\hat{p}^2 + \hat{x}^2\right) + \frac{g^2}{2\omega}\hat{x}^2 = \frac{\omega}{4}\left(\hat{p}^2 + \frac{\Omega^2}{\omega^2}\hat{x}^2\right). \tag{2.5.22}$$

[3]We will later see that this Hamiltonian is relevant to the minimal setup of cavity quantum electrodynamics in the Coulomb gauge.

This means that the above Hamiltonian is nothing but the usual harmonic oscillator, but with a tighter potential with $\Omega^2/\omega^2 \geq 1$. Consequently, the ground state $|0\rangle_b$ is more strongly confined in the x direction compared with the original vacuum $|0\rangle$. Due to the uncertainty relation, this results in an inevitable "expansion" in the p direction. More explicitly, we get

$$\hat{U}_r \begin{pmatrix} \hat{x} \\ \hat{p} \end{pmatrix} \hat{U}_r^\dagger = \begin{pmatrix} e^{-r}\hat{x} \\ e^{r}\hat{p} \end{pmatrix}. \tag{2.5.23}$$

Because position and momentum operators are interchangeable in harmonic oscillators, one can similarly consider a squeezing in a general direction on the x-p plane. A general squeezing operator is given by

$$S(\zeta) \equiv e^{(\zeta \hat{a}^{\dagger 2} - \zeta^* \hat{a}^2)/2}, \quad \zeta = re^{i\theta} \in \mathbb{C}, \tag{2.5.24}$$

which transforms the annihilation and creation operators by

$$\hat{S}^\dagger(\zeta)\hat{a}\hat{S}(\zeta) = \cosh r\hat{a} + e^{i\theta}\sinh r\hat{a}^\dagger. \tag{2.5.25}$$

Summary of Chapter 2

Section 2.1 Fundamental concepts

- A quantum state is described as a vector (or precisely speaking, ray) in a Hilbert space.
- An observable is described by a self-adjoint operator on a Hilbert space.
- Time evolution of a quantum state is given by the Schrödinger equation governed by the self-adjoin operator called the Hamiltonian.
- A measurement process is described as an orthogonal projection onto the corresponding eigenspace.
- A composite system is described by the tensor product.

Section 2.2 Ensembles

- When only a small part of an entire quantum system is accessible, a quantum state is described by an ensemble called density operator.
- A density operator is self-adjoint, positive, and satisfies the convexity.
- Any density operator can be purified, i.e., one can construct a composite pure state that gives a density operator of interest upon doing a partial trace.

Section 2.3 Distance measures

- The distinguishability of two quantum states can be quantified by the fidelity.
- The fidelity can be related to other distance measures such as the L^1 norm through the (in)equalities.

Section 2.4 Qubit

- A general qubit pure state can be represented as a unit-norm vector on the Bloch sphere.
- Similarly, a density operator of a qubit can be represented as unnormalized vector $\mathbf{v}$ in 3D space with $|\mathbf{v}| \leq 1$.

Section 2.5

- Eigenspectrum of a harmonic oscillator is given by using the annihilation and creation operators.
- An energy eigenstate is given by a Fock state.
- An eigenstate of the annihilation operator is a coherent state.
- When a quadratic term is added to the Hamiltonian, eigenstate is in general squeezed along a certain direction on the position-momentum space.

CHAPTER 3

Theory of quantum measurement and open systems

3.1. Introduction: indirect measurement in qubit-boson model

In this Chapter, we give an introduction to theory of quantum measurement and open systems. Before proceeding to a general formalism, let us first consider a simple motivating example, where a system of interest is a single qubit and it interacts with a "meter" degree of freedom modeled by a harmonic oscillator. Physically, this may be considered as a toy model for spontaneous emission process, in which the two-level system (qubit) can be considered as an atom that can emit a photon into a simplified single-mode electromagnetic mode playing the role of the meter.

The model Hamiltonian is

$$\hat{H}_{\rm JC} = \frac{\hbar\Delta}{2}\hat{\sigma}^z + \hbar\omega_c \hat{b}^\dagger \hat{b} + \hbar\gamma(\hat{\sigma}^- \hat{b}^\dagger + \hat{\sigma}^+ \hat{b}), \tag{3.1.1}$$

$$\hat{\sigma}^\pm = \frac{\hat{\sigma}^x \pm i\hat{\sigma}^y}{2}, \quad [\hat{b}, \hat{b}^\dagger] = 1, \tag{3.1.2}$$

which is known as the Jaynes-Cummings model. In fact, this model can be microscopically derived from the fundamental light-matter Hamiltonian after performing certain approximations, as we will see in later Chapters. A notable feature of this Hamiltonian is that it conserves the excitation number

$$N_{\rm ex} = \frac{1}{2}(\hat{\sigma}^z + 1) + \hat{b}^\dagger \hat{b}. \tag{3.1.3}$$

To be concrete, suppose that the initial state is the product state of the excited qubit and the photon vacuum

$$\hat{\rho}_{\rm tot}(0) = |e\rangle\langle e| \otimes |0\rangle\langle 0|, \tag{3.1.4}$$

which belongs to the excitation manifold with $N_{\rm ex} = 1$. The evolved state is

$$\hat{\rho}_{\rm tot}(t) = \hat{U}\hat{\rho}_{\rm tot}(0)\hat{U}^\dagger, \quad \hat{U} = e^{-i\hat{H}_{\rm JC}t}. \tag{3.1.5}$$

We then perform a projection measurement on the meter degree of freedom; since we consider the sector with $N_{\rm ex} = 1$, there are only two possible outcomes corresponding to the following projection operators

$$\hat{P}_0 = |0\rangle\langle 0|, \quad \hat{P}_1 = |1\rangle\langle 1|. \tag{3.1.6}$$

They satisfy the completeness relation (within the Hilbert space of interest here):

$$\hat{I}_A = \sum_{m=0}^{1} \hat{P}_m. \tag{3.1.7}$$

The postmeasurement (unnormalized) state with outcome $m \in \{0, 1\}$ is given by

$$\mathcal{E}_m(\hat{\rho}_S(0)) \equiv \mathrm{Tr}_A \left[\left(\hat{I}_S \otimes \hat{P}_m \right) \hat{\rho}_{\mathrm{tot}}(t) \left(\hat{I}_S \otimes \hat{P}_m \right) \right], \tag{3.1.8}$$

where we note that the trace Tr_A is taken only over the meter degree of freedom, and $\mathcal{E}_m$ is defined by the linear map acting on the *system* initial state:

$$\hat{\rho}_S(0) = |e\rangle\langle e|. \tag{3.1.9}$$

Physically, the linear map $\mathcal{E}_m$ represents the nonunitary evolution of the system conditioned on measurement outcome m. The outcome occurs with the probability

$$p_m = \mathrm{Tr}_S \left[\mathcal{E}_m(\hat{\rho}_S(0)) \right]. \tag{3.1.10}$$

The normalized postmeasurement state is

$$\hat{\rho}_{S,m} = \frac{\mathcal{E}_m(\hat{\rho}_S(0))}{p_m}. \tag{3.1.11}$$

We can rewrite this nonunitary evolution in a more convenient way. To this end, we introduce the *Kraus operators* $\hat{M}_m$ by

$$\hat{M}_m = \langle m|\hat{U}|0\rangle, \tag{3.1.12}$$

where note that the inner product is taken only over the meter degree of freedom and thus $\hat{M}_m$ is an operator that acts on the system Hilbert space. This leads to the expression of the postmeasurement state

$$\mathcal{E}_m(\hat{\rho}_S(0)) = \mathrm{Tr}_A \left[\left(\hat{I}_S \otimes \hat{P}_m \right) \hat{U} \hat{\rho}_S(0) \otimes |0\rangle\langle 0| \hat{U}^\dagger \left(\hat{I}_S \otimes \hat{P}_m \right) \right] \tag{3.1.13}$$

$$= \langle m|\hat{U}|0\rangle \hat{\rho}_S(0) \langle 0|\hat{U}^\dagger|m\rangle \tag{3.1.14}$$

$$= \hat{M}_m \hat{\rho}_S(0) \hat{M}_m^\dagger. \tag{3.1.15}$$

The probability is then expressed by the *positive operator-valued measure* (POVM) $\hat{E}_m$ as follows

$$p_m = \mathrm{Tr}_S \left[\hat{\rho}_S(0) \hat{E}_m \right], \quad \hat{E}_m = \hat{M}_m^\dagger \hat{M}_m. \tag{3.1.16}$$

Importantly, $\hat{E}_m$ are in general nonorthogonal and thus can be considered as a generalization of projection measurement operators $\hat{P}_m$. The Kraus operators and the POVMs satisfy the completeness condition:

$$\sum_{m=0}^{1} \hat{E}_m = \sum_{m=0}^{1} \hat{M}_m^\dagger \hat{M}_m = \hat{I}_S, \tag{3.1.17}$$

leading to

$$\sum_{m=0}^{1} p_m = 1. \tag{3.1.18}$$

So far, we discuss the time evolution that is conditioned on a certain measurement outcome. Another important concept is the nonunitary evolution that is *unconditioned* on measurement outcomes, often called the nonselective evolution defined by

$$\mathcal{E}(\hat{\rho}_S(0)) \equiv \sum_{m=0}^{1} \mathcal{E}_m(\hat{\rho}_S(0)) = \sum_{m=0}^{1} \hat{M}_m \hat{\rho}_S(0) \hat{M}_m^\dagger. \tag{3.1.19}$$

This mapping $\mathcal{E}$ satisfies the linearity, positivity[1], and trace-preserving properties $\mathrm{Tr}[\mathcal{E}(\hat{\rho})] = 1$; we will generalize its notion as the completely positive trace preserving (CPTP) map later.

As shown below, it is often useful to consider the so-called *continuous* measurement limit, for which we take $\gamma \to \infty$ and $\tau \to 0$ while keeping $\gamma^2\tau$ finite. Here, we denote τ as the (short) time duration for a single whole process of the indirect measurement. In this limit, at the leading order of $\gamma\tau \ll 1$, the postmeasurement state when a photon is detected is given by

$$\hat{\rho}_{S,1} = \frac{\tau \hat{L} \hat{\rho}_S(\tau) \hat{L}^\dagger}{p_1}, \tag{3.1.20}$$

where

$$\hat{\rho}_S(\tau) = \hat{U}_S |e\rangle\langle e| \hat{U}_S^\dagger, \;\; \hat{U}_S = e^{-i\Delta\hat{\sigma}^z\tau/2}, \tag{3.1.21}$$

and we define the so-called *jump operator* by

$$\hat{L} \equiv \sqrt{\gamma^2\tau}\hat{\sigma}^-. \tag{3.1.22}$$

In this limit, the Kraus operator corresponding to photon detection ($m = 1$) is given by

$$\hat{M}_1 \simeq \sqrt{\tau}\hat{L} \tag{3.1.23}$$

while the probability is

$$p_1 = \tau \mathrm{Tr}_S \left[\hat{L} \hat{\rho}_S(\tau) \hat{L}^\dagger \right]. \tag{3.1.24}$$

This nonunitary evolution (often called quantum jump) corresponds to the process that, due to the photon detection, an observer acquires the information that the system (two-level atom) de-excites and is thus projected onto the ground state, i.e., $\hat{\rho}_{S,1} = |g\rangle\langle g|$.

Meanwhile, when a photon is not detected during the time interval τ, the postmeasurement state is given by

$$\hat{\rho}_{S,0} = \frac{1}{p_0} \left[\hat{\rho}_S(\tau) - \frac{\tau}{2} \left\{ \hat{L}^\dagger \hat{L}, \hat{\rho}_S(\tau) \right\} \right], \tag{3.1.25}$$

[1] A linear operator $\hat{O} \in \mathcal{L}(\mathcal{H})$ acting on the Hilbert space $\mathcal{H}$ is positive, $\hat{O} \geq 0$, iff $\langle\psi|\hat{O}|\psi\rangle \geq 0$ for $\forall|\psi\rangle \in \mathcal{H}$. A linear mapping $\mathcal{E} : \mathcal{L}(\mathcal{H}) \to \mathcal{L}(\mathcal{H})$ is then said to be positive, $\mathcal{E} \geq 0$, iff $\mathcal{E}(\hat{O}) \geq 0$ for any positive operator $\hat{O} \geq 0$.

and the probability is

$$p_0 = 1 - \tau \mathrm{Tr}_S \left[\hat{L} \hat{\rho}_S(\tau) \hat{L}^\dagger \right]. \tag{3.1.26}$$

The corresponding Kraus operator is

$$\hat{M}_0 = 1 - i \hat{H}_{\mathrm{eff}} \tau / \hbar \tag{3.1.27}$$

where we introduce the non-Hermitian effective Hamiltonian by

$$\hat{H}_{\mathrm{eff}} = \frac{\hbar \Delta}{2} \hat{\sigma}^z - \frac{i}{2} \hat{L}^\dagger \hat{L} = \frac{\hbar \Delta}{2} \hat{\sigma}^z - \frac{i \gamma^2 \tau}{2} |e\rangle\langle e|. \tag{3.1.28}$$

It is important to note that, even in this no-photon-counting process, an observer actually gains the information about the system in the sense that she/he knows that no spontaneous emission has occurred during the time interval τ. This information acquisition indicates that the system is more likely to be in the ground state than in the excited state. It is this tendency that is ascribed to the measurement backaction, which is captured by the non-Hermitian term in $\hat{H}_{\mathrm{eff}}$.

3.2. Positive operator-valued measure

From now on we present a general theory of quantum measurement by considering each notion introduced in the previous section in a more abstract manner. To begin with, motivated by the above simple example, we characterize the POVMs $\hat{E}_m$ by the following properties

- $\hat{E}_m = \hat{E}_m^\dagger$
- $\hat{E}_m \geq 0$
- $\sum_m \hat{E}_m = \hat{I}$

Recall that they are not orthogonal in general. Using the POVMs, the probability of observing measurement outcome m is given by

$$p_m = \mathrm{Tr}[\hat{E}_m \hat{\rho}]. \tag{3.2.1}$$

We note that the Hermiticity and positivity of POVMs ensures that p_m are real and nonnegative, while the completeness relation ensures the normalization $\sum_m p_m = 1$; altogether, p_m can indeed be interpreted as probabilities.

3.3. Completely positive trace-preserving (CPTP) map

We next introduce the notion of a completely positive trace-preserving (CPTP) map $\mathcal{E}$ in a general way. We shall first give a formal definition of the CPTP map $\mathcal{E}$. Consider a Hilbert space $\mathcal{H}$ and a set of linear operators $\mathcal{L}(\mathcal{H})$ acting on $\mathcal{H}$. Since a linear map $\mathcal{E} : \mathcal{L}(\mathcal{H}) \to \mathcal{L}(\mathcal{H})$ is supposed to represent certain time evolution, it should map a density operator $\hat{\rho} \in \mathcal{L}(\mathcal{H})$ to another density operator in the same Hilbert space. This means that $\mathcal{E}$ must be (at least) positive $\mathcal{E} \geq 0$. Since the system of interest is in practice just part of the whole world (i.e., ultimately there always exist external degrees of freedom other than the system), we must also ensure that $\mathcal{E}$ is positive even when it acts on part of a larger Hilbert space. Thus,

it is in fact legitimate to require a stronger condition known as the completely positivity[2]. Altogether, we define the CPTP map by the following conditions:

- $\mathcal{E}(a\hat{\rho} + b\hat{\sigma}) = a\mathcal{E}(\hat{\rho}) + b\mathcal{E}(\hat{\sigma})$
- $\mathcal{E}(\hat{\rho})$ is a density operator, i.e., it is self-adjoint, positive, and satisfies $\mathrm{Tr}[\mathcal{E}(\hat{\rho})] = \mathrm{Tr}[\hat{\rho}] = 1$.
- $\mathcal{E}$ is completely positive, i.e., a linear map $\mathcal{E} \otimes \mathcal{I} : \mathcal{L}(\mathcal{H} \otimes \mathcal{H}_A) \to \mathcal{L}(\mathcal{H} \otimes \mathcal{H}_A)$ is positive for arbitrary (additional) Hilbert space $\mathcal{H}_A$. Here, $\mathcal{I}$ is the identity operator acting on $\mathcal{L}(\mathcal{H}_A)$.

It is worthwhile to note that, if the completely positivity is not satisfied, an initially entangled state in $\mathcal{H} \otimes \mathcal{H}_A$ can lead to negative probabilities after the mapping $\mathcal{E} \otimes \mathcal{I}$ (see e.g., Peres, PRL 77, 1413 (1996)). In this sense, the completely positivity is necessary to ensure that $\mathcal{E}$ indeed gives physically reasonable time evolution even when the initial state is correlated with external world.

We recall that the simple example discussed before indicates that $\mathcal{E}$ has an operator-sum representation (3.1.19) with the Kraus operators $\hat{M}_m$. The map $\mathcal{E}$ then physically represents the nonselective (or unconditional) nonunitary evolution that is ensemble averaged over all the possible measurement outcomes m. These expressions follow from the originally unitary evolution in the larger Hilbert space. This observation naturally motivates the question: given a general CPTP map $\mathcal{E}$ acting on a Hilbert space $\mathcal{H}$, is it possible to embed $\mathcal{H}$ into a larger Hilbert space and to construct a unitary evolution on this extended system that reduces to $\mathcal{E}$ upon tracing out the degrees of freedom outside $\mathcal{H}$? One can answer this question in the affirmative way, as we briefly explain in the next section.

3.4. Kraus operators and the equivalence to indirect measurement model

There is an equivalence between a CPTP map and an indirect measurement model in an extended Hilbert space (exemplified by the simple model above). This means that any nonunitary dynamics of open quantum systems can be considered as a part of a larger closed system equipped with orthogonal projection measurements.

To state this in a more formal manner, let $\{\mathcal{E}_m\}_{m\in M}$ be a set of linear mappings acting on a vector space spanned by a linear operator $\mathcal{L}(\mathcal{H})$. Suppose that they satisfy the following conditions:

- $\mathcal{E} \equiv \sum_m \mathcal{E}_m$ is trace preserving, i.e., $\mathrm{Tr}[\mathcal{E}(\hat{O})] = \mathrm{Tr}[\hat{O}]$ for $\forall \hat{O} \in \mathcal{L}(\mathcal{H})$.
- $\mathcal{E}_m$ is completely positive for $\forall m \in M$.

Then, one can show that [Hellwig & Kraus, Comm. Math. Phys. 16, 142 (1970); Kraus, Ann. Phys. 64, 311 (1971); Stinespring, Proc. Amer. Math. Soc. 6, 211 (1955)], if and only if $\{\mathcal{E}_m\}_{m\in M}$ satisfies the above conditions, there is the following indirect measurement model with some set of $\left\{\mathcal{H}_A, \hat{\rho}_A, \hat{U}, \left\{\hat{P}_m\right\}_{m\in M}\right\}$ (often called Stinespring representation):

$$\mathcal{E}_m(\hat{\rho}) = \mathrm{Tr}_{\mathcal{H}_A}\left[\left(\hat{I} \otimes \hat{P}_m\right)\hat{U}\left(\hat{\rho} \otimes \hat{\rho}_A\right)\hat{U}^\dagger\left(\hat{I} \otimes \hat{P}_m\right)\right], \tag{3.4.1}$$

where $\mathcal{H}_A$ is a Hilbert space and $\hat{\rho}_A$ is a density operator for $\mathcal{H}_A$, $\hat{U}$ is a unitary operator acting on $\mathcal{H} \otimes \mathcal{H}_A$, and $\left\{\hat{P}_m\right\}_{m\in M}$ is a set of projection operators on the subspace of $\mathcal{H}_A$ corresponding to each measurement outcome m.

[2]We remark that positive maps are not necessarily completely positive; we leave constructing such a map to Exercise of this Chapter.

For a given CPTP map $\mathcal{E} = \sum_m \mathcal{E}_m$, this statement guarantees the existence of a meter A and a unitary operator, which will reproduce $\mathcal{E}$ upon tracing out the meter degrees of freedom. However, the constructed meter and the unitary operator are still rather mathematical objects; to deal with a real physical system, in general we need to perform careful analysis of the interaction between the measured system and the meter in light of each physical situation. We will demonstrate such an analysis for a simple example later.

As shown above, the most general measurement process is described by a set of the completely positive maps $\mathcal{E}_m$ whose nonselective mapping $\mathcal{E} = \sum_m \mathcal{E}_m$ is trace reserving. Then, it is useful to note that the measurement process always permits the following representation (often called Kraus representation):

$$\mathcal{E}_m(\hat{\rho}) = \sum_k \hat{M}_{m,k} \hat{\rho} \hat{M}_{m,k}^\dagger. \tag{3.4.2}$$

To see this, it suffices to employ the spectral decomposition

$$\hat{\rho}_A = \sum_i c_i |\psi_i\rangle_{AA}\langle\psi_i|, \quad \hat{P}_m = \sum_j |\phi_{m,j}\rangle_{AA}\langle\phi_{m,j}|, \tag{3.4.3}$$

where $\{|\psi_i\rangle_A\}$ and $\{|\phi_{m,j}\rangle_A\}$ are orthonormal basis in $\mathcal{H}_A$. Then, introducing the Kraus operators by

$$\hat{M}_{m,k} \equiv \hat{M}_{m,(i,j)} = \sqrt{c_i}_A\langle\phi_{m,j}|\hat{U}|\psi_i\rangle_A, \tag{3.4.4}$$

one can show that the (unnormalized) postmeasurement state in Eq. (3.4.1) can be written as in Eq. (3.4.2).

The Kraus representation allows us to express the POVMs by the operator-sum form as

$$\hat{E}_m = \sum_k \hat{M}_{m,k}^\dagger \hat{M}_{m,k}, \quad \sum_m \hat{E}_m = \hat{I}. \tag{3.4.5}$$

The normalized postmeasurement state is given by

$$\hat{\rho}_m = \frac{\mathcal{E}_m(\hat{\rho})}{p_m} \tag{3.4.6}$$

with the probability of observing measurement outcome m being

$$p_m = \mathrm{Tr}[\hat{\rho}\hat{E}_m]. \tag{3.4.7}$$

Conversely, one can show that any Kraus representation can be transformed to some Stinespring representation.

3.5. Bayesian inference and quantum measurement

Bayesian inference is usually discussed in the context of classical estimation theory. In this section, we see that a certain class of quantum measurement processes is in fact completely equivalent to Bayesian inference. A prominent example includes the quantum nondemolition (QND) measurement that has been realized in a beautiful cavity QED experiment (2012 Nobel Prize), as we briefly discuss below.

3.5.1. Diagonal POVM and QND measurement. To motivate the notion of QND measurement, consider a measurement process whose POVM and Kraus operators can be diagonally decomposed into

$$\hat{E}_m = \sum_j c_{m,j} |\psi_j\rangle\langle\psi_j|, \quad \hat{M}_{m,k} = \sum_j c'_{m,k,j} |\psi_j\rangle\langle\psi_j| \tag{3.5.1}$$

by using the common orthogonal basis $\{|\psi_j\rangle\}$ with some coefficients $c_{m,j} = \sum_k |c'_{m,k,j}|^2$. Let us denote the probabilities associated with the projection operators by

$$P(j) = \mathrm{Tr}[\hat{P}_j \hat{\rho}], \quad \hat{P}_j = |\psi_j\rangle\langle\psi_j| \tag{3.5.2}$$

and write the conditional probability distribution of measurement outcomes for $|\psi_j\rangle$ as

$$P(m|j) = \mathrm{Tr}[\hat{E}_m \hat{\rho}_j], \quad \hat{\rho}_j = \frac{\hat{P}_j \hat{\rho} \hat{P}_j}{P(j)}. \tag{3.5.3}$$

Similarly, let $P(j|m)$ be the conditional probability distribution of finding a quantum state in $|\psi_j\rangle$ after obtaining measurement outcome m:

$$P(j|m) = \mathrm{Tr}[\hat{P}_j \hat{\rho}_m], \quad \hat{\rho}_m = \frac{\mathcal{E}_m(\hat{\rho})}{P(m)}. \tag{3.5.4}$$

Then, it satisfies Bayes' theorem

$$P(j|m) = \frac{P(m|j)P(j)}{P(m)}, \quad P(m) = \sum_i P(m|i)P(i). \tag{3.5.5}$$

This follows from the relation

$$P(j|m) = \frac{\mathrm{Tr}[\hat{P}_j \mathcal{E}_m(\hat{\rho})]}{P(m)} = \frac{\mathrm{Tr}[\mathcal{E}_m(P(j)\hat{\rho}_j)]}{P(m)} = \frac{\mathrm{Tr}[\hat{E}_m \hat{\rho}_j]}{P(m)} P(j) = \frac{P(m|j)P(j)}{P(m)}. \tag{3.5.6}$$

If we perform measurement process n times whose measurement outcomes are $\mathbf{m} = \{m_1, m_2, \ldots, m_n\}$, we obtain

$$P_n(j|\mathbf{m}) = \frac{\prod_{l=1}^n P(m_l|j) P_0(j)}{P(\mathbf{m})}, \quad P(\mathbf{m}) = \sum_i \prod_{l=1}^n P(m_l|i) P_0(i). \tag{3.5.7}$$

This is nothing but the usual chain rule of Bayes' relation. Hence, we can reconstruct the probability distribution $P_n(j|\mathbf{m})$ of the postmeasurement quantum state in the $\{|\psi_j\rangle\}$ basis along with the same line of classical estimation theory.

A quantum nondemolition (QND) measurement is an important class of quantum measurements that satisfies the above diagonal condition (3.5.1) and thus essentially reduces to the problem of Bayesian inference. To introduce the notion of QND measurement, consider a measurement process whose nonselective evolution is

$$\mathcal{E}(\hat{\rho}) = \mathrm{Tr}_{\mathcal{H}_A}\left[\hat{U}(\hat{\rho}\otimes\hat{\rho}_A)\hat{U}^\dagger\right], \tag{3.5.8}$$

where the unitary operator $\hat{U}$ acts on the composite system consisting of the system and the meter, and we assume that the meter initial state is pure $\hat{\rho}_A = |\psi_A\rangle\langle\psi_A|$. We also consider a Hermitian operator $\hat{X}$ acting on the system. Then, the measurement is called QND measurement of $\hat{X}$ if the following condition is satisfied:

$$[\hat{X}, \hat{U}]|\psi_A\rangle = 0. \tag{3.5.9}$$

A sufficient condition for this is

$$\hat{X} = \hat{U}^\dagger\hat{X}\hat{U}, \tag{3.5.10}$$

meaning that $\hat{X}$ is the conserved quantity. The name, QND, comes from the fact that such measurement process does not alter the statistics of a certain observable ($\hat{X}$ in our notation) after the measurement, i.e., the following relation holds true for all eigenvalues x of $\hat{X}$ (note that $\hat{P}_x$ is the corresponding projection operator):

$$\mathrm{Tr}[\hat{P}_x\hat{\rho}] = \mathrm{Tr}[\hat{P}_x\mathcal{E}(\hat{\rho})]. \tag{3.5.11}$$

Said differently, the probability distribution of the observable $\hat{X}$ remains the same even after the measurement process.

Using the diagonal representation, one can obtain a simplified expression of a QND measurement operator. To do so, let us use the spectral decomposition of $\hat{X}$,

$$\hat{X} = \sum_x x|x\rangle\langle x|, \tag{3.5.12}$$

as well as the Kraus representation

$$\mathcal{E}(\hat{\rho}) = \sum_{m,k}\hat{M}_{m,k}\hat{\rho}\hat{M}_{m,k}^\dagger, \tag{3.5.13}$$

and the QND condition

$$\langle x|\mathcal{E}(\hat{\rho})|x\rangle = \langle x|\hat{\rho}|x\rangle, \quad \forall x, \hat{\rho}. \tag{3.5.14}$$

It then follows that

$$\sum_{m,k}\hat{M}_{m,k}|x\rangle\langle x|\hat{M}_{m,k}^\dagger = |x\rangle\langle x|, \quad \forall x. \tag{3.5.15}$$

The expectation value of this operator for $|x'\rangle$ with $x \neq x'$ gives

$$\sum_{m,k} |\langle x|\hat{M}_{m,k}|x'\rangle|^2 = 0, \tag{3.5.16}$$

leading to

$$\langle x|\hat{M}_{m,k}|x'\rangle = 0, \quad \forall x \neq x'. \tag{3.5.17}$$

Thus, the Kraus operator and the POVMs are diagonal in the x basis,

$$\hat{M}_{m,k} = \sum_x c'_{m,k,x}|x\rangle\langle x|, \tag{3.5.18}$$

$$\hat{E}_m = \sum_x c_{m,x}|x\rangle\langle x|, \tag{3.5.19}$$

which are nothing but the diagonal condition in Eq. (3.5.1). A QND measurement thus becomes equivalent to the Bayesian inference in the above sense. Building on this fact, below we shall summarize several important properties of QND measurements.

3.5.1.1. *Convergence to measurement basis: wavefunction collapse.* We consider a measurement process satisfying the diagonal condition (3.5.1) in the previous section and call $\{|\psi_i\rangle\}$ as the measurement basis. Suppose that we have performed the measurement n times and obtained the corresponding n measurement outcomes $\{m_k\}_{k=1}^n$. Then, suppose that the measurement outcome m_{n+1} is obtained as a consequence of the $n+1$-th measurement process.

As noted earlier, the probability distribution of the $n+1$-th postmeasurement state is calculated by the Bayes formula

$$P_{n+1}(j|\{m_k\}_{k=1}^{n+1}) = P_n(j|\{m_k\}_{k=1}^n)\frac{P(m_{n+1}|j)}{P_n(m_{n+1})}. \tag{3.5.20}$$

To discuss the probability distribution of the quantum state after an infinite number of measurements, let us denote $P_\infty(j|\{m_k\}_{k=1}^\infty)$ as the probability of finding the quantum state to be j after an infinite number of measurements:

$$P_\infty(j|\{m_k\}_{k=1}^\infty) = P_\infty(j|\{m_k\}_{k=1}^\infty)\frac{P(m|j)}{P_\infty(m)}. \tag{3.5.21}$$

Only the state j for which $P_\infty(j|\{m_k\}_{k=1}^\infty) \neq 0$ leads to a nontrivial condition and let us restrict to such j:

$$P(m|j) = P_\infty(m) = \sum_i P(m|i)P_\infty(i|\{m_k\}_{k=1}^\infty). \tag{3.5.22}$$

This relation can be satisfied by

$$P_\infty(i|\{m_k\}_{k=1}^\infty) = \delta_{ij}, \tag{3.5.23}$$

which means that, in the infinite number limit of measurement processes, the measurement induces the convergence (or wavefunction collapse) of a quantum state into a single particular measurement basis $|\psi_j\rangle$[3].

3.5.1.2. *Born rule of collapsed states.* We next show that the distribution of those collapsed states reproduces the initial distribution $P_0(j)$. To this end, we regard $P_{n+1}(j|\{m_k\}_{k=1}^{n+1})$ as the random variable and consider the average of its value over the measurement outcome m_{n+1}:

$$E[P_{n+1}(j|\{m_k\}_{k=1}^{n+1})] = \sum_{m_{n+1}} P_n(m_{n+1}) P_{n+1}(j|\{m_k\}_{k=1}^{n+1}) \tag{3.5.24}$$

$$= \sum_{m_{n+1}} P(m_{n+1}|j) P_n(j|\{m_k\}_{k=1}^{n}) \tag{3.5.25}$$

$$= P_n(j|\{m_k\}_{k=1}^{n}). \tag{3.5.26}$$

Thus, the expectation value of the next random variable P_{n+1} is equal to the previous one P_n for $\forall j$. It follows then from the convergence theorem of classical probability theory that the infinite limit of a random variable $P_n(j|\{m_k\}_{k=1}^n)$ converges almost surely in the sense of stochastic convergence, and its expectation value is equal to the initial distribution,

$$E[P_\infty(j|\{m_k\}_{k=1}^\infty)] = P_0(j), \quad \forall j. \tag{3.5.27}$$

Physically, this represents the Born rule, i.e., the wavefunction collapse occurs according to the probability distribution determined by the initial wavefunction.

3.5.2. Example: photon QND measurement in cavity QED. To illustrate these general properties, we here consider the minimal example consisting of a single atom system interacting with a cavity photon. We again start from the Jaynes-Cummings-type interaction,

$$\hat{H}_{\rm int} = \hbar\gamma(|e\rangle\langle f|\hat{b}^\dagger + |f\rangle\langle e|\hat{b}), \tag{3.5.28}$$

where $|f\rangle$ is another atomic excited state above $|e\rangle$. At this time we consider a cavity photon as a system of interest while a two-level system is a meter degree of freedom.

To ensure the QND condition and simplify the Hamiltonian, we assume the off-resonant condition $|\delta| \gg \gamma$ for the detuning $\delta = \omega_c - \omega_{fe}$. After adiabatically eliminating the $|f\rangle$ state, at the leading order one gets the interaction Hamiltonian

$$\hat{H}_{\rm int} \simeq \frac{\hbar\gamma^2}{\delta}\hat{b}^\dagger\hat{b}|e\rangle\langle e| \tag{3.5.29}$$

[3]Strictly speaking, there may exist other solution of $P_\infty(i|\{m_k\}_{k=1}^\infty)$ satisfying Eq. (3.5.22) when vectors $\{\mathbf{p}_j; (\mathbf{p}_j)_m = P(m|j)\}$ are not linearly independent.

and the total effective Hamiltonian

$$\hat{H}_{\rm eff} = \hbar\omega_c \hat{n} + \hbar\Omega \hat{n}|e\rangle\langle e|, \quad \Omega = \frac{\gamma^2}{\delta}, \tag{3.5.30}$$

where $\hat{n} = \hat{b}^\dagger \hat{b}$ is the photon-number operator. This observable commutes with the Hamiltonian,

$$[\hat{H}_{\rm eff}, \hat{n}] = 0, \tag{3.5.31}$$

and thus ensures the QND condition (3.5.9).

We assume that the initial meter state is prepared in the excited state:

$$\hat{\rho}_A = |e\rangle\langle e|. \tag{3.5.32}$$

To be specific, we consider the following unitary operator as realized in the actual experiment [Gleyzes et al., Nature 446, 297 (2007)]:

$$\hat{U} = \hat{U}_{R_2} \hat{U}_c \hat{U}_{R_1}, \tag{3.5.33}$$

where $\hat{U}_{R_{1,2}}$ correspond to the interferometric operations known as Ramsey interferometry:

$$\hat{U}_{R_1} = \frac{1}{\sqrt{2}} \begin{pmatrix} 1 & 1 \\ -1 & 1 \end{pmatrix}, \quad \hat{U}_{R_2} = \frac{1}{\sqrt{2}} \begin{pmatrix} 1 & e^{-i\phi} \\ -e^{i\phi} & 1 \end{pmatrix}, \tag{3.5.34}$$

while $\hat{U}_c$ is the light-matter interaction governed by $\hat{H}_{\rm eff}$:

$$\hat{U}_c = e^{-i\hat{H}_{\rm eff}T} = e^{-i\omega_c T\hat{n}} \begin{pmatrix} e^{-i\Omega T\hat{n}} & 0 \\ 0 & 1 \end{pmatrix}. \tag{3.5.35}$$

After the unitary operation, we perform the projection measurement on the two-level system. The resulting measurement outcome is either $m = e$ or $m = g$ depending on the excited or ground state of two-level systems. When $m = e$, the Kraus operator is

$$\hat{M}_e = \langle e|\hat{U}|e\rangle = \frac{e^{-i\omega_c T\hat{n}} \left(e^{-i\Omega T\hat{n}} - e^{-i\phi}\right)}{2} \tag{3.5.36}$$

while for $m = g$ we get

$$\hat{M}_g = \langle g|\hat{U}|e\rangle = \frac{-e^{-i\omega_c T\hat{n}} \left(e^{-i\phi - i\Omega T\hat{n}} + 1\right)}{2}. \tag{3.5.37}$$

The corresponding POVMs are given by

$$\hat{E}_e = \hat{M}_e^\dagger \hat{M}_e = \frac{1 - \cos\left(\Omega T\hat{n} - \phi\right)}{2}, \tag{3.5.38}$$

$$\hat{E}_g = \hat{M}_g^\dagger \hat{M}_g = \frac{1 + \cos\left(\Omega T\hat{n} - \phi\right)}{2}, \tag{3.5.39}$$

which are not orthogonal in general, but satisfy the completeness relation

$$\sum_{m=e,g} \hat{E}_m = \hat{I}. \tag{3.5.40}$$

Following the general theory formulated above, we can write the postmeasurement state and the probability distribution as

$$\hat{\rho}_m = \frac{\hat{M}_m \hat{\rho} \hat{M}_m^\dagger}{p_m}, \quad p_m = \mathrm{Tr}[\hat{\rho}\hat{E}_m], \quad m \in \{e, g\}\,. \tag{3.5.41}$$

Building on our discussion of QND measurement in the previous section, we can immediately obtain the evolution of the postmeasurement probability distribution of the cavity photon number using the Bayes formula

$$P(n|m) = \frac{P(m|n)P_0(n)}{p_m} \tag{3.5.42}$$

where $P_0(n) = \rho_{nn}$ is the initial distribution in the Fock basis and $P(m|n)$ is the conditional probability distribution defined by

$$P(m|n) \equiv \mathrm{Tr}\left[\hat{E}_m \hat{P}_n\right] = \begin{cases} \frac{1-\cos(\Omega T n - \phi)}{2} & m = e \\ \frac{1+\cos(\Omega T n - \phi)}{2} & m = g \end{cases}. \tag{3.5.43}$$

Here, $\hat{P}_n = |n\rangle\langle n|$ is the projection operator on the Fock state with n.

Suppose that we perform the measurement process N times. As shown before, the resulting postmeasurement distribution in the Fock basis is obtained by the chain rule:

$$P_N(n|\,\{m_i\}) = \mathcal{N} \prod_{j=1}^{N} P(m_j|n)P_0(n). \tag{3.5.44}$$

Note that the eigenstates of the observable $\hat{n}$ constitute the complete set of the quantum state of interest. From our general arguments before, we can thus interpret the present measurement process as the "wavefunction collapse" of the cavity photon caused by the observation. More specifically, we conclude that a quantum state eventually converges to a particular Fock state, and the distribution of collapsed states obey the Born rule, i.e., it matches with the initial distribution $P_0(n)$ in the Fock basis.

3.6. Continuous quantum measurement

3.6.1. Quantum trajectories. We here focus on a class of quantum measurements known as *continuous* quantum measurement, which is in fact relevant to many physical systems and lies at the heart of theory of Markovian open quantum systems. Consider the indirect measurement model in which the system in the Hilbert space $\mathcal{H}_S$ repeatedly interacts with the meter in $\mathcal{H}_M$ during a short time interval τ (see Fig. 3.6.1). After each interaction, one performs a projective measurement on the meter, obtains a measurement outcome, and resets it to the common state $|\psi_0\rangle_M$; the latter process ensures that the meter retains no memory about previous measurement outcomes. An observer thus obtains information about the measured system through a sequence of measurement outcomes $\{m_1, m_2, \ldots\}$. We assume that each measurement outcome takes a discrete value from $m_i \in \{0, 1, 2, \ldots, M\}$ $(i = 1, 2, \ldots)$.

We start from the system-meter product state

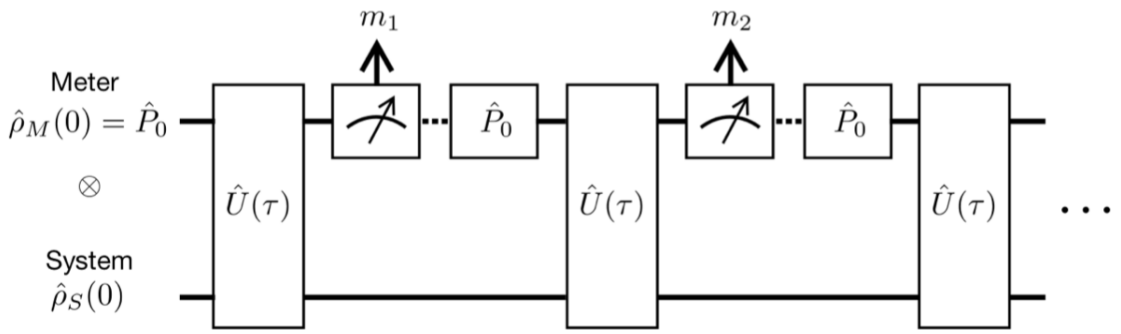

FIGURE 3.6.1. Repeated indirect measurement model.

$$\hat{\rho}_{\rm tot}(0) = \hat{\rho}_S(0) \otimes \hat{P}_0, \quad \hat{P}_0 = |\psi_0\rangle_{MM}\langle\psi_0|, \tag{3.6.1}$$

and assume that the dynamics of the total system is governed by a general Hamiltonian

$$\hat{H} = \hat{H}_S + \hat{V}, \quad \hat{V} = \gamma \sum_{m=1}^{M} \hat{A}_m \otimes \hat{B}_m + \text{H.c.}, \quad \gamma \in \mathbb{R}, \tag{3.6.2}$$

where $\hat{A}_m$ and $\hat{B}_m$ act on $\mathcal{H}_S$ and $\mathcal{H}_M$, respectively. The time scale of $\hat{H}_S$ is assumed to be much longer than τ. We further assume that $\hat{B}_m$ changes the meter state into the subspace of $\mathcal{H}_M$ corresponding to a measurement outcome m, i.e. we impose the relations

$$\hat{P}_{m'}\hat{B}_m = \delta_{m'm}\hat{B}_m \quad (m' = 0, 1, \ldots, M;\ m = 1, 2, \ldots, M), \tag{3.6.3}$$

where $\hat{P}_{m'}$ is a projector onto the subspace of $\mathcal{H}_M$ corresponding to a measurement outcome m'. Note that the reset state is labelled by $m' = 0$. A set of $\hat{P}_{m'}$ satisfies the completeness condition

$$\sum_{m'=0}^{M} \hat{P}_{m'} = \hat{I}. \tag{3.6.4}$$

For each indirect measurement process, there are two possibilities, i.e., either (i) one observes a change in the meter state from the reset state by obtaining an outcome $m = 1, 2, \ldots, M$ or (ii) one observes no change in the state of the meter from the reset state and thus obtains the outcome 0.

In the first case (i), which is often called as the *quantum jump* process, the nonunitary mapping $\mathcal{E}_m$ of the system $\hat{\rho}_S$ corresponding to obtaining an outcome $m = 1, 2, \ldots, M$ is given by

$$\mathcal{E}_m(\hat{\rho}_S) = \mathrm{Tr}_M \left[\hat{P}_m \hat{U}(\tau) \left(\hat{\rho}_S \otimes \hat{P}_0\right) \hat{U}^\dagger(\tau) \hat{P}_m\right] \simeq \tau \hat{L}_m \hat{\rho}_S \hat{L}_m^\dagger, \tag{3.6.5}$$

where we define the total unitary operator $\hat{U}(t) = e^{-i\hat{H}t}$, and Tr_M denotes the trace over the meter. To simplify the expression in the last equality, we here assume the continuous measurement limit:

$$\gamma\tau \ll 1 \text{ while keeping } \gamma^2\tau \text{ finite}. \tag{3.6.6}$$

The operator $\hat{L}_m$ is often called the jump or Lindblad operator and defined by

$$\hat{L}_m = \sqrt{\gamma^2 \tau \langle \hat{B}_m^\dagger \hat{B}_m \rangle_0}\, \hat{A}_m \tag{3.6.7}$$

where $\langle \cdots \rangle_0$ is an expectation value with respect to $|\psi_0\rangle_M$.

In contrast, in the second case (ii) for which one observes no change of the meter state corresponding to the outcome 0, the nonunitary mapping $\mathcal{E}_0$ can be simplified as

$$\mathcal{E}_0(\hat{\rho}_S) = \mathrm{Tr}_M \left[\hat{P}_0 \hat{U}(\tau) \left(\hat{\rho}_S \otimes \hat{P}_0 \right) \hat{U}^\dagger(\tau) \hat{P}_0 \right] \tag{3.6.8}$$

$$\simeq \hat{\rho}_S - i\tau [\hat{H}_S, \hat{\rho}_S] - \frac{\tau}{2} \left\{ \sum_{m=1}^{M} \hat{L}_m^\dagger \hat{L}_m, \hat{\rho}_S \right\} \tag{3.6.9}$$

Clearly, these mappings satisfy the trace-preserving property $\mathrm{Tr}_S[\sum_{m'=0}^{M} \mathcal{E}_{m'}(\hat{\rho}_S)] = 1$.

We next want to formulate this continuous measurement process in the language of stochastic differential equation. To do so, we consider the evolution during a time interval $dt = N\tau$, which is still much shorter than the time scale of the internal dynamics $\hat{H}_S$ but still contains a large number of repetitive interactions with the meter, i.e., $N \gg 1$. The probabilities of observing a change of the meter state scale as

$$p_m = \mathrm{Tr}_S[\mathcal{E}_m(\hat{\rho}_S)] = \tau \mathrm{Tr}_S[\hat{L}_m \hat{\rho}_S \hat{L}_m^\dagger] \sim O((\gamma\tau)^2) \ll 1, \tag{3.6.10}$$

which is negligibly small. Thus, one can assume that such a jump event occurs at most once during each interval dt. Under these conditions, the nonunitary dynamical mappings of the system during the interval dt can be described as

$$\Phi_{m=1,\ldots,M}(\hat{\rho}_S) \equiv \sum_{i=1}^{N} \left(\mathcal{E}_0^{N-i} \circ \mathcal{E}_m \circ \mathcal{E}_0^{i-1} \right)(\hat{\rho}_S) = \hat{M}_m \hat{\rho}_S \hat{M}_m^\dagger + O(dt^2) \tag{3.6.11}$$

$$\Phi_0(\hat{\rho}_S) \equiv \mathcal{E}_0^N(\hat{\rho}_S) = \hat{M}_0 \hat{\rho}_S \hat{M}_0^\dagger + O(dt^2) \tag{3.6.12}$$

Here, we introduce the Kraus operators as

$$\hat{M}_m = \hat{L}_m \sqrt{dt} \quad (m = 1, 2, \ldots, M), \tag{3.6.13}$$

$$\hat{M}_0 = 1 - i\hat{H}_{\mathrm{eff}} dt, \tag{3.6.14}$$

where $\hat{H}_{\mathrm{eff}}$ is an effective non-Hermitian Hamiltonian

$$\hat{H}_{\mathrm{eff}} = \hat{H}_S - \frac{i}{2} \sum_{m=1}^{M} \hat{L}_m^\dagger \hat{L}_m. \tag{3.6.15}$$

An operator $\hat{M}_m$ acts on a quantum state if the jump event with outcome m is observed, which occurs with probability $\mathrm{Tr}_S[\hat{M}_m \hat{\rho}_S \hat{M}_m^\dagger]$. The operator M_0 acts on the state if no jumps are observed during a time interval $[t, t + dt]$, and this no-count process occurs with the probability $\mathrm{Tr}_S[\hat{M}_0 \hat{\rho}_S \hat{M}_0^\dagger]$. Note that

these operators fulfill the completeness condition (aside negligible contributions on the order of $O(dt^2)$):

$$\sum_{m'=0}^{M} \hat{M}_{m'}^{\dagger} \hat{M}_{m'} = \hat{I}_S. \tag{3.6.16}$$

For the sake of simplicity, suppose that the initial state is pure and so is the state $|\psi\rangle_S$ in the course of time evolution. Due to the probabilistic nature of quantum measurement, an appropriate way to formulate the dynamics under measurement is to use a stochastic differential time-evolution equation. We then introduce a discrete random variable dN_m with $m = 1, \ldots, M$, whose mean value is given by

$$\mathbb{E}\left[dN_m\right] = \langle \hat{M}_m^{\dagger} \hat{M}_m \rangle_S = \langle \hat{L}_m^{\dagger} \hat{L}_m \rangle_S dt, \tag{3.6.17}$$

where $\mathbb{E}[\cdot]$ represents the ensemble average over the stochastic process and $\langle \cdots \rangle_S$ denotes an expectation value with respect to a quantum state $|\psi\rangle_S$ of the system. The random variables dN_m satisfy the following stochastic calculus:

$$dN_m dN_n = \delta_{mn} dN_m, \tag{3.6.18}$$

meaning that dN takes either a value of 0 or 1 and thus at most a single jump event can be observed at each time interval dt[4]. The stochastic change of a quantum state $|\psi\rangle_S$ during the time interval $[t, t + dt]$ can now be obtained as

$$|\psi\rangle_S \to |\psi\rangle_S + d|\psi\rangle_S = \left(1 - \sum_{m=1}^{M} dN_m\right) \frac{\hat{M}_0 |\psi\rangle_S}{\sqrt{\langle \hat{M}_0^{\dagger} \hat{M}_0 \rangle_S}} + \sum_{m=1}^{M} dN_m \frac{\hat{M}_m |\psi\rangle_S}{\sqrt{\langle \hat{M}_m^{\dagger} \hat{M}_m \rangle_S}}. \tag{3.6.19}$$

Physically, the first term on the rightmost side describes the no-count process occurring with the probability $1 - \sum_{m=1}^{M} \mathbb{E}[dN_m]$ while the second term describes the detection of a jump process m occurring with a probability $\mathbb{E}[dN_m]$. We note that the denominator in each term is introduced to ensure the normalization of the state vector. We can further rewrite it as

$$d|\psi\rangle_S = \left(-i\hat{H}_{\text{eff}} + \frac{1}{2} \sum_{m=1}^{M} \langle \hat{L}_m^{\dagger} \hat{L}_m \rangle_S\right) dt |\psi\rangle_S + \sum_{m=1}^{M} \left(\frac{\hat{L}_m |\psi\rangle_S}{\sqrt{\langle \hat{L}_m^{\dagger} \hat{L}_m \rangle_S}} - |\psi\rangle_S \right) dN_m. \tag{3.6.20}$$

The first term on the right-hand side describes the non-Hermitian time evolution, in which the factor $\sum_{m=1}^{M} \langle \hat{L}_m^{\dagger} \hat{L}_m \rangle_S / 2$ plays the role of maintaining the normalization of the state vector. The second term describes the state change for the jump event m, where $\hat{L}_m$ acts on the quantum state and causes its discontinuous change. An individual realization of this stochastic differential equation corresponding to a time sequence of specific outcomes is often referred to as the *quantum trajectory*.

3.6.2. Quantum master equation. Taking the ensemble average over all the possible trajectories, one can obtain the differential equation for the nonselective (or unconditional) nonunitary evolution of

[4]Technically, we remark that the stochastic process dN_m is not a simple Poisson process because its intensity depends on a stochastic vector $|\psi\rangle_S$; it is known as a marked point process in the field of stochastic analysis.

density operator. This is known as the master equation in the Gorini-Kossakowski-Sudarshan-Lindblad (GKSL) form. To see this explicitly, let us rewrite the time-evolution equation in the density-operator form $\hat{\rho}_S = |\psi\rangle_{SS}\langle\psi|$:

$$d\hat{\rho}_S = -i\left(\hat{H}_{\rm eff}\hat{\rho}_S - \hat{\rho}_S\hat{H}_{\rm eff}^\dagger\right)dt + \sum_{m=1}^{M}\langle\hat{L}_m^\dagger\hat{L}_m\rangle_S\hat{\rho}_S dt + \sum_{m=1}^{M}\left(\frac{\hat{L}_m\hat{\rho}_S\hat{L}_m^\dagger}{\langle\hat{L}_m^\dagger\hat{L}_m\rangle_S} - \hat{\rho}_S\right)dN_m. \tag{3.6.21}$$

where we take the leading order of $O(dt)$ and use the stochastic calculus. We note that this equation remains valid for a generic density matrix $\hat{\rho}_S$ that is not necessarily pure. Introducing the ensemble-averaged density matrix $\mathbb{E}[\hat{\rho}_S]$ and taking the average over measurement outcomes, one arrives at the GKSL master equation:

$$\frac{d\,\mathbb{E}[\hat{\rho}_S]}{dt} = -i\left(\hat{H}_{\rm eff}\mathbb{E}[\hat{\rho}_S] - \mathbb{E}[\hat{\rho}_S]\hat{H}_{\rm eff}^\dagger\right) + \sum_{m=1}^{M}\hat{L}_m\mathbb{E}[\hat{\rho}_S]\hat{L}_m^\dagger. \tag{3.6.22}$$

The master equation describes the dynamics when no information about measurement outcomes is available to an observer. It can also be applied to analyze dissipative dynamics of a quantum system coupled to a Markovian environment. Roughly speaking, this is because one cannot keep track of all the environmental degrees of freedom and, to describe dissipative dynamics, the best one can do would be to take the trace over them (corresponding to the summation over measurement outcomes above). One can then simplify the dissipative evolution equation of the reduced density matrix $\hat{\rho}_S$ by assuming certain conditions; we will later see sufficient conditions to justify the use of the Markovian description. We note that such conditions are essentially equivalent to the assumptions made in deriving the continuous measurement limit above.

3.6.3. Measurement dynamics vs Dissipation. We have seen that there are two types of dynamics in open quantum systems, namely, conditional or unconditional evolution (also often called selective or nonselective evolution). The conditional dynamics describes the evolution of a quantum system under measurement in the cases when an observer can access information about measurement outcome in some way. In contrast, if measurement outcome is completely unknown, one must take the ensemble average over measurement outcomes, and the dynamics becomes the dissipative one described by the unconditional, Markovian master equation. It is relatively recent development that we have learned that these two types of dynamics can indeed be distinct at both qualitative and quantitative levels, especially in many-body setups, and lead to rich phenomenology in conditional evolution beyond conventional dissipative dynamics.

Here we shall briefly exemplify several classes of such conditional dynamics of continuously measured quantum systems. First of all, we emphasize that an appropriate theoretical description of open quantum dynamics depends on how much information about measurement outcomes is available to an observer. For instance, if one can access the complete information about measurement outcomes, i.e. all the times and types of quantum jumps, the dynamics is described by a single realization of the quantum trajectory:

$$|\psi_{\rm traj}\rangle_S = \prod_{k=1}^{n} \left[\hat{\mathcal{U}}_{\rm eff}(\Delta t_k)\hat{L}_{m_k}\right] \hat{\mathcal{U}}_{\rm eff}(t_1)|\psi_0\rangle_S/\|\cdot\|, \tag{3.6.23}$$

where $0 < t_1 < \cdots < t_n < t$ are the times of quantum jumps whose types are $\{m_1, m_2, \ldots, m_n\}$, $\Delta t_k = t_{k+1} - t_k$ is the time difference with $t_{n+1} \equiv t$, and $\hat{\mathcal{U}}_{\rm eff}(t) = e^{-i\hat{H}_{\rm eff}t}$ is the non-Hermitian time evolution operator. In the context of dissipative systems, this situation may be considered as an ideal case in which one can keep track of all the environmental degrees of freedom.

Meanwhile, even when one cannot access such complete information, we may still have the ability to access partial information about measurement outcomes. One natural situation, which is relevant to certain experiments, is that one can know about the total number of quantum jumps occurring during a certain time interval, but not their types and occurrence times. In such a case, the quantum state is described by the following density matrix conditioned on the number n of quantum jumps that have occurred during a time interval $[0, t]$:

$$\begin{aligned}\hat{\rho}^{(n)}(t) &\propto \sum_{\alpha\in\mathcal{D}_n} |\psi_\alpha\rangle_{SS}\langle\psi_\alpha| \\ &= \sum_{\{m_k\}_{k=1}^n} \int_0^t dt_n \cdots \int_0^{t_2} dt_1 \prod_{k=1}^{n} \left[\hat{\mathcal{U}}_{\rm eff}(\Delta t_k)\hat{L}_{m_k}\right] \hat{\mathcal{U}}_{\rm eff}(t_1)\hat{\rho}_S(0)\hat{\mathcal{U}}_{\rm eff}^\dagger(t_1) \prod_{k=1}^{n} \left[\hat{L}_{m_k}^\dagger \hat{\mathcal{U}}_{\rm eff}^\dagger(\Delta t_k)\right],\end{aligned} \tag{3.6.24}$$

where the ensemble average is taken over the subspace $\mathcal{D}_n$ spanned by all the trajectories having n quantum jumps during $[0, t]$. This is interpreted as coarse-grained dynamics of pure quantum trajectories, where the number of jumps is known while the information about the times and types of jumps are averaged out. The no-jump process $\hat{\rho}^{(0)}(t)$ corresponds to non-Hermitian evolution and is the simplest example of this class of dynamics.

3.6.4. Brief remark on non-Hermitian physics. As we have learned above, dynamics of a quantum system under continuous measurement contains two parts, non-Hermitian evolution and random quantum jumps. Obviously, both of them can be implemented in a numerical calculation, but it is often the case that only the former allows one to resort to analytical/exact theoretical analyses. Such non-Hermitian description can be useful as an effective theoretical tool to understand qualitative physics of open systems. For instance, this is the case when there only exist spontaneous decays or loss processes (but no gain processes) for which phenomena of our interest occur in transient regimes rather than steady states[5]. Otherwise, however, non-Hermitian evolution alone is in general inaccurate and quantum jumps should be included to consistently analyze continuously measured dynamics. Interested students may see the review paper [Adv. Phys. 69, 3 (2020)] and the references therein.

3.6.5. Physical examples.

[5]Technically, this is because, in these lossy systems, the analysis of the Liouvillian of the master equation can significantly be simplified to that of the non-Hermitian operator $\hat{H}_{\rm eff}$, since the Liouvillian possesses the tridiagonal matrix structure and thus shares the same spectral feature with that of $\hat{H}_{\rm eff}$.

Example 1: Photon emission. Let us consider a simple example of photon emission on the basis of the Jaynes-Cummings model (3.1.1) discussed before[6]. The system-meter interaction is

$$\hat{V} \propto \hat{\sigma}^- \hat{b}^\dagger + \hat{\sigma}^+ \hat{b} \tag{3.6.25}$$

and we assume that the reset state is the photon vacuum $|\psi_0\rangle_M = |0\rangle$. The jump operator corresponding to spontaneous emission is

$$\hat{L} = \sqrt{\gamma}\hat{\sigma}^- \tag{3.6.26}$$

and the non-Hermitian effective Hamiltonian is

$$\hat{H}_{\rm eff} = \hat{H}_S - \frac{i\gamma}{2}\hat{\sigma}^+\hat{\sigma}^- = \hat{H}_S - \frac{i\gamma}{2}|e\rangle\langle e|, \tag{3.6.27}$$

which describes the dynamics during the no-count process. We emphasize that, even in the no-count case, an observer actually gains information about the system that no spontaneous emission has been detected. This information acquisition indicates that the system is more likely to be in the ground state than in the excited state. This tendency can be ascribed to the measurement backaction represented by the anti-Hermitian term in $\hat{H}_{\rm eff}$. Meanwhile, when the jump process (described by $\hat{L}_- = \sqrt{\Gamma}\hat{\sigma}^-$) is detected, an observer acquires the information that the system is projected onto the ground state.

Example 2: Damped harmonic oscillator. We next consider a harmonic oscillator as a system of interest, while the meter is also a harmonic oscillator with the reset state chosen to be the ground state $|\psi_0\rangle_M = |0\rangle$. The system-meter interaction is

$$\hat{V} \propto \hat{a}\hat{b}^\dagger + \hat{a}^\dagger \hat{b}. \tag{3.6.28}$$

We can calculate the jump operator as

$$\hat{L} = \sqrt{\gamma}\hat{a}, \tag{3.6.29}$$

which describes the damping of the harmonic oscillator. The corresponding effective non-Hermitian Hamiltonian is

$$\hat{H}_{\rm eff} = \hat{H}_S - \frac{i\gamma}{2}\hat{a}^\dagger\hat{a}. \tag{3.6.30}$$

The unconditional master-equation dynamics is given by

$$\frac{d\,\hat{\rho}}{dt} = -i\omega[\hat{a}^\dagger\hat{a},\hat{\rho}] + \frac{\gamma}{2}\left(2\hat{a}\hat{\rho}\hat{a}^\dagger - \hat{a}^\dagger\hat{a}\hat{\rho} - \hat{\rho}\hat{a}^\dagger\hat{a}\right), \tag{3.6.31}$$

[6]Strictly speaking, photon emission usually arises from interaction between atom and *continuum* photonic modes. We here focus on a single photon mode for the sake of simplicity, and later revisit the related problem in the case of the continuum photon modes.

where we set $\hat{H}_S = \omega \hat{a}^\dagger \hat{a}$. It is a good exercise to check that the expectation value of the oscillator amplitude then exhibits the damping:

$$\frac{da}{dt} \equiv \mathrm{Tr}\left[\hat{a}\frac{d\hat{\rho}}{dt}\right] \to a(t) = a(0)e^{-i\omega t - \gamma t/2}. \tag{3.6.32}$$

Obviously, the steady state is the ground state $\hat{\rho} = |0\rangle\langle 0|$ since there only exists loss process.

Example 3: Lossy many-body systems. Consider a quantum many-body system subject to particle loss processes. The one- or two-body loss processes can effectively be described by the jump operators

$$\hat{L}_{\mathrm{one}}(\boldsymbol{x}) \propto \hat{\Psi}(\boldsymbol{x}), \quad \hat{L}_{\mathrm{two}}(\boldsymbol{x}) \propto \hat{\Psi}(\boldsymbol{x})\hat{\Psi}(\boldsymbol{x}). \tag{3.6.33}$$

The corresponding non-Hermitian Hamiltonian is

$$\hat{H}_{\mathrm{eff}} = \int d\mathbf{x} \left\{ \hat{\Psi}^\dagger(\mathbf{x}) \left[-\frac{\hbar^2\nabla^2}{2m} + V_{\mathrm{r}}(\mathbf{x}) - iV_{\mathrm{i}}(\mathbf{x}) \right] \hat{\Psi}(\mathbf{x}) + \frac{g - i\gamma}{2} \hat{\Psi}^\dagger(\mathbf{x})\hat{\Psi}^\dagger(\mathbf{x})\hat{\Psi}(\mathbf{x})\hat{\Psi}(\mathbf{x}) \right\}, \tag{3.6.34}$$

where $\hat{\Psi}$ ($\hat{\Psi}^\dagger$) is the annihilation (creation) operator of either a fermion or a boson; for the sake of simplicity, we omit spin degrees of freedom. A one-body loss process can be taken into account by an imaginary potential, $-iV_{\mathrm{i}}(\mathbf{x})$, while the two-body loss effectively changes an interaction parameter to a complex value $g - i\gamma$. Suppose that the initial state is an eigenstate of the total particle number $\hat{N} = \int d\mathbf{x}\hat{\Psi}^\dagger(\mathbf{x})\hat{\Psi}(\mathbf{x})$. Then, its expectation value evolves as

$$\frac{dN}{dt} = \frac{d\mathrm{Tr}(\hat{N}\hat{\rho})}{dt} = \frac{1}{i\hbar}\langle \hat{H}_{\mathrm{eff}} - \hat{H}_{\mathrm{eff}}^\dagger \rangle. \tag{3.6.35}$$

Namely, imaginary parts of the eigenvalues of non-Hermitian Hamiltonian directly characterize the loss rate of particles.

It is often useful to describe the system by using tight-binding approximation (especially in ultracold atoms), resulting in

$$H_{\mathrm{eff}} = -J\sum_{m=1}^{N} \left(b_m^\dagger b_{m+1} + \mathrm{H.c.} \right) + \frac{U_{\mathrm{r}} - iU_{\mathrm{i}}}{2} \sum_{m=1}^{N} n_m \left(n_m - 1 \right), \tag{3.6.36}$$

where $\hat{b}_m$ ($\hat{b}_m^\dagger$) is the annihilation (creation) operator of a particle at site m and only a two-body loss is included; an imaginary interaction parameter $-iU_{\mathrm{i}}$ results from two-body loss process. While this model is not exactly solvable, its asymptotically exact spectrum can be obtained by the strong-coupling-expansion analysis in the limit of $U_{\mathrm{r,i}} \gg J$. For instance, the decay rate Γ_{Mott} of the Mott-insulator state at unit filling $\rho = 1$ (i.e., the imaginary part of the corresponding complex eigenvalue) is given by

$$\frac{\Gamma_{\mathrm{Mott}}}{N} = \frac{3J^2U_{\mathrm{i}}}{4\left(U_{\mathrm{r}}^2 + U_{\mathrm{i}}^2\right)}. \tag{3.6.37}$$

Interestingly, the loss rate is suppressed at strong U_{i} as

$$\Gamma_{\mathrm{Mott}} \propto \frac{J^2}{U_{\mathrm{i}}}, \tag{3.6.38}$$

which is known as the *continuous quantum Zeno effect*.

3.6.6. Diffusive limit. We have so far discussed a measurement process in which an operator $\hat{L}_m$ induces a discontinuous change of a quantum state. Below we shall discuss yet another type of continuous measurement associated with a *diffusive* stochastic process.

3.6.6.1. *Wiener process.* To begin with, we introduce the notion of Wiener stochastic process. Roughly speaking, the Wiener process W_t is a continuous random walk that (i) satisfies the initial condition $W_0 = 0$ at $t = 0$ and (2) is a normally distributed random variable with zero mean and width $\sqrt{t}$ at $t > 0$, whose probability distribution is

$$P(W_t, t) = \frac{1}{\sqrt{2\pi t}} e^{-W_t^2/2t}. \tag{3.6.39}$$

We also often denote it by $W_t \in \mathcal{N}(0, t)$. To define its differential, let us first consider the Wiener increment for time interval Δt:

$$\Delta W = W_{t+\Delta t} - W_t, \tag{3.6.40}$$

which has a normal distribution with the following mean and variance:

$$E[\Delta W] = 0, \quad E[(\Delta W)^2] = \Delta t. \tag{3.6.41}$$

Then, we consider its differential limit $\Delta t \to 0$, which effectively gives the time derivative of the Wiener process that we express by

$$\Delta t \to dt, \quad \Delta W \to dW. \tag{3.6.42}$$

We require that this Wiener differential satisfies the stochastic calculus

$$E[dW] = 0, \quad dW^2 = dt. \tag{3.6.43}$$

The latter is often called Itô rule named after Kiyoshi Itô; this condition is indeed reasonable since the random variable $(\Delta W)^2$ has the mean Δt while its fluctuation becomes negligibly small compared to $O(\Delta t)$ quantity in the limit of $\Delta t \to 0$.

3.6.6.2. *Stochastic Schrödinger equation.* Previously, we arrive at the following stochastic differential equation for a quantum system under measurement (see Eq. (3.6.21)):

$$d\hat{\rho} = -i\left(\hat{H}_{\rm eff}\hat{\rho} - \hat{\rho}\hat{H}_{\rm eff}^\dagger\right)dt + \sum_{m=1}^{M}\langle\hat{L}_m^\dagger\hat{L}_m\rangle\hat{\rho}dt + \sum_{m=1}^{M}\left(\frac{\hat{L}_m\hat{\rho}\hat{L}_m^\dagger}{\langle\hat{L}_m^\dagger\hat{L}_m\rangle} - \hat{\rho}\right)dN_m, \tag{3.6.44}$$

with

$$\hat{H}_{\text{eff}} = \hat{H} - \frac{i}{2}\sum_{m=1}^{M} \hat{L}_m^\dagger \hat{L}_m. \tag{3.6.45}$$

We are here interested in the limit that detection rate of quantum jumps is high while an operator $\hat{L}_m$ only induces an infinitesimally small change of a quantum state. To this end, we assume that measurement backaction induced by $\hat{L}_m$ is weak in the sense that it satisfies

$$\hat{L}_m = \sqrt{\Gamma}(1 + \epsilon \hat{a}_m) \tag{3.6.46}$$

for a Hermitian operator $\hat{a}_m$, where Γ characterizes the detection rate of jump events and $\epsilon \ll 1$ is a small dimensionless parameter. We also assume that detections of jump events are so frequent that the expectation value ΔN_m of the number of jump-m events being observed during a time interval Δt is sufficiently large. From the central-limit theorem, ΔN_m can then be approximated as

$$\Delta N_m \simeq \Gamma(1 + 2\epsilon\langle \hat{a}_m \rangle)\Delta t + \sqrt{\Gamma}\,(1 + \epsilon\langle \hat{a}_m \rangle)\,\Delta W_m, \tag{3.6.47}$$

where $\Delta W_m \in \mathcal{N}(0, \Delta t)$ are the (mutually independent) Wiener increments each of which obeys the normal distribution with the zero mean and the variance Δt. We then take the diffusive measurement limit, i.e., $\epsilon \to 0$ and $\Gamma \to \infty$ while $\Gamma\epsilon^2$ is kept constant. It would be a good Exercise to check that the resulting stochastic differential equation in the limit $\Delta t \to 0$ is given by

$$\begin{aligned} d\hat{\rho} = &\left[-i[\hat{H}, \hat{\rho}] - \frac{1}{2}\sum_{m=1}^{M}\left[\hat{l}_m, \left[\hat{l}_m, \hat{\rho}\right]\right]\right] dt \\ &+ \sum_{m=1}^{M}\left\{\hat{l}_m - \langle \hat{l}_m \rangle, \hat{\rho}\right\} dW_m, \end{aligned} \tag{3.6.48}$$

where we introduce operators $\hat{l}_m = \sqrt{\Gamma\epsilon^2}\,\hat{a}_m$ and the (differential) Wiener stochastic processes that satisfy

$$\mathbb{E}[dW_m] = 0, \;\; dW_m dW_n = \delta_{mn} dt. \tag{3.6.49}$$

When a quantum state is pure, the stochastic time-evolution equation can be rewritten as

$$\begin{aligned} d|\psi\rangle = &\left[-i\hat{H} - \frac{1}{2}\sum_{m=1}^{M}\left(\hat{l}_m - \langle \hat{l}_m \rangle\right)^2\right] dt|\psi\rangle \\ &+ \sum_{m=1}^{M}\left(\hat{l}_m - \langle \hat{l}_m \rangle\right) dW_m|\psi\rangle. \end{aligned} \tag{3.6.50}$$

The stochastic Schrödinger equation with the diffusive process is typically applied to analyze nonunitary dynamics of certain quantum optical systems, such as a cavity under homodyne measurement as well as a quantum particle under continuous position measurement.

3.6.6.3. *Example: continuous position measurement.* As a concrete example of a diffusive continuous measurement, we here consider a single quantum particle subject to continuous position measurement. In this case, the effective "jump" operator corresponds to a position operator:

$$\hat{l} = \sqrt{\kappa}\hat{x}, \tag{3.6.51}$$

resulting in the time-evolution equations:

$$d|\psi\rangle = \left[1 - i\hat{H} - \frac{\kappa}{2}(\hat{x} - \langle\hat{x}\rangle)^2\right] dt|\psi\rangle + \sqrt{\kappa}(\hat{x} - \langle\hat{x}\rangle)dW|\psi\rangle, \tag{3.6.52}$$

$$d\hat{\rho} = \left(-i[\hat{H}, \hat{\rho}] - \frac{\kappa}{2}[\hat{x}, [\hat{x}, \hat{\rho}]]\right) dt + \sqrt{\kappa}\left\{\hat{x} - \langle\hat{x}\rangle, \hat{\rho}\right\} dW. \tag{3.6.53}$$

Suppose that the unitary part is simply governed by the free-particle Hamiltonian:

$$\hat{H} = \frac{\hat{p}^2}{2m}, \tag{3.6.54}$$

and also that the initial state is a Gaussian state with zero mean $\langle\hat{x}\rangle = 0$. It is then a good Exercise to derive the following differential relations of the expectation values:

$$d\langle\hat{x}\rangle = \frac{\langle\hat{p}\rangle}{m}dt + \sqrt{4\kappa}V_x dW \tag{3.6.55}$$

$$d\langle\hat{p}\rangle = 2\sqrt{\kappa}C_{xp}dW \tag{3.6.56}$$

$$dV_x = \frac{2}{m}C_{xp}dt - 4\kappa V_x^2 dt \tag{3.6.57}$$

$$dV_p = \kappa(1 - 4C_{xp}^2)dt \tag{3.6.58}$$

$$dC_{xp} = \frac{V_p}{m}dt - 4\kappa V_x C_{xp}dt \tag{3.6.59}$$

where we define the variances as $V_O \equiv \langle\hat{O}^2\rangle - \langle\hat{O}\rangle^2$ and covariance by $C_{xp} = \langle\{\hat{x}, \hat{p}\}\rangle/2 - \langle\hat{x}\rangle\langle\hat{p}\rangle$, and use Wick's theorem (see also Chapter 4).

These relations explicitly show that the means and variances are decoupled from the higher-order moments. This means that, if the initial state is completely characterized by the moments up to second order, i.e., it is a Gaussian state, a quantum state remains Gaussian during time evolution under measurement. In fact, one can show that, even if the initial state is non-Gaussian, at sufficiently long time, a quantum state reduces to a certain Gaussian state due to the measurement backaction.

One can also calculate the heating rate, i.e., the increase rate of the kinetic energy K:

$$dK \equiv d\left\langle\frac{\hat{p}^2}{2m}\right\rangle = \frac{1}{2m}\left(dV_p + d(\langle\hat{p}\rangle^2)\right) = \frac{1}{2m}\left(\kappa dt + 4\langle\hat{p}\rangle\sqrt{\kappa}C_{xp}\, dW\right) \tag{3.6.60}$$

resulting in

$$\mathbb{E}[K(t)] = K(0) + \frac{\kappa t}{2m}. \tag{3.6.61}$$

This means that the position measurement continuously disturbs momentum and thus causes the inevitable heating that leads to t linear increase of the kinetic energy. Physically, it can be interpreted as, for example, a consequence of recoil energy due to photon scattering when particle position is probed by light scattering, like the one performed in optical microscopy.

Position measurement also induces the decoherence. For the sake of simplicity, consider the infinite mass case $m \to \infty$; then the nonselective evolution simplifies to

$$d\hat{\rho} = -\frac{\kappa}{2}[\hat{x}, [\hat{x}, \hat{\rho}]]dt. \tag{3.6.62}$$

We expand the density operator in the position basis

$$\hat{\rho} = \int dxdy\, |x\rangle\langle y|\, \rho_{xy}, \quad \rho_{xy} \equiv \langle x|\hat{\rho}|y\rangle. \tag{3.6.63}$$

We then see that the position measurement causes the exponential decay of the off-diagonal elements

$$\frac{d\rho_{xy}}{dt} = -\frac{\kappa}{2}\,(x-y)^2\,\rho_{xy}. \tag{3.6.64}$$

Note that the decoherence rate is proportional to the square of the distance between the two elements, namely, macroscopic coherence is fragile against decoherence.

3.7. Master equation from Born-Markov approximations

In the context of continuous quantum measurement, the dynamics is governed by the GKSL master equation when an external observer cannot access to any information about meter degrees of freedom, i.e., measurement outcomes. There, the best one can do is to take the (unbiased) ensemble average over all the possible outcomes, which in turn results in the nonunitary evolution of a density operator; even if the initial state is pure, the irreversible information leaking from the system into meter degrees of freedom (outside the system Hilbert space) results in a mixed state after nonunitary evolution.

In fact, besides quantum measurement, the master-equation description itself is applicable to a certain class of dissipative systems, known as Markovian open systems. Roughly speaking, there one considers a quantum system that is weakly coupled to external environments that possess negligibly small memory. More precisely, the Markovian description is valid when the following approximations can be justified[7]:

(1) Born approximation: System-environment interaction γ is sufficiently weak such that if the total system has no system–environmental correlations at the initial time, an evolved state at a later time must also remain so.

(2) Markov approximation: the environmental correlation time $\tau_{\rm env}$ is much shorter than the relaxation time scale $\tau_{\rm rel}$ of the whole dynamics including both the system and the environment; $\tau_{\rm rel}$

[7]While these conditions are usually well-justified in quantum optics/AMO systems, it is important to keep in mind that this is in general not the case in, for example, condensed matter physics.

can typically be estimated as $\tau_{\rm rel} \propto \Delta/\mu^2$ with Δ being typical level spacing in the internal dynamics of the system and μ being the strength of the system–environment coupling.

(3) "Secular" approximation: there is a time scale separation such that $1/\Delta \ll \tau_{\rm rel}$, which ensures that the jump operators $\hat{L}_m$ in the master equation are time independent.

Building on these approximations, below we shall re-derive the master equation, but at this time starting from a theory of dissipative systems rather than quantum measurement.

We assume that the initial state has no system-environmental correlations:

$$\hat{\rho}_{SE}(0) = \hat{\rho}_S(0) \otimes \hat{\rho}_E, \tag{3.7.1}$$

and describe the total system-environment density operator as $\hat{\rho}_{SE}$ that obeys the unitary evolution:

$$\frac{d\hat{\rho}_{SE}}{dt} = -i[\hat{H}, \hat{\rho}_{SE}], \quad \hat{H} = \hat{H}_S + \hat{H}_E + \hat{H}_{SE}, \tag{3.7.2}$$

where $\hat{H}_S$ ($\hat{H}_E$) acts only on system (environmental) degrees of freedom, and $\hat{H}_{SE}$ is the system-environment interaction. The reduced system density operator is

$$\hat{\rho}(t) \equiv {\rm Tr}_E[\hat{\rho}_{SE}(t)] \tag{3.7.3}$$

and our goal is to show that its dynamics is governed by the GKSL master equation.

To begin with, it is useful to introduce the interaction picture:

$$\hat{\tilde{\rho}}_{SE}(t) = e^{i(\hat{H}_S+\hat{H}_E)t}\hat{\rho}_{SE}(t)e^{-i(\hat{H}_S+\hat{H}_E)t} \tag{3.7.4}$$

$$\hat{\tilde{H}}_{SE}(t) = e^{i(\hat{H}_S+\hat{H}_E)t}\hat{H}_{SE}e^{-i(\hat{H}_S+\hat{H}_E)t}. \tag{3.7.5}$$

Then, the time evolution of the whole system is given by

$$\frac{d\hat{\tilde{\rho}}_{SE}}{dt} = -i[\hat{\tilde{H}}_{SE}, \hat{\tilde{\rho}}_{SE}]. \tag{3.7.6}$$

Integration of this equation from t to $t + \Delta t$ results in

$$\hat{\tilde{\rho}}_{SE}(t+\Delta t) = \hat{\tilde{\rho}}_{SE}(t) - i\int_t^{t+\Delta t} dt'\,[\hat{\tilde{H}}_{SE}(t'), \hat{\tilde{\rho}}_{SE}(t')]. \tag{3.7.7}$$

We iterate this procedure for $\hat{\tilde{\rho}}_{SE}(t')$ one more time and obtain

$$\hat{\tilde{\rho}}_{SE}(t+\Delta t) = \hat{\tilde{\rho}}_{SE}(t) - i\int_t^{t+\Delta t} dt'\,[\hat{\tilde{H}}_{SE}(t'), \hat{\tilde{\rho}}_{SE}(t)] - \int_t^{t+\Delta t} dt' \int_t^{t'} dt''[\hat{\tilde{H}}_{SE}(t'), [\hat{\tilde{H}}_{SE}(t''), \hat{\tilde{\rho}}_{SE}(t'')]] \tag{3.7.8}$$

We now use the Born approximation, which leads to

$$\hat{\tilde{\rho}}_{SE}(t) \simeq \hat{\tilde{\rho}}(t) \otimes \hat{\tilde{\rho}}_E. \tag{3.7.9}$$

When considering the trace over the environment, this results in the following simplification

$$\mathrm{Tr}_E[[\hat{\tilde{H}}_{SE}(t'),\hat{\tilde{\rho}}_{SE}(t)]] \simeq \hat{\tilde{\rho}}(t)\mathrm{Tr}_E[[\hat{\tilde{H}}_{SE}(t'),\hat{\tilde{\rho}}_E]] = \hat{\tilde{\rho}}(t)\mathrm{Tr}_E[[\hat{H}_{SE},\hat{\rho}_E]] = 0. \tag{3.7.10}$$

The last equality can always be attained by absorbing (if any) mean values into the definition of the system Hamiltonian. Physically, this means that there are fluctuations only around zero mean in the system-environment interaction.

To further simplify the analysis, we use the Markov approximation; this allows us to set the intermediate time scale $\tau_{\mathrm{rel}} \gg \Delta t \gg \tau_{\mathrm{env}}$ and thus, at the lowest order of Δt and together with the Born approximation ($\hat{\tilde{\rho}}_{SE}(t'') \simeq \hat{\tilde{\rho}}(t) \otimes \hat{\tilde{\rho}}_E$), leading to

$$\Delta\hat{\tilde{\rho}}(t) \simeq -\int_0^\infty d\tau \int_t^{t+\Delta t} dt'\, \mathrm{Tr}_E\left[[\hat{\tilde{H}}_{SE}(t'),[\hat{\tilde{H}}_{SE}(t'-\tau),\hat{\tilde{\rho}}(t)\otimes\hat{\tilde{\rho}}_E]]\right] \tag{3.7.11}$$

where $\tau \equiv t' - t''$ and we take the range of integration $[0, t'-t] \sim [0,\infty]$ since $\Delta t \gg \tau_{\mathrm{env}}$. This is known as the Redfield equation; we note that it is known that this equation does not in general lead to the positivity map, and the resulting density operators may be nonpositive.

To construct a physically consistent description satisfying the positivity, we employ further simplifications. To this end, we assume that the system-environment interaction satisfies the following conditions:

$$\hat{H}_{SE} = \sum_m \hat{L}_m \otimes \hat{R}_m + \mathrm{H.c.}, \tag{3.7.12}$$

$$\hat{\tilde{L}}_m(t) = e^{i\hat{H}_S t}\hat{L}_m e^{-i\hat{H}_S t} = \hat{L}_m e^{-i\omega_m t}, \tag{3.7.13}$$

$$\mathrm{Tr}_E\left[\hat{\tilde{\rho}}_E\hat{\tilde{R}}_m(t_1)\hat{\tilde{R}}_n^\dagger(t_2)\right] = \mathrm{Tr}_E\left[\hat{\tilde{\rho}}_E\hat{\tilde{R}}_m(t_1)\hat{\tilde{R}}_n(t_2)\right] = \mathrm{Tr}_E\left[\hat{\tilde{\rho}}_E\hat{\tilde{R}}_m^\dagger(t_1)\hat{\tilde{R}}_n^\dagger(t_2)\right] = 0. \tag{3.7.14}$$

These conditions are satisfied in typical situations considered in this lecture[8] (see, e.g., Eq. (5.3.49)), while a derivation in a more general setup is possible (see e.g., the textbook by H.-P. Breuer, "The Theory of Open Quantum Systems", Oxford University Press (2007)).

Building on these simplifications, we then use the final condition, the so-called secular condition, which allows us to set the time scale $\tau_{\mathrm{rel}} \gg \Delta t \gg 1/(\omega_m - \omega_n)$, leading to

$$\int_t^{t+\Delta t} dt'\, e^{i(\omega_m-\omega_n)t'} \simeq \Delta t\, \delta_{mn}. \tag{3.7.15}$$

This effectively eliminates the time dependence in the "jump" operators $\hat{\tilde{L}}_m(t)$ acting on the density operator. Altogether, from Eq. (3.7.11), we arrive at

[8] Imagine, for example, a typical situation, for which there only exist energy conserving terms like $\hat{L}_m \propto \hat{a}_m$ with $\hat{R}_m \propto b_m^\dagger$, where $\hat{a}, \hat{b}^\dagger$ are bosonic annihilation/creation operators and $\hat{\rho}_E$ is the vacuum state. Technically, this treatment can be justified when the rotating wave approximation is valid as we see later.

$$\frac{\Delta\hat{\tilde{\rho}}(t)}{\Delta t} \simeq \sum_m \left[C_m \left(\hat{L}_m \hat{\tilde{\rho}}(t) \hat{L}_m^\dagger - \hat{L}_m^\dagger \hat{L}_m \hat{\tilde{\rho}}(t) \right) + \text{H.c.} \right], \tag{3.7.16}$$

where we define

$$C_m \equiv \int_0^\infty d\tau \, e^{i\omega_m \tau} \, \mathrm{Tr}_E \left[\hat{\tilde{\rho}}_E \hat{\tilde{R}}_m^\dagger(\tau) \hat{\tilde{R}}_m(0) \right] = \frac{\gamma_m + i\kappa_m}{2}, \quad \gamma_m, \kappa_m \in \mathbb{R}. \tag{3.7.17}$$

Taking the differential limit $\Delta t \to 0$, we obtain a more familiar form as follows:

$$\frac{d\hat{\rho}}{dt} = -i \left(\hat{H}_{\text{eff}} \hat{\rho}(t) - \hat{\rho}(t) \hat{H}_{\text{eff}}^\dagger \right) + \sum_m \gamma_m \hat{L}_m \hat{\rho}(t) \hat{L}_m^\dagger \tag{3.7.18}$$

with

$$\hat{H}_{\text{eff}} \equiv \hat{H}_S + \hat{\Sigma} - \frac{i}{2} \sum_m \gamma_m \hat{L}_m^\dagger \hat{L}_m, \tag{3.7.19}$$

where the self-energy term $\hat{\Sigma}$ is

$$\hat{\Sigma} = \frac{1}{2} \sum_m \kappa_m \hat{L}_m^\dagger \hat{L}_m. \tag{3.7.20}$$

This term is often called Lamb shift, since it gives an analogue of the vacuum-fluctuation induced energy shifts in the system; we will revisit this point later when we learn about quantum theory of electrodynamics.

3.8. Short remark on the validity of master equation approaches

Before proceeding further, let us make a few remarks on the Markovian master-equation approaches. Firstly, we note that when a system of interest gets strongly correlated with an external environment, the nonvanishing system-environment entanglement in general invalidates the Born-Markov approximations used above. Such a situation is ubiquitous in condensed matter systems (a.k.a quantum impurity problems) and also relevant to certain state-of-the-art AMO systems, such as strongly coupled light-matter systems. In these cases, the master equation approaches are no longer valid, and ideally, one has to explicitly take into account both system and enviromental degrees of freedom on equal footing. Historically, this line of studes date back to the pionering works by Feynman and Vernon or Caldeira and Leggett. For further developments, you may refer to Sec. 4.3.3 of Adv. Phys. 69, 249 (2020) or lecture note that can be found in this link (in Japanese).

Summary of Chapter 3

Section 3.1-3.4 Indirect measurement model, POVM, CPTP map

- In the indirect measurement model, a projection measurement is performed on meter that interacts with a system of interest. The measurement operators $\left\{\hat{M}_{m,k}\right\}$ acting on a density operator of the system, $\hat{\rho} \to \sum_k \hat{M}_{m,k}\hat{\rho}\hat{M}_{m,k}^\dagger$, are in general nonorthogonal and called Kraus operators. The probability distribution p_m of measurement outcome m is characterized by the positive operator-valued measure (POVM): $\hat{E}_m = \sum_k \hat{M}_{m,k}^\dagger \hat{M}_{m,k}$ and $p_m = \mathrm{Tr}[\hat{E}_m\hat{\rho}]$.
- Consider a linear mapping $\mathcal{E}$ between density operators on part of the whole Hilbert space. To ensure that $\mathcal{E}$ gives physically reasonable time evolution (the target vector $\mathcal{E}(\hat{\rho})$ can indeed be interpreted as a density operator), we must make it completely positive and trace-preserving (CPTP) map.
- For any CPTP map $\mathcal{E}$, one can construct an indirect measurement model in such a way that its nonselective evolution matches with $\mathcal{E}$. In other words, $\mathcal{E}$ always permits Stinespring representation, $\mathcal{E}(\hat{\rho}) = \mathrm{Tr}_A[\hat{U}(\hat{\rho}\otimes\hat{\rho}_A)\hat{U}^\dagger]$, or Kraus representation $\mathcal{E}(\hat{\rho}) = \sum_\alpha \hat{M}_\alpha\hat{\rho}\hat{M}_\alpha^\dagger$.

Section 3.5 Bayesian inference and QND measurement

- If a measurement process satisfies the diagonal condition (both POVM and Kraus operators can be diagonalized by the same basis), the probability distribution of the postmeasurement state in this basis satisfies Bayes' relation.
- A quantum nondemolition (QND) measurement is a measurement process that does not alter the statistics of a certain observable even after the measurement.
- Since a QND measurement satisfies the diagonal condition, the probability distribution satisfies Bayes' theorem in the eigenbasis of the QND observable $\hat{X}$. After many repetitions of measurements, a quantum state eventually converges to a particular eigenstate $\hat{X}$, and the distribution of those "collapsed" states obey the Born rule (it is given by the initial distribution in the eigenbasis of $\hat{X}$).

Section 3.6 Continuous quantum measurement

- Taking the weak and frequent limit of the repeated indirect measurement model, the dynamics of measured system can be described by the stochastic Schrödinger equation. Each realization of this stochastic equation is called quantum trajectory.
- The stochastic dynamics consists of two parts, deterministic non-Hermitian evolution and random events causing discrete state changes often called quantum jumps.
- Upon the ensemble average over all the possible trajectories, the nonselective evolution is given by the GKSL master equation. This master equation can also be derived from the Born-Markov approximations.
- When the detection rate of quantum jumps is high but their influences are weak, one can replace the stochastic process by the Wiener process.

3.9. Exercises

Exercise 3.1 (Continuous position measurement: 2 points). Consider a single particle subject to continuous position measurement

$$d|\psi\rangle = \left[-i\hat{H} - \frac{\kappa}{2}(\hat{x} - \langle\hat{x}\rangle)^2\right] dt|\psi\rangle + \sqrt{\kappa}(\hat{x} - \langle\hat{x}\rangle)dW|\psi\rangle \tag{3.9.1}$$

with the Hamiltonian

$$\hat{H} = \frac{\hat{p}^2}{2m} + V(\hat{x}). \tag{3.9.2}$$

Using the Itô calculus, derive the following time evolution equation for a density operator

$$d\hat{\rho} = \left(-i[\hat{H}, \hat{\rho}] - \frac{\kappa}{2}[\hat{x}, [\hat{x}, \hat{\rho}]]\right) dt + \sqrt{\kappa}\left\{\hat{x} - \langle\hat{x}\rangle, \hat{\rho}\right\} dW. \tag{3.9.3}$$

Next, suppose that the initial state is a Gaussian state (i.e., a state that is fully characterized by the moments up to the second order) with zero mean $\langle\hat{x}\rangle = 0$. Derive the time evolution equations for the mean values $\langle\hat{x}\rangle$, $\langle\hat{p}\rangle$ and $V_{x,p}$, C_{xp} in the case of $V(x) = m\omega^2 x^2/2$. Show that the state remains a Gaussian state during the time evolution. Explain why this is in general not the case for a non-harmonic potential.

Finally, derive the time evolution equation of the following Wigner function in the case of the harmonic potential

$$W(x,p) \equiv \frac{1}{2\pi}\int_{-\infty}^{\infty} dy\, e^{ipy}\langle x + y/2|\mathbb{E}[\hat{\rho}]|x - y/2\rangle, \tag{3.9.4}$$

and discuss its relation to the Fokker-Planck equation.

Exercise 3.2 (Continuous measurement of indistinguishable particles: 2 points). Consider two noninteracting particles trapped in the harmonic potential, where the single-particle Hamiltonian is given by $\hat{H} = \hat{p}^2/2m + m\omega^2 x^2/2$. The particles are either distinguishable particles or identical bosons/fermions of mass m. First, calculate the particle squared distance $\langle(x_1 - x_2)^2\rangle$ for each case. To simplify the analysis, you may assume that two particles reside in energy eigenstates.

Second, generalize your consideration to the case of two particles under continuous position measurement, and derive the time evolution equation; do the results depend on the distinguishability of the particles? If possible, try to numerically calculate the time evolution of the squared distance $\langle(x_1 - x_2)^2\rangle$ by choosing a certain initial state.

Exercise 3.3 (Completely positivity: 1 point). Give an example of positive, but not completely positive maps acting on a density operator and explain why it is so.

CHAPTER 4

Foundations of quantum optics

4.1. Introduction

Here we shall cover several fundamental concepts of quantum optics and modern quantum science. We start from quantization of the electromagnetic field, introduce Bosonic/Fermionic Gaussian states, learn about variational principles, and briefly review physics of superconducting qubits. These contents not only constitute fundamental building blocks of quantum optics, but also play important roles in a broader context of quantum science, such as condensed matter physics or recent efforts toward applying variational algorithms to Noisy Intermediate-Scale Quantum computer (NISQ).

4.2. Quantization of the electromagnetic field

4.2.1. Classical electromagnetism review. We first review the free evolution of the classical electromagnetic field (i.e., without any couplings to matter degrees of freedom); we will quantize the full light-matter Hamiltonian including matter in the next Chapter.

Our starting point is the following free Maxwell's equations

$$\nabla \cdot \mathbf{E} = 0, \;\; \nabla \cdot \mathbf{B} = 0, \;\; \nabla \times \mathbf{E} = -\partial_t \mathbf{B}, \;\; \nabla \times \mathbf{B} = \frac{1}{c^2}\partial_t \mathbf{E}. \tag{4.2.1}$$

To rewrite these equations, we first note the Helmholtz theorem, which states that a vector field $\mathbf{V}(\mathbf{r})$ can be uniquely decomposed into transverse and longitudinal parts as follows:

$$\mathbf{V}(\mathbf{r}) = \mathbf{V}^{\perp}(\mathbf{r}) + \mathbf{V}^{\parallel}(\mathbf{r}), \tag{4.2.2}$$

$$\nabla \cdot \mathbf{V}^{\perp} = 0, \tag{4.2.3}$$

$$\nabla \times \mathbf{V}^{\parallel} = \mathbf{0}. \tag{4.2.4}$$

This theorem, together with the equations $\nabla \cdot \mathbf{B} = 0$, $\nabla \cdot \mathbf{E} = 0$, and $\nabla \times \mathbf{E} = -\partial_t \mathbf{B}$, lead to the following expressions for some vector field $\mathbf{A}(\mathbf{r}, t)$ (called the vector potential):

$$\mathbf{B} = \mathbf{B}^{\perp} = \nabla \times \mathbf{A} \tag{4.2.5}$$

$$\mathbf{E} = \mathbf{E}^{\perp} = -\partial_t \mathbf{A}^{\perp}. \tag{4.2.6}$$

Decomposing the final equation $\nabla \times \mathbf{B} = \frac{1}{c^2}\partial_t \mathbf{E}$ into transverse and longitudinal parts, we obtain

$$-\nabla^2 \mathbf{A}^{\perp} = \frac{1}{c^2}\partial_t \mathbf{E}^{\perp} = -\frac{1}{c^2}\partial_t^2 \mathbf{A}^{\perp} \tag{4.2.7}$$

for the transverse part, and

$$-\nabla^2 \mathbf{A}^{\parallel} + \nabla(\nabla \cdot \mathbf{A}^{\parallel}) = \mathbf{0} \tag{4.2.8}$$

for the longitudinal part. It is now obvious that the longitudinal part of the vector potential $\mathbf{A}^{\parallel}$ is completely decoupled from dynamical degrees of freedom. Thus, we can always ensure the condition (known as the Coulomb gauge):

$$\mathbf{A}^{\parallel} = \mathbf{0} \iff \nabla \cdot \mathbf{A} = 0. \tag{4.2.9}$$

We assume that this condition will always be satisfied in the following discussions in this Chapter. Altogether, the Maxwell's equations now reduce to the time evolution of the transverse vector field $\mathbf{A} = \mathbf{A}^{\perp}$ (for the sake of notational simplicity, we shall omit $\perp$ from now on)

$$\nabla^2 \mathbf{A} = \frac{1}{c^2} \partial_t^2 \mathbf{A}, \tag{4.2.10}$$

which can be related to the electric and magnetic fields via

$$\mathbf{B} = \nabla \times \mathbf{A}, \;\; \mathbf{E} = -\partial_t \mathbf{A}. \tag{4.2.11}$$

One can check that this equation of motion also follows from the Lagrangian:

$$L = \frac{\epsilon_0}{2} \int d^3 r \left[(\partial_t \mathbf{A})^2 - c^2 (\nabla \times \mathbf{A})^2 \right]. \tag{4.2.12}$$

The canonical momentum is

$$\mathbf{\Pi} \equiv \frac{\delta L}{\delta(\partial_t \mathbf{A})} = \epsilon_0 \partial_t \mathbf{A} = -\epsilon_0 \mathbf{E} \tag{4.2.13}$$

while we get

$$\frac{\delta L}{\delta \mathbf{A}} = -\epsilon_0 c^2 \nabla \times (\nabla \times \mathbf{A}) = \epsilon_0 c^2 \nabla^2 \mathbf{A}, \tag{4.2.14}$$

resulting in the Euler-Lagrange equation

$$\frac{d}{dt} \frac{\delta L}{\delta(\partial_t \mathbf{A})} = \frac{\delta L}{\delta \mathbf{A}} \iff \nabla^2 \mathbf{A} = \frac{1}{c^2} \partial_t^2 \mathbf{A}. \tag{4.2.15}$$

The corresponding Hamiltonian is

$$H = \int d^3 r \, \mathbf{\Pi} \cdot \partial_t \mathbf{A} - L = \int d^3 r \left[\frac{\mathbf{\Pi}^2}{2\epsilon_0} + \frac{\epsilon_0 c^2}{2} (\nabla \times \mathbf{A})^2 \right]. \tag{4.2.16}$$

In terms of the electric and magnetic fields, this is nothing but the well known expression of the total energy of the electromagnetic field:

$$H = \int d^3r \left[\frac{\epsilon_0}{2}\mathbf{E}^2 + \frac{\epsilon_0 c^2}{2}\mathbf{B}^2 \right]. \tag{4.2.17}$$

Using the mode expansion, one can further rewrite this Hamiltonian (which is useful for our purpose of quantization of electromagnetic fields in the next section). To this end, we note that the equation of motion (4.2.15) can be solved by using the ansatz $\mathbf{A}_\omega(\mathbf{r},t) = \mathbf{A}_\omega(\mathbf{r})e^{-i\omega t} + \text{c.c.}$, resulting in the Helmholtz equation:

$$\left(\nabla^2 + \frac{\omega^2}{c^2}\right)\mathbf{A}_\omega(\mathbf{r}) = \mathbf{0}. \tag{4.2.18}$$

A specific eigensolution depends on boundary conditions and let us denote a set of these eigenfrequencies by $\{\omega_n\}$. We can now express a general solution as a linear combination of those eigenmodes:

$$\mathbf{A}(\mathbf{r},t) = \sum_n \alpha_n \mathbf{f}_n(\mathbf{r})e^{-i\omega_n t} + \text{c.c.}, \tag{4.2.19}$$

where α_n are mode amplitudes and $\mathbf{f}_n$ are the orthonormal mode functions satisfying the eigenequation:

$$\left(\nabla^2 + \frac{\omega_n^2}{c^2}\right)\mathbf{f}_n(\mathbf{r}) = \mathbf{0}, \quad \int d^3r\, \mathbf{f}_n^\dagger(\mathbf{r})\mathbf{f}_m(\mathbf{r}) = \delta_{nm}. \tag{4.2.20}$$

It is a good exercise to show that, using these eigenmodes, the Hamiltonian can be rewritten as

$$H = \sum_n \left[\frac{P_n^2}{2\epsilon_0} + \frac{\epsilon_0\omega_n^2}{2}Q_n^2 \right] = \sum_n \epsilon_0\omega_n^2(\alpha_n^*\alpha_n + \alpha_n\alpha_n^*), \tag{4.2.21}$$

where we define

$$Q_n \equiv \alpha_n + \alpha_n^*, \quad P_n \equiv i\epsilon_0\omega_n(\alpha_n^* - \alpha_n). \tag{4.2.22}$$

Note that the free electromagnetic Hamiltonian is equivalent to a collection of independent harmonic oscillators with eigenfrequencies ω_n; we may then regard P_n and Q_n as effective momentum and position variables.

4.2.2. Quantization of electromagnetic fields. The quantization of the electromagnetic field can now be done by promoting classical variables Q_n, P_n to operators $\hat{Q}_n, \hat{P}_n$ and assuming the following commutation relations:

$$[\hat{Q}_n, \hat{P}_m] = i\hbar\delta_{nm}. \tag{4.2.23}$$

This is equivalent to the following replacement of the amplitude variables by the annihilation operators obeying the commutation relation:

$$\alpha_n \to \sqrt{\frac{\hbar}{2\epsilon_0\omega_n}}\hat{a}_n, \quad [\hat{a}_n, \hat{a}_m^\dagger] = \delta_{nm}. \tag{4.2.24}$$

The quantized Hamiltonian is

$$\hat{H} = \sum_n \hbar\omega_n \left(\hat{a}_n^\dagger \hat{a}_n + \frac{1}{2}\right), \tag{4.2.25}$$

from which it is now clear that the excitations of the quantum electromagnetic field correspond to elementary (i.e., particle-like) excitations which are called *photons*. The quantized vector field (in the Heisenberg representation) is expressed by

$$\hat{\mathbf{A}}(\mathbf{r}, t) = \sum_n \sqrt{\frac{\hbar}{2\epsilon_0\omega_n}} \left(\mathbf{f}_n(\mathbf{r})\hat{a}_n e^{-i\omega_n t} + \text{H.c.}\right). \tag{4.2.26}$$

This is a general expression that holds true for arbitrary boundary conditions.

It is useful to consider the case of free space that corresponds to imposing the periodic boundary conditions in a box of volume $V = L^3$. Since the vector potential is transverse, it contains two independent polarization modes $\lambda = 1, 2$ other than the wavevector $\mathbf{k}$ and each eigenmode is labeled by

$$n \to (\mathbf{k}, \lambda). \tag{4.2.27}$$

The photon operators and the mode functions thus obey

$$[\hat{a}_{\mathbf{k}\lambda}, \hat{a}_{\mathbf{k}'\lambda'}^\dagger] = \delta_{\mathbf{k}\mathbf{k}'}\delta_{\lambda\lambda'}, \tag{4.2.28}$$

$$\mathbf{f}_{\mathbf{k}\lambda}(\mathbf{r}) = \frac{1}{\sqrt{V}}\boldsymbol{\epsilon}_{\mathbf{k}\lambda}e^{i\mathbf{k}\cdot\mathbf{r}}, \quad \omega_{\mathbf{k}} = ck, \tag{4.2.29}$$

$$\mathbf{k}\cdot\boldsymbol{\epsilon}_{\mathbf{k}\lambda} = 0, \quad k_\alpha = \frac{2\pi n_\alpha}{L}, \quad n_\alpha \in \mathbb{Z}, \quad \alpha \in \{x, y, z\}. \tag{4.2.30}$$

Note that the mode functions satisfy the orthonormal relation:

$$\int dV\ \mathbf{f}_{\mathbf{k}\lambda}^\dagger \cdot \mathbf{f}_{\mathbf{k}'\lambda'} = \delta_{\mathbf{k}\mathbf{k}'}\delta_{\lambda\lambda'}. \tag{4.2.31}$$

The vector potential (4.2.26) can then be obtained by

$$\hat{\mathbf{A}}(\mathbf{r}, t) = \sum_{\mathbf{k}\lambda} \sqrt{\frac{\hbar}{2\epsilon_0\omega_{\mathbf{k}}V}} \left(\boldsymbol{\epsilon}_{\mathbf{k}\lambda}\hat{a}_{\mathbf{k}\lambda}e^{i\mathbf{k}\cdot\mathbf{r} - i\omega_{\mathbf{k}}t} + \text{H.c.}\right). \tag{4.2.32}$$

Let $\mathbf{e}_\alpha$ be the unit vector in the direction $\alpha \in \{x, y, z\}$. It is often useful to note the relation

$$\sum_\lambda (\boldsymbol{\epsilon}_{\mathbf{k}\lambda}\cdot\mathbf{e}_\alpha)(\boldsymbol{\epsilon}_{\mathbf{k}\lambda}\cdot\mathbf{e}_\beta) = \delta_{\alpha\beta} - \frac{k_\alpha k_\beta}{|\mathbf{k}|^2}, \tag{4.2.33}$$

which follows from the fact that the left hand side represents the projection onto the subspace spanned by the transverse vector fields. Another useful relation can be obtained in the thermodynamic limit $V \to \infty$, where the summation is replaced by the integral

$$\frac{1}{V}\sum_{\mathbf{k}} \to \int \frac{d^3k}{(2\pi)^3}. \tag{4.2.34}$$

This induces the replacements of the annihilation/creation operators and their commutation relation as follows:

$$\hat{a}_{\mathbf{k}\lambda} \to \frac{1}{\sqrt{V}}\hat{a}_{\mathbf{k}\lambda}, \tag{4.2.35}$$

$$[\hat{a}_{\mathbf{k}\lambda}, \hat{a}^\dagger_{\mathbf{k}'\lambda'}] = \delta_{\mathbf{k}\mathbf{k}'}\delta_{\lambda\lambda'} \to [\hat{a}_{\mathbf{k}\lambda}, \hat{a}^\dagger_{\mathbf{k}'\lambda'}] = (2\pi)^3\delta(\mathbf{k}-\mathbf{k}')\delta_{\lambda\lambda'}. \tag{4.2.36}$$

4.2.3. Commutation relations of quantized fields. We can use the relations in the previous section to derive the commutation relations of quantized fields in free space. To demonstrate this, we here consider the following commutation relation between $\hat{\mathbf{A}}$ and $\hat{\mathbf{E}}$:

$$\begin{aligned}[\hat{A}_\alpha(\mathbf{r},t), -\epsilon_0\hat{E}_\beta(\mathbf{r}',t)] &= \frac{i\hbar}{2}\sum_{\mathbf{k}\lambda}((\mathbf{f}_{\mathbf{k}\lambda})_\alpha(\mathbf{f}^*_{\mathbf{k}\lambda})_\beta + \text{c.c.}) \\ &= \frac{i\hbar}{2}\int\frac{d^3k}{(2\pi)^3}\left(\delta_{\alpha\beta} - \frac{k_\alpha k_\beta}{k^2}\right)e^{i\mathbf{k}\cdot(\mathbf{r}-\mathbf{r}')} + \text{c.c.}.\end{aligned} \tag{4.2.37}$$

Using the formula of the transverse delta function:

$$\int\frac{d^3k}{(2\pi)^3}\left(\delta_{\alpha\beta} - \frac{k_\alpha k_\beta}{k^2}\right)e^{i\mathbf{k}\cdot\mathbf{r}} = \frac{2}{3}\delta_{\alpha\beta}\delta(\mathbf{r}) - \frac{1}{4\pi r^3}\left(\delta_{\alpha\beta} - \frac{3r_\alpha r_\beta}{r^2}\right) \equiv \delta^\perp_{\alpha\beta}(\mathbf{r}), \tag{4.2.38}$$

we get

$$[\hat{A}_\alpha(\mathbf{r},t), -\epsilon_0\hat{E}_\beta(\mathbf{r}',t)] = i\hbar\delta^\perp_{\alpha\beta}(\mathbf{r}-\mathbf{r}'). \tag{4.2.39}$$

While these operators appear to behave as the position-like operator $\hat{\mathbf{A}}$ and the momentum-like operator $\hat{\mathbf{\Pi}} = -\epsilon_0\mathbf{E}$ as inferred from the Lagrangian above, we must keep in mind that the Coulomb-gauge constraint $\nabla\cdot\hat{\mathbf{A}} = 0$ restricts the vector variables into the transverse subspace. This fact leads to the above unusual commutation relation with the modified, transverse delta function. In the wavevector space, one can check that this relation is equivalent to the commutation relation for the transverse modes corresponding to $[\hat{a}_{\mathbf{k}\lambda}, \hat{a}^\dagger_{\mathbf{k}'\lambda'}] = \delta_{\mathbf{k}\mathbf{k}'}\delta_{\lambda\lambda'}$, while the longitudinal parts vanish due to the the Coulomb-gauge constraint.

It is also notable that the commutator (4.2.39) is nonvanishing even at $|\mathbf{r}-\mathbf{r}'| \neq 0$ that lies outside the light cone. However, in fact one can show that all the equal-time commutators among $\hat{\mathbf{E}}$ and $\hat{\mathbf{B}}$ vanish at different positions, which ensure the causality (see Exercise). This indicates that the vector potential $\hat{\mathbf{A}}$ itself is not a *local* observable (although its global property may lead to observable effects such as the Aharonov-Bohm effect).

4.3. Bosonic Gaussian states

Theory of Bosonic Gaussian states allows us to fully characterize time evolution of the free quantized electromagnetic modes discussed in the previous section from a general perspective and thus play an important role in quantum optics, especially in the context of photonic quantum computation. We here introduce some basic concepts of Bosonic Gaussian states starting from a single-mode case and also discuss its application to a quantum many-body system.

4.3.1. Introduction: single mode. To understand the notion of Gaussian states, we first consider a single-mode case whose position and momentum operators are defined by (see also Sec. 2.5 in Chapter 2):

$$\hat{x} = \hat{a} + \hat{a}^\dagger, \quad \hat{p} = i(\hat{a}^\dagger - \hat{a}), \tag{4.3.1}$$

$$[\hat{x}, \hat{p}] = 2i, \quad [\hat{a}, \hat{a}^\dagger] = 1. \tag{4.3.2}$$

The vacuum state $|0\rangle$ of this mode is defined by

$$\hat{a}|0\rangle = 0. \tag{4.3.3}$$

The Gaussian (pure) state is basically a state that can be obtained from the vacuum by acting the unitary operator $\hat{U}_{\rm GS}$ (called Gaussian unitary) that is an exponential of $\hat{a}, \hat{a}^\dagger$ terms up to second order:

$$|\psi\rangle = \hat{U}_{\rm GS}|0\rangle. \tag{4.3.4}$$

For a single-mode case, a general Gaussian unitary operator can be generated by a combination of three unitary operators (we will later show this statement from a general argument). The first one is a squeezing operator defined by

$$S(r) = e^{\frac{r}{2}(\hat{a}^{\dagger 2} - \hat{a}^2)}, \quad r \in \mathbb{R}, \tag{4.3.5}$$

which acts as

$$\hat{S}^\dagger(r)\hat{a}\hat{S}(r) = \cosh r\hat{a} + \sinh r\hat{a}^\dagger. \tag{4.3.6}$$

As we discussed before, this corresponds to the squeezing along the x/p direction (see Eq. (2.5.23)).

The second one is a phase shift, which corresponds to time evolution governed by the harmonic-oscillator Hamiltonian:

$$\hat{R}(\theta) = e^{i\theta\hat{a}^\dagger\hat{a}}, \quad \theta \in \mathbb{R}. \tag{4.3.7}$$

The final one is the displacement operator

$$\hat{D}(\alpha) = e^{\alpha\hat{a}^\dagger - \alpha^*\hat{a}}, \quad \alpha \in \mathbb{C} \tag{4.3.8}$$

which acts as

$$\hat{D}^\dagger(\alpha)\hat{a}\hat{D}(\alpha) = \hat{a} + \alpha. \tag{4.3.9}$$

A generic single-mode Gaussian state is then given by combining the three operations as follows:

$$|\psi(\alpha,\theta,r)\rangle = \hat{D}(\alpha)\hat{R}(\theta)\hat{S}(r)|0\rangle \tag{4.3.10}$$

$$= e^{\alpha\hat{a}^\dagger - \alpha^*\hat{a}} e^{i\theta\hat{a}^\dagger\hat{a}} e^{\frac{r}{2}(\hat{a}^{\dagger 2} - \hat{a}^2)}|0\rangle. \tag{4.3.11}$$

As noted above, it is now clear that a Gaussian state is constructed by a unitary operator that is an exponential of the function including $\hat{a}, \hat{a}^\dagger$ terms up to second order.

While this is the expression in terms of $\hat{a}, \hat{a}^\dagger$ operators, we will later see that it is useful to switch to the $\hat{x}, \hat{p}$ representation. We first note that the displacement operator in the $\hat{x}, \hat{p}$ representation can be rewritten by using a real vector $\boldsymbol{\xi} \in \mathbb{R}^2$ as

$$\hat{D}_{\boldsymbol{\xi}} \equiv \exp\left[\frac{i}{2}\begin{pmatrix} \hat{x} & \hat{p} \end{pmatrix}\begin{pmatrix} 0 & 1 \\ -1 & 0 \end{pmatrix}\begin{pmatrix} \xi_1 \\ \xi_2 \end{pmatrix}\right] \tag{4.3.12}$$

$$= \exp\left(\frac{i}{2}\hat{\boldsymbol{\phi}}^{\mathrm{T}}\sigma\boldsymbol{\xi}\right). \tag{4.3.13}$$

We here introduce the vector-valued operator $\hat{\boldsymbol{\phi}}$ and the matrix σ by

$$\hat{\boldsymbol{\phi}} = \begin{pmatrix} \hat{x} \\ \hat{p} \end{pmatrix}, \quad \sigma \equiv i\sigma^y = \begin{pmatrix} 0 & 1 \\ -1 & 0 \end{pmatrix}. \tag{4.3.14}$$

The displacement operator acts as

$$\hat{D}_{\boldsymbol{\xi}}^\dagger\hat{\boldsymbol{\phi}}\hat{D}_{\boldsymbol{\xi}} = \hat{\boldsymbol{\phi}} + \boldsymbol{\xi} \iff \hat{D}_{\boldsymbol{\xi}}^\dagger\begin{pmatrix} \hat{x} \\ \hat{p} \end{pmatrix}\hat{D}_{\boldsymbol{\xi}} = \begin{pmatrix} \hat{x} + \xi_1 \\ \hat{p} + \xi_2 \end{pmatrix}. \tag{4.3.15}$$

A generic single-mode Gaussian state can then be expressed by the $\hat{x}, \hat{p}$ representation as follows:

$$|\psi(\phi_1,\phi_2,\theta,r)\rangle = e^{\frac{i}{2}(\hat{x}\phi_2 - \hat{p}\phi_1)} e^{\frac{i\theta}{4}\left(\hat{x}^2 + \hat{p}^2\right)} e^{-\frac{ir}{4}(\hat{x}\hat{p} + \hat{p}\hat{x})}|0\rangle, \tag{4.3.16}$$

$$\phi_1 = 2\mathrm{Re}[\alpha], \quad \phi_2 = 2\mathrm{Im}[\alpha], \quad \phi_{1,2} \in \mathbb{R}. \tag{4.3.17}$$

One can relate four real parameters, $\phi_1, \phi_2, \theta, r$, of a single-mode Gaussian state to its first and second moments of $\hat{\boldsymbol{\phi}}$. On one hand, the mean value of $\hat{\boldsymbol{\phi}}$ is simply obtained by

$$\langle\psi|\hat{\boldsymbol{\phi}}|\psi\rangle = \langle 0|\hat{D}_{\boldsymbol{\phi}}^\dagger\hat{\boldsymbol{\phi}}\hat{D}_{\boldsymbol{\phi}}|0\rangle = \boldsymbol{\phi}, \tag{4.3.18}$$

and thus directly related to the variables $\phi_{1,2}$ in $|\psi\rangle$. On the other hand, the covariance matrix is defined by

$$(\Gamma_\phi)_{\xi\eta} \equiv \frac{1}{2}\langle\psi|\left\{\delta\hat{\phi}_\xi, \delta\hat{\phi}_\eta\right\}|\psi\rangle, \quad \delta\hat{\boldsymbol{\phi}} = \hat{\boldsymbol{\phi}} - \boldsymbol{\phi}, \quad \xi,\eta \in \{1,2\} \tag{4.3.19}$$

and its matrix elements are the functions of the variables θ, r. It is a good Exercise to obtain the expression of Γ_ϕ in terms of θ, r and show the following relation:

$$\chi_\psi(\boldsymbol{\xi}) \equiv \langle\psi|\hat{D}_{\boldsymbol{\xi}}|\psi\rangle = \exp\left[-\frac{1}{8}\boldsymbol{\xi}^{\mathrm{T}}\sigma^{\mathrm{T}}\Gamma_\phi\sigma\boldsymbol{\xi} + \frac{i}{2}\boldsymbol{\phi}^{\mathrm{T}}\sigma\boldsymbol{\xi}\right], \quad \boldsymbol{\xi}\in\mathbb{R}^2. \tag{4.3.20}$$

Here, $\chi_\psi(\boldsymbol{\xi})$ is known as the characteristic function and will play a central role in our discussions of multi-mode Gaussian states below. This equation means that the single-mode bosonic Gaussian state is fully characterized by the Gaussian characteristic function $\chi_\psi(\boldsymbol{\xi})$ whose first and second moments are determined by the mean vector $\boldsymbol{\phi}$ and covariance matrix Γ_ϕ defined in Eqs. (4.3.18) and (4.3.19).

4.3.2. Multiple modes.

Characteristic function. Let us now formulate a general theory of Bosonic Gaussian states with multiple modes. To do so, we denote bosonic annihiliation and creation operators of mode $i\in\{1,2,\ldots,N_b\}$ as $\hat{a}_i$ and $\hat{a}_i^\dagger$, and introduce a vector of the $\hat{x},\hat{p}$ operators by

$$\hat{\boldsymbol{\phi}} = (\hat{x}_1,\hat{x}_2,\ldots,\hat{x}_{N_b},\hat{p}_1,\hat{p}_2,\ldots,\hat{p}_{N_b})^{\mathrm{T}}, \tag{4.3.21}$$

$$\hat{x}_i = \hat{a}_i + \hat{a}_i^\dagger, \quad \hat{p}_i = i\left(\hat{a}_i^\dagger - \hat{a}_i\right), \tag{4.3.22}$$

$$\left[\hat{a}_i,\hat{a}_j^\dagger\right] = \delta_{ij}, \quad [\hat{a}_i,\hat{a}_j] = 0, \quad i,j\in\{1,2,\ldots,N_b\}. \tag{4.3.23}$$

With this definition, the $\hat{x},\hat{p}$ operators (which we represented as a component of the operator-valued vector $\hat{\boldsymbol{\phi}}$) obey the commutation relation

$$\left[\hat{\phi}_\xi,\hat{\phi}_\eta\right] = 2i\sigma_{\xi\eta}, \quad \sigma \equiv i\sigma^y\otimes \mathrm{I}_{N_b} = \begin{pmatrix} 0 & \mathrm{I}_{N_b} \\ -\mathrm{I}_{N_b} & 0 \end{pmatrix}, \quad \xi,\eta\in\{1,2,\ldots,2N_b\}. \tag{4.3.24}$$

The displacement operator, which is also known as the Weyl operator, is characterized by $2N_b$ real variables $\boldsymbol{\xi}$:

$$\hat{D}_{\boldsymbol{\xi}} = e^{\frac{i}{2}\hat{\boldsymbol{\phi}}^{\mathrm{T}}\sigma\boldsymbol{\xi}}, \quad \hat{D}_{\boldsymbol{\xi}}^\dagger\hat{\boldsymbol{\phi}}\hat{D}_{\boldsymbol{\xi}} = \hat{\boldsymbol{\phi}} + \boldsymbol{\xi}, \quad \boldsymbol{\xi}\in\mathbb{R}^{2N_b}. \tag{4.3.25}$$

This operator is complete in the sense that any N_b-mode bosonic many-body operator can be expressed as a certain linear superposition of $\hat{D}_{\boldsymbol{\xi}}$. To represent this more explicitly, we introduce the *characteristic function* of operator $\hat{A}$ by

$$\chi_A(\boldsymbol{\xi}) \equiv \mathrm{Tr}\left[\hat{A}\hat{D}_{\boldsymbol{\xi}}\right]. \tag{4.3.26}$$

Its inverse transformation allows us to express $\hat{A}$ as a linear superposition of the displacement operators:

$$\hat{A} = \int_{\mathbb{R}^{2N_b}} \frac{d^{2N_b}\boldsymbol{\xi}}{(4\pi)^{N_b}}\,\chi_A(\boldsymbol{\xi})\hat{D}_{\boldsymbol{\xi}}^\dagger. \tag{4.3.27}$$

This formula can be shown by using the relation

$$\mathrm{Tr}\left[\hat{D}_{\boldsymbol{\zeta}}\right] = (4\pi)^{N_b}\delta(\boldsymbol{\zeta}). \tag{4.3.28}$$

Thus, there is a one-to-one correspondence between an operator $\hat{A}$ and a complex function χ_A; in this respect, this transformation is sort of the Fourier transformation. In analogy with the Parseval relation in the Fourier analysis, one can show the relation:

$$\mathrm{Tr}\left[\hat{A}\hat{B}\right] = \int_{\mathbb{R}^{2N_b}} \frac{d^{2N_b}\boldsymbol{\xi}}{(4\pi)^{N_b}}\, \chi_A(-\boldsymbol{\xi})\chi_B(\boldsymbol{\xi}). \tag{4.3.29}$$

When an operator is Hermitian, the characteristic function satisfies

$$\chi_A^*(\boldsymbol{\xi}) = \chi_A(-\boldsymbol{\xi}). \tag{4.3.30}$$

Using these relations, the purity of a density operator $\hat{\rho}$ is expressed as

$$\mathrm{Tr}[\hat{\rho}^2] = \int_{\mathbb{R}^{2N_b}} \frac{d^{2N_b}\boldsymbol{\xi}}{(4\pi)^{N_b}}\, \chi_\rho(-\boldsymbol{\xi})\chi_\rho(\boldsymbol{\xi}) = \int_{\mathbb{R}^{2N_b}} \frac{d^{2N_b}\boldsymbol{\xi}}{(4\pi)^{N_b}}\, \left|\chi_\rho(\boldsymbol{\xi})\right|^2. \tag{4.3.31}$$

In fact, from the definition of the characteristic function, one can show that any correlation functions of $\hat{\rho}$ is obtained by certain derivatives of χ_ρ:

$$\mathrm{Tr}\left[\hat{\rho}\left[\hat{x}_1^{p_1}\cdots\hat{x}_{N_b}^{p_{N_b}}\hat{p}_1^{q_1}\cdots\hat{p}_{N_b}^{q_{N_b}}\right]_{\mathcal{S}}\right] \tag{4.3.32}$$

$$= 2^{\sum_i q_i+p_i} i^{\sum_i q_i - p_i}\, \frac{\partial^{q_1}}{\partial\xi_1^{q_1}}\cdots\frac{\partial^{q_{N_b}}}{\partial\xi_{N_b}^{q_{N_b}}}\frac{\partial^{p_1}}{\partial\xi_{1+N_b}^{p_1}}\cdots\frac{\partial^{p_{N_b}}}{\partial\xi_{2N_b}^{p_{N_b}}}\bigg|_{\boldsymbol{\xi}=\mathbf{0}} \chi_\rho(\boldsymbol{\xi}) \tag{4.3.33}$$

Here, $[\cdots]_{\mathcal{S}}$ is the totally symmetric ordering; for example, $[\hat{x}_i\hat{p}_j]_{\mathcal{S}} = (\hat{x}_i\hat{p}_j + \hat{p}_j\hat{x}_i)/2$ (see Exercise for a useful formula to simplify its calculation). It is also noteworthy that the *Wigner function* gives alternative expression of the characteristic function, which is defined by the Fourier transformation as follows:

$$W(\boldsymbol{\zeta}) = \int_{\mathbb{R}^{2N_b}} \frac{d^{2N_b}\boldsymbol{\xi}}{(4\pi)^{2N_b}} e^{-\frac{i}{2}\boldsymbol{\zeta}^{\mathrm{T}}\sigma\boldsymbol{\xi}}\chi(\boldsymbol{\xi}). \tag{4.3.34}$$

Bosonic Gaussian states. We call $\hat{\rho}_{\mathrm{G}}$ a *Bosonic Gaussian state* when it is completely characterized by the correlation functions up to the second-order moment. In terms of the characteristic function, this definition is equivalent to requiring the following (Gaussian) functional form:

$$\chi_{\rho_{\mathrm{G}}}(\boldsymbol{\xi}) = \exp\left[-\frac{1}{8}\boldsymbol{\xi}^{\mathrm{T}}\sigma^{\mathrm{T}}\Gamma_\phi\sigma\boldsymbol{\xi} + \frac{i}{2}\boldsymbol{\phi}^{\mathrm{T}}\sigma\boldsymbol{\xi}\right], \tag{4.3.35}$$

where χ_{ρ_G} is the characteristic function of a Gaussian state $\hat{\rho}_{\mathrm{G}}$:

$$\hat{\rho}_{\mathrm{G}} = \int_{\mathbb{R}^{2N_b}} \frac{d^{2N_b}\boldsymbol{\xi}}{(4\pi)^{N_b}}\, \chi_{\rho_G}(\boldsymbol{\xi})\hat{D}_{\boldsymbol{\xi}}^\dagger. \tag{4.3.36}$$

Here, a vector-valued displacement variable $\boldsymbol{\phi}$ and a covariance matrix Γ_ϕ characterize the first- and second-order moments of a Gaussian state:

$$\boldsymbol{\phi} = \langle\hat{\boldsymbol{\phi}}\rangle_{\mathrm{G}}, \quad (\Gamma_\phi)_{\xi\eta} = \frac{1}{2}\left\langle\left\{\delta\hat{\phi}_\xi, \delta\hat{\phi}_\eta\right\}\right\rangle_{\mathrm{G}}, \tag{4.3.37}$$

$$\langle\cdots\rangle_{\mathrm{G}} \equiv \mathrm{Tr}[\hat{\rho}_{\mathrm{G}}\cdots], \quad \delta\hat{\boldsymbol{\phi}} = \hat{\boldsymbol{\phi}} - \boldsymbol{\phi}. \tag{4.3.38}$$

The covariance matrix Γ_ϕ contains complete information about two-point correlation functions, such as $\langle\delta\hat{x}\delta\hat{p}\rangle$, $\langle\delta\hat{x}\delta\hat{x}\rangle$ or $\langle\delta\hat{p}\delta\hat{p}\rangle$ type functions. From the definition, it follows that Γ_ϕ is a real-symmetric $2N_b\times 2N_b$ matrix. One can show that it satisfies the following generalized Heisenberg uncertainty relation:

$$\Gamma_\phi + i\sigma \geq 0. \tag{4.3.39}$$

When we use a basis in which Γ_ϕ is diagonal, this relation simplifies to the well-known uncertainty relation for each mode:

$$\left\langle \delta\hat{x}_i^2 \right\rangle \left\langle \delta\hat{p}_i^2 \right\rangle \geq 1. \tag{4.3.40}$$

In fact, the uncertainty relation (4.3.39) itself holds true for arbitrary density operator $\hat{\rho}$ besides a Gaussian state (see Exercise).

A general Bosonic Gaussian state $\hat{\rho}_{\rm G}$ is completely characterized by a set of variables $(\boldsymbol{\phi}, \Gamma_\phi)$ where $\boldsymbol{\phi}$ is arbitrary $2N_b$ dimensional real vector and Γ_ϕ is a real-symmetric $2N_b \times 2N_b$ matrix satisfying the condition (4.3.39). This follows from the fact that, for a given Gaussian state, the relation (4.3.39) is equivalent to the positivity of a density operator $\hat{\rho}_{\rm G} \geq 0$ (see Exercise). We note that the relation (4.3.39) automatically ensures the positivity of covariance matrix $\Gamma_\phi \geq 0$, since Eq. (4.3.39) also indicates $\Gamma_\phi - i\sigma \geq 0$ because of $\sigma = -\sigma^{\rm T}$.

It is sometimes useful to switch to the $\hat{a}, \hat{a}^\dagger$ representation. To this end, we introduce the complex variables by

$$\lambda_i = \frac{\xi_i + i\xi_{i+N_b}}{2}, \quad \lambda_i^* = \frac{\xi_i - i\xi_{i+N_b}}{2}. \tag{4.3.41}$$

Using the vector notation

$$\boldsymbol{\lambda} = (\lambda_1, \lambda_2, \ldots, \lambda_{N_b})^{\rm T}, \quad \hat{\boldsymbol{a}} = (\hat{a}_1, \hat{a}_2, \ldots, \hat{a}_{N_b})^{\rm T}, \tag{4.3.42}$$

the Weyl operator is rewritten as

$$\hat{D}_{\boldsymbol{\lambda}} = e^{\hat{\boldsymbol{a}}^\dagger \boldsymbol{\lambda} - \hat{\boldsymbol{a}}^{\rm T} \boldsymbol{\lambda}^*}. \tag{4.3.43}$$

The $\hat{x}, \hat{p}$ and $\hat{a}, \hat{a}^\dagger$ representations can in general be interchanged by using the following linear transformation:

$$\hat{\boldsymbol{\phi}} = T \begin{pmatrix} \hat{\boldsymbol{a}} \\ \hat{\boldsymbol{a}}^* \end{pmatrix}, \quad T \equiv \begin{pmatrix} {\rm I}_{N_b} & {\rm I}_{N_b} \\ -i{\rm I}_{N_b} & i{\rm I}_{N_b} \end{pmatrix}. \tag{4.3.44}$$

This leads to the following relation that connects the two different expressions of the covariance matrix:

$$\Gamma_b \equiv \left\langle \begin{pmatrix} \delta\hat{\boldsymbol{a}} \\ \delta\hat{\boldsymbol{a}}^* \end{pmatrix} \begin{pmatrix} \delta\hat{\boldsymbol{a}}^\dagger & \delta\hat{\boldsymbol{a}}^{\rm T} \end{pmatrix} \right\rangle_{\rm G} = \frac{1}{2}{\rm I}_{2N_b} + \frac{1}{4} T^\dagger \Gamma_\phi T, \tag{4.3.45}$$

where we denote $\delta\hat{\boldsymbol{a}} = \hat{\boldsymbol{a}} - \langle\hat{\boldsymbol{a}}\rangle_{\rm G}$ and Γ_b is the covariance matrix in the $\hat{a}, \hat{a}^\dagger$ representation and contains complete information about $\langle\delta\hat{a}\delta\hat{a}^\dagger\rangle$, $\langle\delta\hat{a}\delta\hat{a}\rangle$ or $\langle\delta\hat{a}^\dagger\delta\hat{a}^\dagger\rangle$ type functions.

Gaussian unitary operation. We next characterize a set of all the possible unitary operations that map a Gaussian state to another Gaussian state. To do so, we introduce the symplectic group that is defined by a set of real matrix S satisfying

$$S\sigma S^{\mathrm{T}} = \sigma. \tag{4.3.46}$$

Physically, this transformation S represents a linear transformation that keeps the commutation relation (4.3.24). Using a certain S, we can show that the covariance matrix can be diagonalized as (called Williamson decomposition):

$$S\Gamma S^{\mathrm{T}} = \mathrm{diag}\left(\kappa_1, \ldots, \kappa_{N_b}, \kappa_1, \ldots, \kappa_{N_b}\right) \tag{4.3.47}$$

where $1 \leq \kappa_1 \cdots \leq \kappa_{N_b}$ are known as the Williamson eigenvalues. To show this, we rewrite this equality as

$$S = (D \oplus D)^{1/2} O \Gamma^{-1/2} \tag{4.3.48}$$

where O is an orthogonal matrix and $D = \mathrm{diag}(\kappa_1, \ldots, \kappa_{N_b})$. Since S is symplectic, we arrive at

$$O\Gamma^{-1/2}\sigma\Gamma^{-1/2}O^{\mathrm{T}} = \begin{pmatrix} 0 & D^{-1} \\ -D^{-1} & 0 \end{pmatrix}. \tag{4.3.49}$$

This relation says nothing but there exists an orthogonal matrix O that transforms a real antisymmetric matrix, $\Gamma^{-1/2}\sigma\Gamma^{-1/2}$, to a canonical form given in the right-hand side; this is the well-known fact in linear algebra.

Using the Williamson decomposition, we can now characterize arbitrary Gaussian unitary operations. Consider a Gaussian unitary operation that maps a Gaussian state with the mean vector and covariance matrix $(\boldsymbol{\phi}, \Gamma_\phi)$ to another one with $(\boldsymbol{\phi}', \Gamma'_\phi)$. The Williamson decomposition ensures that there exists a symplectic transformation S that relates two covariance matrices:

$$\Gamma'_\phi = S\Gamma_\phi S^{\mathrm{T}}. \tag{4.3.50}$$

As inferred from the definition of Γ_ϕ, this transformation is equivalent to inducing the symplectic transformation onto $\hat{\boldsymbol{\phi}}$ as $S\hat{\boldsymbol{\phi}}$. Meanwhile, the mean vectors can be mapped by simply using the displacement $\boldsymbol{\phi} \to \boldsymbol{\phi}'$. Altogether, we conclude that a Gaussian operation of interest here is induced by a unitary operator acting as

$$\hat{U}^\dagger_{S,\boldsymbol{\Delta}} \hat{\boldsymbol{\phi}} \hat{U}_{S,\boldsymbol{\Delta}} = S\hat{\boldsymbol{\phi}} + \boldsymbol{\Delta}, \quad \boldsymbol{\Delta} = \boldsymbol{\phi}' - S\boldsymbol{\phi}. \tag{4.3.51}$$

Indeed, the transformed state

$$\hat{\rho}'_{\mathrm{G}} = \hat{U}_{S,\boldsymbol{\Delta}} \hat{\rho}_{\mathrm{G}} \hat{U}^\dagger_{S,\boldsymbol{\Delta}} \tag{4.3.52}$$

has the mean vector $\boldsymbol{\phi}' = S\boldsymbol{\phi} + \boldsymbol{\Delta}$ and the covariance matrix $\Gamma'_\phi = S\Gamma_\phi S^{\mathrm{T}}$ by construction.

To obtain a more explicit form of a Gaussian unitary operation $\hat{U}_{S,\boldsymbol{\Delta}}$, we note the fact that a symplectic matrix can be written as

$$S = e^{\sigma R}, \quad R = R^{\mathrm{T}}. \tag{4.3.53}$$

Using this real symmetric matrix R, we can show that the following unitary operator satisfies the required condition (4.3.51):

$$\hat{U}_{S,\boldsymbol{\Delta}} = \exp\left[i\hat{H}_{\boldsymbol{\Delta}}\right] \exp\left[-i\hat{H}_S\right], \ \hat{H}_{\boldsymbol{\Delta}} = \frac{1}{2}\hat{\boldsymbol{\phi}}^{\mathrm{T}}\sigma\boldsymbol{\Delta}, \ \hat{H}_S = \frac{1}{4}\hat{\boldsymbol{\phi}}^{\mathrm{T}}R\hat{\boldsymbol{\phi}}. \tag{4.3.54}$$

We remark that this expression can be regarded as a time evolution governed by "Hamiltonian", $\hat{H}_{\boldsymbol{\Delta}}$, $\hat{H}_S$, that are quadratic in terms of $\hat{x}, \hat{p}$, or equivalently, $\hat{a}, \hat{a}^\dagger$ operators. Conversely, the time evolution induced by any quadratic Hamiltonian can be written in this form by using suitable R and $\boldsymbol{\Delta}$. In particular, one can thus conclude that if an initial state is Gaussian, it remains so during the time evolution governed by a quadratic (i.e., noninteracting) Hamiltonian.

To understand physical meaning of the symplectic transformation S, we can use the Euler/Bloch-Messiah decomposition of S:

$$S = KDL, \tag{4.3.55}$$

where K and L are symplectic and orthogonal real matrices, and D is the following diagonal matrix

$$D = \mathrm{diag}\left(e^{r_1}, e^{r_2}, \ldots, e^{r_{N_b}}, e^{-r_1}, e^{-r_2}, \ldots, e^{-r_{N_b}}\right), \quad r_i \in \mathbb{R}. \tag{4.3.56}$$

Said differently, any symplectic transformation can be decomposed into coordinate transformation (i.e., (generalized) rotation), followed by a squeezing operation of each mode with squeezed parameters $\{r_j\}$, and again followed by another coordinate transformation.

Example: Gaussian pure state. Let us focus on the case of Gaussian *pure* states. From the purity $\mathrm{Tr}[\hat{\rho}_{\mathrm{G}}^2] = 1/\sqrt{\det(\Gamma_\phi)}$ (see Exercise), a Gaussian state is pure if and only if all the Williamson eigenvalues satisfy $\kappa_1 = \ldots = \kappa_{N_b} = 1$. Thus, a covariance matrix for a pure Gaussian state can be decomposed by a symplectic matrix S as

$$\Gamma_\phi = S^{\mathrm{T}}S. \tag{4.3.57}$$

It then follows that

$$(\sigma\Gamma_\phi)^2 = -\mathrm{I}_{2N_b}. \tag{4.3.58}$$

Equivalently, one can consider the relation (4.3.58) as the necessary and sufficient condition for $\hat{\rho}_{\mathrm{G}}$ being pure.

A general pure Gaussian state $\hat{\rho}_{\mathrm{G}} = |\psi\rangle\langle\psi|$, which has mean vector $\boldsymbol{\phi}$ and covariance matrix Γ_ϕ, is obtained by acting a Gaussian unitary operation on the vacuum as

$$|\psi\rangle = \hat{U}_{S,\boldsymbol{\phi}}|0\rangle = e^{\frac{i}{2}\hat{\boldsymbol{\phi}}^{\mathrm{T}}\sigma\boldsymbol{\phi}}e^{-\frac{i}{4}\hat{\boldsymbol{\phi}}^{\mathrm{T}}R\hat{\boldsymbol{\phi}}}|0\rangle, \tag{4.3.59}$$

where $S = e^{\sigma R}$ with $R = R^{\mathrm{T}}$ satisfies $\Gamma_\phi = SS^{\mathrm{T}}$. Indeed, its first-order moment satisfies

$$\langle\hat{\boldsymbol{\phi}}\rangle = \langle 0|\hat{U}_{S,\boldsymbol{\phi}}^\dagger\hat{\boldsymbol{\phi}}\hat{U}_{S,\boldsymbol{\phi}}|0\rangle = \langle 0|S\hat{\boldsymbol{\phi}} + \boldsymbol{\phi}|0\rangle = \boldsymbol{\phi}, \tag{4.3.60}$$

and second-order moment is

$$\frac{1}{2}\left\langle\left\{\delta\hat{\phi}_\xi,\delta\hat{\phi}_\eta\right\}\right\rangle=\frac{1}{2}\left\langle 0\left|\left\{\left(S\delta\hat{\phi}\right)_\xi,\left(S\delta\hat{\phi}\right)_\eta\right\}\right|0\right\rangle=\left(SS^{\mathrm{T}}\right)_{\xi\eta}=\left(\Gamma_\phi\right)_{\xi\eta}. \tag{4.3.61}$$

In particular, when there is only a single mode ($N_b = 1$), the Euler/Bloch-Messiah decomposition leads to

$$S=\begin{pmatrix}\cos\theta & -\sin\theta\\ \sin\theta & \cos\theta\end{pmatrix}\begin{pmatrix}e^r & 0\\ 0 & e^{-r}\end{pmatrix}\begin{pmatrix}\cos\phi & -\sin\phi\\ \sin\phi & \cos\phi\end{pmatrix}. \tag{4.3.62}$$

The first rotation trivially acts on the vacuum, i.e., it does not alter the state. Thus, together with a displacement, a general single-mode Gaussian state is characterized by

$$|\psi(\phi_1,\phi_2,\theta,r)\rangle=e^{\frac{i}{2}(\hat{x}\phi_2-\hat{p}\phi_1)}e^{\frac{i\theta}{4}\left(\hat{x}^2+\hat{p}^2\right)}e^{-\frac{ir}{4}(\hat{x}\hat{p}+\hat{p}\hat{x})}|0\rangle \tag{4.3.63}$$

or in the $\hat{a},\hat{a}^\dagger$ expression

$$|\psi(\alpha,\theta,r)\rangle=e^{\alpha\hat{a}^\dagger-\alpha^*\hat{a}}e^{i\theta\hat{a}^\dagger\hat{a}}e^{\frac{r}{2}\left(\hat{a}^2-\hat{a}^{\dagger 2}\right)}|0\rangle, \tag{4.3.64}$$

as we discussed in the introduction of this Chapter.

4.3.3. Application to weakly interacting BEC. A multi-mode bosonic Gaussian state fully characterizes energy eigenmodes of the free electromagnetic field in arbitrary geometry (i.e., under general boundary conditions). In fact, a bosonic Gaussian state is also very useful in condensed matter physics. As an illustrative example, here we shall apply it to the analysis of a weakly interacting Bose gas at zero temperature. This problem is not exactly solvable and one has to resort to some approximative methods. We review a simple variational theory using a subclass of bosonic Gaussian states, which is actually nothing but the usual Bogoliubov theory (that you may already be familiar with). One advantage of discussing the problem in terms of a Gaussian state is that one can easily generalize the analysis to a wider variational manifold spanned by the whole bosonic Gaussian states as discussed later.

We want to obtain the ground state of a weakly interacting Bose gas:

$$\hat{H}=\int d\boldsymbol{r}\hat{\psi}^\dagger_{\boldsymbol{r}}\left(-\frac{\hbar^2\nabla^2}{2m}\right)\hat{\psi}_{\boldsymbol{r}}+\frac{U}{2}\int d\boldsymbol{r}\hat{\psi}^\dagger_{\boldsymbol{r}}\hat{\psi}^\dagger_{\boldsymbol{r}}\hat{\psi}_{\boldsymbol{r}}\hat{\psi}_{\boldsymbol{r}}. \tag{4.3.65}$$

To begin with, let us consider the noninteracting case $U = 0$; the exact ground state is then obtained as the Bose-Einstein condensate (BEC), in which all the particles occupy the zero momentum single-particle states:

$$|\Psi^{U=0}_{\mathrm{GS}}\rangle\propto\hat{a}^{\dagger N}_{\boldsymbol{k}=\boldsymbol{0}}|\mathrm{vac}\rangle, \tag{4.3.66}$$

where N is the total number of bosons. An essential feature of this state is the presence of the off-diagonal long-range order (ODLRO):

$$\lim_{|\boldsymbol{r}|\to\infty}\langle\hat{\psi}^\dagger_{\boldsymbol{r}}\hat{\psi}_{\boldsymbol{0}}\rangle=\frac{N}{V}\neq 0. \tag{4.3.67}$$

The central idea of variational analysis is to use a simpler variational state that still captures the essential physical feature expected in the exact ground state. When considering (noninteracting) BEC, a natural choice is the coherent state:

$$|\Psi_{\rm var}^{U=0}\rangle = e^{\sqrt{N}\left(\hat{a}_{\boldsymbol{k}=\boldsymbol{0}}^\dagger - \hat{a}_{\boldsymbol{k}=\boldsymbol{0}}\right)}|{\rm vac}\rangle, \tag{4.3.68}$$

which clearly has nonvanishing ODLRO and thus keeps the essential feature of the present case. An advantage of using a coherent state is that it can often significantly simplify the theoretical analysis in more complex problems; while this state is not an eigenstate of the particle number, one can neglect its fluctuation in the thermodynamic limit. Even in mesoscopic regimes (say, $N \sim O(10^2)$), we will later see that the expectation value of the total particle number $\hat{N}$ can be exactly conserved during the variational time evolution. In this sense, one can consistently take into account the particle conservation into theory even if a variational state is not a particle-number eigenstate.

Building on this observation, we next switch on a weakly repulsive interaction $U > 0$. We expect that the ground state should be expressed by slightly modifying the noninteracting variational state $|\Psi_{\rm var}^{U=0}\rangle$. More specifically, the interaction should "excite" a certain amount of zero-momentum bosons leading to the suppressed condensate particle number $N_0 < N$. Because of the momentum conservation, the "excited" bosons must behave as a creation of a pair of particles with momentum $\boldsymbol{k}$ and $-\boldsymbol{k}$. This physical intuition leads to the following variational form for the interacting ground state

$$|\Psi_{\rm var}^{U>0}\rangle = e^{\sum_{\boldsymbol{k}\neq\boldsymbol{0}} \frac{r_{\boldsymbol{k}}}{2}\left(\hat{a}_{\boldsymbol{k}}\hat{a}_{-\boldsymbol{k}} - \hat{a}_{\boldsymbol{k}}^\dagger\hat{a}_{-\boldsymbol{k}}^\dagger\right)} e^{\sqrt{N_0}\left(\hat{a}_{\boldsymbol{k}=\boldsymbol{0}}^\dagger - \hat{a}_{\boldsymbol{k}=\boldsymbol{0}}\right)}|{\rm vac}\rangle, \tag{4.3.69}$$

which spans a certain subspace within the whole Bosonic Gaussian states. We then consider the squeezing parameters $r_{\boldsymbol{k}}$ as variational parameters determined by minimizing the expectation value of total energy.

In fact, this whole discussion is equivalent to the standard Bogoliubov theory. To see this, following the usual mean-field treatment, we expand as $\hat{a}_{\boldsymbol{k}} = \sqrt{N_0}\delta_{\boldsymbol{k},\boldsymbol{0}} + \delta\hat{a}_{\boldsymbol{k}}$ and neglect the higher order terms of $\delta\hat{a}$, leading to the mean-field Hamiltonian

$$\hat{H}_{\rm MF} = \frac{nUN}{2} + \sum_{\boldsymbol{k}\neq\boldsymbol{0}}\left[\left(\epsilon_{\boldsymbol{k}} + nU\right)\hat{a}_{\boldsymbol{k}}^\dagger\hat{a}_{\boldsymbol{k}} + \frac{nU}{2}\left(\hat{a}_{\boldsymbol{k}}^\dagger\hat{a}_{-\boldsymbol{k}}^\dagger + \hat{a}_{\boldsymbol{k}}\hat{a}_{-\boldsymbol{k}}\right)\right], \quad n = \frac{N}{V}. \tag{4.3.70}$$

Since this is a quadratic Hamiltonian, we can diagonalize it by the Bogoliubov transformation

$$\hat{b}_{\boldsymbol{k}} = \cosh r_{\boldsymbol{k}}\hat{a}_{\boldsymbol{k}} + \sinh r_{-\boldsymbol{k}}\hat{a}_{-\boldsymbol{k}}^\dagger = \hat{U}^\dagger\hat{a}_{\boldsymbol{k}}\hat{U}, \tag{4.3.71}$$

$$\hat{U} = e^{-\sum_{\boldsymbol{k}\neq\boldsymbol{0}} \frac{r_{\boldsymbol{k}}}{2}\left(\hat{a}_{\boldsymbol{k}}\hat{a}_{-\boldsymbol{k}} - \hat{a}_{\boldsymbol{k}}^\dagger\hat{a}_{-\boldsymbol{k}}^\dagger\right)}, \tag{4.3.72}$$

where the squeezing parameters are given by

$$\sinh 2r_{\boldsymbol{k}} = \frac{nU}{\sqrt{\epsilon_{\boldsymbol{k}}\left(\epsilon_{\boldsymbol{k}} + 2nU\right)}}. \tag{4.3.73}$$

The resulting diagonalized mean-field Hamiltonian is

$$\hat{H}_{\rm MF} = {\rm const.} + \sum_{\boldsymbol{k}\neq\boldsymbol{0}}\sqrt{\epsilon_{\boldsymbol{k}}\left(\epsilon_{\boldsymbol{k}} + 2nU\right)}\hat{b}_{\boldsymbol{k}}^\dagger\hat{b}_{\boldsymbol{k}}. \tag{4.3.74}$$

Its ground state is given by the squeezed vacuum $|\mathrm{vac}\rangle_{b_{\boldsymbol{k}\neq\boldsymbol{0}}} = \hat{U}^\dagger|\mathrm{vac}\rangle$. Together with the BEC part, we can now write the mean-field ground state as

$$|\Psi_{\mathrm{MF}}^{U>0}\rangle = |\mathrm{vac}\rangle_{b_{\boldsymbol{k}\neq\boldsymbol{0}}}|\mathrm{BEC}_{\boldsymbol{k}=\boldsymbol{0}}^{N_0}\rangle, \tag{4.3.75}$$

$$= e^{\sum_{\boldsymbol{k}\neq\boldsymbol{0}}\frac{r_{\boldsymbol{k}}}{2}\left(\hat{a}_{\boldsymbol{k}}\hat{a}_{-\boldsymbol{k}}-\hat{a}_{\boldsymbol{k}}^\dagger\hat{a}_{-\boldsymbol{k}}^\dagger\right)}\, e^{\sqrt{N_0}\left(\hat{a}_{\boldsymbol{k}=\boldsymbol{0}}^\dagger-\hat{a}_{\boldsymbol{k}=\boldsymbol{0}}\right)}|\mathrm{vac}\rangle, \tag{4.3.76}$$

which is nothing but the above Gaussian variational state (4.3.69).

We argued that one advantage of using variational states is that one can significantly simplify the theoretical analysis. In the present context, this can be inferred from, for example, the following factorization when evaluating the expectation value of the interaction term:

$$\sum_{\boldsymbol{k},\boldsymbol{p},\boldsymbol{q}}\left\langle\hat{a}_{\boldsymbol{k}+\boldsymbol{q}}^\dagger\hat{a}_{\boldsymbol{p}-\boldsymbol{q}}^\dagger\hat{a}_{\boldsymbol{k}}\hat{a}_{\boldsymbol{p}}\right\rangle \simeq N_0^2 + N_0\sum_{\boldsymbol{k}\neq\boldsymbol{0}}\left(4\left\langle\hat{a}_{\boldsymbol{k}}^\dagger\hat{a}_{\boldsymbol{k}}\right\rangle + \left\langle\hat{a}_{\boldsymbol{k}}^\dagger\hat{a}_{-\boldsymbol{k}}^\dagger\right\rangle + \langle\hat{a}_{\boldsymbol{k}}\hat{a}_{-\boldsymbol{k}}\rangle\right). \tag{4.3.77}$$

Note that the right-hand side only contains second-order correlation functions that are completely characterized by a Gaussian state. Then, the procedure of minimizing the variational energy $\langle\hat{H}\rangle_{\mathrm{var}}$ with respect to $\{r_{\boldsymbol{k}}\}$ can also be considered as the optimization of the covariance matrix Γ_ϕ of a Gaussian state for minimizing a loss function $\langle\hat{H}\rangle_{\mathrm{var}}$. We will develop a general variational formalism along this line later.

4.4. Fermionic Gaussian states

Coherent state, or more generally, Gaussian state is historically discussed mainly in the context of bosonic systems. One can in fact introduce similar notions also in the case of fermionic states as we discuss in this section. Similar to bosonic cases, the Fermionic Gaussian states lie at the heart of such standard mean-field theory as Hartree-Fock method or Bardeen-Cooper-Schrieffer (BCS) theory of superconductors.

4.4.1. Introduction: single mode. As an introduction, we first consider the single-mode case of spin-1/2 fermion. The annihilation and creation operators satisfy the following anticommutation relations:

$$\left\{\hat{c}_\sigma, \hat{c}_{\sigma'}^\dagger\right\} = \delta_{\sigma\sigma'}, \quad \{\hat{c}_\sigma, \hat{c}_{\sigma'}\} = 0, \quad \sigma \in \{\uparrow,\downarrow\}. \tag{4.4.1}$$

To motivate the notion of Gaussian states, consider a single-mode fermionic state characterized by the following expectation values[1]:

$$\langle\hat{c}_\uparrow^\dagger\hat{c}_\uparrow\rangle_\theta = \sin^2\theta, \quad \langle\hat{c}_\uparrow^\dagger\hat{c}_\downarrow^\dagger\rangle_\theta = \langle\hat{c}_\downarrow\hat{c}_\uparrow\rangle_\theta = \sin\theta\cos\theta. \tag{4.4.2}$$

Such a state is given by a superposition of the following two states:

$$\hat{c}_\uparrow^\dagger\hat{c}_\downarrow^\dagger|0\rangle, \quad |0\rangle \tag{4.4.3}$$

with coefficients

$$|\Psi(\theta)\rangle = \left(\cos\theta + \sin\theta\hat{c}_\uparrow^\dagger\hat{c}_\downarrow^\dagger\right)|0\rangle. \tag{4.4.4}$$

[1]As shown later, this physically implies the condensation of paring state of two fermions in BCS superconductors.

This state can be written by using a unitary operator

$$\hat{U}_\theta = e^{-\theta\left(\hat{c}_\uparrow^\dagger \hat{c}_\downarrow^\dagger + \hat{c}_\uparrow \hat{c}_\downarrow\right)} \tag{4.4.5}$$

as follows:

$$|\Psi(\theta)\rangle = \hat{U}_\theta^\dagger |0\rangle = \hat{U}_{-\theta}|0\rangle. \tag{4.4.6}$$

To see this, we note the relation

$$\hat{U}_\theta^\dagger \begin{pmatrix} \hat{c}_\uparrow \\ \hat{c}_\downarrow^\dagger \end{pmatrix} \hat{U}_\theta = \begin{pmatrix} \cos\theta & -\sin\theta \\ \sin\theta & \cos\theta \end{pmatrix} \begin{pmatrix} \hat{c}_\uparrow \\ \hat{c}_\downarrow^\dagger \end{pmatrix}, \tag{4.4.7}$$

which, for example, leads to the expectation value $\langle\Psi(\theta)|\hat{c}_\downarrow \hat{c}_\uparrow|\Psi(\theta)\rangle$:

$$\langle 0|\hat{U}_\theta \hat{c}_\downarrow \hat{c}_\uparrow \hat{U}_\theta^\dagger|0\rangle = \langle 0|\hat{U}_{-\theta}^\dagger \hat{c}_\downarrow \hat{c}_\uparrow \hat{U}_{-\theta}|0\rangle \tag{4.4.8}$$

$$= \langle 0| \left(-\sin\theta \hat{c}_\uparrow^\dagger + \cos\theta \hat{c}_\downarrow\right)\left(\cos\theta \hat{c}_\uparrow + \sin\theta \hat{c}_\downarrow^\dagger\right)|0\rangle \tag{4.4.9}$$

$$= \sin\theta\cos\theta. \tag{4.4.10}$$

Altogether, the simplest fermionic Gaussian state is given by

$$|\Psi(\theta)\rangle = \left(\cos\theta + \sin\theta \hat{c}_\uparrow^\dagger \hat{c}_\downarrow^\dagger\right)|0\rangle = e^{\theta\left(\hat{c}_\uparrow^\dagger \hat{c}_\downarrow^\dagger + \hat{c}_\uparrow \hat{c}_\downarrow\right)}|0\rangle. \tag{4.4.11}$$

For later use, let us also introduce the Majorana representation of fermionic operators:

$$\hat{\psi}_{1\sigma} = \hat{c}_\sigma + \hat{c}_\sigma^\dagger, \;\; \hat{\psi}_{2\sigma} = i(\hat{c}_\sigma^\dagger - \hat{c}_\sigma), \tag{4.4.12}$$

which satisfy the anticommutation relations

$$\left\{\hat{\psi}_{\xi\sigma}, \hat{\psi}_{\eta\sigma'}\right\} = 2\delta_{\xi\eta}\delta_{\sigma\sigma'} \quad \xi,\eta \in \{1,2\}. \tag{4.4.13}$$

This operator is "real" in the sense that it satisfies $\hat{\psi}_{\xi\sigma} = \hat{\psi}_{\xi\sigma}^\dagger$; roughly speaking, this corresponds to the $\hat{x}, \hat{p}$ representation in the bosonic case discussed before. However, different from the bosonic $\hat{x}, \hat{p}$ operators, the Majorana operators either anticommute with each other or satisfy $\hat{\psi}_{1\sigma}^2 = \hat{\psi}_{2\sigma}^2 = 1$. The above state can be expressed in terms of the Majorana operators as

$$|\Psi(\theta)\rangle = e^{\theta\left(\hat{c}_\uparrow^\dagger \hat{c}_\downarrow^\dagger + \hat{c}_\uparrow \hat{c}_\downarrow\right)}|0\rangle = e^{\frac{\theta}{2}\left(\hat{\psi}_{1\uparrow}\hat{\psi}_{1\downarrow} - \hat{\psi}_{2\uparrow}\hat{\psi}_{2\downarrow}\right)}|0\rangle. \tag{4.4.14}$$

4.4.2. Multiple modes. We now generalize the argument to the case of N_f-mode fermionic system (for the sake of simplicity, we omit the spin degrees of freedom here). The annihilation and creation operators for each mode satisfy

$$\left\{\hat{c}_i, \hat{c}_j^\dagger\right\} = \delta_{ij}, \;\; \{\hat{c}_i, \hat{c}_j\} = 0, \quad i,j \in \{1,2,\ldots,N_f\}. \tag{4.4.15}$$

In the Majorana representation, they satisfy

$$\hat{\psi}_{1,i} = \hat{c}_i + \hat{c}_i^\dagger, \;\; \hat{\psi}_{2,i} = i\left(\hat{c}_i^\dagger - \hat{c}_i\right) \tag{4.4.16}$$

$$\left\{\hat{\psi}_\xi, \hat{\psi}_\eta\right\} = 2\delta_{\xi\eta}, \quad \hat{\psi}_\xi = \hat{\psi}_\xi^\dagger, \quad \xi, \eta \in \{1, 2, \ldots, 2N_f\}\,. \tag{4.4.17}$$

We then introduce the operator-valued vector in the Majorana representation by

$$\hat{\boldsymbol{\psi}} = \left(\hat{\psi}_{1,1}, \hat{\psi}_{1,2}, \ldots, \hat{\psi}_{1,N_f}, \hat{\psi}_{2,1}, \hat{\psi}_{2,2}, \ldots, \hat{\psi}_{2,N_f}\right)^{\mathrm{T}}, \tag{4.4.18}$$

which gives an analog of $\hat{\boldsymbol{\phi}}$ vector in the bosonic case above.

Similar to the bosonic case, one can construct the Fermionic Gaussian states by starting from the corresponding Weyl operator, coherent states, and characteristic functions as detailed later. Here, however, we shall begin with a more explicit and straightforward introduction of Fermionic Gaussian states.

Specifically, we define the *Fermionic Gaussian states* by a density operator described by

$$\hat{\rho}_{\mathrm{G}} = \mathcal{N} \exp\left[-\frac{i}{4}\hat{\boldsymbol{\psi}}^{\mathrm{T}} X \hat{\boldsymbol{\psi}}\right], \tag{4.4.19}$$

where X is arbitrary $2N_f \times 2N_f$ real antisymmetric matrix and $\mathcal{N}$ is the normalization factor. This state is completely characterized by the following two-point correlation function:

$$(\Gamma_\psi)_{\xi\eta} = \frac{i}{2}\left\langle\left[\hat{\psi}_\xi, \hat{\psi}_\eta\right]\right\rangle_{\mathrm{G}}, \quad \langle\cdots\rangle_{\mathrm{G}} \equiv \mathrm{Tr}[\hat{\rho}_{\mathrm{G}}\cdots], \tag{4.4.20}$$

where the covariance matrix Γ_ψ is also real antisymmetric matrix. Recall that the Bosonic Gaussian states were characterized by the mean vector $\boldsymbol{\phi}$ in addition to the covariance matrix Γ_ϕ; in contrast, the Fermionic Gaussian states here have no mean vectors since there is no BEC. To see the relation between X in $\hat{\rho}_{\mathrm{G}}$ and Γ_ψ, we note that real antisymmetric matrix can be transformed to the following canonical form by using an orthogonal matrix O:

$$OXO^{\mathrm{T}} = \begin{pmatrix} 0 & D \\ -D & 0 \end{pmatrix}, \quad D = \mathrm{diag}\left(\beta_1, \ldots, \beta_{N_f}\right), \quad \beta_i \in \mathbb{R}. \tag{4.4.21}$$

We also introduce the corresponding state vector by

$$\hat{\tilde{\boldsymbol{\psi}}} = O\hat{\boldsymbol{\psi}} \tag{4.4.22}$$

and denote the annihilation and creation operators for this as $\hat{\tilde{c}}_i$ and $\hat{\tilde{c}}_i^\dagger$; note that these operators also satisfy the anticommutation relations since O is orthogonal. In this canonical frame, the density matrix becomes

$$\hat{\rho}_{\mathrm{G}} = \mathcal{N} \exp\left[-\sum_{j=1}^{N_f} \beta_j \hat{\tilde{c}}_j^\dagger \hat{\tilde{c}}_j\right]. \tag{4.4.23}$$

The corresponding covariance matrix can be obtained as

$$O\Gamma_\psi O^{\mathrm{T}} = \begin{pmatrix} 0 & -\tanh(D/2) \\ \tanh(D/2) & 0 \end{pmatrix}. \tag{4.4.24}$$

Since this has pure imaginary eigenvalues $\pm i\tanh(\beta_j/2)$, the covariance matrix satisfies

$$-\mathrm{I}_{2N_f} \le i\Gamma_\psi \le \mathrm{I}_{2N_f} \iff -\Gamma_\psi^2 \le \mathrm{I}_{2N_f}. \tag{4.4.25}$$

Conversely, for a given $2N_f \times 2N_f$ real antisymmetric matrix Γ_ψ satisfying this condition, there exists a Fermionic Gaussian state whose covariance matrix is given by Γ_ψ.

You can check that $\hat{\rho}_{\rm G}$ is pure if and only if $\beta_i \to \pm\infty \ \forall i$, which leads to

$$\hat{\rho}_{\rm G}^2 = \hat{\rho}_{\rm G} \iff \Gamma_\psi^2 = -{\rm I}_{2N_f}. \tag{4.4.26}$$

More generally, the purity of $\hat{\rho}_{\rm G}$ is given by (see Exercise)

$${\rm Tr}[\hat{\rho}_{\rm G}^2] = \sqrt{\det\left[\left({\rm I}_{2N_f} - \Gamma_\psi^2\right)/2\right]}. \tag{4.4.27}$$

A general multi-point correlation function is given by the certain product of matrix elements of Γ_ψ as follows (known as Wick's theorem):

$${\rm Tr}\left[\hat{\rho}_{\rm G}\hat{\psi}_1^{p_1}\hat{\psi}_2^{p_2}\cdots\hat{\psi}_{2N_f}^{p_{2N_f}}\right] = {\rm Pf}\left[(-i)\Gamma_\psi|_P\right], \ \ p_\xi \in \{0,1\}, \tag{4.4.28}$$

where $\Gamma_\psi|_P$ describes the submatrix that only contains the raws and columns for which $p_\xi = 1$, and Pf is the Pfaffian which is defined for antisymmetric $2n \times 2n$ matrix M as follows:

$${\rm Pf}(M) = \frac{1}{2^n n!}\sum_{\sigma\in S_{2n}} {\rm sgn}(\sigma) M_{\sigma(1)\sigma(2)}\cdots M_{\sigma(2n-1)\sigma(2n)}. \tag{4.4.29}$$

Here, S_{2n} is the permutation group. The Pfaffian satisfies the following important property:

$${\rm Pf}(M)^2 = \det(M). \tag{4.4.30}$$

For instance, the four-point correlation function for $\xi_1 < \xi_2 < \xi_3 < \xi_4$ is given by

$${\rm Tr}\left[\hat{\rho}_{\rm G}\hat{\psi}_{\xi_1}\hat{\psi}_{\xi_2}\hat{\psi}_{\xi_3}\hat{\psi}_{\xi_4}\right] = -\left((\Gamma_\psi)_{\xi_1\xi_2}(\Gamma_\psi)_{\xi_3\xi_4} - (\Gamma_\psi)_{\xi_1\xi_3}(\Gamma_\psi)_{\xi_2\xi_4} + (\Gamma_\psi)_{\xi_1\xi_4}(\Gamma_\psi)_{\xi_2\xi_3}\right). \tag{4.4.31}$$

We note that, conversely, a density operator satisfying Wick's theorem is given by a certain Fermionic Gaussian state. We will prove Wick's theorem later by using Fermionic *coherent* states.

It is also useful to employ the Nambu representation (corresponding to $\hat{a}, \hat{a}^\dagger$ representation in the bosonic case):

$$\begin{pmatrix} \hat{\boldsymbol{c}} \\ \hat{\boldsymbol{c}}^* \end{pmatrix}, \ \ \hat{\boldsymbol{c}} = \left(\hat{c}_1, \hat{c}_2, \ldots, \hat{c}_{N_f}\right)^{\rm T}, \tag{4.4.32}$$

which can be related to the Majorana representation via

$$\hat{\boldsymbol{\psi}} = T\begin{pmatrix} \hat{\boldsymbol{c}} \\ \hat{\boldsymbol{c}}^* \end{pmatrix}, \ \ T \equiv \begin{pmatrix} 1 & 1 \\ -i & i \end{pmatrix} \otimes {\rm I}_{N_f} = \begin{pmatrix} {\rm I}_{N_f} & {\rm I}_{N_f} \\ -i{\rm I}_{N_f} & i{\rm I}_{N_f} \end{pmatrix}. \tag{4.4.33}$$

The correlation function in the Nambu representation is given by

$$\Gamma_f \equiv \left\langle \begin{pmatrix} \hat{\boldsymbol{c}} \\ \hat{\boldsymbol{c}}^* \end{pmatrix} \begin{pmatrix} \hat{\boldsymbol{c}}^\dagger & \hat{\boldsymbol{c}}^{\rm T} \end{pmatrix} \right\rangle_{\rm G} = \frac{1}{2}{\rm I}_{2N_f} - \frac{i}{4}T^\dagger\Gamma_\psi T. \tag{4.4.34}$$

Gaussian unitary operation. We next consider a unitary operation that maps a Fermionic Gaussian state to another Gaussian state (Gaussian operation). To this end, note that the parameters $\{\beta_i\}$ in Eq.

(4.4.23) are invariant under unitary transformation. This means that, for any two Gaussian states that are related by a unitary operation, there exists an orthogonal matrix O that relates their covariance matrices as

$$\tilde{\Gamma}_\psi = O\Gamma_\psi O^{\mathrm{T}}. \tag{4.4.35}$$

Thus, a set of Gaussian unitary operations is characterized by the unitary operation $\hat{U}_O$ that induces this change, which in the state vector corresponds to the transformation

$$\hat{\tilde{\boldsymbol{\psi}}} = \hat{U}_O^\dagger \hat{\boldsymbol{\psi}} \hat{U}_O = O\hat{\boldsymbol{\psi}}. \tag{4.4.36}$$

Recall that the orthogonal group is generated by the reflections and rotations; accordingly, Gaussian unitary operations consist of those two parts. First, the reflections (corresponding to $\hat{\psi}_\xi \to \hat{\psi}_\xi$, $\hat{\psi}_\eta \to -\hat{\psi}_\eta$, $\forall \eta \neq \xi$) are induced by the following unitary operator

$$\hat{U}_O = \hat{\psi}_\xi. \tag{4.4.37}$$

A set of operators given by the product of $\left\{\hat{\psi}_\xi\right\}$ generates the reflection transformations. Second, the rotations are given by the following matrix with a real antisymmetric matrix X:

$$O = e^X, \quad X = -X^{\mathrm{T}}. \tag{4.4.38}$$

This rotation is induced by the following unitary operator:

$$\hat{U}_O = \exp\left[-i\hat{H}_O\right], \ \hat{H}_O = \frac{i}{4}\hat{\boldsymbol{\psi}}^{\mathrm{T}} X \hat{\boldsymbol{\psi}}. \tag{4.4.39}$$

These transformations correspond to the special orthogonal group and contain the identity operator in the limit $X \to 0$. Physically, one may consider this unitary as a time evolution governed by a quadratic Hamiltonian. Conversely, if the initial state is Gaussian and the Hamiltonian is quadratic, the state remains Gaussian during the unitary evolution.

In the Nambu representation, these Gaussian operations are given by

$$\begin{pmatrix} \hat{\tilde{\boldsymbol{c}}} \\ \hat{\tilde{\boldsymbol{c}}}^* \end{pmatrix} = U \begin{pmatrix} \hat{\boldsymbol{c}} \\ \hat{\boldsymbol{c}}^* \end{pmatrix}, \tag{4.4.40}$$

where $U \equiv T^{-1}OT$ is the unitary matrix.

Finally, it is useful to explicitly include the spin-1/2 degrees of freedom of fermions:

$$\hat{\boldsymbol{\psi}} = \left(\hat{\psi}_{1,1\uparrow}, \ldots, \hat{\psi}_{1,N_f\uparrow}, \hat{\psi}_{1,1\downarrow}, \ldots, \hat{\psi}_{1,N_f\downarrow}, \hat{\psi}_{2,1\uparrow}, \ldots, \hat{\psi}_{2,N_f\uparrow}, \hat{\psi}_{2,1\downarrow}, \ldots, \hat{\psi}_{2,N_f\downarrow}\right)^{\mathrm{T}}. \tag{4.4.41}$$

One can show that the Gaussian unitary (corresponding to the rotations) can be written in the following canonical form by using a suitable basis:

$$\hat{U}_O = e^{\frac{1}{4}\hat{\boldsymbol{\psi}}^{\mathrm{T}} X \hat{\boldsymbol{\psi}}} = e^{\sum_{i=1}^{N_f} \theta_i \left(\hat{c}_{i\uparrow}^\dagger \hat{c}_{i\downarrow}^\dagger + \hat{c}_{i\uparrow}\hat{c}_{i\downarrow}\right)} e^{\sum_{i=1}^{N_f} \varphi_i \left(\hat{c}_{i\uparrow}^\dagger \hat{c}_{i\downarrow} + \hat{c}_{i\uparrow}\hat{c}_{i\downarrow}^\dagger\right)}, \quad \theta_i, \varphi_i \in \mathbb{R}. \tag{4.4.42}$$

This expression is particularly useful when we consider an application to the BCS superconductors as detailed later.

Example: Fermionic Gaussian pure state. We here focus on a *pure* Fermionic Gaussian state and summarize several important properties. In the same manner as in the bosonic case, a general pure Fermionic Gaussian state is given by acting a Gaussian unitary operator on the vacuum:

$$|\psi\rangle = \hat{U}\left[\left\{\hat{\psi}_\xi\right\}, \left\{e^{\frac{X_{\xi\eta}}{2}\hat{\psi}_\xi\hat{\psi}_\eta}\right\}\right]|0\rangle. \tag{4.4.43}$$

Here, $\hat{U}$ represents a set of operators generated by a product of unitary operators generating the reflection (4.4.37) and rotation (4.4.39). While this is not in general a particle-number eigenstate, it can always be taken as an eigenstate of the following parity operator:

$$\hat{P} = (-1)^{\sum_{i=1}^{N_f}\hat{c}_i^\dagger\hat{c}_i} = (-i)^{N_f}\hat{\psi}_1\hat{\psi}_2\cdots\hat{\psi}_{2N_f} \equiv (-i)^{N_f}\prod_{\xi=1}^{2N_f}\hat{\psi}_\xi, \tag{4.4.44}$$

$$\hat{P}|\psi\rangle = P|\psi\rangle, \quad P \in \{1,-1\}. \tag{4.4.45}$$

This follows from the fact that $\hat{P}$ commutes with the rotation and anticommutes with the reflection, while the vacuum is parity even:

$$\left\{\hat{P},\hat{\psi}_\xi\right\} = 0, \quad \left[\hat{P}, e^{\frac{X_{\xi\eta}}{2}\hat{\psi}_\xi\hat{\psi}_\eta}\right] = 0, \quad \hat{P}|0\rangle = |0\rangle. \tag{4.4.46}$$

For a given Gaussian state, its parity is given by its covariance matrix as follows:

$$P = (-1)^{N_f}\mathrm{Pf}(\Gamma_\psi). \tag{4.4.47}$$

Another useful formula for pure Gaussian states is the overlap:

$$|\langle\psi_1|\psi_2\rangle|^2 = \begin{cases} (-2)^{N_f}P\mathrm{Pf}\left(\Gamma_{\psi_1}+\Gamma_{\psi_2}\right) & P = P_1 = P_2 \\ 0 & P_1 \neq P_2 \end{cases}. \tag{4.4.48}$$

We will derive these formulas later by using Fermionic coherent states.

If a Gaussian state is an eigenstate of particle numbers, it reduces to the well-known Slater determinant state:

$$|\psi_{\mathrm{Slater}}\rangle = \left(\hat{c}_1^\dagger\right)^{p_1}\left(\hat{c}_2^\dagger\right)^{p_2}\cdots\left(\hat{c}_{N_f}^\dagger\right)^{p_{N_f}}|0\rangle, \quad p_i \in \{0,1\}. \tag{4.4.49}$$

A Gaussian unitary operation restricted to particle-number conserving subspace corresponds to a unitary that does not mix annihilation and creation operators (i.e., a unitary operator only contains the exponential of $\hat{c}^\dagger\hat{c}$ terms). Specifically, it acts as

$$\hat{U}_{O_{\mathrm{Slater}}}|\psi_{\mathrm{Slater}}\rangle = \left(\hat{\tilde{c}}_1^\dagger\right)^{p_1}\left(\hat{\tilde{c}}_2^\dagger\right)^{p_2}\cdots\left(\hat{\tilde{c}}_{N_f}^\dagger\right)^{p_{N_f}}|0\rangle, \quad \hat{\tilde{c}}_i = \sum_{i=1}^{N_f}U_{ij}\hat{c}_j. \tag{4.4.50}$$

Here, $N_f \times N_f$ unitary matrix U corresponds to a basis change. Thus, the Hartree-Fock theory is a method that identifies the optimal Slater-determinant state by using U_{ij} as variational parameters. However, note

that a general Gaussian state is wider than a simple Slater-determinant state and can, for example, be used to analyze BCS superconductors.

To see this more explicitly, we consider a parity-even Gaussian state including the spin degrees of freedom:

$$|\psi\rangle = e^{\frac{1}{4}\hat{\boldsymbol{\psi}}^{\mathrm{T}} X \hat{\boldsymbol{\psi}}}|0\rangle. \tag{4.4.51}$$

Here, the antisymmetric matrix X is related to the covariance matrix via

$$(\Gamma_\psi)_{\xi\eta} = \frac{i}{2}\langle\psi|\left[\hat{\psi}_\xi, \hat{\psi}_\eta\right]|\psi\rangle = -\left(e^X \sigma e^{-X}\right)_{\xi\eta}, \tag{4.4.52}$$

which can be obtained by using Eq. (4.4.35) in the case that the right hand side is the covariance matrix of the vacuum, $-\sigma$. Using the canonical form introduced above, one can express the Gaussian state as

$$|\psi\rangle = e^{\sum_{i=1}^{N_f}\theta_i\left(\hat{c}^\dagger_{i\uparrow}\hat{c}^\dagger_{i\downarrow}+\hat{c}_{i\uparrow}\hat{c}_{i\downarrow}\right)}|0\rangle = \prod_{i=1}^{N_f}\left(\cos\theta_i + \sin\theta_i \hat{c}^\dagger_{i\uparrow}\hat{c}^\dagger_{i\downarrow}\right)|0\rangle, \tag{4.4.53}$$

which is nothing but the well-known BCS variational states[2]. Said differently, any Gaussian state written as Eq. (4.4.51) can be expressed by this BCS form in a suitable basis. Finally, as a corollary of this fact, we note that any pure Gaussian state is a ground state of a certain quadratic Hamiltonian. Indeed, one can construct such "parent Hamiltonian" as

$$\hat{H}_0 = \sum_i \left(\cos(2\theta_i)\left[\hat{c}^\dagger_{i\uparrow}\hat{c}_{i\uparrow} + \hat{c}^\dagger_{i\downarrow}\hat{c}_{i\downarrow}\right] - \sin(2\theta_i)\left[\hat{c}^\dagger_{i\uparrow}\hat{c}^\dagger_{i\downarrow} + \hat{c}_{i\downarrow}\hat{c}_{i\uparrow}\right]\right). \tag{4.4.54}$$

In the simplest example of a single-mode spin-1/2 fermionic system, the canonical form is given by

$$\hat{\boldsymbol{\psi}} = \left(\hat{\psi}_{1\uparrow}, \hat{\psi}_{1\downarrow}, \hat{\psi}_{2\uparrow}, \hat{\psi}_{2\downarrow}\right)^{\mathrm{T}} \tag{4.4.55}$$

and

$$X = \begin{pmatrix} & \theta & & \\ -\theta & & & \\ & & & -\theta \\ & & \theta & \end{pmatrix} \tag{4.4.56}$$

leading to

$$|\psi\rangle = \hat{U}_O|0\rangle = e^{\frac{1}{4}\hat{\boldsymbol{\psi}}^{\mathrm{T}} X \hat{\boldsymbol{\psi}}}|0\rangle = e^{\frac{\theta}{2}\left(\hat{\psi}_{1\uparrow}\hat{\psi}_{1\downarrow} - \hat{\psi}_{2\uparrow}\hat{\psi}_{2\downarrow}\right)}|0\rangle = e^{\theta\left(\hat{c}^\dagger_\uparrow\hat{c}^\dagger_\downarrow + \hat{c}_\uparrow\hat{c}_\downarrow\right)}|0\rangle. \tag{4.4.57}$$

This is nothing but the elemental example we discussed before in the introduction of this section.

Fermionic coherent states and characteristic function. We now introduce the fermionic analog of coherent states and apply it to derive several useful formulas we introduced above. A crucial difference from the bosonic case is that fermionic coherent states are eigenstates of annihilation operators with eigenvalues being given by the Grassmann number:

[2] Strictly speaking, the BCS states usually consist of the pairing between different modes k and $-k$, but one can easily change the present expression into that form.

$$\{\eta_i, \eta_j\} = \{\eta_i^*, \eta_j\} = \left\{\eta_i^*, \eta_j^*\right\} = 0, \quad \forall i, j \in \{1, 2, \ldots, N_f\}. \tag{4.4.58}$$

Here, η_i^* is the complex conjugate of η_i. We define that the Grassmann number anticommutes with fermionic operators:

$$\{\eta_i, \hat{c}_i\} = \left\{\eta_i, \hat{c}_i^\dagger\right\} = 0. \tag{4.4.59}$$

We also define the Hermitian conjugate of η such that it is given in the similar manner as in operators:

$$(\eta_i \eta_j)^\dagger = \eta_j^* \eta_i^*. \tag{4.4.60}$$

The fermionic analog of the Weyl operator (a.k.a displacement operator) is then defined by

$$\hat{D}_{\boldsymbol{\eta}} \equiv e^{\hat{\boldsymbol{c}}^\dagger \boldsymbol{\eta} - \boldsymbol{\eta}^\dagger \hat{\boldsymbol{c}}} = \prod_{i=1}^{N_f} \left[1 + \hat{c}_i^\dagger \eta_i - \eta_i^* \hat{c}_i + \left(\hat{c}_i^\dagger \hat{c}_i - \frac{1}{2}\right) \eta_i^* \eta_i\right]. \tag{4.4.61}$$

One can check that it indeed satisfies the property

$$\hat{D}_{\boldsymbol{\eta}}^\dagger \hat{c}_i \hat{D}_{\boldsymbol{\eta}} = \hat{c}_i + \eta_i, \tag{4.4.62}$$

resulting in the *fermionic coherent state*:

$$\hat{c}_i \hat{D}_{\boldsymbol{\eta}} |0\rangle = \eta_i \hat{D}_{\boldsymbol{\eta}} |0\rangle. \tag{4.4.63}$$

In contrast to the bosonic case, acting the displacement operator on the fully occupied state $|1\rangle \equiv \prod_i \hat{c}_i^\dagger |0\rangle$, one can construct an eigenstate of the creation operator:

$$\hat{c}_i^\dagger \hat{D}_{\boldsymbol{\eta}} |1\rangle = \eta_i^* \hat{D}_{\boldsymbol{\eta}} |1\rangle. \tag{4.4.64}$$

We now switch to the Majorana representation:

$$\xi_{1,i} = \eta_i + \eta_i^*, \;\; \xi_{2,i} = i(\eta_i^* - \eta_i), \tag{4.4.65}$$

where

$$\boldsymbol{\xi} = (\boldsymbol{\xi}_1, \boldsymbol{\xi}_2)^{\mathrm{T}} \tag{4.4.66}$$

are real Grassmann numbers. The displacement operator then becomes

$$\hat{D}_{\boldsymbol{\xi}} = e^{\frac{1}{2}\hat{\boldsymbol{\psi}}^{\mathrm{T}} \boldsymbol{\xi}}, \;\; \hat{D}_{\boldsymbol{\xi}}^\dagger \hat{\boldsymbol{\psi}} \hat{D}_{\boldsymbol{\xi}} = \hat{\boldsymbol{\psi}} + \boldsymbol{\xi}. \tag{4.4.67}$$

Using the Majorana representation, arbitrary Grassmann-valued function can be expanded as

$$f(\boldsymbol{\xi}) = \sum_{n=0}^{2N_f} \sum_{i_1 < i_2 < \cdots < i_n} f_{i_1 i_2 \cdots i_n} \xi_{i_1} \xi_{i_2} \cdots \xi_{i_n} \tag{4.4.68}$$

To introduce the integration of Grassmann-valued function, we define as follows:

$$\int d\xi_i = 0, \;\; \int d\xi_{j_n} \cdots d\xi_{j_1} \xi_{i_1} \cdots \xi_{i_n} = \epsilon \begin{pmatrix} i_1, \cdots, i_n \\ j_1, , \cdots, j_n \end{pmatrix}, \tag{4.4.69}$$

where $(i_1, \ldots, i_n)$ is a set of mutually different integer numbers, and the right hand side gives zero when it is different from another set $(j_1, \ldots, j_n)$, while provides 1 or -1 if these two sets are the same and connected by the even or odd permutations, respectively.

As an example, let us consider the following integral:

$$\int d\xi_i d\xi_j e^{-\xi_i \xi_j} = \int d\xi_i d\xi_j \left(1 - \xi_i \xi_j\right) = \int d\xi_i d\xi_j \xi_j \xi_i = 1. \tag{4.4.70}$$

More generally, for a given antisymmetric matrix M, one can obtain the following Gaussian formulas:

$$\int \mathcal{D}\boldsymbol{\xi} \, \exp\left(\frac{1}{2}\boldsymbol{\xi}^{\mathrm{T}} M \boldsymbol{\xi}\right) = \mathrm{Pf}\left(M\right), \quad \int \mathcal{D}\boldsymbol{\xi} \equiv \int d\xi_{2N_f} \cdots d\xi_1, \tag{4.4.71}$$

$$\int \mathcal{D}\boldsymbol{\xi} \exp\left(\boldsymbol{\zeta}^{\mathrm{T}}\boldsymbol{\xi} + \frac{1}{2}\boldsymbol{\xi}^{\mathrm{T}} M \boldsymbol{\xi}\right) = \mathrm{Pf}(M) \exp\left(\frac{1}{2}\boldsymbol{\zeta}^{\mathrm{T}} M^{-1} \boldsymbol{\zeta}\right). \tag{4.4.72}$$

One important advantage of using the fermionic coherent states is the simplification in certain calculations, such as

$$\mathrm{Tr}\left[\hat{A}\hat{B}\right] = (-2)^{N_f} \int \mathcal{D}\boldsymbol{\zeta}\mathcal{D}\boldsymbol{\xi} e^{\boldsymbol{\xi}^{\mathrm{T}}\boldsymbol{\zeta}} A_{\boldsymbol{\xi}} B_{\boldsymbol{\zeta}}, \tag{4.4.73}$$

where we assign the Grassmann-valued function $A_{\boldsymbol{\xi}}$ for each operator $\hat{A}$ via the following replacement of the Majorana representation:

$$\hat{A} = \sum_{\{p_i\}} A_{p_1 \cdots p_{2N_f}} \hat{\psi}_1^{p_1} \cdots \hat{\psi}_{2N_f}^{p_{2N_f}} \rightarrow A_{\boldsymbol{\xi}} = \sum_{\{p_i\}} A_{p_1 \cdots p_{2N_f}} \xi_1^{p_1} \cdots \xi_{2N_f}^{p_{2N_f}} \tag{4.4.74}$$

with

$$p_i \in \{0, 1\}. \tag{4.4.75}$$

Using this mapping between an operator and a Grassman-valued function, a Gaussian density operator

$$\hat{\rho}_{\mathrm{G}} = \mathcal{N} \exp\left[-\frac{i}{4}\hat{\boldsymbol{\psi}}^{\mathrm{T}} X \hat{\boldsymbol{\psi}}\right] \tag{4.4.76}$$

corresponds to the function

$$\rho_{\mathrm{G},\boldsymbol{\xi}} = \frac{1}{2^{N_f}} \exp\left(\frac{i}{2}\boldsymbol{\xi}^{\mathrm{T}} \Gamma_\psi \boldsymbol{\xi}\right), \tag{4.4.77}$$

where Γ_ψ is the covariance matrix of $\hat{\rho}_{\mathrm{G}}$ (see Exercise).

Similar to the bosonic case, one can introduce the fermionic analog of the characteristic function as follows:

$$\chi_A(\boldsymbol{\xi}) \equiv \mathrm{Tr}\left[\hat{A}\hat{D}_{\boldsymbol{\xi}}\right] = 2^{N_f} A_{\boldsymbol{\xi}/2}. \tag{4.4.78}$$

As inferred from the last equality here, the Grassmann-valued function introduced above itself is essentially the characteristic function aside constants. In particular, the characteristic function of a Gaussian density operator is

$$\chi_{\rho_{\mathrm{G}}}(\boldsymbol{\xi}) = \exp\left[\frac{i}{8}\boldsymbol{\xi}^{\mathrm{T}} \Gamma_\psi \boldsymbol{\xi}\right]. \tag{4.4.79}$$

One can also use this condition as the definition of a Fermionic Gaussian state in the similar way as we have done in the bosonic case.

Using the characteristic function, one can expand a general operator acting on fermionic states as the integral over Grassmann variables:

$$\hat{A} = \int \mathcal{D}\boldsymbol{\zeta}\, \chi_A(\boldsymbol{\zeta}) \hat{E}_{\boldsymbol{\zeta}}, \tag{4.4.80}$$

where

$$\hat{E}_{\boldsymbol{\zeta}} = 4^{N_f} \int \mathcal{D}\boldsymbol{\lambda} e^{\frac{i}{8}\boldsymbol{\zeta}^{\mathrm{T}}\sigma\boldsymbol{\zeta} - \frac{1}{2}\boldsymbol{\lambda}^{\mathrm{T}}\boldsymbol{\zeta}} \hat{D}_{\boldsymbol{\lambda}}|0\rangle\langle 0|\hat{D}_{\boldsymbol{\lambda}}. \tag{4.4.81}$$

You can check this formula by using the relation

$$\mathrm{Tr}\left[\hat{E}_{\boldsymbol{\zeta}}\hat{D}_{\boldsymbol{\xi}}\right] = \delta\left(\boldsymbol{\zeta} - \boldsymbol{\xi}\right) \equiv (\zeta_1 - \xi_1)\cdots(\zeta_{2N_f} - \xi_{2N_f}). \tag{4.4.82}$$

Here, $\delta(\boldsymbol{\zeta} - \boldsymbol{\xi})$ is the delta function of Grassmann variables. It is a good Exercise to check this relation from the equalities

$$\mathrm{Tr}\left[\hat{O}\hat{D}_{\boldsymbol{\xi}}|0\rangle\langle 0|\hat{D}_{\boldsymbol{\xi}'}\right] = \langle 0|\hat{D}^{\dagger}_{\boldsymbol{\xi}'}\hat{O}\hat{D}_{\boldsymbol{\xi}}|0\rangle, \tag{4.4.83}$$

$$\hat{D}_{\boldsymbol{\xi}}\hat{D}_{\boldsymbol{\lambda}} = \hat{D}_{\boldsymbol{\xi}+\boldsymbol{\lambda}} e^{\frac{1}{4}\boldsymbol{\lambda}^{\mathrm{T}}\boldsymbol{\xi}}, \tag{4.4.84}$$

$$\langle 0|\hat{D}^{\dagger}_{\boldsymbol{\lambda}}\hat{D}_{\boldsymbol{\xi}+\boldsymbol{\lambda}}|0\rangle = e^{\frac{1}{4}\boldsymbol{\lambda}^{\mathrm{T}}\boldsymbol{\xi} - \frac{i}{8}\boldsymbol{\xi}^{\mathrm{T}}\sigma\boldsymbol{\xi}}. \tag{4.4.85}$$

As an application of Fermionic coherent representations, let us derive some formulas we used before. First, Wick's theorem (4.4.28) can be derived as follows:

$$\mathrm{Tr}\left[\hat{\rho}_{\mathrm{G}}\hat{\psi}_1^{p_1}\hat{\psi}_2^{p_2}\cdots\hat{\psi}_{2N_f}^{p_{2N_f}}\right] = (-1)^{N_f}\int \mathcal{D}\boldsymbol{\zeta}\mathcal{D}\boldsymbol{\xi} e^{\boldsymbol{\xi}^{\mathrm{T}}\boldsymbol{\zeta}} e^{\frac{i}{2}\boldsymbol{\xi}^{\mathrm{T}}\Gamma_\psi\boldsymbol{\xi}}\zeta_1^{p_1}\cdots\zeta_{2N_f}^{p_{2N_f}} \tag{4.4.86}$$

$$= (-1)^{N_f}\int \mathcal{D}\boldsymbol{\xi}\mathcal{D}\boldsymbol{\zeta} e^{\boldsymbol{\xi}^{\mathrm{T}}\boldsymbol{\zeta}}\zeta_1^{p_1}\cdots\zeta_{2N_f}^{p_{2N_f}} e^{\frac{i}{2}\boldsymbol{\xi}^{\mathrm{T}}\Gamma_\psi\boldsymbol{\xi}} \tag{4.4.87}$$

$$= (-1)^{\sum_i p_i/2}\int \mathcal{D}\boldsymbol{\xi}\xi_1^{1-p_1}\cdots\xi_{2N_f}^{1-p_{2N_f}} e^{\frac{i}{2}\boldsymbol{\xi}^{\mathrm{T}}\Gamma_\psi\boldsymbol{\xi}} \tag{4.4.88}$$

$$= (-1)^{\sum_i p_i/2}\int \mathcal{D}\boldsymbol{\xi} e^{\frac{i}{2}\boldsymbol{\xi}^{\mathrm{T}}\Gamma_\psi|_P\boldsymbol{\xi}} = \mathrm{Pf}\left[(-i\Gamma_\psi)|_P\right]. \tag{4.4.89}$$

Second, the parity formula (4.4.47) can be obtained by using the expression $\hat{P} = (-i)^{N_f}\prod_{\xi=1}^{2N_f}\hat{\psi}_\xi$ and applying this formula to the case of $p_1 = \cdots = p_{2N_f} = 1$. Finally, the inner product formula (4.4.48) is

similarly obtained by

$$|\langle\psi_1|\psi_2\rangle|^2 = \mathrm{Tr}[\hat{\rho}_{\mathrm{G},1}\hat{\rho}_{\mathrm{G},2}] \tag{4.4.90}$$

$$= (-2)^{-N_f}\int \mathcal{D}\boldsymbol{\zeta}\mathcal{D}\boldsymbol{\xi}e^{\boldsymbol{\xi}^{\mathrm{T}}\boldsymbol{\zeta}}e^{\frac{i}{2}\boldsymbol{\xi}^{\mathrm{T}}\Gamma_{\psi,1}\boldsymbol{\xi}}e^{\frac{i}{2}\boldsymbol{\zeta}^{\mathrm{T}}\Gamma_{\psi,2}\boldsymbol{\zeta}} \tag{4.4.91}$$

$$= (-2)^{-N_f}\,\mathrm{Pf}\,(i\Gamma_{\psi,2})\int \mathcal{D}\boldsymbol{\xi}e^{\frac{i}{2}\boldsymbol{\xi}^{\mathrm{T}}(\Gamma_{\psi,1}-\Gamma_{\psi,2}^{-1})\boldsymbol{\xi}} \tag{4.4.92}$$

$$= (-2)^{-N_f}\,\mathrm{Pf}\,(i\Gamma_{\psi,2})\,\mathrm{Pf}\,(i(\Gamma_{\psi,1}+\Gamma_{\psi,2})) \tag{4.4.93}$$

$$= (-2)^{-N_f}\,P\mathrm{Pf}\,(\Gamma_{\psi,1}+\Gamma_{\psi,2}) \tag{4.4.94}$$

Here, we used the Gaussian integration formula (4.4.72), the parity formula $P = (-1)^{N_f}\mathrm{Pf}(\Gamma_{\psi,1})$, and the relation $\Gamma_{\psi,2}^{-1} = -\Gamma_{\psi,2}$ that holds true in a pure state.

4.4.3. Application to BCS superconductors. As an application of Fermionic Gaussian states, we here briefly review the theory of BCS superconductors. To this end, consider the BCS model consisting of attractively interacting fermions:

$$\hat{H} = \sum_{\boldsymbol{k}\sigma}\epsilon_{\boldsymbol{k}}\hat{c}^\dagger_{\boldsymbol{k}\sigma}\hat{c}_{\boldsymbol{k}\sigma} - \frac{g}{\Omega}\sum_{\boldsymbol{k}\boldsymbol{k}'\boldsymbol{q}}\hat{c}^\dagger_{\boldsymbol{k}+\boldsymbol{q}\uparrow}\hat{c}^\dagger_{-\boldsymbol{k}\downarrow}\hat{c}_{-\boldsymbol{k}'+\boldsymbol{q}\downarrow}\hat{c}_{\boldsymbol{k}'\uparrow}. \tag{4.4.95}$$

Here, $\epsilon_{\boldsymbol{k}} = \hbar^2k^2/(2m) - \mu$ is the single-particle energy including the chemical potential and $\Omega = \sum_{\boldsymbol{k}}1$ is the total mode number. The second term describes the effective attractive interaction arising from, e.g., phonon-mediated interaction. The essential feature of the ground state of this model is the formation and condensation of paring between two fermions with different spins (known as the Cooper pairs). This leads to the emergence of the ODLRO in the following sense:

$$\langle\hat{c}^\dagger_{\boldsymbol{r}_1\uparrow}\hat{c}^\dagger_{\boldsymbol{r}_2\downarrow}\hat{c}_{\boldsymbol{r}_3\downarrow}\hat{c}_{\boldsymbol{r}_4\uparrow}\rangle \to O\left(\frac{N^2}{V^2}\right)\neq 0,\quad \hat{c}_{\boldsymbol{r}\sigma} = \frac{1}{\sqrt{V}}\sum_{\boldsymbol{k}}\hat{c}_{\boldsymbol{k}\sigma}e^{i\boldsymbol{k}\cdot\boldsymbol{r}}, \tag{4.4.96}$$

where the limit $\to$ represents the long-distance limit between $(\boldsymbol{r}_1,\boldsymbol{r}_2)$ and $(\boldsymbol{r}_3,\boldsymbol{r}_4)$. To capture this feature, one straightforward choice would be to take a quantum state of the following form (the momentum conservation leads to the paring between $\boldsymbol{k}$ and $-\boldsymbol{k}$):

$$\prod_{\boldsymbol{k}}\left(g_{\boldsymbol{k}}\hat{c}^\dagger_{\boldsymbol{k}\uparrow}\hat{c}^\dagger_{-\boldsymbol{k}\downarrow}\right)|\mathrm{vac}\rangle, \tag{4.4.97}$$

which consists of the products of two-fermion states. Despite the conceptual simplicity, this wavefunction is not very useful especially when one wants to analyze certain physical quantities by calculating the expectation values with respect to this state. This motivates us to construct a more simple and tractable variational state, which still captures the same essential physical feature (i.e., nonvanishing ODLRO).

To do so, recall that the Gaussian state has nonvanishing expectation values of $\langle\hat{c}^\dagger_\uparrow\hat{c}^\dagger_\downarrow\rangle$ or $\langle\hat{c}_\downarrow\hat{c}_\uparrow\rangle$, which can lead to nonzero ODLRO. The following fermionic Gaussian state is thus a natural candidate to describe the ground-state physics of the BCS model:

$$|\Psi^{\mathrm{BCS}}_{\mathrm{var}}\rangle = \prod_{\boldsymbol{k}}\left(\cos\theta_{\boldsymbol{k}} + \sin\theta_{\boldsymbol{k}}\hat{c}^\dagger_{\boldsymbol{k}\uparrow}\hat{c}^\dagger_{-\boldsymbol{k}\downarrow}\right)|\mathrm{vac}\rangle = e^{\sum_{\boldsymbol{k}}\theta_{\boldsymbol{k}}\left(\hat{c}^\dagger_{\boldsymbol{k}\uparrow}\hat{c}^\dagger_{-\boldsymbol{k}\downarrow}+\hat{c}_{\boldsymbol{k}\uparrow}\hat{c}_{-\boldsymbol{k}\downarrow}\right)}|\mathrm{vac}\rangle. \tag{4.4.98}$$

Indeed, this state features the ODLRO

$$\langle \hat{c}^\dagger_{\boldsymbol{r}\uparrow}\hat{c}^\dagger_{\boldsymbol{r}\downarrow}\hat{c}_{\boldsymbol{0}\downarrow}\hat{c}_{\boldsymbol{0}\uparrow}\rangle \to \langle \hat{c}^\dagger_{\boldsymbol{r}\uparrow}\hat{c}^\dagger_{\boldsymbol{r}\downarrow}\rangle\langle \hat{c}_{\boldsymbol{0}\downarrow}\hat{c}_{\boldsymbol{0}\uparrow}\rangle = \frac{\left(\sum_{\boldsymbol{k}} \sin\theta_{\boldsymbol{k}}\cos\theta_{\boldsymbol{k}}\right)^2}{V^2} \sim O\left(\frac{N^2}{V^2}\right), \tag{4.4.99}$$

and thus captures the condensation of the Cooper pairs. While $|\Psi^{\rm BCS}_{\rm var}\rangle$ is not an eigenstate of the particle number, this does not cause problems in the variational analysis, since (similar to the coherent-state description of the BEC discussed before) the fluctuations can be neglected in the thermodynamic limit.

The variational parameters $\theta_{\boldsymbol{k}}$ of $|\Psi^{\rm BCS}_{\rm var}\rangle$ are optimized by minimizing the expectation value of the total energy:

$$\min_{\theta_{\boldsymbol{k}}} \langle \Psi^{\rm BCS}_{\rm var}|\hat{H}|\Psi^{\rm BCS}_{\rm var}\rangle. \tag{4.4.100}$$

Since the expectation values can be decomposed into the products of two-point correlation functions via Wick's theorem, one can check that this procedure is equivalent to the usual mean-field analysis. To see this, let us follow the standard mean-field procedure; we expand the following operator around the mean field $\Delta_{\boldsymbol{k}}$,

$$\hat{c}_{-\boldsymbol{k}\downarrow}\hat{c}_{\boldsymbol{k}\uparrow} \equiv \Delta_{\boldsymbol{k}} + \delta\hat{\Delta}_{\boldsymbol{k}}, \quad \Delta_{\boldsymbol{k}} \equiv \langle \hat{c}_{-\boldsymbol{k}\downarrow}\hat{c}_{\boldsymbol{k}\uparrow}\rangle \in \mathbb{R}, \tag{4.4.101}$$

and neglect the higher-order terms of the fluctuations $\delta\Delta_{\boldsymbol{k}}$. The resulting mean-field Hamiltonian is

$$\hat{H}_{\rm MF} = \sum_{\boldsymbol{k}\sigma} \epsilon_{\boldsymbol{k}}\hat{c}^\dagger_{\boldsymbol{k}\sigma}\hat{c}_{\boldsymbol{k}\sigma} - g\Omega\bar{\Delta}^2 - g\bar{\Delta}\sum_{\boldsymbol{k}}\left(\hat{c}^\dagger_{\boldsymbol{k}\uparrow}\hat{c}^\dagger_{-\boldsymbol{k}\downarrow} + \hat{c}_{-\boldsymbol{k}\downarrow}\hat{c}_{\boldsymbol{k}\uparrow}\right), \tag{4.4.102}$$

where we define

$$\bar{\Delta} \equiv \frac{1}{\Omega}\sum_{\boldsymbol{k}} \Delta_{\boldsymbol{k}}. \tag{4.4.103}$$

One can diagonalize the quadratic Hamiltonian $\hat{H}_{\rm MF}$ by using the following unitary transformation (cf. Eq. (4.4.7)):

$$\begin{pmatrix} \hat{d}_{\boldsymbol{k}\uparrow} \\ \hat{d}^\dagger_{-\boldsymbol{k}\downarrow} \end{pmatrix} = \hat{U}^\dagger \begin{pmatrix} \hat{c}_{\boldsymbol{k}\uparrow} \\ \hat{c}^\dagger_{-\boldsymbol{k}\downarrow} \end{pmatrix} \hat{U} = \begin{pmatrix} \cos\theta_{\boldsymbol{k}} & -\sin\theta_{\boldsymbol{k}} \\ \sin\theta_{\boldsymbol{k}} & \cos\theta_{\boldsymbol{k}} \end{pmatrix} \begin{pmatrix} \hat{c}_{\boldsymbol{k}\uparrow} \\ \hat{c}^\dagger_{-\boldsymbol{k}\downarrow} \end{pmatrix} \tag{4.4.104}$$

with

$$\hat{U} = e^{-\sum_{\boldsymbol{k}}\theta_{\boldsymbol{k}}\left(\hat{c}^\dagger_{\boldsymbol{k}\uparrow}\hat{c}^\dagger_{-\boldsymbol{k}\downarrow} + \hat{c}_{\boldsymbol{k}\uparrow}\hat{c}_{-\boldsymbol{k}\downarrow}\right)}, \tag{4.4.105}$$

where the parameters are defined by

$$\cos(\theta_{\boldsymbol{k}}) = \sqrt{\frac{E_{\boldsymbol{k}} + \epsilon_{\boldsymbol{k}}}{2E_{\boldsymbol{k}}}}, \quad \sin(\theta_{\boldsymbol{k}}) = \sqrt{\frac{E_{\boldsymbol{k}} - \epsilon_{\boldsymbol{k}}}{2E_{\boldsymbol{k}}}}, \quad E_{\boldsymbol{k}} = \sqrt{\bar{\Delta}^2 + (\epsilon_{\boldsymbol{k}} - \mu)^2}. \tag{4.4.106}$$

The diagonalized Hamiltonian is

$$\hat{H}_{\rm MF} = \text{const.} + \sum_{\boldsymbol{k}\sigma} E_{\boldsymbol{k}}\hat{d}^\dagger_{\boldsymbol{k}\sigma}\hat{d}_{\boldsymbol{k}\sigma}. \tag{4.4.107}$$

Thus, the mean-field ground state is given by the vacuum of $\hat{d}$ operators

$$|\Psi_{\rm MF}^{\rm BCS}\rangle = |{\rm vac}\rangle_d, \tag{4.4.108}$$

which corresponds to the squeezed vacuum in the original $\hat{c}$ operators:

$$|\Psi_{\rm MF}^{\rm BCS}\rangle = |{\rm vac}\rangle_d = \hat{U}^\dagger|{\rm vac}\rangle \tag{4.4.109}$$

$$= e^{\sum_{\boldsymbol{k}}\theta_{\boldsymbol{k}}\left(\hat{c}^\dagger_{\boldsymbol{k}\uparrow}\hat{c}^\dagger_{-\boldsymbol{k}\downarrow}+\hat{c}_{\boldsymbol{k}\uparrow}\hat{c}_{-\boldsymbol{k}\downarrow}\right)}|{\rm vac}\rangle \tag{4.4.110}$$

$$= \prod_{\boldsymbol{k}}\left(\cos\theta_{\boldsymbol{k}} + \sin\theta_{\boldsymbol{k}}\hat{c}^\dagger_{\boldsymbol{k}\uparrow}\hat{c}^\dagger_{-\boldsymbol{k}\downarrow}\right)|{\rm vac}\rangle \tag{4.4.111}$$

Indeed, this state satisfies

$$\hat{d}_{\boldsymbol{k}\sigma}|{\rm vac}\rangle_d = \hat{U}^\dagger\hat{c}_{\boldsymbol{k}\sigma}\hat{U}\hat{U}^\dagger|{\rm vac}\rangle = \hat{U}^\dagger\hat{c}_{\boldsymbol{k}\sigma}|{\rm vac}\rangle = 0. \tag{4.4.112}$$

The mean-field ground state $|\Psi_{\rm MF}^{\rm BCS}\rangle$ is nothing but the the Gaussian variational state $|\Psi_{\rm var}^{\rm BCS}\rangle$ in Eq. (4.4.98).

Finally, we note that the variational parameters $\theta_{\boldsymbol{k}}$ are determined by the following self-consistent condition

$$\bar{\Delta} \equiv \frac{1}{\Omega}\sum_{\boldsymbol{k}}\Delta_{\boldsymbol{k}} = \frac{1}{\Omega}\sum_{\boldsymbol{k}}\langle\hat{c}_{-\boldsymbol{k}\downarrow}\hat{c}_{\boldsymbol{k}\uparrow}\rangle = \frac{1}{\Omega}\sum_{\boldsymbol{k}}\sin\theta_{\boldsymbol{k}}\cos\theta_{\boldsymbol{k}}, \tag{4.4.113}$$

leading to

$$\bar{\Delta} = \frac{1}{\Omega}\sum_{\boldsymbol{k}}\frac{g\bar{\Delta}}{2\sqrt{\bar{\Delta}^2+\epsilon_{\boldsymbol{k}}^2}}. \tag{4.4.114}$$

In the superconducting phase ($\bar{\Delta}\neq 0$), we arrive at

$$1 = \frac{1}{\Omega}\sum_{\boldsymbol{k}}\frac{g}{2\sqrt{\bar{\Delta}^2+\epsilon_{\boldsymbol{k}}^2}}. \tag{4.4.115}$$

Again, from a perspective of Gaussian states, these mean-field procedures are equivalent to finding the optimal values of $\theta_{\boldsymbol{k}}$ (or said differently, the covariance matrix) of the Gaussian variational state that minimize the total energy. In the next section, we will develop a more systematic variational approach to perform the optimization over the entire Gaussian manifold. For this purpose, we first need to introduce the concept of the variational principle.

4.5. Variational principle

4.5.1. Introduction. The difficulty of exactly solving quantum many-body problems arises from the vast Hilbert space that cannot (in general) be handled by classical computers. Unless a faithful quantum computer is realized, the best we can do at this stage would be to design a wavefunction that avoids the difficulty of exponential divergence while still captures essential physical features in a system of interest.

Suppose that we can construct such a class of variational states that possess both the efficiency and flexibility. To apply them to actual physical systems, we want to obtain the approximative solutions within

this variational subspace that represent either the ground state or the time-evolved state in nonequilibrium situations. How can one optimize the parameters of those variational states for these purposes?

The time-dependent variational principle (TDVP) provides a general and systematic framework to achieve this aim, which is the main subject of this section. The idea of the variational principle plays an important role also in the context of certain quantum algorithms including Variational Quantum Eigensolver (VQE) on NISQ devices, and more generally, in the field of classical machine learning.

Below we will first review a general theory of the TDVP for both imaginary and real time evolutions; the former can be used to analyze the ground state while the latter is applicable to study nonequilibrium dynamics. We then apply this formalism to Bosonic and Fermionic Gaussian states introduced above.

4.5.2. Complex-valued variational manifold. We first consider a variational state $|\Psi_{\boldsymbol{z}}\rangle$ that is parameterized by complex parameters $\boldsymbol{z}$. We assume that it is always normalized as $\langle\Psi_{\boldsymbol{z}}|\Psi_{\boldsymbol{z}}\rangle = 1$ below. If we naively write down the time-evolution equation, we get

$$\frac{d}{dt}|\Psi_{\boldsymbol{z}(t)}\rangle \stackrel{?}{=} -i\hat{H}|\Psi_{\boldsymbol{z}(t)}\rangle. \tag{4.5.1}$$

The left-hand side is given by the derivative of the variational state, $\frac{d}{dt}|\Psi_{\boldsymbol{z}(t)}\rangle$, and thus lies in the restricted subspace of the whole Hilbert space. Meanwhile, on the right hand side, the Hamiltonian in general contains complex interaction terms and thus the state $-i\hat{H}|\Psi_{\boldsymbol{z}(t)}\rangle$ can lie outside the restricted subspace corresponding to the left hand side. This means that one cannot equate these two states in general. Said differently, the vector on the left hand side belongs to the tangential space of the variational manifold, while that on the right hand side in general does not.

Thus, we have to approximate the time-evolution equation on the variational manifold in some way. For this purpose, the best approximation can be made by minimizing the following quantity:

$$\min_{\boldsymbol{z}(t)} \left\| \left(\frac{d}{dt} + i\hat{H} \right) |\Psi_{\boldsymbol{z}(t)}\rangle \right\|. \tag{4.5.2}$$

From a geometric point of view, this is equivalent to the following condition:

$$\frac{d}{dt}|\Psi_{\boldsymbol{z}(t)}\rangle = \hat{\mathrm{P}}_{\partial} \left(-i\hat{H} \right) |\Psi_{\boldsymbol{z}(t)}\rangle \tag{4.5.3}$$

where $\hat{\mathrm{P}}_{\partial}$ is the projection of a state vector onto the tangential space $\mathcal{T}_{\boldsymbol{z}(t)}$ of the variational manifold, which is a complex vector space spanned by the basis vectors $\left\{ \frac{\partial|\Psi_{\boldsymbol{z}(t)}\rangle}{\partial z_i} \right\}$. More explicitly, we can express it as

$$\hat{\mathrm{P}}_{\partial}|\Psi\rangle \equiv \arg\min_{|v\rangle\in\mathcal{T}_{\boldsymbol{z}}} \||\Psi\rangle - |v\rangle\| \tag{4.5.4}$$

$$\mathcal{T}_{\boldsymbol{z}} \equiv \left\{ |v\rangle \,\middle|\, |v\rangle = \sum_i c_i \frac{\partial|\Psi_{\boldsymbol{z}}\rangle}{\partial z_i},\ c_i \in \mathbb{C} \right\}. \tag{4.5.5}$$

Equation (4.5.3) is known as the McLachlan variational principle.

Similarly, the minimization condition (4.5.2) can also be satisfied by ensuring the following equality:

$$\hat{\mathrm{P}}_\partial i\frac{d}{dt}|\Psi_{\boldsymbol{z}(t)}\rangle = \hat{\mathrm{P}}_\partial \hat{H}|\Psi_{\boldsymbol{z}(t)}\rangle. \tag{4.5.6}$$

This is known as the action variational principle. To see this, recall that the action can be defined by

$$S = \int dt\, L, \quad L = \langle\Psi_{\boldsymbol{z}^*(t)}|\left(i\frac{d}{dt} - \hat{H}\right)|\Psi_{\boldsymbol{z}(t)}\rangle, \tag{4.5.7}$$

and consider the variation $\delta_{\boldsymbol{z}^*}S$ with respect to the change $\boldsymbol{z}^* \to \boldsymbol{z}^* + \delta\boldsymbol{z}^*$:

$$\delta_{\boldsymbol{z}^*}S = \sum_i \delta z_i^* \frac{\partial\langle\Psi_{\boldsymbol{z}^*(t)}|}{\partial z_i^*}\left(i\frac{d}{dt} - \hat{H}\right)|\Psi_{\boldsymbol{z}(t)}\rangle = 0, \quad \forall\delta z_i^* \tag{4.5.8}$$

$$\iff \hat{\mathrm{P}}_\partial\left(i\frac{d}{dt} - \hat{H}\right)|\Psi_{\boldsymbol{z}(t)}\rangle = 0. \tag{4.5.9}$$

This indeed gives the variational principle in Eq. (4.5.6).

We note that, in the present complex-valued case, the McLachlan and action variational principles are equivalent. The reason is that the tangential space $\mathcal{T}_{\boldsymbol{z}}$ is invariant under the multiplication by i, i.e., the operations $\hat{\mathrm{P}}_\partial$ and i commute with each other $[\hat{\mathrm{P}}_\partial, i] = 0$.

The resulting time evolution equation of the variational parameters $\boldsymbol{z}(t)$ can be obtained by multiplying $\frac{\partial|\Psi_{\boldsymbol{z}(t)}\rangle}{\partial z_i}$ from left in Eq. (4.5.3):

$$\sum_j g_{ij}\frac{dz_j}{dt} = -ih_i, \tag{4.5.10}$$

$$g_{ij} \equiv \frac{\partial\langle\Psi_{\boldsymbol{z}^*(t)}|}{\partial z_i^*}\frac{\partial|\Psi_{\boldsymbol{z}(t)}\rangle}{\partial z_j}, \quad h_i = \frac{\partial\langle\Psi_{\boldsymbol{z}^*(t)}|}{\partial z_i^*}\hat{H}|\Psi_{\boldsymbol{z}(t)}\rangle. \tag{4.5.11}$$

4.5.3. Real-valued variational manifold. We next consider a variational state $|\Psi_{\boldsymbol{x}}\rangle$ that is parameterized by real variables $\boldsymbol{x}$; it turns out that one has to be careful about a choice of the variational principles in this case. As done before, we consider the minimization problem

$$\min_{\boldsymbol{x}(t)}\left\|\left(\frac{d}{dt} + i\hat{H}\right)|\Psi_{\boldsymbol{x}(t)}\rangle\right\|. \tag{4.5.12}$$

This leads to the two variational principles as discussed above, which are distinct in the present case because the operations $\hat{\mathrm{P}}_\partial$ and i do not commute with each other $[\hat{\mathrm{P}}_\partial, i] \neq 0$ in general. Indeed, the tangential space of real-valued variational manifold is the real vector space spanned by the basis vectors $\left\{\frac{\partial|\Psi_{\boldsymbol{x}(t)}\rangle}{\partial x_i}\right\}$ and thus

$$\hat{\mathrm{P}}_\partial|\Psi\rangle = \arg\min_{|v\rangle\in\mathcal{T}_{\boldsymbol{x}}}\||\Psi\rangle - |v\rangle\| \tag{4.5.13}$$

$$\mathcal{T}_{\boldsymbol{x}} \equiv \left\{|v\rangle\,\middle|\,|v\rangle = \sum_i a_i\frac{\partial|\Psi_{\boldsymbol{x}}\rangle}{\partial x_i},\ a_i \in \mathbb{R}\right\} \tag{4.5.14}$$

It is clear that this tangential space $\mathcal{T}_{\boldsymbol{x}}$ is not necessarily invariant under the multiplication by i, i.e., the vector $i|v\rangle$ may lie outside of $\mathcal{T}_{\boldsymbol{x}}$.

Keeping this important point in mind, let us first consider the McLachlan variational principle:

$$\frac{d}{dt}|\Psi_{\boldsymbol{x}(t)}\rangle = \hat{\mathrm{P}}_\partial \left(-i\hat{H}\right)|\Psi_{\boldsymbol{x}(t)}\rangle. \tag{4.5.15}$$

Multiplying $\frac{\partial|\Psi_{\boldsymbol{x}(t)}\rangle}{\partial z_i}$ from the left and taking the real parts, we get the time-evolution equations of the variational parameters for this variational principle:

$$\sum_j g^{\mathrm{R}}_{ij}\frac{dx_j}{dt} = \mathrm{Re}\left[-iv_i\right], \tag{4.5.16}$$

$$g^{\mathrm{R}}_{ij} \equiv \mathrm{Re}\left[\frac{\partial\langle\Psi_{\boldsymbol{x}(t)}|}{\partial x_i}\frac{\partial|\Psi_{\boldsymbol{x}(t)}\rangle}{\partial x_j}\right], \quad v_i = \frac{\partial\langle\Psi_{\boldsymbol{x}(t)}|}{\partial x_i}\hat{H}|\Psi_{\boldsymbol{x}(t)}\rangle. \tag{4.5.17}$$

Meanwhile, the action variational principle leads to

$$\hat{\mathrm{P}}_\partial i\frac{d}{dt}|\Psi_{\boldsymbol{x}(t)}\rangle = \hat{\mathrm{P}}_\partial\hat{H}|\Psi_{\boldsymbol{x}(t)}\rangle. \tag{4.5.18}$$

Multiplying $\frac{\partial|\Psi_{\boldsymbol{x}(t)}\rangle}{\partial z_i}$ from the left and taking the real parts, at this time we get

$$\sum_j g^{\mathrm{I}}_{ij}\frac{dx_j}{dt} = -\mathrm{Re}[v_i], \tag{4.5.19}$$

$$g^{\mathrm{I}}_{ij} \equiv \mathrm{Im}\left[\frac{\partial\langle\Psi_{\boldsymbol{x}(t)}|}{\partial x_i}\frac{\partial|\Psi_{\boldsymbol{x}(t)}\rangle}{\partial x_j}\right]. \tag{4.5.20}$$

Note that these two variational time-evolution equations (4.5.16) and (4.5.19) are in general inequivalent.

The two variational principles we encountered above have both advantages and shortcomings. Specifically, in the McLachlan variational principle the symmetries and the corresponding conservation laws of the system are consistently satisfied during the variational time evolutions. To see this, suppose that we have $\hat{O}$ such that $[\hat{O},\hat{H}]=0$ and $\hat{O}|\psi\rangle$ belongs to the tangential space. Then, its expectation value evolves as

$$\frac{d}{dt}\langle\hat{O}\rangle_{\boldsymbol{x}(t)} = \langle\Psi_{\boldsymbol{x}(t)}|(i\hat{H})\hat{\mathrm{P}}_\partial\hat{O} - \hat{O}\hat{\mathrm{P}}_\partial(i\hat{H})|\Psi_{\boldsymbol{x}(t)}\rangle \tag{4.5.21}$$

$$= \langle\Psi_{\boldsymbol{x}(t)}|(i\hat{H})\hat{O}\hat{\mathrm{P}}_\partial - \hat{\mathrm{P}}_\partial\hat{O}(i\hat{H})|\Psi_{\boldsymbol{x}(t)}\rangle \tag{4.5.22}$$

$$= i\langle\Psi_{\boldsymbol{x}(t)}|[\hat{H},\hat{O}]|\Psi_{\boldsymbol{x}(t)}\rangle = 0, \tag{4.5.23}$$

showing that $\hat{O}$ is conserved during the variational evolution. However, we emphasize that one cannot in general choose the Hamiltonian $\hat{H}$ itself as $\hat{O}$ since $\hat{H}$ may not keep the tangential space invariant (i.e., $[\hat{H},\hat{\mathrm{P}}_\partial]\neq 0$). This means that the McLachlan variational principle in general does not conserve the total energy.

In contrast, one can show that the action variational principle always conserves the total energy, while it does not satisfy the other possible symmetries and conservation laws in general (see Exercise).

4.5.4. Imaginary time evolution. Let us next consider the imaginary-time evolution:

$$\frac{d}{d\tau}|\Psi_\tau\rangle = -\left(\hat{H} - \langle\hat{H}\rangle_\tau\right)|\Psi_\tau\rangle \tag{4.5.24}$$

$$\iff |\Psi_\tau\rangle = \frac{e^{-\hat{H}\tau}|\Psi_\tau\rangle}{\left\|e^{-\hat{H}\tau}|\Psi_\tau\rangle\right\|}. \tag{4.5.25}$$

This is especially useful when one is interested in the ground-state physics, since the state converges to the ground state in $\tau \to \infty$ if the initial state has nonzero overlap with the ground state.

We want to find the best approximation for the imaginary-time evolution within a certain variational manifold. This can be achieved by the following minimization:

$$\min_{\boldsymbol{x}(\tau)} \left\| \left[\frac{d}{d\tau} + \left(\hat{H} - E_{\rm var}\right)\right] |\Psi_{\boldsymbol{x}(\tau)}\rangle \right\| \tag{4.5.26}$$

$$E_{\rm var} = \langle\Psi_{\boldsymbol{x}(\tau)}|\hat{H}|\Psi_{\boldsymbol{x}(\tau)}\rangle. \tag{4.5.27}$$

Note that in the present case there is no i factor (as we found for real-time evolution) and thus the McLachlan and action principles are equivalent and lead to the same results for both real-valued and complex-valued variational states.

To be concrete, here we consider the McLachlan variational principle leading to

$$\frac{d}{d\tau}|\Psi_{\boldsymbol{x}(\tau)}\rangle = \hat{\rm P}_\partial\left(E_{\rm var} - \hat{H}\right)|\Psi_{\boldsymbol{x}(\tau)}\rangle = -\hat{\rm P}_\partial\hat{H}|\Psi_{\boldsymbol{x}(\tau)}\rangle. \tag{4.5.28}$$

Here we use $\hat{\rm P}_\partial|\Psi_{\boldsymbol{x}}\rangle = 0$ that follows from the definition (4.5.13). The variational imaginary time evolution of the variational parameters are given by multiplying $\frac{\partial|\Psi_{\boldsymbol{x}(t)}\rangle}{\partial x_i}$ from left and taking the real parts:

$$\sum_j g^{\rm R}_{ij}\frac{dx_j}{d\tau} = -{\rm Re}\left[v_i\right]. \tag{4.5.29}$$

Because of the positivity of $g^{\rm R}_{ij}$, one can show that the variational energy monotonically decreases during the imaginary time evolution:

$$\frac{dE_{\rm var}}{d\tau} \le 0. \tag{4.5.30}$$

If $g^{\rm R}_{ij}$ has the inverse, we can rewrite the time evolution equation as

$$\frac{dx_j}{d\tau} = -\sum_i \left[(g^{\rm R})^{-1}\right]_{ji}{\rm Re}\left[v_i\right]. \tag{4.5.31}$$

It is worthwhile to note that this equation can be considered as the generalized stochastic gradient descent on the curved space whose metric is given by $g^{\rm R}$. In the fields of machine learning or information geometry, this gives an analogue of the so-called Natural Gradient descent or the Riemannian gradient descent. For the sake of comparison, we recall that the simplest stochastic gradient method is defined by

$$x_j(\tau + \delta\tau) = x_j(\tau) - \eta\delta\tau\frac{\partial}{\partial x_j}\langle\hat{H}\rangle_\tau \tag{4.5.32}$$

which is widely used especially in the field of machine learning. When the metric is not flat, the modified gradient descent (4.5.31) can in practice converge more efficiently than the simplest form of the stochastic gradient descent.

We note that, in the imaginary time evolution, energy or other quantities are not conserved in general even if there exist certain symmetries. However, (if necessary) one can ensure a conservation of, e.g., particle number by further restricting the projection operation $\hat{\mathrm{P}}_\partial$ onto a certain subspace associated with a conserved quantity at each time step. In practice, this can be achieved by adding the penalty term to the Hamiltonian (e.g., like $\lambda(\hat{N}-N_0)^2$ for the particle number conservation with N_0 being the initial particle number).

4.5.5. Application to Gaussian states. It is a good demonstration to apply the time-dependent variational principle above to the case of Gaussian variational states. First, we recall that pure Fermionic Gaussian states are in general expressed by

$$|\psi\rangle = \hat{U}_{\mathrm{G}}\left[\left\{\hat{\psi}_\xi\right\}, \left\{e^{\frac{X_{\xi\eta}}{2}\hat{\psi}_\xi\hat{\psi}_\eta}\right\}\right]|0\rangle, \quad X_{\xi\eta}\in\mathbb{R}. \tag{4.5.33}$$

In particular, if the Gaussian state is given by using only the rotations, we can express it as

$$|\psi\rangle = e^{\frac{1}{4}\hat{\boldsymbol{\psi}}^{\mathrm{T}}X\hat{\boldsymbol{\psi}}}|0\rangle, \quad X\in\mathbb{R}^{2N_f\times 2N_f}, \quad X=-X^{\mathrm{T}}, \tag{4.5.34}$$

whose covariance matrix is given by

$$\Gamma_\psi = -e^{X}\sigma e^{-X}, \quad \sigma = \begin{pmatrix} 0 & \mathrm{I}_{N_f} \\ -\mathrm{I}_{N_f} & 0 \end{pmatrix}. \tag{4.5.35}$$

Several remarks are in order. First, it is redundant to use X as variational parameters of Fermionic Gaussian states. It is the covariance matrix Γ_ψ that completely characterizes Gaussian states without unnecessary redundancies. Indeed, one can check that different choices of X can lead to the same Γ_ψ in Eq. (4.5.35). Second, while Gaussian variational states are parametrized by real variables, the corresponding tangential space satisfies $[\hat{\mathrm{P}}_\partial, i]=0$ and thus the McLachlan and action variational principles are equivalent. Consequently, energy and other conserved quantities (if any) are consistently conserved during the variational time evolutions. To see this explicitly, we can obtain the tangential space of the Gaussian states by taking the derivative with respect to the variational parameters Γ_ψ. One can show that the result is

$$\mathcal{T}_{\mathrm{f}} \equiv \left\{ |v\rangle \,\middle|\, |v\rangle = \hat{U}_{\mathrm{G}}\left(\sum_{1\le i<j}^{N_f} c_{ij}\hat{c}_i^\dagger\hat{c}_j^\dagger\right)|0\rangle,\ c_{ij}\in\mathbb{C} \right\}, \tag{4.5.36}$$

which is invariant under the multiplication by i, leading to $[\hat{\mathrm{P}}_\partial, i]=0$. The same applies to Bosonic Gaussian states.

Let us now derive the time-evolution equations of the variational parameters Γ_ψ. While this can be done by using Eq. (4.5.16), here let us follow a more direct procedure. To this end, we represent a pure Fermionic Gaussian state by

$$|\psi_t\rangle = \hat{U}_{\rm G}|0\rangle,\ \ \hat{U}_{\rm G}^\dagger \hat{\boldsymbol{\psi}} \hat{U}_{\rm G} = O\hat{\boldsymbol{\psi}},\ \ \Gamma_\psi = -O\sigma O^{\rm T},\ \ OO^{\rm T} = {\rm I}_{2N_f}, \tag{4.5.37}$$

and note the following relation (you can check this by expanding $\hat{H}$ in terms of $\hat{\boldsymbol{\psi}}$):

$$\hat{\rm P}_\partial \hat{H}|\psi_t\rangle = \hat{\rm P}_\partial \hat{U}_{\rm G}\left(\frac{i}{4}\hat{\boldsymbol{\psi}}^{\rm T} O^{\rm T}\mathcal{H}O\hat{\boldsymbol{\psi}} + \hat{\delta}\right)|0\rangle \tag{4.5.38}$$

$$= \hat{U}_{\rm G}\left(:\frac{i}{4}\hat{\boldsymbol{\psi}}^{\rm T} O^{\rm T}\mathcal{H}O\hat{\boldsymbol{\psi}}:\right)|0\rangle, \tag{4.5.39}$$

$$\mathcal{H} \equiv 4\frac{\delta E_{\rm var}}{\delta \Gamma_\psi} = 4\frac{\delta \langle \hat{H}\rangle_{\rm G}}{\delta \Gamma_\psi}, \tag{4.5.40}$$

where : : represents the normal order (i.e., $:\hat{A}: \equiv \hat{A} - \langle 0|\hat{A}|0\rangle$), while $\hat{\delta}$ denotes higher-order terms of $\hat{\boldsymbol{\psi}}$ that is projected out by $\hat{\rm P}_\partial$. Using these equations, we obtain the time evolution equation of the covariance matrix by

$$\frac{d(\Gamma_\psi)_{\xi\eta}}{dt} = \frac{i}{2}\langle\psi_t|[\hat{\psi}_\xi, \hat{\psi}_\eta]\frac{d|\psi_t\rangle}{dt} + {\rm c.c.} \tag{4.5.41}$$

$$= {\rm Re}\left[\langle 0|\hat{U}_{\rm G}^\dagger[\hat{\psi}_\xi, \hat{\psi}_\eta]\hat{\rm P}_\partial \hat{H}|\psi_t\rangle\right] \tag{4.5.42}$$

$$= {\rm Re}\left[\langle 0|[\left(O\hat{\boldsymbol{\psi}}\right)_\xi, \left(O\hat{\boldsymbol{\psi}}\right)_\eta] : \frac{i}{4}\hat{\boldsymbol{\psi}}^{\rm T} O^{\rm T}\mathcal{H}O\hat{\boldsymbol{\psi}} : |0\rangle\right] \tag{4.5.43}$$

$$= -{\rm Re}\left[\left(i\left(1 - i\Gamma_\psi\right)\mathcal{H}\left(1 + i\Gamma_\psi\right)\right)_{\xi\eta}\right]. \tag{4.5.44}$$

Here we used Wick's theorem to derive the last equality:

$$\langle 0|\hat{\psi}_\alpha\hat{\psi}_\beta|0\rangle = \left({\rm I}_{2N_f} + i\sigma\right)_{\alpha\beta}. \tag{4.5.45}$$

We then arrive at the final result

$$\frac{d\Gamma_\psi}{dt} = \mathcal{H}\Gamma_\psi - \Gamma_\psi\mathcal{H} \tag{4.5.46}$$

which gives the variational real time evolution of the Fermionic Gaussian states. The imaginary time evolution can also be obtained in the similar manner, resulting in

$$\frac{d\Gamma_\psi}{d\tau} = -{\rm Im}\left[i\left(1 - i\Gamma_\psi\right)\mathcal{H}\left(1 + i\Gamma_\psi\right)\right] \tag{4.5.47}$$

$$= -\mathcal{H} - \Gamma_\psi\mathcal{H}\Gamma_\psi. \tag{4.5.48}$$

We next consider a pure Bosonic Gaussian state labelled by

$$|\phi\rangle = \hat{U}_{\rm G}|0\rangle = e^{\frac{i}{2}\hat{\boldsymbol{\phi}}^{\rm T}\sigma\boldsymbol{\Delta}}e^{-\frac{i}{4}\hat{\boldsymbol{\phi}}^{\rm T}R\hat{\boldsymbol{\phi}}}|0\rangle, \tag{4.5.49}$$

$$\sigma = \begin{pmatrix} 0 & {\rm I}_{N_b} \\ -{\rm I}_{N_b} & 0 \end{pmatrix},\ \ \boldsymbol{\Delta} \in \mathbb{R}^{2N_b},\ \ R \in \mathbb{R}^{2N_b\times 2N_b}\ \ R = R^{\rm T}, \tag{4.5.50}$$

$$\Gamma_\phi = SS^{\rm T},\ \ S = e^{\sigma R},\ \ S\sigma S^{\rm T} = \sigma. \tag{4.5.51}$$

Similar to the fermionic case, we have to keep in mind that the variables $(\mathbf{\Delta}, \Gamma_\phi)$ are the correct choice as variational parameters (while R is redundant). The tangential space is then given by

$$\mathcal{T}_{\rm b} \equiv \left\{ |v\rangle \,\middle|\, |v\rangle = \hat{U}_{\rm G} \left(\sum_{1\le i\le j}^{N_b} c_{ij} \hat{b}_i^\dagger \hat{b}_j^\dagger + \sum_{i=1}^{N_b} c_i \hat{b}_i^\dagger \right) |0\rangle,\ c_{ij} \in \mathbb{C} \right\} \tag{4.5.52}$$

which satisfies $[\hat{\rm P}_\partial, i] = 0$.

Following the similar steps above for the fermionic case, one can obtain the real time evolution equations. The results are (see Exercise):

$$\frac{d\mathbf{\Delta}}{dt} = \sigma \mathcal{H}_{\mathbf{\Delta}},\ \ \frac{d\Gamma_\phi}{dt} = \sigma \mathcal{H}_\Gamma \Gamma_\phi - \Gamma_\phi \mathcal{H}_\Gamma \sigma, \tag{4.5.53}$$

$$\mathcal{H}_{\mathbf{\Delta}} \equiv 2\frac{\delta E_{\rm var}}{\delta \mathbf{\Delta}},\ \ \mathcal{H}_\Gamma = 4\frac{\delta E_{\rm var}}{\delta \Gamma_\phi}. \tag{4.5.54}$$

The imaginary time evolution is given by

$$\frac{d\mathbf{\Delta}}{d\tau} = -\Gamma_\phi \mathcal{H}_{\mathbf{\Delta}},\ \ \frac{d\Gamma_\phi}{d\tau} = -\sigma \mathcal{H}_\Gamma \sigma - \Gamma_\phi \mathcal{H}_\Gamma \Gamma_\phi \tag{4.5.55}$$

$$\mathcal{H}_{\mathbf{\Delta}} \equiv 2\frac{\delta E_{\rm var}}{\delta \mathbf{\Delta}},\ \ \mathcal{H}_\Gamma = 4\frac{\delta E_{\rm var}}{\delta \Gamma_\phi}. \tag{4.5.56}$$

These sets of equations of motion are exact if the Hamiltonian is quadratic, while give approximative solutions when there exist interaction terms. One can use the imaginary time evolution and take $\tau \to \infty$ to obtain the variational ground state, while the real time evolution allows us to analyze nonequilibrium dynamics of the system.

4.6. Superconducting qubits

4.6.1. LC circuits. We next briefly discuss the physics of superconducting qubits, one of the most promising building blocks toward realizing quantum computers. To begin with, imagine that we have electrical circuits at low temperature that is well below the critical temperature T_c of the superconductor. Then, the resistance R goes down to zero and, as long as the circuit is well isolated from environmental degrees of freedom, the circuit can be operated in quantum regime.

It is such situation that we are interested in here, and our starting point is the following quantized Hamiltonian of a simple LC circuit:

$$\hat{H} = \frac{\hat{Q}^2}{2C} + \frac{1}{2} C\omega^2 \hat{\Phi}^2,\ \ \omega \equiv \frac{1}{\sqrt{LC}}, \tag{4.6.1}$$

where $\hat{Q}$ is the charge on the capacitor and $\hat{\Phi}$ is the flux in the inductor, which are the canonically conjugate variables satisfying

$$[\hat{\Phi}, \hat{Q}] = i\hbar. \tag{4.6.2}$$

In analogy with the harmonic oscillator, $\hat{\Phi}$ and $\hat{Q}$ can be considered as the analogues of position and momentum operators, respectively. This equivalence motivates us to introduce the annihilation and creation operators by

$$\hat{\Phi} = \sqrt{\frac{\hbar}{2\omega C}}(\hat{a} + \hat{a}^\dagger), \quad \hat{Q} = i\sqrt{\frac{\hbar\omega C}{2}}(\hat{a}^\dagger - \hat{a}), \tag{4.6.3}$$

$$[\hat{a}, \hat{a}^\dagger] = 1. \tag{4.6.4}$$

The resulting Hamiltonian is

$$\hat{H} = \hbar\omega\left(\hat{a}^\dagger\hat{a} + \frac{1}{2}\right). \tag{4.6.5}$$

From this expression, it is now clear that an excitation of quantized LC circuit corresponds to an electromagnetic elementary excitation (a.k.a photon) of frequency ω, which is typically in the microwave regime.

4.6.2. Josephson junction. As shown above, the LC circuit is equivalent to the harmonic oscillator corresponding to a quadratic Hamiltonian, which means that at most one can only perform a Gaussian operation that essentially generates a linear transformation of photon modes (see the discussions in the previous sections). We want to introduce *nonlinearity* to realize circuit operations that are inaccessible in the linear regime. In fact, it is such nonlinearity that eventually allows one to implement effectively two-level systems, namely, qubits.

For this purpose, we shall explain about the Josephson junction that effectively replaces the linear inductance in the circuit by the nonlinear inductance corresponding to the energy:

$$\frac{1}{2}C\omega^2\hat{\Phi}^2 \to -E_J\cos\left(\frac{2\pi\hat{\Phi}}{\Phi_0}\right), \quad \Phi_0 = h/2e. \tag{4.6.6}$$

To derive this result, we recall the BCS theory of superconductors explained before; the superconducting phase was well captured by the ground state of the following quadratic Hamiltonian:

$$\hat{H}_{\mathrm{MF}} = \sum_{\boldsymbol{k}\sigma}\epsilon_{\boldsymbol{k}}\hat{c}^\dagger_{\boldsymbol{k}\sigma}\hat{c}_{\boldsymbol{k}\sigma} - g\Omega|\bar{\Delta}|^2 - g\sum_{\boldsymbol{k}}\left(\bar{\Delta}\hat{c}^\dagger_{\boldsymbol{k}\uparrow}\hat{c}^\dagger_{-\boldsymbol{k}\downarrow} + \bar{\Delta}^*\hat{c}_{-\boldsymbol{k}\downarrow}\hat{c}_{\boldsymbol{k}\uparrow}\right), \tag{4.6.7}$$

where at this time we take the order parameter to be a generic form with a phase:

$$\bar{\Delta} = |\bar{\Delta}|e^{i\varphi}, \quad \varphi \in [0, 2\pi). \tag{4.6.8}$$

Its ground state is given by the vacuum of the quasiparticle operator $\hat{d}_{\boldsymbol{k}}$ and can be expressed as the Gaussian state in terms of $\hat{c}_{\boldsymbol{k}}$ operators as follows:

$$|\Psi_\varphi\rangle = \prod_{\boldsymbol{k}}\left(\cos\theta_{\boldsymbol{k}} + \sin\theta_{\boldsymbol{k}}e^{i\varphi}\hat{c}^\dagger_{\boldsymbol{k}\uparrow}\hat{c}^\dagger_{-\boldsymbol{k}\downarrow}\right)|\mathrm{vac}\rangle, \tag{4.6.9}$$

which is obviously 2π-periodic

$$|\Psi_\varphi\rangle = |\Psi_{\varphi+2\pi}\rangle. \tag{4.6.10}$$

We then note that its Fourier transformation gives the projection onto the eigenspace of total number of Cooper pairs with eigenvalue N:

$$|\Psi_N\rangle = \int_0^{2\pi} \frac{d\varphi}{2\pi} e^{-iN\varphi} |\Psi_\varphi\rangle = \hat{P}_N |\Psi_{\varphi=0}\rangle, \quad N \in \mathbb{Z}. \tag{4.6.11}$$

We may consider the variational superconductor wavefunctions, $|\Psi_\varphi\rangle$ and $|\Psi_N\rangle$, as effective "position" and "momentum" eigenstates of the one-body wavefunction on the circle $\varphi \in [0, 2\pi)$. To obtain the φ basis representation of the operator $\hat{N}$, we can use the relation

$$N|\Psi_N\rangle = \int_0^{2\pi} \frac{d\varphi}{2\pi} \left(i\frac{d}{d\varphi} e^{-iN\varphi} \right) |\Psi_\varphi\rangle = \int_0^{2\pi} \frac{d\varphi}{2\pi} e^{-iN\varphi} \left(-i\frac{d}{d\varphi} |\Psi_\varphi\rangle \right), \tag{4.6.12}$$

where we used the fact that N is an integer number and $|\Psi_\varphi\rangle$ is 2π periodic. One may thus identify as

$$N \to -i\frac{d}{d\varphi}. \tag{4.6.13}$$

Precisely speaking, this identification is equivalent to the quantization procedure associated with the following operators

$$\hat{N}, \quad \hat{T} = e^{-i\varphi}, \tag{4.6.14}$$

which satisfy the commutation relation

$$[\hat{T}, \hat{N}] = \hat{T}. \tag{4.6.15}$$

One can check that this leads to the N basis representation of the operator $\hat{T}$:

$$\hat{T} = \sum_N |N-1\rangle\langle N|. \tag{4.6.16}$$

Note that the phase φ itself cannot be an operator while $\hat{T}$ is, since the phase must satisfy the 2π periodicity[3]. Physically, $\hat{N}$ can be interpreted as the number of Cooper pairs in the superconductor, each of which consists of two electrons as noted above. Then, the role of $\hat{T}$ is to increase the number of Cooper pairs by one.

Suppose now that we have two BCS superconductors and they are linked by a thin insulator; then, electron pairs can tunnel across the potential barrier with certain nonvanishing probabilities. This tunneling is, at the lowest order process, described by the following effective Hamiltonian:

$$\hat{H}_J = -\frac{E_J}{2} \left(\hat{T}_1^\dagger \hat{T}_2 + \text{H.c.} \right) = -E_J \cos\varphi, \quad \varphi \equiv \varphi_1 - \varphi_2. \tag{4.6.17}$$

[3]Suppose that we can treat the phase as an operator $\hat{\varphi}$ that obeys $[\hat{\varphi}, \hat{N}] = i$. However, we get $\langle\Psi_N|[\hat{\varphi}, \hat{N}]|\Psi_N\rangle = (N - N)\langle\Psi_N|\hat{\varphi}|\Psi_N\rangle = 0$, which contradicts with the commutation relation.

The variable φ describes the phase difference between two conductors and we have $E_J > 0$ which means that the phase match is energetically favored. The transfer of the Cooper pairs will also lead to the nonzero electric dipole between the superconductors that induces the electrostatic energy, which can be described by

$$\hat{H}_C = 4E_C \left(\hat{N} - N_g\right)^2, \tag{4.6.18}$$

where $E_C = e^2/2C$ is the capacitance energy with C being the total capacitance of the circuit, the factor of 4 comes from the fact that the Cooper pair has charge $2e$, and N_g is the global charge bias in the unit of $2e$. The resulting total Hamiltonian of the Josephson junction is

$$\hat{H}_{JJ} = \hat{H}_C + \hat{H}_J = 4E_C \left(\hat{N} - N_g\right)^2 - E_J \cos\varphi. \tag{4.6.19}$$

To make a comparison with the circuit Hamiltonian discussed before, it is also useful to express $\hat{H}_{JJ}$ in terms of the charge and flux variables as

$$\hat{H}_{JJ} = \frac{\left(\hat{Q} - 2eN_g\right)^2}{2C} - E_J \cos\left(\frac{2\pi\Phi}{\Phi_0}\right), \tag{4.6.20}$$

$$\hat{Q} = 2e\hat{N}, \quad \Phi = \frac{\Phi_0}{2\pi}\varphi = \frac{\hbar}{2e}\varphi, \tag{4.6.21}$$

which explains the replacement in Eq. (4.6.6).

4.6.3. Superconducting qubits: realizing effectively two-level systems. There are in fact several ways to realize effectively two-level systems (qubits) by operating the Josephson junction in different parameter regimes. As a first approach, we shall consider the regime in which the charge energy is dominant $E_C \gg E_J$ (the so-called Cooper-pair-Box regime). It is then useful to work in the N basis, leading to the Hamiltonian

$$\hat{H}_{JJ} = 4E_C \left(\hat{N} - N_g\right)^2 - \frac{E_J}{2} \sum_N \left(|N\rangle\langle N+1| + \text{H.c.}\right). \tag{4.6.22}$$

At $E_J = 0$, the energy eigenstates are given by the charge eigenstates $\{|N\rangle\}$ and the ground and first excited states correspond to the ones that provide the two lowest values of $(N - N_g)^2$. Without Josephson energy E_J, this setup merely leads to the equal energy spacing that is unfavorable for the purpose of realizing qubits, since the resonant operation inevitably induces the transitions between many different levels besides the lowest two levels we are interested in. With the nonlinear term $E_J > 0$, however, energy levels are now inhomogeneously shifted and the energy degeneracies can be lifted, allowing one to use the two lowest levels as effective qubits. This type of qubits is known as the *charge qubits*.

In practice, the charge qubit is sensitive to the environmental voltage noise that comes through the fluctuations of N_g, which ultimately leads to the decoherence. To circumvent this difficulty, one possible way is to work in another regime $E_C \ll E_J$ (the so-called transmon regime). In the language of the

one-body wavefunction, this corresponds to the deep potential (or equivalently large mass) that associates with the small "position" fluctuations $\langle\varphi^2\rangle - \langle\varphi\rangle^2 \ll 1$. This allows us to treat the phase variable φ as an effectively continuous variable without 2π-periodicity restriction. Expanding the $\cos(\varphi)$ term, we then arrive at the effective Hamiltonian,

$$\hat{H}_{JJ} \simeq 4E_C\left(\hat{N} - N_g\right)^2 + \frac{1}{2}E_J\hat{\varphi}^2 - \frac{1}{4!}E_J\hat{\varphi}^4, \tag{4.6.23}$$

which is equivalent to the weakly anharmonic oscillator. Due to this anharmonicity, the energy degeneracies are lifted and thus one can use the two lowest energy eigenstates as an effective qubit; a quantum operation can be performed by using a process that is only resonant to the first excitation energy. This type of qubits is known as the *transmon qubits*.

4.6.4. Light-matter interaction: circuit QED. Finally, we shall briefly mention how superconducting qubits can be electromagnetically coupled to microwave photons. To be concrete, suppose that we capacitively couple the Josephson junction to the LC circuit discussed at the beginning of this section. The corresponding Hamiltonian can be simply obtained by replacing the (normalized) gate voltage N_g by that of the LC circuit $\hat{N}_g$, resulting in

$$\hat{H} = 4E_C\left(\hat{N} - \hat{N}_g\right)^2 - E_J\cos\varphi + \hbar\omega_r\hat{a}^\dagger\hat{a}, \tag{4.6.24}$$

where we define

$$\hat{N}_g = \frac{C_g}{C}\frac{\hat{Q}}{2e} = \frac{C_g}{2e}\sqrt{\frac{\hbar\omega}{2C}}i(\hat{a}^\dagger - \hat{a}). \tag{4.6.25}$$

Here, we used Eq. (4.6.3) and C_g is the gate capacitance connecting the Josephson junction with the LC circuit. While we here discuss the coupling to only a single electromagnetic mode (as realized in cavity resonators), more generally, one can couple the Josephson junction to continuum number of electromagnetic modes by using a certain type of resonators such as waveguides.

These systems offer an ideal platform to study the physics of light-matter interaction, namely, the interaction between collective excitations of electrons (matter) in the superconductors and quantized microwave photons (light) in the LC circuit. This subfield of quantum optics is often referred to as *circuit quantum electrodynamics (QED)* together with *cavity / waveguide QED*; we will give a short introduction for this topic in the next Chapter.

Summary of Chapter 4

Section 4.2 Quantization of the electromagnetic field

- The free quantum electromagnetic Hamiltonian is equivalent to a collection of independent harmonic oscillators with eigenfrequencies $\{\omega_n\}$, which are determined by solving the Helmholtz equation, $(\nabla^2 + \omega^2/c^2)\mathbf{A}_\omega = \mathbf{0}$, under certain boundary conditions. The corresponding elementary excitation is called photon.
- In nonrelativistic quantum electrodynamics, the Coulomb gauge is commonly used and leads to the unusual commutation relation between the vector potential and electromagnetic fields with transverse delta function, which apparently violates the locality. This indicates that the vector potential is not a local observable, but still may influence global property like in the Aharanov-Bohm effect.

Section 4.3 Bosonic Gaussian states

- A bosonic quantum many-body state is called Gaussian state when it is completely characterized by only the correlation functions up to the second-order moment. Time evolution generated by a quadratic bosonic Hamiltonian, such as the free quantum electromagnetic fields, is given by a bosonic Gaussian unitary.
- When a bosonic Gaussian state is used as a variational ansatz for analyzing weakly interacting BEC, it naturally incorporates the usual treatment including Bogoliubov or Gross-Pitaevskii theory.

Section 4.4 Fermionic Gaussian states

- A fermionic Gaussian state is completely characterized by the two-point correlation function. Examples include the Slater determinant and BCS states. Time evolution generated by a quadratic fermionic Hamiltonian is given by a fermionic Gaussian unitary.
- A coherent state can be constructed also in fermionic systems and is useful for the purpose of obtaining several formulas of Gaussian states.

Section 4.5 Variational principle

- Time-dependent variational principle (TDVP) gives an optimal way to approximate the exact time evolution on the variational manifold at each local time. Variational imaginary time evolution can be viewed as natural gradient descent on the variational manifold.
- When applied to Gaussian variational states, TDVP allows us to derive a set of equations of motion that can be used to analyze ground-state properties or nonequilibrium dynamics of many-body systems.

Section 4.6 Superconducting qubits

- When two BCS superconductors are linked by a thin insulator (Josephson junction), its effective Hamiltonian essentially reduces to that of a single quantum particle subject to periodic cosine potential.
- The nonlinear inductance in Josephson junction leads to unequal energy spacing and allows one to use the two lowest energy eigenstates as effectively two-level systems, qubits. Depending on the parameter regimes, they are often called charge or transmon qubits.

4.7. Exercises

Exercise 4.1 (Field commutation relations: 1 point). Calculate the following unequal-time commutation relations among $\hat{\mathbf{E}}$ and $\hat{\mathbf{B}}$ in free space:

$$[\hat{E}_\alpha(\mathbf{r},t),\hat{E}_\beta(\mathbf{r}',t')] \tag{4.7.1}$$

$$[\hat{B}_\alpha(\mathbf{r},t),\hat{B}_\beta(\mathbf{r}',t')] \tag{4.7.2}$$

$$[\hat{E}_\alpha(\mathbf{r},t),\hat{B}_\beta(\mathbf{r}',t')] \tag{4.7.3}$$

Explain how one can interpret the results in terms of the light cone at $|\mathbf{r}-\mathbf{r}'|=c|t-t'|$.

Exercise 4.2 (Single-mode bosonic pure Gaussian state: 1 point). Consider the following single-mode pure bosonic Gaussian state:

$$|\psi(\phi_1,\phi_2,\theta,r)\rangle = e^{\frac{i}{2}(\hat{x}\phi_2-\hat{p}\phi_1)}e^{\frac{i\theta}{4}\left(\hat{x}^2+\hat{p}^2\right)}e^{-\frac{ir}{4}(\hat{x}\hat{p}+\hat{p}\hat{x})}|0\rangle,\quad \phi_{1,2},\theta,r\in\mathbb{R}. \tag{4.7.4}$$

Derive the expression of the covariance matrix in terms of the real parameters $\phi_{1,2},\theta,r$:

$$(\Gamma_\phi)_{\xi\eta}\equiv\frac{1}{2}\langle\psi|\left\{\delta\hat{\phi}_\xi,\delta\hat{\phi}_\eta\right\}|\psi\rangle,\quad \delta\hat{\boldsymbol{\phi}}=\hat{\boldsymbol{\phi}}-\boldsymbol{\phi},\quad \xi,\eta\in\{1,2\}, \tag{4.7.5}$$

where $\hat{\boldsymbol{\phi}}=(\hat{x},\hat{p})^{\mathrm{T}}$. Similarly, derive the expression of the characteristic function in terms of $\boldsymbol{\phi},\theta,r,\boldsymbol{\xi}$ and check the following relation:

$$\chi_\psi(\boldsymbol{\xi})\equiv\langle\psi|\hat{D}_{\boldsymbol{\xi}}|\psi\rangle=\exp\left[-\frac{1}{8}\boldsymbol{\xi}^{\mathrm{T}}\sigma^{\mathrm{T}}\Gamma_\phi\sigma\boldsymbol{\xi}+\frac{i}{2}\boldsymbol{\phi}^{\mathrm{T}}\sigma\boldsymbol{\xi}\right],\quad \boldsymbol{\xi}\in\mathbb{R}^2. \tag{4.7.6}$$

Exercise 4.3 (McCoy's formula: 1 point). Show McCoy's formula for the operators $\hat{x},\hat{p}$ satisfying $[\hat{x},\hat{p}]=2i$:

$$[\hat{x}^m\hat{p}^n]_{\mathcal{S}}=\frac{1}{2^m}\sum_{l=0}^{m}\begin{pmatrix}m\\l\end{pmatrix}\hat{x}^l\hat{p}^n\hat{x}^{m-l}=\exp\left(-i\frac{\partial}{\partial\hat{x}}\frac{\partial}{\partial\hat{p}}\right)\hat{x}^m\hat{p}^n. \tag{4.7.7}$$

Here, $[\cdots]_{\mathcal{S}}$ represents the totally symmetric ordering (for example, $[\hat{x}_i\hat{p}_j]_S=(\hat{x}_i\hat{p}_j+\hat{p}_j\hat{x}_i)/2$).

Exercise 4.4 (Bosonic Gaussian states: 2 points).

- Express the Wigner function (4.3.34) as the integral over N_b real variables (cf. Eq. (3.9.4)) [you can replace the trace $\mathrm{Tr}[\cdots]$ by the integral over position variables $\boldsymbol{x}$ and perform the integration over $2N_b$ variables $\boldsymbol{\xi}$].

- Derive the expression of the overlap between two Bosonic Gaussian states $\mathrm{Tr}[\hat{\rho}_1\hat{\rho}_2]$; you may use the following formula for a real, symmetric, positive definite matrix A and real vector $\boldsymbol{v}$:

$$\int_{\mathbb{R}^N} d^N r\; e^{-\frac{1}{2}\boldsymbol{r}^{\mathrm{T}}A\boldsymbol{r}+\boldsymbol{v}^{\mathrm{T}}\boldsymbol{r}} = \sqrt{\frac{(2\pi)^N}{\det(A)}} e^{\frac{1}{2}\boldsymbol{v}^{\mathrm{T}}A^{-1}\boldsymbol{v}}. \tag{4.7.8}$$

  Show that the obtained formula in particular leads to the simplified expression of the purity $\mathrm{Tr}[\hat{\rho}^2] = 1/\sqrt{\det(\Gamma_\phi)}$ of a Bosonic Gaussian state.

Exercise 4.5 (Generalized uncertainty relation: 1 point). Show the generalized uncertainty relation for a general (i.e., not necessarily Gaussian) density operator $\hat{\rho}$ of bosons:

$$\Gamma_\phi + i\sigma \geq 0, \tag{4.7.9}$$

by using the bosonic commutation relations:

$$\left[\hat{\phi}_\xi, \hat{\phi}_\eta\right] = 2i\sigma_{\xi\eta}, \quad \sigma \equiv i\sigma^y \otimes \mathrm{I}_{N_b} = \begin{pmatrix} 0 & \mathrm{I}_{N_b} \\ -\mathrm{I}_{N_b} & 0 \end{pmatrix}. \tag{4.7.10}$$

Here, $(\Gamma_\phi)_{\xi\eta} = \frac{1}{2}\mathrm{Tr}\left[\hat{\rho}\left\{\delta\hat{\phi}_\xi, \delta\hat{\phi}_\eta\right\}\right]$ is the covariance matrix of $\hat{\rho}$. In particular, when $\hat{\rho}$ is a bosonic Gaussian state, show that the condition (4.7.9) is equivalent to the positivity of $\hat{\rho}$.

Exercise 4.6 (Fermionic Gaussian states: 2 points). Consider a general multi-mode Fermionic Gaussian state $\hat{\rho}$. Show that its purity is given by $\mathrm{Tr}[\hat{\rho}^2] = \sqrt{\det\left[\left(\mathrm{I}_{2N_f} - \Gamma_\psi^2\right)/2\right]}$. Show also that the characteristic function of a Gaussian state (4.4.76) is given by (4.4.77) [you may use the canonical form (4.4.21) and note the relations $\hat{\psi}_{1,2}^2 = 1$ or $\xi^2 = 0$].

Exercise 4.7 (Conservation laws in variational analysis: 1 point). Consider a real-valued variational state. Show that the action variational principle (4.5.18) ensures the energy conservation, but it does not in general satisfy the other conservation laws.

Exercise 4.8 (Variational time-evolution equations: 1 point). Derive a set of the variational time-evolution equations (4.5.53) and (4.5.55) for Bosonic Gaussian states [you can follow the same procedure as done for the fermionic case above].

CHAPTER 5

Quantum light-matter interaction

We here introduce a theory of nonrelativistic quantum electrodynamics (QED) by including matter degrees of freedom in the theory of quantized electromagnetic field introduced in the previous Chapter. We first do this within the Coulomb gauge, and introduce several unitary transformations that are useful, e.g., to introduce simplified effective models or analyze strong light-matter interaction. We briefly mention the relevance of these discussions to cavity/waveguide/circuit QED systems that are of current interest in the fields of quantum optics, quantum information science, and quantum chemistry.

5.1. Classical electrodynamics review

Before developing quantum theory, we shall start from reviewing the theory of classical electrodynamics.

5.1.1. Equations of motion. The dynamics of classical electromagnetic fields interacting with classical charged particles are governed by Maxwell's equations:

$$\nabla \cdot \mathbf{E} = \frac{\rho}{\epsilon_0}, \;\; \nabla \cdot \mathbf{B} = 0, \;\; \nabla \times \mathbf{E} = -\partial_t \mathbf{B}, \;\; \nabla \times \mathbf{B} = \frac{1}{c^2}\partial_t \mathbf{E} + \frac{1}{\epsilon_0 c^2}\mathbf{j}. \tag{5.1.1}$$

Here, we represent the charge density, current density, and the particle velocity as follows:

$$\rho(\mathbf{r}) = \sum_\alpha q_\alpha \delta(\mathbf{r} - \mathbf{r}_\alpha(t)), \;\; \mathbf{j}(\mathbf{r}) = \sum_\alpha q_\alpha \mathbf{v}_\alpha \delta(\mathbf{r} - \mathbf{r}_\alpha(t)), \;\; \mathbf{v}_\alpha \equiv d_t \mathbf{r}_\alpha. \tag{5.1.2}$$

Each charged particle obeys the equation of motion:

$$m_\alpha d_t^2 \mathbf{r}_\alpha = q_\alpha \left[\mathbf{E}(\mathbf{r}_\alpha(t), t) + \mathbf{v}_\alpha \times \mathbf{B}(\mathbf{r}_\alpha(t), t)\right]. \tag{5.1.3}$$

From the Helmholtz theorem, we can introduce the vector potential $\mathbf{A}$ and the scalar potential ϕ via

$$\mathbf{B} = \nabla \times \mathbf{A}, \;\; \mathbf{E} = -\partial_t \mathbf{A} - \nabla\phi. \tag{5.1.4}$$

We then write down the Lagrangian of the total system by

$$L = \sum_\alpha \frac{1}{2} m_\alpha (d_t \mathbf{r}_\alpha)^2 + \int d^3 r \left(\frac{\epsilon_0}{2} \left[\mathbf{E}^2 - c^2 \mathbf{B}^2\right] + \mathbf{j} \cdot \mathbf{A} - \rho\phi \right) \tag{5.1.5}$$

$$= \sum_\alpha \frac{1}{2} m_\alpha (d_t \mathbf{r}_\alpha)^2 + \int d^3 r \left(\frac{\epsilon_0}{2} \left[(\partial_t \mathbf{A} + \nabla\phi)^2 - c^2 \left(\nabla \times \mathbf{A}\right)^2 \right] + \mathbf{j} \cdot \mathbf{A} - \rho\phi \right). \tag{5.1.6}$$

One can check that the Euler-Lagrange equations for generalized coordinates, $\mathbf{A}$, ϕ, and $\{\mathbf{r}_\alpha\}$, reproduce Maxwell's equations (5.1.1) and the equation of motion (5.1.3). At first sight, it might seem that the Lagrangian has the following set of dynamical variables:

$$\{\mathbf{A}, \partial_t \mathbf{A}, \phi, \partial_t \phi\}\,, \quad \{\mathbf{r}_\alpha, \mathbf{v}_\alpha\}\,. \tag{5.1.7}$$

As shown below, in fact this choice of dynamical variables is redundant since they are not independent degrees of freedom. Thus, the present system is a *constrained* dynamical system and, to complete the canonical quantization, we have to carefully identify the correct (nonredundant) dynamical degrees of freedom in this system.

To this end, we introduce the Fourier transformation of arbitrary field variable by

$$\mathbf{V}(\mathbf{r}) = \int \frac{d^3k}{(2\pi)^3}\, \mathbf{V}_\mathbf{k} e^{i\mathbf{k}\cdot\mathbf{r}}, \tag{5.1.8}$$

$$\mathbf{V}_\mathbf{k} = \int d^3r\, \mathbf{V}(\mathbf{r}) e^{-i\mathbf{k}\cdot\mathbf{r}}. \tag{5.1.9}$$

When it is vector-valued, we recall that the Helmholtz theorem allows us to decompose it into transverse and longitudinal parts as

$$\mathbf{V}(\mathbf{r}) = \mathbf{V}^\perp(\mathbf{r}) + \mathbf{V}^\parallel(\mathbf{r}), \tag{5.1.10}$$

where each component satisfies

$$\nabla \cdot \mathbf{V}^\perp(\mathbf{r}) = 0 \iff \mathbf{k} \cdot \mathbf{V}^\perp_\mathbf{k} = 0, \tag{5.1.11}$$

$$\nabla \times \mathbf{V}^\parallel(\mathbf{r}) = \mathbf{0} \iff \mathbf{k} \times \mathbf{V}^\parallel_\mathbf{k} = \mathbf{0}. \tag{5.1.12}$$

More specifically, the transverse part can be obtained by using the transverse delta function:

$$(\mathbf{V}^\perp_\mathbf{k})_i = \sum_j \left(\delta_{ij} - \frac{k_i k_j}{|\mathbf{k}|^2}\right) (\mathbf{V}_\mathbf{k})_j. \tag{5.1.13}$$

In real space, this can be read as

$$(\mathbf{V}^\perp(\mathbf{r}))_i = \sum_j \int d^3r'\, \delta^\perp_{ij}(\mathbf{r} - \mathbf{r}')(\mathbf{V}(\mathbf{r}'))_j, \tag{5.1.14}$$

where $\delta^\perp_{ij}(\mathbf{r})$ is defined in Eq. (4.2.38).

Using these expressions, we can rewrite Maxwell's equations in the Fourier space as

$$\mathbf{E}^\parallel_\mathbf{k} = -\frac{i\rho_\mathbf{k}}{\epsilon_0 k^2}\mathbf{k}, \quad \mathbf{B}^\parallel_\mathbf{k} = \mathbf{0}, \quad i\mathbf{k} \times \mathbf{E}^\perp_\mathbf{k} = -\partial_t \mathbf{B}^\perp_\mathbf{k}, \quad i\mathbf{k} \times \mathbf{B}^\perp_\mathbf{k} = \frac{1}{c^2}\partial_t \mathbf{E}^\perp_\mathbf{k} + \frac{1}{\epsilon_0 c^2}\mathbf{j}^\perp_\mathbf{k} \tag{5.1.15}$$

with

$$\rho_{\mathbf{k}} = \sum_{\alpha} \frac{q_\alpha}{(2\pi)^3} e^{-i\mathbf{k}\cdot\mathbf{r}_\alpha}, \quad \mathbf{j}_{\mathbf{k}} = \sum_{\alpha} \frac{q_\alpha \mathbf{v}_\alpha}{(2\pi)^3} e^{-i\mathbf{k}\cdot\mathbf{r}_\alpha}. \tag{5.1.16}$$

Note that the longitudinal part of the last equation, $\nabla \times \mathbf{B} = \frac{1}{c^2}\partial_t \mathbf{E} + \frac{1}{\epsilon_0 c^2}\mathbf{j}$, leads to the following equality

$$\mathbf{0} = \partial_t \mathbf{E}^{\parallel}_{\mathbf{k}} + \mathbf{j}^{\parallel}_{\mathbf{k}}/\epsilon_0 \iff 0 = \partial_t \rho_{\mathbf{k}} + i\mathbf{k}\cdot\mathbf{j}_{\mathbf{k}}, \tag{5.1.17}$$

which merely indicates the charge conservation and does not provide additional constraints. It is now clear that the correct choice of the independent dynamical degrees of freedom is the one that contributes to the actual time evolution in Eq. (5.1.15), that is,

$$\left\{\mathbf{E}^{\perp}_{\mathbf{k}}, \mathbf{B}^{\perp}_{\mathbf{k}}\right\}, \quad \{\mathbf{r}_\alpha, \mathbf{v}_\alpha\}, \tag{5.1.18}$$

while the longitudinal fields always obey the constraints $\mathbf{E}^{\parallel}_{\mathbf{k}} = -\frac{i\rho_{\mathbf{k}}}{\epsilon_0 k^2}\mathbf{k}$ and $\mathbf{B}^{\parallel}_{\mathbf{k}} = \mathbf{0}$. Said differently, it suffices to give the initial conditions of the variables $\left\{\mathbf{E}^{\perp}_{\mathbf{k}}, \mathbf{B}^{\perp}_{\mathbf{k}}\right\}, \{\mathbf{r}_\alpha, \mathbf{v}_\alpha\}$ for the purpose of fully predicting the dynamics of the present system; the whole time evolution is then obtained by solving Eqs. (5.1.15) and (5.1.3) with these initial conditions. We remark that, since $\mathbf{E}^{\perp}_{\mathbf{k}}, \mathbf{B}^{\perp}_{\mathbf{k}}$ obey the first-derivative time-evolution equation, we don't need to specify the initial "velocity" of these variables.

5.1.2. Redundancy in the dynamical variables and the Coulomb gauge. As mentioned before, the original Lagrangian appeared to have 8 dynamical variables for electromagnetic degrees of freedom:

$$\{\mathbf{A}, \partial_t \mathbf{A}, \phi, \partial_t \phi\}. \tag{5.1.19}$$

However, as we have seen at the last part in the previous section, there should be only 4 dynamical variables, which correspond to the transverse fields $\left\{\mathbf{E}^{\perp}_{\mathbf{k}}, \mathbf{B}^{\perp}_{\mathbf{k}}\right\}$. To proceed with the quantization, we thus must omit the redundant, extra 4 degrees of freedom from the theory.

To do so, we first note that $\partial_t \phi$ does not appear in any equations of motion and ϕ can be related to other variables via the constraint

$$\phi_{\mathbf{k}} = \frac{1}{k^2}\left(i\mathbf{k}\cdot\partial_t \mathbf{A}^{\parallel}_{\mathbf{k}} + \frac{\rho_{\mathbf{k}}}{\epsilon_0}\right), \tag{5.1.20}$$

which follows from the first equality in Eq. (5.1.15). This fact means that $\partial_t \phi$ and ϕ are not actual dynamical degrees of freedom, but can be eliminated from the theory through this constraint.

Now there are 6 variables. To identify another constraint, we recall the relations between electromagnetic fields and the potentials in the Fourier space:

$$\mathbf{B}^{\perp}_{\mathbf{k}} = i\mathbf{k}\times\mathbf{A}^{\perp}_{\mathbf{k}}, \quad \mathbf{E}^{\perp}_{\mathbf{k}} = -\partial_t \mathbf{A}^{\perp}_{\mathbf{k}}, \quad \mathbf{E}^{\parallel}_{\mathbf{k}} = -\partial_t \mathbf{A}^{\parallel}_{\mathbf{k}} - i\mathbf{k}\phi_{\mathbf{k}}. \tag{5.1.21}$$

Since we know that the variables $\left\{\mathbf{E}^{\perp}_{\mathbf{k}}, \mathbf{B}^{\perp}_{\mathbf{k}}\right\}$ constitute the independent dynamical degrees of freedom, we can conclude that it suffices to consider only the transverse component of the vector potential $\mathbf{A}$ as

dynamical variables. This can be achieved most easily by imposing the following gauge condition, which is known as the Coulomb gauge:

$$\nabla \cdot \mathbf{A}(\mathbf{r}) = 0 \iff \mathbf{A}^{\parallel}(\mathbf{r}) = \mathbf{A}^{\parallel}_{\mathbf{k}} = \mathbf{0}. \tag{5.1.22}$$

Altogether, we now identify that, in terms of the potentials, the 4 independent dynamical degrees of freedom correspond to the transverse components of the vector potential and their "velocity":

$$\left\{\mathbf{A}^{\perp}, \partial_t \mathbf{A}^{\perp}\right\}. \tag{5.1.23}$$

For the sake of notational simplicity, from now on, we shall abbreviate $\perp$ in $\mathbf{A}^{\perp}$ and assume that the vector potential is always transverse.

To derive the Hamiltonian, we have to express the Lagrangian in terms of only independent dynamical variables $\{\mathbf{A}, \partial_t \mathbf{A}\}, \{\mathbf{r}_\alpha, \mathbf{v}_\alpha\}$. To this end, we eliminate the longitudinal electric field $\mathbf{E}^{\parallel}$ and the scalar potential ϕ in the original Lagrangian,

$$L = \sum_\alpha \frac{1}{2} m_\alpha (d_t \mathbf{r}_\alpha)^2 + \int d^3 r \left(\frac{\epsilon_0}{2} \left[\mathbf{E}^2 - c^2 \mathbf{B}^2\right] + \mathbf{j} \cdot \mathbf{A} - \rho\phi \right), \tag{5.1.24}$$

in the following way

$$\int d^3 r \left(\frac{\epsilon_0}{2} |\mathbf{E}^{\parallel}(\mathbf{r})|^2 - \rho\phi \right) = -\frac{1}{2} \int d^3 r |\nabla \phi(\mathbf{r})|^2 = -V_{\mathrm{C}} \tag{5.1.25}$$

$$V_{\mathrm{C}} \equiv \frac{1}{4\pi\epsilon_0} \sum_{\alpha > \beta} \frac{q_\alpha q_\beta}{|\mathbf{r}_\alpha - \mathbf{r}_\beta|}, \tag{5.1.26}$$

which gives the electrostatic contributions. Using the relation

$$\mathbf{E}^{\perp} = \mathbf{A}, \;\; \mathbf{B} = \nabla \times \mathbf{A}, \tag{5.1.27}$$

we then arrive at

$$L = \sum_\alpha \frac{1}{2} m_\alpha (d_t \mathbf{r}_\alpha)^2 - V_{\mathrm{C}} + \int d^3 r \left(\frac{\epsilon_0}{2} \left[(\partial_t \mathbf{A})^2 - c^2 (\nabla \times \mathbf{A})^2\right] + \mathbf{j} \cdot \mathbf{A} \right). \tag{5.1.28}$$

One can now derive the canonical momentum as

$$\mathbf{p}_\alpha \equiv \frac{\partial L}{\partial (d_t \mathbf{r}_\alpha)} = m d_t \mathbf{r}_\alpha + q_\alpha \mathbf{A}(\mathbf{r}_\alpha), \tag{5.1.29}$$

$$\mathbf{\Pi} \equiv \frac{\delta L}{\delta (\partial_t \mathbf{A})} = \epsilon_0 \partial_t \mathbf{A}, \tag{5.1.30}$$

which leads to the Hamiltonian

$$H = \sum_\alpha \mathbf{p}_\alpha \cdot d_t \mathbf{r}_\alpha + \int d^3 r\, \mathbf{\Pi} \cdot \partial_t \mathbf{A} - L \tag{5.1.31}$$

$$= \sum_\alpha \frac{\left[\mathbf{p}_\alpha - q_\alpha \mathbf{A}(\mathbf{r}_\alpha)\right]^2}{2m_\alpha} + V_{\mathrm{C}} + \int d^3 r \left[\frac{\mathbf{\Pi}^2}{2\epsilon_0} + \frac{\epsilon_0 c^2}{2}(\nabla \times \mathbf{A})^2\right]. \tag{5.1.32}$$

To simplify the expression, let us assume the periodic boundary conditions and use the mode expansion of $\mathbf{A}$ and $\mathbf{\Pi}$ in terms of mode functions $\mathbf{f}_{\mathbf{k}\lambda}(\mathbf{r}) = \boldsymbol{\epsilon}_{\mathbf{k}\lambda} e^{i\mathbf{k}\cdot\mathbf{r}}/\sqrt{V}$ (cf. Eqs. (4.2.29) and (4.2.19) in Chapter 4):

$$\mathbf{A}(\mathbf{r}) = \sum_{\mathbf{k}\lambda} \left(\alpha_{\mathbf{k}\lambda} \boldsymbol{\epsilon}_{\mathbf{k}\lambda} \frac{e^{i\mathbf{k}\cdot\mathbf{r}}}{\sqrt{V}} + \text{c.c.}\right), \tag{5.1.33}$$

$$\mathbf{\Pi}(\mathbf{r}) = \sum_{\mathbf{k}\lambda} \left(-i\epsilon_0 \omega_{\mathbf{k}} \alpha_{\mathbf{k}\lambda} \boldsymbol{\epsilon}_{\mathbf{k}\lambda} \frac{e^{i\mathbf{k}\cdot\mathbf{r}}}{\sqrt{V}} + \text{c.c.}\right) \tag{5.1.34}$$

with the dispersion relation

$$\omega_{\mathbf{k}} = ck. \tag{5.1.35}$$

Then, the electromagnetic part of the total Hamiltonian can be rewritten as

$$\int d^3 r \left[\frac{\mathbf{\Pi}^2}{2\epsilon_0} + \frac{\epsilon_0 c^2}{2}(\nabla \times \mathbf{A})^2\right] = \sum_{\mathbf{k}\lambda} \left[\frac{P_{\mathbf{k}\lambda}^2}{2\epsilon_0} + \frac{\epsilon_0 \omega_{\mathbf{k}}^2}{2} Q_{\mathbf{k}\lambda}^2\right], \tag{5.1.36}$$

where we define the generalized coordinates and momentum variables by

$$Q_{\mathbf{k}\lambda} \equiv \alpha_{\mathbf{k}\lambda} + \alpha_{\mathbf{k}\lambda}^*, \quad P_{\mathbf{k}\lambda} \equiv i\epsilon_0 \omega_{\mathbf{k}} (\alpha_{\mathbf{k}\lambda}^* - \alpha_{\mathbf{k}\lambda}). \tag{5.1.37}$$

5.2. Quantized electrodynamics Hamiltonians

5.2.1. Quantum electrodynamics in the Coulomb gauge. It is now straightforward to quantize the classical electrodynamic Hamiltonian in the Coulomb gauge obtained above:

$$H_{\mathrm{C}} = \sum_\alpha \frac{\left[\mathbf{p}_\alpha - q_\alpha \mathbf{A}(\mathbf{r}_\alpha)\right]^2}{2m_\alpha} + V_{\mathrm{C}} + \sum_{\mathbf{k}\lambda} \left[\frac{P_{\mathbf{k}\lambda}^2}{2\epsilon_0} + \frac{\epsilon_0 \omega_{\mathbf{k}}^2}{2} Q_{\mathbf{k}\lambda}^2\right], \tag{5.2.1}$$

$$\mathbf{A}(\mathbf{r}) = \sum_{\mathbf{k}\lambda} \left(\alpha_{\mathbf{k}\lambda} \boldsymbol{\epsilon}_{\mathbf{k}\lambda} \frac{e^{i\mathbf{k}\cdot\mathbf{r}}}{\sqrt{V}} + \text{c.c.}\right). \tag{5.2.2}$$

Specifically, we require that the particle coordinate and momentum obey the canonical commutation relations

$$[(\hat{\mathbf{r}}_\alpha)_i, (\hat{\mathbf{p}}_\beta)_j] = i\hbar \delta_{\alpha\beta} \delta_{ij}, \tag{5.2.3}$$

while the same also applies to the generalized coordinates and momentum for electromagnetic degrees of freedom:

$$[\hat{Q}_{\mathbf{k}\lambda}, \hat{P}_{\mathbf{k}'\lambda'}] = i\hbar\delta_{\mathbf{k}\mathbf{k}'}\delta_{\lambda\lambda'}. \tag{5.2.4}$$

In terms of normal variables $\alpha_{\mathbf{k}\lambda}$, the latter is equivalent to the following replacement:

$$\alpha_{\mathbf{k}\lambda} \to \sqrt{\frac{\hbar}{2\epsilon_0\omega_{\mathbf{k}}}}\hat{a}_{\mathbf{k}\lambda} \tag{5.2.5}$$

where $\hat{a}_{\mathbf{k}\lambda}$ is the bosonic annihilation operator satisfying the commutation relation:

$$[\hat{a}_{\mathbf{k}\lambda}, \hat{a}^\dagger_{\mathbf{k}'\lambda'}] = \delta_{\mathbf{k}\mathbf{k}'}\delta_{\lambda\lambda'}. \tag{5.2.6}$$

Summarizing, the quantized electrodynamic Hamiltonian is finally given by

$$\hat{H}_{\rm C} = \sum_\alpha \frac{\left[\hat{\mathbf{p}}_\alpha - q_\alpha\hat{\mathbf{A}}(\hat{\mathbf{r}}_\alpha)\right]^2}{2m_\alpha} + V_{\rm C} + \sum_{\mathbf{k}\lambda}\hbar\omega_{\mathbf{k}}\hat{a}^\dagger_{\mathbf{k}\lambda}\hat{a}_{\mathbf{k}\lambda} \tag{5.2.7}$$

with the vector potential being

$$\hat{\mathbf{A}}(\mathbf{r}) = \sum_{\mathbf{k}\lambda}\sqrt{\frac{\hbar}{2\epsilon_0\omega_{\mathbf{k}}V}}\left(\hat{a}_{\mathbf{k}\lambda}\boldsymbol{\epsilon}_{\mathbf{k}\lambda}e^{i\mathbf{k}\cdot\mathbf{r}} + \text{H.c.}\right). \tag{5.2.8}$$

Note that the present formulation in the Coulomb gauge remains valid as far as we are interested in low-energy behavior in the sense $\hbar\omega \ll mc^2$. To describe high-energy process at $\hbar\omega \geq mc^2$, such as creation of electron-positron pairs, we have to treat also matter degrees of freedom as excitations of field operators on equal footing. There, rather than the Coulomb gauge, it is more natural to use the gauge condition that is manifestly relativistic invariant.

5.2.2. Unitary transformation. One can employ a unitary transformation to analyze the obtained QED Hamiltonian in another reference of frame other than the Coulomb gauge. The most general form for such unitary transformation is[1]

$$\hat{U} = \exp\left[\frac{i}{\hbar}f\left(\{\hat{\mathbf{r}}_\alpha, \hat{\mathbf{p}}_\alpha\}; \left\{\hat{a}_{\mathbf{k}\lambda}, \hat{a}^\dagger_{\mathbf{k}\lambda}\right\}\right)\right], \tag{5.2.9}$$

where f is some function of particle and photon operators, $\{\hat{\mathbf{r}}_\alpha, \hat{\mathbf{p}}_\alpha\}$ and $\left\{\hat{a}_{\mathbf{k}\lambda}, \hat{a}^\dagger_{\mathbf{k}\lambda}\right\}$. In the transformed frame, all the observables $\hat{O}$ (including the Hamiltonian, position operators, field amplitudes, etc) are related to the original expressions in the Coulomb gauge via

$$\hat{\tilde{O}} = \hat{U}^\dagger\hat{O}\hat{U}, \tag{5.2.10}$$

while a quantum state is transformed to be

$$|\tilde{\Psi}\rangle = \hat{U}^\dagger|\Psi\rangle. \tag{5.2.11}$$

[1] In principle, one can also include manifestly time-dependent variables, which may be useful when there exists classical external drivings.

Of course, all the frames must ultimately give the same physical results. In practice, however, one cannot exactly solve the exact QED Hamiltonian and usually resort to a variety of approximations as discussed below. After performing such approximations, different references of frames in general lead to different predictions since the validity of making certain approximations can depend on a choice of frames. This means that some frames may significantly simplify the analysis compared to other frames, and thus it is often crucial how to choose a correct frame of reference depending on different regimes/physical phenomena at hand.

5.2.3. Gauge transformation. One particular class of unitary transformations corresponds to merely adding the time-derivative term to the Lagrangian, which is nothing but the gauge transformation. Specifically, the corresponding unitary transformation takes the form

$$\hat{U} = \exp\left[\frac{i}{\hbar} f\left(\{\hat{\mathbf{r}}_\alpha\}\,;\hat{\mathbf{A}}\right)\right], \tag{5.2.12}$$

which means that f is a function of only generalized coordinates $\hat{\mathbf{r}}_\alpha$ and $\hat{\mathbf{A}}$; the latter means that it includes $\hat{a}, \hat{a}^\dagger$ operators only through the vector potential $\hat{\mathbf{A}}$.

To see that this indeed corresponds to the gauge transformation, consider adding the time-derivative term to the classical Lagrangian:

$$\tilde{L}(\{\mathbf{r}_\alpha, d_t\mathbf{r}_\alpha\}\,;\mathbf{A},\partial_t\mathbf{A}) = L(\{\mathbf{r}_\alpha, d_t\mathbf{r}_\alpha\}\,;\mathbf{A},\partial_t\mathbf{A}) + \frac{df}{dt} \tag{5.2.13}$$

$$= L(\{\mathbf{r}_\alpha, d_t\mathbf{r}_\alpha\}\,;\mathbf{A},\partial_t\mathbf{A}) + \sum_\alpha d_t\mathbf{r}_\alpha \frac{\partial f}{\partial \mathbf{r}_\alpha} + \partial_t\mathbf{A}\frac{\partial f}{\partial \mathbf{A}}. \tag{5.2.14}$$

The new canonical momentum variables are

$$\tilde{\mathbf{p}}_\alpha \equiv \frac{\partial \tilde{L}}{\partial(d_t\mathbf{r}_\alpha)} = m d_t\mathbf{r}_\alpha - e\mathbf{A}(\mathbf{r}_\alpha) + \frac{\partial f}{\partial \mathbf{r}_\alpha} = \mathbf{p}_\alpha + \frac{\partial f}{\partial \mathbf{r}_\alpha} \tag{5.2.15}$$

and

$$\tilde{\mathbf{\Pi}} \equiv \frac{\delta \tilde{L}}{\delta(\partial_t\mathbf{A})} = \epsilon_0\partial_t\mathbf{A} + \frac{\partial f}{\partial \mathbf{A}}. \tag{5.2.16}$$

The corresponding new Hamiltonian is

$$\tilde{H} = \sum_\alpha \tilde{\mathbf{p}}_\alpha \cdot d_t\mathbf{r}_\alpha + \int d^3r\, \tilde{\mathbf{\Pi}}\cdot\partial_t\mathbf{A} - \tilde{L} \tag{5.2.17}$$

$$= \sum_\alpha \frac{\left[\tilde{\mathbf{p}}_\alpha - q_\alpha\mathbf{A}(\mathbf{r}_\alpha)\right]^2}{2m_\alpha} + V_{\mathrm{C}} + \int d^3r \left[\frac{\tilde{\mathbf{\Pi}}^2}{2\epsilon_0} + \frac{\epsilon_0 c^2}{2}(\nabla\times\mathbf{A})^2\right]. \tag{5.2.18}$$

This means that the form of the Hamiltonian is invariant under the gauge transformation, while one has to replace the canonical momentum by the transformed ones via

$$\mathbf{p}_\alpha \to \tilde{\mathbf{p}}_\alpha, \quad \mathbf{\Pi} \to \tilde{\mathbf{\Pi}}. \tag{5.2.19}$$

It is now clear that, in the language of quantum mechanics, the above unitary transformation (5.2.12) indeed induces such replacement[2]:

$$\hat{\tilde{\mathbf{p}}}_\alpha = \hat{U}^\dagger \hat{\mathbf{p}}_\alpha \hat{U} = \hat{\mathbf{p}}_\alpha + \frac{\partial f}{\partial \hat{\mathbf{r}}_\alpha} \tag{5.2.20}$$

$$\hat{\tilde{\mathbf{\Pi}}} = \hat{U}^\dagger \hat{\mathbf{\Pi}} \hat{U} = \hat{\mathbf{\Pi}} + \frac{\partial f}{\partial \hat{\mathbf{A}}}. \tag{5.2.21}$$

We note that gauge transformation is just a special subclass among all the possible unitary transformations, and there still exists a much wider class of unitary transformations that do not reduce to the gauge transformations; we will see such examples later.

5.3. Long wavelength approximation

Consider a globally charge-neutral system (such as a neutral atom) that consists of nuclei and localized electrons, whose center of mass is positioned at $\mathbf{r} = \mathbf{0}$. If the dynamics of those particles are well localized in the length scales that are much shorter than typical wavelengths of photons, we can perform the long-wavelength approximation:

$$\hat{\mathbf{A}}(\hat{\mathbf{r}}_\alpha) \simeq \hat{\mathbf{A}}(\mathbf{0}). \tag{5.3.1}$$

From now on, we impose this condition and abbreviate the position variable as $\hat{\mathbf{A}} \equiv \hat{\mathbf{A}}(\mathbf{0})$. For the sake of simplicity, suppose that there is essentially a single valence electron in a neutral system that contributes to the electrodynamics, and its motion around the nuclei can be modeled by using a simplified effective potential $V(\mathbf{r})$. We then arrive at the following QED Hamiltonian in the Coulomb gauge:

$$\hat{H}_{\rm C} = \frac{\left[\hat{\mathbf{p}} + e\hat{\mathbf{A}}\right]^2}{2m_e} + V(\hat{\mathbf{r}}) + \sum_{\mathbf{k}\lambda} \hbar\omega_{\mathbf{k}} \hat{a}^\dagger_{\mathbf{k}\lambda} \hat{a}_{\mathbf{k}\lambda}, \tag{5.3.2}$$

$$\hat{\mathbf{A}} = \sum_{\mathbf{k}\lambda} \sqrt{\frac{\hbar}{2\epsilon_0 \omega_{\mathbf{k}} V}} \left(\hat{a}_{\mathbf{k}\lambda} \boldsymbol{\epsilon}_{\mathbf{k}\lambda} + \text{H.c.}\right). \tag{5.3.3}$$

Below we shall illustrate the applications of several unitary transformations to this type of Hamiltonians under the long-wavelength approximation.

5.3.1. Power-Zienau-Woolley transformation and dipole interaction. Let us first consider a concrete example of the gauge transformation known as the Power-Zienau-Woolley (PZW) transformation:

$$\hat{U} = \exp\left[\frac{i}{\hbar} f\left(\hat{\mathbf{r}}; \hat{\mathbf{A}}\right)\right], \quad f \equiv -e\hat{\mathbf{r}} \cdot \hat{\mathbf{A}}, \tag{5.3.4}$$

[2]Strictly speaking, the condition (5.2.21) may include redundant degrees of freedom depending on a choice of the gauge conditions in the original Hamiltonian. In that case, it must be modified such that it is expressed by only using the independent dynamical degrees of freedom.

which transforms the particle momentum as

$$\hat{\tilde{\mathbf{p}}} = \hat{U}^\dagger \hat{\mathbf{p}} \hat{U} = \hat{\mathbf{p}} + \frac{\partial f}{\partial \hat{\mathbf{r}}} = \hat{\mathbf{p}} - e\hat{\mathbf{A}}. \tag{5.3.5}$$

To determine how the electromagnetic canonical momentum $\hat{\mathbf{\Pi}}$ changes under this transformation, we recall that in the Coulomb gauge it is related to the transverse electric field via $\hat{\mathbf{\Pi}} = -\epsilon_0 \hat{\mathbf{E}}^\perp$. We thus obtain

$$(\hat{\tilde{\mathbf{E}}}^\perp(\mathbf{r}))_i = \hat{U}^\dagger (\hat{\mathbf{E}}^\perp(\mathbf{r}))_i \hat{U} \tag{5.3.6}$$

$$= (\hat{\mathbf{E}}^\perp(\mathbf{r}))_i + \frac{ie}{\hbar}\left[\hat{\mathbf{r}}\cdot\hat{\mathbf{A}}, (\hat{\mathbf{E}}^\perp(\mathbf{r}))_i\right] \tag{5.3.7}$$

$$= (\hat{\mathbf{E}}^\perp(\mathbf{r}))_i + \frac{e}{\epsilon_0}\sum_j \delta^\perp_{ij}(\mathbf{r})(\hat{\mathbf{r}})_j \tag{5.3.8}$$

where we used the commutation relation (4.2.39). One can check that the magnetic field $\hat{\mathbf{B}}$ remains invariant under the transformation. Using the relation

$$\sum_{\mathbf{k}\lambda} \hbar\omega_{\mathbf{k}} \hat{a}^\dagger_{\mathbf{k}\lambda}\hat{a}_{\mathbf{k}\lambda} + \text{const.} = \frac{\epsilon_0}{2}\int d^3r \left[\hat{\mathbf{E}}^{\perp 2}(\mathbf{r}) + c^2\hat{\mathbf{B}}^2(\mathbf{r})\right], \tag{5.3.9}$$

we then arrive at the transformed Hamiltonian in the PZW gauge:

$$\hat{H}_{\text{PZW}} = \hat{U}^\dagger \hat{H}_{\text{C}} \hat{U} \tag{5.3.10}$$

$$= \frac{\hat{\mathbf{p}}^2}{2m_e} + V(\hat{\mathbf{r}}) + e\hat{\mathbf{r}}\cdot\hat{\mathbf{E}}^\perp + D_{P^2}(\hat{\mathbf{r}}) + \sum_{\mathbf{k}\lambda}\hbar\omega_{\mathbf{k}}\hat{a}^\dagger_{\mathbf{k}\lambda}\hat{a}_{\mathbf{k}\lambda}, \tag{5.3.11}$$

where we recall that we abbreviate the position variables in the electromagnetic fields: $e\hat{\mathbf{r}}\cdot\hat{\mathbf{E}}^\perp \equiv e\hat{\mathbf{r}}\cdot\hat{\mathbf{E}}^\perp(\mathbf{0})$. This $\mathbf{r}\cdot\mathbf{E}$ term describes the light-matter interaction in this frame, which is called the dipole interaction term. There is additional term corresponding to the dipole self-energy:

$$D_{P^2}(\hat{\mathbf{r}}) \equiv \frac{e^2}{2\epsilon_0}\int d^3r \sum_{ijm} \hat{r}_i\hat{r}_j \delta^\perp_{im}(\mathbf{r})\delta^\perp_{jm}(\mathbf{r}). \tag{5.3.12}$$

$$= \frac{e^2}{2\epsilon_0}\int \frac{d^3k}{(2\pi)^3}\sum_{ijm}\hat{r}_i\hat{r}_j\left(\delta_{im} - \frac{k_ik_m}{k^2}\right)\left(\delta_{jm} - \frac{k_jk_m}{k^2}\right). \tag{5.3.13}$$

While this term appears to be divergent, it is in fact nondiverging since we must restrict the k integration up to a certain momentum cutoff, above which the long wavelength approximation becomes inapplicable. At the cost of introducing the dipole self-energy, we note that the PZW Hamiltonian no longer possesses $\hat{A}^2$ term that was present in the Coulomb gauge.

5.3.2. Matrix elements in different gauges and TRK sum rule. Since the long wavelength approximation should remain valid in both Coulomb and PZW gauges (at least in the weak light-matter coupling regimes), we expect that the different gauges must provide the same physical predictions, despite the apparently different expressions of the Hamiltonians.

To explicitly demonstrate this equivalence for one- and two-photon processes, consider an external driving by a weak monochromatic classical field at frequency ω:

$$\mathbf{A}(\mathbf{r}=\mathbf{0},t) = A\boldsymbol{\epsilon}\cos(\omega t) \tag{5.3.14}$$

$$\mathbf{E}(\mathbf{r}=\mathbf{0},t) = \omega A\boldsymbol{\epsilon}\sin(\omega t) \tag{5.3.15}$$

with $\boldsymbol{\epsilon} = (1,0,0)^{\mathrm{T}}$. At the leading order, we can neglect the $\hat{A}^2$ term in $\hat{H}_{\mathrm{C}}$ and the D_{P^2} term in $\hat{H}_{\mathrm{PZW}}$. In the Coulomb gauge, the first-order time-dependent perturbation theory with respect to the interaction term $\hat{H}_{\mathrm{int,C}} = \frac{e}{m}\hat{\mathbf{p}}\cdot\mathbf{A}$ in $\hat{H}_{\mathrm{C}}$ leads to the transition rate

$$w_{1\mathrm{C}} = \frac{\pi A^2}{2\hbar^2}|f_{nm}|^2\delta(\omega_{nm}-\omega), \tag{5.3.16}$$

where f_{nm} is

$$f_{nm} \equiv \frac{e}{m}\langle n|\hat{p}|m\rangle, \quad \hat{p} = \boldsymbol{\epsilon}\cdot\hat{\mathbf{p}}, \tag{5.3.17}$$

which includes the matrix elements of the momentum operator between two internal energy eigenstates of the neutral atom, having an energy difference $\hbar\omega_{nm} \equiv E_n - E_m$.

In the PZW gauge, the similar perturbation calculation with respect to the interaction term $\hat{H}_{\mathrm{int,PZW}} = e\hat{\mathbf{r}}\cdot\mathbf{E}$ in $\hat{H}_{\mathrm{PZW}}$ results in the transition rate

$$w_{1\mathrm{PZW}} = \frac{\pi A^2}{2\hbar^2}|\tilde{f}_{nm}|^2\delta(\omega_{nm}-\omega), \tag{5.3.18}$$

where $\tilde{f}_{nm}$ is given by

$$\tilde{f}_{nm} \equiv ie\omega\langle n|\hat{r}|m\rangle, \quad \hat{r} = \boldsymbol{\epsilon}\cdot\hat{\mathbf{r}}, \tag{5.3.19}$$

which, in this case, includes the matrix elements of the position operator.

We want to check that these two different gauges predict the same transition rate, namely,

$$f_{nm} = \tilde{f}_{nm} \Rightarrow w_{1\mathrm{C}} = w_{1\mathrm{PZW}}. \tag{5.3.20}$$

This equivalence follows from the relation between matrix elements of momentum and position operators in the energy basis:

$$\langle n|\hat{p}|m\rangle = -i\frac{m}{\hbar}\langle n|[\hat{r},\hat{H}_0]|m\rangle = im\omega_{nm}\langle n|\hat{r}|m\rangle, \tag{5.3.21}$$

where we define the single-particle Hamiltonian by

$$\hat{H}_0 = \frac{\hat{\mathbf{p}}^2}{2m_e} + V(\hat{\mathbf{r}}) \tag{5.3.22}$$

and use $\hat{H}_0|n\rangle = E_n|n\rangle$.

Similarly, one can also check the gauge equivalence for two-photon transition processes. The second-order time-dependent perturbation theory in the Coulomb gauge leads to

$$w_{2\mathrm{C}} = \frac{\pi A^4}{8\hbar^2}|g_{nm}|^2\delta(\omega_{nm} - 2\omega), \tag{5.3.23}$$

where

$$g_{nm} \equiv \left(\frac{e}{m}\right)^2 \sum_l \frac{\langle n|\hat{p}|l\rangle\langle l|\hat{p}|m\rangle}{\omega - \omega_{lm}}. \tag{5.3.24}$$

The transition rate in the PZW gauge is

$$w_{2\mathrm{PZW}} = \frac{\pi A^4}{8\hbar^2}|\tilde{g}_{nm}|^2\delta(\omega_{nm} - 2\omega) \tag{5.3.25}$$

with

$$\tilde{g}_{nm} \equiv -\omega^2 e^2 \sum_l \frac{\langle n|\hat{r}|l\rangle\langle l|\hat{r}|m\rangle}{\omega - \omega_{lm}}. \tag{5.3.26}$$

One can check that the equivalence between these results,

$$g_{nm} = \tilde{g}_{nm} \Rightarrow w_{2\mathrm{C}} = w_{2\mathrm{PZW}}, \tag{5.3.27}$$

directly follows from the Thomas-Reiche-Kuhn (TRK) sum rule (see Exercise):

$$\sum_l (\omega_{ln} + \omega_{lm}) \langle n|\hat{r}|l\rangle\langle l|\hat{r}|m\rangle = \frac{\hbar}{m}\delta_{nm}. \tag{5.3.28}$$

The TRK sum rule can be shown as follows:

$$\sum_l (\omega_{ln} + \omega_{lm}) \langle n|\hat{r}|l\rangle\langle l|\hat{r}|m\rangle = -\frac{i}{m}\sum_l (\langle n|\hat{r}|l\rangle\langle l|\hat{p}|m\rangle - \langle n|\hat{p}|l\rangle\langle l|\hat{r}|m\rangle) \tag{5.3.29}$$

$$= -\frac{i}{m}\langle n|[\hat{r},\hat{p}]|m\rangle = \frac{\hbar}{m}\delta_{nm}, \tag{5.3.30}$$

where we used Eq. (5.3.21) to obtain the first equality.

5.3.3. Unitary transformations beyond gauge transformations. As noted earlier, there also exist unitary transformations that do not reduce to the gauge transformations. Some of them are useful for the purpose of analyzing quantum light-matter systems in certain regimes; let us briefly look at such examples below.

5.3.3.1. *Pauli-Fierz-Kramers transformation.* The first example is the Pauli-Fierz-Kramers transformation, by which the light-matter interaction can be absorbed by the field-induced shift of the particle position together with the fluctuation in the particle potential. To simplify the argument, we consider 1D case as follows:

$$\hat{H}_{\rm C} = \frac{\left[\hat{p} + e\hat{A}\right]^2}{2m_e} + V(\hat{x}) + \sum_k \hbar\omega_k \hat{a}_k^\dagger \hat{a}_k, \tag{5.3.31}$$

$$\hat{A} = \sum_k f_k \left(\hat{a}_k + \hat{a}_k^\dagger\right). \tag{5.3.32}$$

Starting from this Coulomb-gauge Hamiltonian, we define the unitary transformation

$$\hat{U} = \exp\left(-\frac{i}{\hbar}\hat{p}\hat{Z}\right), \quad \hat{Z} \equiv \sum_k (-ie)\frac{f_k}{m_e\omega_k}\left(\hat{a}_k^\dagger - \hat{a}_k\right), \tag{5.3.33}$$

which includes the particle momentum $\hat{p}$, and the field operator $\hat{Z}$ that does not reduce to $\hat{A}$; thus it cannot be described as a gauge transformation.

The unitary transformation acts on each operator as

$$\hat{U}^\dagger \hat{x} \hat{U} = \hat{x} + \hat{Z} \tag{5.3.34}$$

$$\hat{U}^\dagger \hat{a}_k \hat{U} = \hat{a}_k - \frac{e f_k}{m_e \hbar \omega_k}\hat{p}. \tag{5.3.35}$$

The coefficients in $\hat{Z}$ are chosen in such a way that the $\hat{p}\cdot\hat{A}$ term in the Coulomb gauge is cancelled by the term arising from the shift of the $\hat{a}^\dagger\hat{a}$ term. The resulting transformed Hamiltonian is

$$\hat{H}_{\rm PFK} = \hat{U}^\dagger \hat{H}_{\rm C} \hat{U} \tag{5.3.36}$$

$$= \frac{\left[1 - 2\sum_k \frac{e^2 f_k^2}{m_e\hbar\omega_k}\right]}{2m_e}\hat{p}^2 + \frac{e^2}{2m_e}\left(\hat{A} - \sum_k \frac{2ef_k^2}{m_e\hbar\omega_k}\hat{p}\right)^2 + V(\hat{x}+\hat{Z}) + \sum_k \hbar\omega_k \hat{a}_k^\dagger \hat{a}_k \tag{5.3.37}$$

$$\simeq \frac{1}{2m_e}\hat{p}^2 + V(\hat{x}+\hat{Z}) + \sum_k \hbar\omega_k \hat{a}_k^\dagger \hat{a}_k, \tag{5.3.38}$$

where the last expression holds true only for a weak light-matter coupling. An advantage of this expression is that, at the lowest order of e, the light-matter interaction is incorporated only through the potential term V, and this feature can simplify calculations of transition amplitudes for certain scattering processes.

5.3.3.2. *Asymptotically decoupling transformation.* The Pauli-Fierz-Kramers transformation introduced above is not very satisfactory in the sense that, at strong light-matter coupling, the higher-order terms in Eq. (5.3.37) must contribute to dynamics in a rather complicated manner.

To circumvent this difficulty, one can introduce the asymptotically decoupling (AD) unitary transformation, which can completely disentangle light and matter degrees of freedom in the strong-coupling limit. To do so, we first note that one can diagonalize the quadratic photon part in $\hat{H}_{\rm C}$ as

$$\frac{e^2\hat{A}^2}{2m_e} + \sum_k \hbar\omega_k \hat{a}_k^\dagger \hat{a}_k = \sum_n \hbar\Omega_n \hat{b}_n^\dagger \hat{b}_n + \text{const.} \tag{5.3.39}$$

This is always possible by using a certain bosonic Gaussian transformation we studied in the previous Chapter. In terms of new photon operators $\hat{b}_n, \hat{b}_n^\dagger$, one can show that the Hamiltonian takes the following

form (see Exercise):

$$\hat{H}_{\rm C} = \frac{\hat{p}^2}{2m_e} + V(\hat{x}) - \hat{p}\sum_n \zeta_n(\hat{b}_n + \hat{b}_n^\dagger) + \sum_n \hbar\Omega_n \hat{b}_n^\dagger \hat{b}_n. \tag{5.3.40}$$

We then define the unitary transformation

$$\hat{U} = \exp\left(-\frac{i}{\hbar}\hat{p}\hat{\Xi}\right), \quad \hat{\Xi} \equiv \sum_k i\frac{\zeta_n}{\Omega_n}\left(\hat{b}_n^\dagger - \hat{b}_n\right), \tag{5.3.41}$$

which again does not reduce to a gauge transformation since it includes the operators $\hat{p}$ and $\hat{\Xi} \neq \hat{A}$. This transformation acts on each operator as

$$\hat{U}^\dagger \hat{x} \hat{U} = \hat{x} + \hat{\Xi}, \tag{5.3.42}$$

$$\hat{U}^\dagger \hat{b}_n \hat{U} = \hat{b}_n + \frac{\zeta_n}{\hbar\Omega_n}\hat{p}. \tag{5.3.43}$$

Note that the coefficients in $\hat{\Xi}$ are chosen in such a way that, at this time, the interaction term $-\hat{p}\sum_n \zeta_n(\hat{b}_n + \hat{b}_n^\dagger)$ in $\hat{H}_{\rm C}$ is cancelled by the term arising from the displacement of $\hat{b}^\dagger\hat{b}$ term. After some calculations which we leave to Exercise, the transformed Hamiltonian is given by a very simplified form:

$$\hat{H}_{\rm AD} = \hat{U}^\dagger \hat{H}_{\rm C} \hat{U} \tag{5.3.44}$$

$$= \frac{\hat{p}^2}{2m_{\rm eff}} + V(\hat{x} + \hat{\Xi}) + \sum_n \hbar\Omega_n \hat{b}_n^\dagger \hat{b}_n \tag{5.3.45}$$

with the mass being renormalized to

$$m_{\rm eff} \equiv m_e\left(1 + 2\sum_k \frac{e^2 f_k^2}{m_e \hbar\omega_k}\right). \tag{5.3.46}$$

This expression of the Hamiltonian may look similar to the Pauli-Fierz-Kramers form (5.3.38), however, the crucial point is that the present one (5.3.45) is *exact* and valid for arbitrary light-matter coupling strengths (as far as the long wavelength approximation is meaningful). As we will revisit later, an advantage of this frame is that the effective light-matter coupling strength (characterized by ζ_n/Ω_n) asymptotically vanishes in the strong coupling limit $e \to \infty$. This "asymptotic freedom" can simplify the analysis of strong coupling physics in quantum light-matter systems.

5.3.4. Spontaneous emission: Wigner-Weisskopf theory. We here illustrate an application of nonrelativistic QED to yet another elemental process, namely, *spontaneous emission* of a photon from an excited atom. Suppose that the emission is induced by the light-matter interaction between an atomic dipole, which can be modeled by an effectively two-level system, and vacuum electromagnetic field in free space. Projecting the PZW-gauge Hamiltonian (5.3.11) onto the two-level manifold, the total Hamiltonian is obtained by

$$\hat{H}_{\rm PZW} = \hbar\omega_a\left(\frac{\hat{\sigma}^z + 1}{2}\right) - \hat{\sigma}^x \sum_{\mathbf{k}\lambda}(g_{\mathbf{k}}\hat{a}_{\mathbf{k}\lambda} + {\rm H.c.}) + \sum_{\mathbf{k}\lambda}\hbar\omega_{\mathbf{k}}\hat{a}_{\mathbf{k}\lambda}^\dagger\hat{a}_{\mathbf{k}\lambda}, \tag{5.3.47}$$

where we introduce the coupling strengths and the dipole matrix element by

$$g_{\mathbf{k}} = \sqrt{\frac{\omega_{\mathbf{k}}}{2\hbar\epsilon_0 V}}\mathbf{d}\cdot\boldsymbol{\epsilon}_{\mathbf{k}\lambda}e^{i\mathbf{k}\cdot\mathbf{r}},\quad \mathbf{d}\equiv\langle e|(-e\hat{\mathbf{r}})|g\rangle. \tag{5.3.48}$$

To further simplify the analysis, one can perform the rotating wave approximation and the Born-Markov approximation, which can be justified when the light-matter interaction is sufficiently weak. The former leads to the interaction term

$$\hat{H}_{SE} = -\left(\hat{\sigma}^+\sum_{\mathbf{k}\lambda} g_{\mathbf{k}}\hat{a}_{\mathbf{k}\lambda} + \hat{\sigma}^-\sum_{\mathbf{k}\lambda} g^*_{\mathbf{k}}\hat{a}^\dagger_{\mathbf{k}\lambda}\right), \tag{5.3.49}$$

while the latter allows us to treat the problem of spontaneous emission within the framework of Markovian open systems by integrating out the electromagnetic field. Following the general argument given in Chapter 3, we obtain the total decay rate (see Eq. (3.7.17)):

$$\Gamma = 2\sum_{\mathbf{k}\lambda}\int_0^\infty d\tau|g_{\mathbf{k}}|^2 e^{i\omega_a\tau}\langle 0|\hat{a}_{\mathbf{k}}e^{-i\omega_{\mathbf{k}}\tau}\hat{a}^\dagger_{\mathbf{k}}|0\rangle \tag{5.3.50}$$

$$= \int_0^\infty \frac{2k^2dk}{\pi^2}\frac{ck}{2\hbar\epsilon_0}\frac{|\mathbf{d}|^2}{3}\pi\delta(\omega_a - ck) \tag{5.3.51}$$

$$= \frac{\omega_a^3|\mathbf{d}|^2}{3\pi\epsilon_0\hbar c^3} \tag{5.3.52}$$

where we assume the isotropic atom

$$|\mathbf{d}\cdot\boldsymbol{\epsilon}_{\mathbf{k}\lambda}|^2 = \frac{1}{3}|\mathbf{d}|^2 \tag{5.3.53}$$

and used the relations

$$\frac{1}{V}\sum_{\mathbf{k}} \to \int\frac{d^3k}{(2\pi)^3},\quad \omega_{\mathbf{k}} = ck, \tag{5.3.54}$$

$$\int_0^\infty d\tau e^{i(\omega_a-\omega_{\mathbf{k}})\tau} = \pi\delta(\omega_a-\omega_{\mathbf{k}}) + \mathrm{P.v.}\frac{i}{\omega_a-\omega_{\mathbf{k}}}. \tag{5.3.55}$$

The resulting Markovian master equation for the spontaneous emission is (see Eq. (3.7.18))

$$\frac{d\hat{\rho}}{dt} = -\frac{i}{\hbar}\left(\hat{H}_{\text{eff}}\hat{\rho} - \hat{\rho}\hat{H}^\dagger_{\text{eff}}\right) + \Gamma\hat{\sigma}^-\hat{\rho}\hat{\sigma}^+, \tag{5.3.56}$$

$$\hat{H}_{\text{eff}} \equiv \hbar\omega_a\left(\frac{\hat{\sigma}^z+1}{2}\right) - \frac{i\hbar\Gamma}{2}\hat{\sigma}^+\hat{\sigma}^- = \hbar\left(\omega_a - \frac{i\Gamma}{2}\right)\left(\frac{\hat{\sigma}^z+1}{2}\right). \tag{5.3.57}$$

If an observer can access information about electromagnetic modes (by, for example, photodetectors) and knows that no photon is emitted, the initial state then evolves under the effective non-Hermitian Hamiltonian which is characterized by a complex energy $\hbar(\omega_a - i\Gamma/2)$. In contrast, if an observer does not know about when a photon is emitted, the correct description is the master equation and the initially pure state evolves into a mixed density matrix.

To check that the obtained decay rate is indeed small as appropriate for validating the master-equation description, we can rewrite

$$\Gamma = \frac{4\alpha_{\rm QED}\omega_a^3|\mathbf{d}|^2}{3c^2e^2},\quad \alpha_{\rm QED} \equiv \frac{e^2}{4\pi\epsilon_0\hbar c} \simeq \frac{1}{137}. \tag{5.3.58}$$

Thus, we have $\Gamma/\omega_a \sim \alpha_{\rm QED}(r_a/\lambda_a)^2 \ll 1$ where r_a is the size of the atomic dipole $r_a = |\mathbf{d}|/e$ and λ_a is the wavelength for atomic transition and we used the long-wavelength condition $r_a/\lambda_a \ll 1$.

5.4. Brief introduction to Cavity/Waveguide QED

As we have seen in the previous section, the light-matter interaction between a quantum emitter and quantum electromagnetic field in free space is very weak, which ultimately has its origin in the smallness of the fine structure constant $\alpha_{\rm QED}$. This can be problematic especially in the fields of quantum information technologies or quantum optics, since one needs strong light-matter interaction to efficiently and faithfully operate, convert, and propagate quantum information in-between (artificial) atoms and photons.

One way to circumvent this difficulty is to confine electromagnetic fields into a tiny box, namely, *cavity*. This confinement effectively enhances the quantum light-matter interaction since the coupling strength is proportional to $1/\sqrt{V}$ with V being the mode volume. The resulting strong quantum light-matter coupling allows one to study the interaction between atoms and photons in (typically a few) discrete electromagnetic modes at the fundamental level of single quanta. This field, which studies quantum electrodynamics of atoms and photons confined in cavity, is known as *cavity QED*. More recently, similar strong coupling is also achieved for (artificial) atoms coupled to photons in continuum modes; this emerging field is coined as *waveguide QED*, since continuum electromagnetic modes are typically realized in certain waveguide resonators. Below we shall briefly address some of basics in these fields.

5.4.1. Two-level approximation: quantum Rabi model and Dicke model. To introduce a simplified model for describing cavity QED systems, we typically assume that only a single electromagnetic mode in a cavity is dominantly coupled to an atomic dipole. We then start from the effective QED Hamiltonian in the Coulomb gauge:

$$\hat{H}_{\rm C} = \frac{\left[\hat{p} + e\hat{A}\right]^2}{2m_e} + V(\hat{x}) + \hbar\omega_c\hat{a}^\dagger\hat{a},\quad \hat{A} = f\left(\hat{a} + \hat{a}^\dagger\right), \tag{5.4.1}$$

where f is the mode amplitude depending on the cavity geometry and ω_c is the cavity frequency. A standard choice of a potential $V(x)$ for modeling an atomic dipole is the double well potential,

$$V(x) = v\left(1 - \frac{x^2}{D^2}\right)^2, \tag{5.4.2}$$

which has two degenerate minima at $x = \pm D$; then, it can represent the spectrum of atomic dipole of size $\simeq -eD$. The two lowest energy levels play the role of the ground and first excited states, and we may project the Hamiltonian onto such two-level manifold (i.e., the two-level approximation) to further simplify the analysis.

For the purpose of performing the two-level approximation, it is advantageous to switch to the PZW gauge:

$$\hat{H}_{\rm PZW} = \hat{U}^\dagger \hat{H}_{\rm C} \hat{U}, \tag{5.4.3}$$

$$= \frac{\hat{p}^2}{2m_e} + V(\hat{x}) + mg^2\hat{x}^2 + ig\sqrt{m\hbar\omega_c}\hat{x}(\hat{a}^\dagger - \hat{a}) + \hbar\omega_c \hat{a}^\dagger\hat{a}, \tag{5.4.4}$$

where the PZW transformation is given by

$$\hat{U} = e^{\frac{-ie\hat{x}\hat{A}}{\hbar}}, \;\; g \equiv -ef\sqrt{\frac{\omega_c}{m\hbar}}. \tag{5.4.5}$$

While the Coulomb and PZW gauges must provide the same results if no approximation is made, the two-level approximation can in fact make differences between them. In other words, the validity of the two-level approximation in fact depends on a choice of reference frames. It is now understood that the PZW gauge is well suited for obtaining a two-level description up to the regimes in which the light-matter coupling strength reaches to an order of elementary excitation energies $\hbar\omega_{a,c}$ (known as ultrastrong coupling regimes).

To derive the two-level model in the PZW gauge, we consider the two lowest levels of the renormalized single-particle Hamiltonian $\hat{H}_0 = \frac{\hat{p}^2}{2m_e} + V(\hat{x}) + mg^2\hat{x}^2$ in Eq .(5.4.4); note that the last term, $mg^2\hat{x}^2$, represents the dipole self-energy. We denote the two-level manifold of $\hat{H}_0$ by $\{|g\rangle, |e\rangle\}$ and introduce the Pauli operators as

$$\hat{\sigma}^z = |e\rangle\langle e| - |g\rangle\langle g|, \;\; \hat{\sigma}^x = |e\rangle\langle g| + |g\rangle\langle e|. \tag{5.4.6}$$

Projecting the matter part of $\hat{H}_{\rm PZW}$ onto this manifold, we obtain the two-level effective model, often called the *quantum Rabi model*, as follows:

$$\hat{H}_{\rm Rabi} = \frac{\hbar\omega_a}{2}\hat{\sigma}^z + \hbar\lambda\hat{\sigma}^x\left(\hat{a}^\dagger + \hat{a}\right) + \hbar\omega_c\hat{a}^\dagger\hat{a}, \tag{5.4.7}$$

where $\lambda \equiv f\omega_c d/\hbar$ with $d = \langle e|(-e\hat{x})|g\rangle$ and we replaced $\hat{a} \to i\hat{a}$.

These arguments can straightforwardly be generalized to the case of N atomic dipoles coupled to a cavity electromagnetic mode. Specifically, we start from the Coulomb-gauge Hamiltonian

$$\hat{H}_{\rm C} = \sum_{i=1}^{N}\left[\frac{\left[\hat{p}_i + e\hat{A}\right]^2}{2m_e} + V(\hat{x}_i)\right] + \hbar\omega_c\hat{a}^\dagger\hat{a}, \tag{5.4.8}$$

and perform the multi-dipole PZW transformation $\hat{U} = \exp\left[\frac{-ie\sum_i \hat{x}_i\hat{A}}{\hbar}\right]$, after which we project the transformed Hamiltonian onto the two-level manifold, and obtain

$$\hat{H}_{\rm Dicke} = \frac{\hbar\omega_a}{2}\sum_{i=1}^{N}\hat{\sigma}_i^z + \hbar\lambda\sum_{i=1}^{N}\hat{\sigma}_i^x\left(\hat{a}^\dagger + \hat{a}\right) + \hbar\omega_c\hat{a}^\dagger\hat{a} + \frac{\hbar\lambda^2}{\omega_c}\left(\sum_{i=1}^{N}\hat{\sigma}_i^x\right)^2. \tag{5.4.9}$$

The last term arises from the dipole self-energy of multiple atoms, which can also be interpreted as the cavity-mediated dipole-dipole coupling. Strictly speaking, this Hamiltonian should be referred to as the generalized Dicke model, since the original Dicke model usually refers to the model without the self-energy term. In fact, the original Dicke model eventually becomes invalid at large λ and is known to give rise to qualitatively inaccurate predictions, such as an occurrence of the (equilibrium) superradiant transition at sufficiently large λ (see Exercise).

5.4.2. Rotating wave approximation: Jaynes-Cummings model. Consider a single atomic dipole coupled to a cavity electromagnetic mode. If the atomic frequency is near resonant and the light-matter interaction is weak in the sense $|\omega_a - \omega_c|, \lambda \ll \omega_{a,c}$, we can neglect the contributions from the counter rotating terms $\hat{\sigma}^+\hat{a}^\dagger$ and $\hat{\sigma}^-\hat{a}$ in the Rabi model (5.4.7), which are off-resonant and thus rotate rapidly in the rotating wave frame. This allows us to further simplify the two-level model (5.4.7) as follows:

$$\hat{H}_{\rm JC} = \frac{\hbar\omega_a}{2}\hat{\sigma}^z + \hbar\lambda\left(\hat{a}^\dagger\hat{\sigma}^- + \hat{a}\hat{\sigma}^+\right) + \hbar\omega_c\hat{a}^\dagger\hat{a}. \tag{5.4.10}$$

This Hamiltonian is known as the *Jaynes-Cummings model* and has a conserved quantity

$$\hat{N}_{\rm ex} = \hat{a}^\dagger\hat{a} + \frac{\hat{\sigma}^z + 1}{2}. \tag{5.4.11}$$

The ground state with $N_{\rm ex} = 0$ is unique and given by $|g\rangle|0\rangle$, while other sector at nonzero $N_{\rm ex}$ is spanned by two states $|e\rangle|N_{\rm ex}-1\rangle$ and $|g\rangle|N_{\rm ex}\rangle$. The spectrum is then obtained by just solving the 2×2 eigenvalue problem. For instance, at the resonant condition $\omega_a = \omega_c$, excitation energies are given by

$$E_{N_{\rm ex},\pm} = N_{\rm ex}\omega_a \pm \lambda\sqrt{N_{\rm ex}}. \tag{5.4.12}$$

The corresponding energy eigenstates hybridize light and matter degrees of freedom and are often called as *dressed* states.

The energy splittings $2\lambda\sqrt{N_{\rm ex}}$ depend on the excitation number $N_{\rm ex}$, which have interesting physical consequences. To see this, consider exciting an atom by a low-photon external pumping at frequency ω. In the limit of $\lambda \to 0$, all the transition processes become resonant at $\omega = \omega_a$. At $\lambda \neq 0$, however, the $N_{\rm ex}$ dependence of energy splittings allow one to choose ω such that only a specific process is resonant. Thus, in the ideal case where the linewidth is sufficiently small compared to λ, one can realize an effectively nonlinear optical medium. For instance, if one chooses $\omega = \omega_a - \lambda$, only a single photon can be excited since two (and higher) photon excitation processes are off-resonant and suppressed, leading to effective "photon blockade".

5.4.3. Strong-coupling physics: asymptotic freedom. The two-level description discussed above ultimately breaks down when the coupling strength reaches and surpasses elementary excitation energies $\omega_{a,c}$. Physically, this is because at such strong couplings the photon and atoms are strongly entangled and

thus they form hybridized states consisting of superposition of high-lying energy modes in both photon and atomic levels. It is this strong entanglement that invalidates the level truncations necessary to derive the two-level models.

To circumvent this difficulty, we can perform the asymptotically decoupling unitary transformation that we introduced in the previous section. To see this, we first rewrite the Coulomb-gauge Hamiltonian (5.4.1) as

$$\hat{H}_{\rm C} = \frac{\hat{p}^2}{2m_e} + V(\hat{x}) - g\sqrt{\frac{\hbar}{m\Omega}}\hat{p}(\hat{b}+\hat{b}^\dagger) + \hbar\Omega\hat{b}^\dagger\hat{b}, \tag{5.4.13}$$

$$\Omega \equiv \sqrt{\omega_c^2 + 2g^2}, \tag{5.4.14}$$

where we perform the Bogoliubov transformation $\hat{b}+\hat{b}^\dagger = \sqrt{\Omega/\omega_c}(\hat{a}+\hat{a}^\dagger)$. We then use the unitary transformation to get

$$\hat{H}_{\rm AD} = \hat{U}^\dagger\hat{H}_{\rm C}\hat{U} \tag{5.4.15}$$

$$= \frac{\hat{p}^2}{2m_{\rm eff}} + V(\hat{x}+\hat{\Xi}) + \hbar\Omega\hat{b}^\dagger\hat{b} \tag{5.4.16}$$

where we introduce

$$m_{\rm eff} = m_e(1+2(g/\omega_c)^2), \quad \hat{\Xi} = i\xi(\hat{b}^\dagger - \hat{b}), \tag{5.4.17}$$

$$\hat{U} = \exp\left[-\frac{i\hat{p}\hat{\Xi}}{\hbar}\right]. \tag{5.4.18}$$

Here, the length scale ξ characterizes the effective light-matter coupling strength in the transformed frame and defined by

$$\xi \equiv g\sqrt{\frac{\hbar}{m\Omega^3}} = \sqrt{\frac{\hbar g^2}{m(\omega_c^2+2g^2)^{3/2}}}. \tag{5.4.19}$$

Note that ξ converges as $\xi \propto g^{-1/2} \to 0$ in the strong-coupling limit $g \gg \omega_c$. This means that atoms and photons are asymptotically decoupled in the strong coupling regimes. One can then easily study strong-coupling physics of light-matter systems in this frame, which is otherwise difficult to analyze in general.

5.4.4. Waveguide QED Hamiltonian and Spin-Boson model. We have so far assumed that atoms are coupled to only a single electromagnetic mode. If we couple atoms to electromagnetic modes of waveguide resonators instead of cavity, atoms in general couple to *continuum* electromagnetic modes. The discussions above for cavity QED can be extended to the case of such waveguide QED setups possessing multiple continuum photon modes.

A particularly well-known model in this context is the continuum-mode counterpart of the Rabi model, which is also known as the *spin-boson model*:

$$\hat{H}_{\rm SB} = \frac{\hbar\omega_a}{2}\hat{\sigma}^z + \hat{\sigma}^x \sum_k \hbar\lambda_k \left(\hat{a}^\dagger + \hat{a}\right) + \sum_k \hbar\omega_k \hat{a}^\dagger \hat{a}. \tag{5.4.20}$$

The spin-boson model has historically been extensively studied in the context of open quantum systems, as it can describe dissipative dynamics of a spin-1/2 coupled to bosonic baths. Unless λ_k is sufficiently weak, the master equation approach is in general insufficient and thus this model belongs to a class of non-Markovian (or nonperturbative) open quantum systems. It is interesting to note that its ground state can exhibit the quantum phase transition of the Berezinskii-Kosterlitz-Thouless (BKT) type. Under certain conditions, this transition can be identified as the antiferromagnetic-to-ferromagnetic transition in the anisotropic Kondo model. However, to apply the spin-boson description to waveguide QED systems, we have to keep in mind that this two-level description can be a good effective model only when a number of assumptions used above are plausible. When some of those assumptions (such as the two-level approximation etc) break down (which might be the case especially at strong light-matter couplings), we have to go back to the original QED Hamiltonian and reexamine the validity of the analysis.

5.4.5. Circuit realizations. As we briefly mentioned in the previous Chapter, one can use superconducting circuits to study the physics of quantum light-matter interaction; this field is often coined as circuit QED. To complete the analogy between circuit QED and cavity QED, let us recall the Hamiltonians in each case:

$$\hat{H}_{\rm circuit} = 4E_C \left(\hat{N} - \hat{N}_g\right)^2 - E_J \cos\varphi + \hbar\omega_r \hat{a}^\dagger \hat{a}, \quad \hat{N}_g \propto \hat{a}^\dagger + \hat{a}, \tag{5.4.21}$$

$$\hat{H}_{\rm cavity} = \frac{\left[\hat{p} + e\hat{A}\right]^2}{2m_e} + V(\hat{x}) + \hbar\omega_c \hat{a}^\dagger \hat{a}, \quad \hat{A} \propto \hat{a} + \hat{a}^\dagger. \tag{5.4.22}$$

It is now clear that these two models are essentially equivalent if we identify the potential in the cavity QED Hamiltonian as the periodic potential $V(x) \propto \cos(2\pi x/\lambda)$.

In circuit QED, the Josephson junction plays the role of an artificial atom which is coupled to microwave photons in LC circuit. If we couple a Josephson junction to a more complex circuit with infinite length, this artificial atom will interact with continuum of microwave photons, thus offering an ideal platform to study physics of waveguide QED[3]. Owing to low frequency of photons in circuit setups (typically in microwave regimes), it is usually easier to attain strong light-matter couplings in circuit setups than conventional cavity QED setups (typically in optical regimes). Circuit QED systems are thus also one of the most ideal experimental platforms for exploring physics of strong quantum light-matter interaction.

[3]Strictly speaking, the analogy with the waveguide QED Hamiltonian may not be perfect in this case, since the $\hat{A}^2$ may in fact take a slightly different form depending on circuit geometry in circuit QED Hamiltonian.

Summary of Chapter 5

Section 5.1-5.3 Quantum electrodynamics in the Coulomb gauge and unitary transformations

- To eliminate the redundant degrees of freedom, one can impose the Coulomb gauge condition, after which the standard canonical quantization procedure allows us to obtain the QED Hamiltonian (5.2.7).
- The unitary transformation that only includes the particle positions $\hat{\mathbf{r}}_\alpha$ and the vector potential $\hat{\mathbf{A}}$ generates a gauge transformation. One example is the Power-Zienau-Woolley transformation, after which the interaction is described by the $\mathbf{r} \cdot \mathbf{E}$ term at the leading order.
- There also exist unitary transformations that go beyond gauge transformations. Examples include the Pauli-Fierz-Kramers or asymptotically decoupling transformations, which can be particularly useful in strong light-matter coupling regimes.

Section 5.4 Brief introduction to cavity/waveguide QED

- If a dipole is dominantly coupled to only a single electromagnetic mode, we can use the two-level effective model called the quantum Rabi model. This model can be faithfully derived from the QED Hamiltonian in the PZW gauge up to ultrastrong coupling regimes. Its N-dipole generalization gives the (generalized) Dicke model.
- When the rotating wave approximation is valid, one can further simplify the model to the Jaynes-Cummings Hamiltonian.
- A single two-level system coupled to continuum electromagnetic modes can be modeled by the spin-boson model.
- When light-matter coupling strength reaches/surpasses energy scales of elementary excitations, both the two-level and rotating wave approximations break down in general. In such regimes, one may use the asymptotically decoupling transformation to simplify the analysis.

5.5. Exercises

Exercise 5.1 (PZW gauge without long-wave approximation: 2 points). Introduce the atomic polarization density by

$$\hat{\mathbf{P}}(\mathbf{r}) \equiv -e\hat{\mathbf{r}} \int_0^1 du\, \delta(\mathbf{r} - u\hat{\mathbf{r}}). \tag{5.5.1}$$

Consider the gauge transformation (called the PZW transformation) corresponding to the following unitary operator:

$$\hat{U} = \exp\left[\frac{i}{\hbar}\int d^3r\, \hat{\mathbf{P}}(\mathbf{r}) \cdot \hat{\mathbf{A}}(\mathbf{r})\right]. \tag{5.5.2}$$

Check that this reduces to Eq. (5.3.4) after performing the long-wave approximation.

We here aim to derive the transformed Hamiltonian without resorting to the long-wave approximation. To do so, consider the exact Coulomb-gauge Hamiltonian

$$\hat{H}_{\rm C} = \frac{\left[\hat{\mathbf{p}} + e\hat{\mathbf{A}}(\hat{\mathbf{r}})\right]^2}{2m_e} + V(\hat{\mathbf{r}}) + \sum_{\mathbf{k}\lambda} \hbar\omega_{\mathbf{k}} \hat{a}^\dagger_{\mathbf{k}\lambda}\hat{a}_{\mathbf{k}\lambda}, \tag{5.5.3}$$

with

$$\hat{\mathbf{A}}(\mathbf{r}) = \sum_{\mathbf{k}\lambda} \sqrt{\frac{\hbar}{2\epsilon_0\omega_{\mathbf{k}}V}} \left(\hat{a}_{\mathbf{k}\lambda}\boldsymbol{\epsilon}_{\mathbf{k}\lambda}e^{i\mathbf{k}\cdot\mathbf{r}} + \text{H.c.}\right). \tag{5.5.4}$$

Show that the PZW transformation above leads to the following transformed Hamiltonian:

$$\begin{aligned}\hat{H}_{\rm PZW} &= \hat{U}^\dagger \hat{H}_{\rm C} \hat{U} \\ &= \frac{\left(\hat{\mathbf{p}} - e\hat{\mathbf{r}} \times \int_0^1 du\, u\hat{\mathbf{B}}(u\hat{\mathbf{r}})\right)^2}{2m_e} + V(\hat{\mathbf{r}}) - \int d^3r\, \hat{\mathbf{P}}^\perp(\mathbf{r}) \cdot \hat{\mathbf{E}}^\perp(\mathbf{r}) \qquad (5.5.5)\\ &+ \frac{1}{2\epsilon_0}\int d^3r\, \hat{\mathbf{P}}^{\perp 2}(\mathbf{r}) + \sum_{\mathbf{k}\lambda} \hbar\omega_{\mathbf{k}}\hat{a}^\dagger_{\mathbf{k}\lambda}\hat{a}_{\mathbf{k}\lambda}. \qquad (5.5.6)\end{aligned}$$

You may use the relations

$$\sum_{\mathbf{k}\lambda} \hbar\omega_{\mathbf{k}}\hat{a}^\dagger_{\mathbf{k}\lambda}\hat{a}_{\mathbf{k}\lambda} + \text{const.} = \frac{\epsilon_0}{2}\int d^3r \left[\hat{\mathbf{E}}^{\perp 2}(\mathbf{r}) + c^2\hat{\mathbf{B}}^2(\mathbf{r})\right], \tag{5.5.7}$$

$$[\hat{A}_\alpha(\mathbf{r}, t), -\epsilon_0\hat{E}_\beta(\mathbf{r}', t)] = i\hbar\delta^\perp_{\alpha\beta}(\mathbf{r} - \mathbf{r}'). \tag{5.5.8}$$

Exercise 5.2 (Applications of TRK sum rule: 2 points). (a) Show the equivalence between expressions of matrix elements for two-photon scattering process in different gauges:

$$g_{nm} = \tilde{g}_{nm} \tag{5.5.9}$$

where

$$g_{nm} \equiv \left(\frac{e}{m}\right)^2 \sum_l \frac{\langle n|\hat{p}|l\rangle\langle l|\hat{p}|m\rangle}{\omega - \omega_{lm}}, \quad \tilde{g}_{nm} \equiv -\omega^2 e^2 \sum_l \frac{\langle n|\hat{r}|l\rangle\langle l|\hat{r}|m\rangle}{\omega - \omega_{lm}} \tag{5.5.10}$$

with the two-photon resonant frequency

$$\omega = \frac{\omega_{nm}}{2}. \tag{5.5.11}$$

You may use the TRK sum rule:

$$\sum_l (\omega_{ln} + \omega_{lm}) \langle n|\hat{r}|l\rangle\langle l|\hat{r}|m\rangle = \frac{\hbar}{m}\delta_{nm}. \tag{5.5.12}$$

(b) Consider the Dicke model (5.4.9) at large, but finite number N of electric dipoles. Use the TRK sum rule to show that the energy difference between the first excited state and the ground state does not vanish at any finite light-matter coupling strength[4]. What would happen if the last term (self-energy term) in Eq. (5.4.9) is neglected? You may use the Holstein-Primakoff approximation:

$$\sum_{i=1}^{N} \hat{\sigma}_i^+ \simeq \sqrt{N}\hat{b}^\dagger, \quad \sum_{i=1}^{N} \hat{\sigma}^z \simeq -N + 2\hat{b}^\dagger\hat{b}, \tag{5.5.13}$$

where $\hat{b}, \hat{b}^\dagger$ are bosonic operators obeying $[\hat{b}, \hat{b}^\dagger] = 1$.

Exercise 5.3 (Mass renormalization in the asymptotically decoupled frame: 2 points). Consider the Coulomb-gauge Hamiltonian in the long-wave approximation:

$$\hat{H}_{\rm C} = \frac{\left[\hat{p} + e\hat{A}\right]^2}{2m_e} + V(\hat{x}) + \sum_k \hbar\omega_k \hat{a}_k^\dagger \hat{a}_k, \tag{5.5.14}$$

$$\hat{A} = \sum_k f_k \left(\hat{a}_k + \hat{a}_k^\dagger\right). \tag{5.5.15}$$

(a) The quadratic photon part can be diagonalized as

$$\frac{e^2\hat{A}}{2m_e} + \sum_k \hbar\omega_k \hat{a}_k^\dagger \hat{a}_k = \sum_n \hbar\Omega_n \hat{b}_n^\dagger \hat{b}_n + \text{const.} \tag{5.5.16}$$

[4]This argument essentially forbids realization of the equilibrium superradiant transition in cavity QED systems with a single electromagnetic mode, which is often called "no-go theorem". Note, however, that possibility of realizing superradiant transition is not excluded in general multi-mode cases.

via the canonical transformation

$$\hat{a}_k = \sum_n (O)_{kn} \left[\cosh(r_{nk}) \hat{b}_n - \sinh(r_{nk}) \hat{b}_n^\dagger \right], \tag{5.5.17}$$

where $r_{nk} \in \mathbb{R}$ are squeezing parameters while O is an orthogonal matrix. Determine the expression of r_{nk} and derive the relation satisfied by O.

(b) In terms of $\hat{b}$ operators, the Hamiltonian can be written as

$$\hat{H}_{\rm C} = \frac{\hat{p}^2}{2m_e} + V(\hat{x}) - \hat{p} \sum_n \zeta_n (\hat{b}_n + \hat{b}_n^\dagger) + \sum_n \hbar \Omega_n \hat{b}_n^\dagger \hat{b}_n. \tag{5.5.18}$$

Determine the expression of ζ_n by using O. Using the relation derived in (a), show the following relation

$$\frac{1}{1 - 2\sum_n \frac{m_e \zeta_n^2}{\hbar \Omega_n}} = 1 + 2 \sum_k \frac{e^2 f_k^2}{m_e \hbar \omega_k}. \tag{5.5.19}$$

Check that this relation leads to the simplified expression of the mass renormalization in $m_{\rm eff}$ of the AD-frame Hamiltonian:

$$\hat{H}_{\rm AD} = \hat{U}^\dagger \hat{H}_{\rm C} \hat{U} = \frac{\hat{p}^2}{2m_{\rm eff}} + V(\hat{x} + \hat{\Xi}) + \sum_n \hbar \Omega_n \hat{b}_n^\dagger \hat{b}_n \tag{5.5.20}$$

where

$$\hat{U} = \exp\left(-\frac{i}{\hbar} \hat{p} \hat{\Xi} \right), \quad \hat{\Xi} \equiv \sum_k i \frac{\zeta_n}{\Omega_n} \left(\hat{b}_n^\dagger - \hat{b}_n \right) \tag{5.5.21}$$

and

$$m_{\rm eff} = m_e \left(1 + 2 \sum_k \frac{e^2 f_k^2}{m_e \hbar \omega_k} \right). \tag{5.5.22}$$

Exercise 5.4 (Spontaneous emission: 1 point). Consider the isotropic two-level atom coupled to vacuum electromagnetic field. Derive the formula (5.3.52) of the spontaneous emission rate from Fermi's golden rule.

CHAPTER 6

Machine learning and quantum science

6.1. Introduction

The field of machine learning, especially artificial neural networks, has witnessed remarkable developments in recent years, and is revolutionizing science and technology. Deep neural networks are now routinely applied to classify or recognize patterns/images, translate sentences or speech between different languages, predict traffic or market trading, and to attain self-driving cars, device/robot controls, and superhuman performance in table/video games. In the context of physical science (especially quantum science), the idea of machine learning has also led to many interesting developments in these years. In the next two Chapters, we try to give brief and introductory descriptions about some of key concepts/topics in this rapidly growing field.

In machine learning, there are mainly three classes of problems, namely, supervised, unsupervised, and reinforcement learning. *Supervised learning* handles data consisting of a pair of vectors $\{\mathbf{x}_i, \mathbf{y}_i\}_{i=1}^n$ with $\mathbf{y}$ being often called a label and n being the number of data. The goal of supervised learning is to estimate a function f that relates these two vectors via $\mathbf{y} = f(\mathbf{x})$. We call it as "supervised" since the correct answer (i.e., label) $\mathbf{y}_i$ is given for each $\mathbf{x}_i$ by "teacher", and machine is trained by "teacher" according to this dataset. In contrast, *unsupervised learning* deals with data that only contains some set of vectors $\{\mathbf{x}_i\}_{i=1}^n$ that is supposed to be randomly generated by a certain probability distribution $p(\mathbf{x})$. Typically, unsupervised learning aims to either extract essential features/structures behind the data or even (approximately) construct the distribution $p(\mathbf{x})$ itself by using some tractable ansatz. Since there is no "teacher" who tells us the label, it is called "unsupervised".

In these two classes of learning problems, the trained machine can at most reproduce or imitate the ways that are taught or predicted by the original dataset; machines thus cannot have sort of creativity, in the sense that they would neither realize performance beyond the teacher nor predict something new that is not expected from the dataset.

Roughly speaking, *reinforcement learning* aims to train machines to acquire that sort of creativity for achieving better performance by repeating a huge number of trials and errors. In reinforcement learning, data is not given in advance in contrast to supervised/unsupervised learning, but machine itself acquires knowledge about data to find the best solution by interacting with an environment. Each solution associates with some figure of merit called "reward", and on the basis of its value, the machine tries to search a better solution from the repetitions of trials and errors. In this sense, there is a feedback loop between the machine (also called agent) and environment, and in fact its theoretical framework fits well with theory of open quantum systems (or more specifically, continuous quantum measurement) as we discuss later.

Below we begin by introducing some basic concepts of machine learning and black-box optimizations. Building on these understandings, in the next Chapter, we proceed to learn about (deep) reinforcement learning.

6.2. Basic concepts

6.2.1. Supervised learning.

6.2.1.1. *Function approximation, cost function, and training.* As noted above, the goal of supervised learning is to identify a function approximation f that relates inputs $\mathbf{x}$ to outputs $\mathbf{y}$. We do this by hypothesizing a certain functional form f_θ parameterized by θ:

$$\mathbf{y} = f_\theta(\mathbf{x}). \tag{6.2.1}$$

Given a training dataset $\{\mathbf{x}_i, \mathbf{y}_i\}_{i=1}^n$, we then try to optimize θ in such a way that the resulting f_θ imitates the training dataset best.

To do so, we have to quantify how well the obtained function f_θ reproduces the training dataset. For this purpose, we introduce the *cost function* that usually decomposes into the sum of each data:

$$L(\theta) = \frac{1}{n}\sum_{i=1}^{n} \lambda(\mathbf{x}_i, \mathbf{y}_i; \theta). \tag{6.2.2}$$

One common way is to use the mean squared error as the cost function:

$$L(\theta) = \frac{1}{n}\sum_{i=1}^{n} |\mathbf{y}_i - f_\theta(\mathbf{x}_i)|^2 , \tag{6.2.3}$$

while the specific form of the cost function in general changes depending on type of the problem or a choice of f_θ.

After specifying the cost function, we next have to specify how in practice we attempt to find the optimal θ^* that would minimize $L(\theta)$. A process of finding the optimal values θ^* is commonly referred to as *training*, and the most common way for this is to simply apply the *gradient descent* method. Recall that we have already encountered the similar idea in the context of imaginary-time evolution of variational states in Chapter 4. At each time step, the gradient descent updates the parameters according to

$$\theta_{\tau+\delta\tau} = \theta_\tau - \eta \nabla_\theta L, \tag{6.2.4}$$

where η is some positive and small quantity, often called the learning rate. This means that we change the parameters along the negative gradient of the cost function. In practice, however, it often takes too much time to evaluate L by using all the possible training data. This difficulty can be circumvented by restricting the ensemble average in L to only a small subset of data called *mini batch*:

$$\theta_{\tau+\delta\tau} = \theta_\tau - \eta \nabla_\theta L_{\text{batch}}, \quad L_{\text{batch}} = \frac{1}{n_{\text{batch}}}\sum_{i=1}^{n_{\text{batch}}} |\mathbf{y}_i - f_\theta(\mathbf{x}_i)|^2 \tag{6.2.5}$$

with $n_{\text{batch}} < n$. This is often referred to as *stochastic gradient descent* in the sense that we use an approximation of the negative gradient, which brings certain noise compared to the "exact" gradient descent calculated from all the possible data. As we mentioned in Chapter 4, from a geometrical point of view, the gradient descent may be considered as the discrete-time version of the imaginary time evolution on the variational manifold spanned by f_θ.

It is important to note that the choice of a functional ansatz f_θ is crucial in supervised learning, but its exact form is unknown a priori in most of practical problems. So, on what basis can we specify such ansatz? A possible guiding principle for this is actually similar to the spirit of variational approach we discussed in Chapter 4. Specifically, we shall choose a functional ansatz that is (1) *flexible*, i.e., its representation capacity is large enough such that it can fit well with reasonably different patterns in practical problems (2) *tractable and efficient*, i.e., there is some efficient algorithm to optimize θ within a reasonable amount of time and numerical computing resource, and (3) *scalable*, i.e., it can easily be scaled up to handle high-dimensional data. Below we briefly discuss several illustrative examples in supervised learning.

Example 1: Kernel method, support vector machine, and variational quantum circuits. Suppose that we have dataset $\{\mathbf{x}_i, y_i\}_{i=1}^n$. The kernel method aims to predict output $y \in \mathbb{R}$ for a given input $\mathbf{x} \in \mathbb{R}^m$ by using the functional form,

$$y = \sum_{i=1}^{n} \alpha_i k(\mathbf{x}, \mathbf{x}_i), \tag{6.2.6}$$

where $\{\alpha_i\}$ are parameters of this model and k is a certain fixed (nonlinear) function called *kernel*. One of the most common choice is to use the Gaussian kernel

$$k(\mathbf{x}, \mathbf{x}') = \exp\left(-\beta \left|\mathbf{x} - \mathbf{x}'\right|^2\right). \tag{6.2.7}$$

In this choice, the kernel method tries to fit the data by using a linear superposition of many Gaussian functions as in Eq. (6.2.6).

The cost function is typically given by the mean squared error

$$L(\alpha) = \frac{1}{n} \sum_{i=1}^{n} \left| y_i - \sum_{j=1}^{n} \alpha_j k(\mathbf{x}_i, \mathbf{x}_j) \right|^2 + \sigma^2 \sum_{ij=1}^{n} \alpha_i k(\mathbf{x}_i, \mathbf{x}_j) \alpha_j, \tag{6.2.8}$$

where the last term is the regularization term that is introduced to avoid the overfitting or divergence of the parameters $\{\alpha_i\}$.

In fact, in the present problem, we can analytically identify the optimal α^* that minimizes the cost function (see Exercise):

$$\alpha_i^* = \sum_{j=1}^{n} \left(K + \sigma^2 I\right)_{ij}^{-1} y_j, \tag{6.2.9}$$

where I is the $n \times n$ identity matrix and we define the kernel matrix by

$$(K)_{ij} = k(\mathbf{x}_i, \mathbf{x}_j). \tag{6.2.10}$$

The resulting trained function is

$$y = \sum_{i=1}^{n} \alpha_i^* k(\mathbf{x}, \mathbf{x}_i) = \sum_{ij=1}^{n} k(\mathbf{x}, \mathbf{x}_i) \left(K + \sigma^2 I\right)_{ij}^{-1} y_j. \tag{6.2.11}$$

This allows us to estimate output y for a given unknown input $\mathbf{x}$.

It is worthwhile to note that the kernel method also gives a functional ansatz of the so-called *support vector machine*. Consider a binary classification problem with output $y \in \{-1, 1\}$. For a given input $\mathbf{x}$, the support vector machine predicts which class the input vector belongs to, i.e., it gives a positive (negative) class if the function takes a positive (negative) value:

$$y = \mathrm{sign}\left(\sum_{i=1}^{n} \alpha_i^* k(\mathbf{x}, \mathbf{x}_i) + b^*\right) \in \{-1, 1\}, \tag{6.2.12}$$

where we introduce a bias parameter b. In practice, the optimized vector α^* may have mostly zero components. One can then simplify the evaluation of the function by restricting the summation over only for dataset that have nonzero α_i^*, rather than over all the possible data.

We also note that, in fact, the kernel method has a close connection with some type of quantum machine learning algorithms. In the context of quantum machine learning, one typically encodes an input vector $\mathbf{x}$ into a quantum state $|\psi(\mathbf{x})\rangle$. One can then introduce the kernel function by using the inner product between two different quantum states by

$$k(\mathbf{x}, \mathbf{x}') = \left|\langle\psi(\mathbf{x})|\psi(\mathbf{x}')\rangle\right|^2, \tag{6.2.13}$$

and use the function ansatz $y = \sum_{i=1}^{n} \alpha_i k(\mathbf{x}, \mathbf{x}_i)$ in the same manner as above, but at this time the kernel function is evaluated from the overlap of quantum states.

A specific form of the kernel depends on type of available quantum computer and how one encodes the information into a quantum state. As a simple example, let us first consider a harmonic oscillator and suppose that input data is encoded by a displacement operator

$$|\psi(x)\rangle = \hat{D}(x)|0\rangle = e^{x(\hat{a}^\dagger - \hat{a})}|0\rangle. \tag{6.2.14}$$

For high-dimensional input data, we consider

$$|\psi(\mathbf{x})\rangle \equiv \prod_i |\psi(x_i)\rangle. \tag{6.2.15}$$

Then, the kernel actually corresponds to the usual Gaussian kernal:

$$k(\mathbf{x}, \mathbf{x}') = \left|\langle\psi(\mathbf{x})|\psi(\mathbf{x}')\rangle\right|^2 = \exp\left(-\left|\mathbf{x} - \mathbf{x}'\right|^2\right). \tag{6.2.16}$$

Experimentally, this choice would be relevant to photonic quantum computers in which a harmonic oscillator represents each electromagnetic mode.

Let us next consider a two-level system and its encoding:

$$|\psi(x)\rangle = \exp\left(-\frac{i}{2}x\hat{\sigma}^x\right)|\uparrow_z\rangle = \cos\left(\frac{x}{2}\right)|\uparrow_z\rangle - i\sin\left(\frac{x}{2}\right)|\downarrow_z\rangle \tag{6.2.17}$$

$$|\psi(\mathbf{x})\rangle \equiv \prod_i |\psi(x_i)\rangle. \tag{6.2.18}$$

This corresponds to the following kernel function

$$k(\mathbf{x},\mathbf{x}') = \left|\langle\psi(\mathbf{x})|\psi(\mathbf{x}')\rangle\right|^2 = \prod_i \cos^2\left(\frac{x_i - x_i'}{2}\right). \tag{6.2.19}$$

This situation should be relevant to a quantum computer consisting of, e.g., the superconducting qubits we explained in Chapter 4. One can then use these kernel functions (which can be evaluated on a quantum computer) as a functional ansatz to fit real-life data. Very roughly speaking, the idea along this line can be considered as one of what has been envisioned in the emerging field of quantum machine learning.

In practice, numerical cost of the kernel method is mainly set by the cost of calculating the inverse matrix $\left(K + \sigma^2 I\right)^{-1}$, which basically scales as $O(n^3)$ with n being the number of training data. Even if training has been performed in some way, the function evaluation requires the summation over dataset and its cost scales linear with n. Thus, the kernel method can in general be applied to a problem with rather modest size of data, such as $n \leq O(10^3)$. This limitation will become a major difficulty when we have to deal with a large dataset, namely, "big data". A possible solution for this is to introduce supervised learning using deep neural networks, as we briefly discuss next.

Example 2: Neural network and classifying phases of matter. Deep learning basically uses the following multilayer feed-forward neural network as a nonlinear functional ansatz f_θ:

$$f_\theta(\mathbf{x}) = g(w_L \cdots g(w_2\, g(w_1\mathbf{x}))), \tag{6.2.20}$$

where $\mathbf{x}$ is the input vector, w_i are weight matrices that map input vector at each layer i to another vector that becomes an input vector to the next layer, and g is some nonlinear function called activation function. Typical choices for g are

$$g_{\rm sigmoid}(x) = \frac{1}{1+e^{-x}}, \quad g_{\rm ReLU}(x) = \begin{cases} x & x \geq 0 \\ 0 & x < 0 \end{cases}, \tag{6.2.21}$$

where ReLU stands for the Rectified Linear Unit function. One may also introduce the bias vector and consider the affine transformation $w_i\mathbf{x} + \mathbf{b}$. Although it is not the purpose of this course to explain about details of deep learning, we here remark that there is an efficient and simple algorithm (based on the stochastic gradient descent and chain-rule calculations of derivatives) to train this function in a reasonable

amount of time even for vastly large dataset. From empirical success of deep learning, we know that the trained function f_{θ^*} found by this algorithm would fit well training data set and, surprisingly, somehow generalizes well (i.e., it can predict well for unknown input). Interestingly, this seems to be the case when the network is deep and has many layers, for which the function appears to be overparametrized. Currently, it is a commonly held view that there is still little theoretical understanding behind this unreasonable success of deep learning.

One of the most well-known applications of the multilayer feed-forward neural network (or precisely, so-called convolutional neural network) is the problem of image classification. It basically gets 2D image as an input data and predicts which class that image belongs to, say, cat or dog. In the context of physics, the success of deep learning in this problem inspires physicists to apply it to the problem of classifying phases of matter. From a close analogy with the variational approach in quantum many-body physics, deep neural networks also motivate quantum physicists to use them as variational ansatz for quantum many-body wavefunctions, as we briefly discuss later. Interested students may refer to, for example, [Rev. Mod. Phys. 91, 045002 (2019)].

6.2.2. Unsupervised learning. In unsupervised learning, we deal with data $\{\mathbf{x}_i\}_{i=1}^n$ without labels and typically aim to extract essential information about the probability distribution that generates training dataset. In some cases, one attempts to directly construct the probability distribution itself by using a certain functional ansatz and optimizing it to find the best approximations of the distribution. There are many different ways for doing this, but here let us only mention two of the most well-known examples.

Example 3: Autoencoder. Suppose that we have dataset which should possess certain structure, but we do not know what structure it specifically represents since the data has no labels; one may imagine, for instance, a set of 2D images of animals for some unknown different species. How can one identify the possible structure behind the data? The idea of *autoencoder* is to use neural networks to extract key features of dataset by compressing the original data into a much smaller vector space, but without loosing essential information. Specifically, it attempts to reproduce its input vector itself as output vector:

$$\mathbf{x} \simeq f_\theta(\mathbf{x}) \tag{6.2.22}$$

by optimizing θ in neural networks whose middle layers have much fewer neurons than those in the input/output layers. In this way, at the middle layers, data is significantly compressed and lives in much smaller vector space, while hopefully this compression can be done without loosing too much information about data, i.e., keeping the most relevant features of the input data. The intuition behind this is that (as long as the learning is successful) the trained network is supposed to reconstruct the input data only from the limited amount of information encoded in the restricted middle layer. The neurons in this middle layer is often called *latent variables*, since they represent the relevant features of input data which are a priori unknown. The philosophy behind autoencoder may fit well with physics, namely, the idea that there must exist only a few key principles behind data generated from the laws of physics that we want to understand; naturally, autoencoder has already found many applications in physical science. One of the recent illustrative applications is an automated discovery of state variables from observations of experimental data

[Nat. Comp. Sci. 2, 433 (2022)].

Example 4: Restricted Boltzmann machine and neural network states. Suppose that dataset $\{\mathbf{x}_i\}_{i=1}^n$ is generated by some unknown probability distribution $p(\mathbf{x})$. We want to construct a model that imitates this distribution by using a flexible, efficient, and scalable variational ansatz $p_\theta(\mathbf{x})$. In practice, we do not know the exact form of a true distribution $p(\mathbf{x})$, but can access about the empirical "data" distribution $p_{\rm Data}(\mathbf{x})$ that gives its approximation:

$$p_{\rm Data}(\mathbf{x}) = \frac{1}{n}\sum_{i=1}^{n} \delta_{\mathbf{x},\mathbf{x}_i}. \tag{6.2.23}$$

The most common way for the optimization, i.e., training of the model $p_\theta(\mathbf{x})$, is to use the cross entropy

$$L(\theta) = -\sum_{\mathbf{x}} p_{\rm Data}(\mathbf{x}) \ln p_\theta(\mathbf{x}) = -\frac{1}{n}\sum_{i=1}^{n} \ln p_\theta(\mathbf{x}_i). \tag{6.2.24}$$

We can rewrite it (aside constant) by

$$L(\theta) = D\left[p_{\rm Data}(\mathbf{x})||p_\theta(\mathbf{x})\right] + \text{const.}, \tag{6.2.25}$$

where we define the relative entropy for given probability distributions p, q via

$$D\left[p(\mathbf{x})||q(\mathbf{x})\right] \equiv \sum_{\mathbf{x}} p(\mathbf{x}) \ln \frac{p(\mathbf{x})}{q(\mathbf{x})}. \tag{6.2.26}$$

The relative entropy vanishes $D = 0$ if and only if the two distributions coincide, i.e., $p(\mathbf{x}) = q(\mathbf{x})$ for $\forall \mathbf{x}$. Roughly speaking, the relative entropy thus quantifies how much there is difference between two distributions. The minimization of the cost function above then corresponds to the process that makes the model p_θ similar to the empirical distribution $p_{\rm Data}$ as much as possible.

The *restricted Boltzmann machine* (RBM) is one example of possible variational ansatz p_θ, which is defined by

$$p_\theta(\mathbf{v}) = \sum_{\mathbf{h}} p_\theta(\mathbf{v},\mathbf{h}) \equiv \sum_{\mathbf{h}} \frac{e^{-E_\theta(\mathbf{v},\mathbf{h})}}{Z}, \tag{6.2.27}$$

$$E_\theta(\mathbf{v},\mathbf{h}) \equiv -\mathbf{a}\cdot\mathbf{v} - \mathbf{b}\cdot\mathbf{h} - \mathbf{v}^{\rm T} W \mathbf{h}, \quad Z \equiv \sum_{\mathbf{v},\mathbf{h}} e^{-E_\theta(\mathbf{v},\mathbf{h})}. \tag{6.2.28}$$

where $\mathbf{v}$ are actual variables for representing data and called "visible" units, while the "hidden" units $\mathbf{h}$ are summed over before giving the model and do not appear in $p_\theta(\mathbf{v})$. These units are typically binary variables $v_i, h_i \in \{0,1\}$. The model parameters θ include real vectors $\mathbf{a}, \mathbf{b}$ and matrix W; we emphasize that there are no direct couplings among hidden variables $\mathbf{h}$ and also among $\mathbf{v}$. This particular structure of the couplings is the reason for calling this model "restricted" since the coupling network of $\mathbf{v}, \mathbf{h}$ can then be represented by the connection between the *single* hidden layer and the visible layer.

An apparent difficulty in this variational ansatz is that it is computationally intractable to perform the summation over exponentially large number of configurations for $\mathbf{v}$ and $\mathbf{h}$ in the partition function Z and thus to evaluate $p_\theta(\mathbf{v})$. That said, it is noteworthy that one can still efficiently evaluate the conditional distribution as follows:

$$p_\theta(\mathbf{h}|\mathbf{v}) \equiv \frac{p_\theta(\mathbf{v},\mathbf{h})}{p_\theta(\mathbf{v})} = \prod_i \frac{e^{z_i h_i}}{1+e^{z_i h_i}}, \quad \mathbf{z} \equiv \mathbf{b} + W\mathbf{v}. \tag{6.2.29}$$

A similar expression can be obtained for $p_\theta(\mathbf{v}|\mathbf{h})$. This fact simplifies the calculation of the gradient of the loss function $\nabla_\theta L$ to some extent, but the computational difficulty of Z itself is unavoidable anyway. We mention that there are still several heuristic approaches to tackle this difficulty, such as the method so-called contrastive divergence.

In the context of quantum many-body physics, the RBM inspires physicists to introduce the following variational many-body states often called neural network states[1] [Science 355, 602 (2017)]:

$$|\Psi_{\mathrm{RBM}}\rangle = \sum_{\boldsymbol{\sigma}} \Psi_{\boldsymbol{\sigma}} |\boldsymbol{\sigma}\rangle \tag{6.2.30}$$

$$\Psi_{\boldsymbol{\sigma}} \equiv \frac{1}{Z} \sum_{\mathbf{h}} \exp\left[\mathbf{a}\cdot\boldsymbol{\sigma} + \mathbf{b}\cdot\mathbf{h} + \boldsymbol{\sigma}^{\mathrm{T}} W \mathbf{h}\right]. \tag{6.2.31}$$

where $\boldsymbol{\sigma} \in \{0,1\}^n$ are binary variables representing spin-1/2 states and $|\boldsymbol{\sigma}\rangle$ corresponds to the basis states. It is known that any many-body state can then be arbitrarily well approximated by an RBM state if the number of hidden units is larger than the number of configurations $|\boldsymbol{\sigma}\rangle$ satisfying $|\Psi_{\boldsymbol{\sigma}}| > 0$. Intuitively, one may say that the correlations of physical variables $\boldsymbol{\sigma}$ are effectively induced by hidden variables $\mathbf{h}$ and they can be nonlocal if the coupling W is long-ranged[2]. In practice, to find the optimal RBM variational state for, e.g., the ground state of some many-body Hamiltonian, one can use the stochastic gradient descent and standard techniques which are common in variational Monte Carlo method.

6.3. Black-box optimization

To minimize a cost function, one has to choose some optimization algorithms. As introduced above, the most elemental way for this is to use the (stochastic) gradient descent. In Chapter 4, we have also mentioned that one can improve this method and use the so-called natural gradient descent when the geometry of the variational manifold is appropriately taken into account. From a broader perspective, there exist other types of optimization methods that do not rely on the local gradient as used in the aforementioned examples, but on some heuristic algorithms, some of which are inspired by ecology. These methods are heuristic in the sense that they usually lack solid theoretical justifications, while are empirically known to be effective in many challenging optimization problems.

[1] Precisely speaking, neural network states often refer to a slightly generalized version of the RBM states, in the sense that the network structure of physical $\boldsymbol{\sigma}$ and hidden $\mathbf{h}$ variables is not necessarily restricted to the bipartite graph with a single hidden layer as in RBM.

[2] If couplings W are short-ranged or sparse, one can show that the RBM states have only small entanglement, i.e., they obey the area law, and thus can be efficiently represented by the matrix product states.

Algorithm 1 Random search

Initialize: θ
while till convergence of F **do**
    Get: fitness value $F(\theta)$
    Sample a new parameter set θ^{new} from θ
    if $F(\theta^{\text{new}}) > F(\theta)$ **then**
        $\theta \leftarrow \theta^{\text{new}}$

We here cover several examples of such heuristic optimization algorithms, also known as *black-box optimizations*. In this approach, to optimize the objective (that is not in a solvable, closed form function) with respect to parameters θ, we do not need to calculate its derivative or even require the differentiability, but use the value of the *fitness function* $F(\theta)$, which gives a certain measure about the optimality of a solution. This fitness function may be the objective function itself, but needs not to be so. While the gradient-based optimization methods tend to be trapped in local minima, black-box optimizations are gradient-free and can often circumvent this difficulty; this is the reason why black-box optimizations are often also referred to as *global* search methods. Below we assume that the optimization problems is formulated in such a way that the goal is to *maximize* the fitness function (which is consistent with the usual convention in the literature).

Random search. The simplest example of black-box optimization would be the random search. Firstly, it randomly chooses an initial value θ_0 and calculates the fitness $F(\theta_0)$. We then stochastically generate a new set of parameters θ_0^{new} starting from θ_0 by using some given probability distribution. Calculating the fitness $F(\theta_0^{\text{new}})$ for this parameter set, and if the new one is better than the old one, i.e., $F(\theta_0^{\text{new}}) > F(\theta_0)$, we accept the change and set the parameters at the next step as $\theta_1 = \theta_0^{\text{new}}$, otherwise we set $\theta_1 = \theta_0$. This procedure will be repeated many times until the convergence of the fitness. As a probability distribution for selecting a new candidate parameter θ_t^{new} from θ_t, we typically use the uniform distribution over the hypersphere with a fixed radius centered at θ_t. The algorithm is summarized in Algorithm 1.

Evolutionary strategy. A major difficulty in random search is its low sample efficiency; it literally searches the whole parameter space randomly and it often fails or takes too much time to finally reach the correct optimal solution. In this context, the evolutionary strategies refer to methods that aim to improve the search efficiency by developing a heuristic algorithm inspired by the evolution process. While there are many variants of evolutionary strategies, here we consider one concrete example, known as the covariance matrix adaptation evolution strategy (CMA-ES).

Algorithm 2 CMA-ES

Initialize: θ, η, σ
while till convergence of F **do**
    Sample n random vectors $\{\epsilon_i\}_{i=1}^n$, each component sampled from $\mathcal{N}(0,1)$
    Get: fitness values $F_i = F(\theta + \sigma\epsilon_i)$ for $i = 1, 2, \ldots, n$
    $\theta \leftarrow \theta + \eta \frac{1}{n} \sum_{i=1}^n \epsilon_i F_i$

Algorithm 3 Genetic algorithm

Initialize: $\{\theta_i\}_{i=1}^n$, σ, $m(\leq n)$
while till convergence of F **do**
  Get: fitness values $F_i = F(\theta_i)$ for all i
  Sort $\{\theta_i\}$ in the descending order of $\{F_i\}$
  $\theta'_1 = \theta_1$, $F'_1 = F_1$
  for $i = 2, 3, \ldots, n$ **do**
    Sample k from $1, 2, \ldots, m$. Sample random vector ϵ, each component from $\mathcal{N}(0, 1)$
    $\theta'_i = \theta_k + \sigma\epsilon$
  $\theta_i \leftarrow \theta'_i$ for all i

The algorithm of the CMA-ES is summarized in Algorithm 2. The key point is that we use a minibatch of random vectors $\{\epsilon_i\}_{i=1}^n$ and use the averaged fitness $\frac{1}{n}\sum_{i=1}^n \epsilon_i F_i$ as a (finite step) differential direction at the next generation. In this sense, one can say that this algorithm is in the similar spirit of the gradient descent algorithms, but the advantage here is that one does not need to explicitly calculate the derivative or even assume the differentiability of the fitness function. While we here discuss the simplest CMA-ES where only θ is updated, it can in general also update the parameters in the Gaussian sample distribution, i.e., its mean and covariance matrix, at each generation. In this case, under certain conditions, the update of the parameters of the sample distribution in the CMA-ES can be interpreted as the discretized version of the natural gradient descent over the space of sample distributions.

Genetic algorithm. Another well-known black-box optimization method is the so-called genetic algorithms. This class of methods generate a population of individual sets of parameters $\{\theta_i\}_{i=1}^n$, calculate the fitness values for a new individual (mutant) obtained by combining some of old individuals (parents), and pick up the best mutants that are used to create the next generation. While there are again many variants of genetic algorithms, we give the simplest version of the algorithms in Algorithm 4 as an illustration.

Differential evolution. The above algorithms are elementary, representative examples of black box optimization algorithms, and can already be useful for certain problems as we will see their applications

Algorithm 4 Differential evolution

Initialize: $\theta_i \in \mathbb{R}^d$ for $i = 1, 2, \ldots, n$, $f > 0$, $C_r > 0$
Get: fitness values $F_i = F(\theta_i)$ for all i
while till convergence of F **do**
  for $i = 1, 2, \ldots, n$ **do**
    Sample mutually exclusive integers $k, l, m \neq i$ from $1, 2, \ldots, n$
    $\mu_i = \theta_k + f(\theta_l - \theta_m)$
    Sample β from $1, 2, \ldots, d$
    for $\alpha = 1, 2, \ldots, d$ **do**
      $$(\theta'_i)_\alpha = \begin{cases} (\mu_i)_\alpha & \text{if } \alpha = \beta \text{ or } \mathrm{rand}_{\alpha,\beta}[0,1] \leq C_r \\ (\theta_i)_\alpha & \text{otherwise} \end{cases}$$
    Get: fitness value $F'_i = F(\theta'_i)$
    if $F'_i \geq F_i$ **then**
      $\theta_i \leftarrow \theta'$, $F_i \leftarrow F'_i$

to deep reinforcement learning in the next Chapter. That said, there have been many proposed ways to improve the performance of those algorithms and, for the purpose of solving actual problems at your hand, it may be useful to introduce a more sophisticated algorithm here.

The differential evolution is known to be one of the most competitive black-box optimization algorithms in high-dimensional nonconvex search space. Its basic idea is similar to the above algorithms, but it includes several heuristic improvements that are empirically known to be able to realize more efficient search. The algorithm is summarized in Algorithm 4. The key parameter is the crossover factor C_r which characterizes how often the mutation occurs in producing the offspring individuals. A larger C_r leads to more frequent mutations and thus expedites the exploration while a lower C_r tends to expedite the exploitation of the current information about the search space. To optimize the exploration-exploitation balance, it may be advantageous to randomly use different sets of parameters at each generation, say $(f, C_r) = (1, 0.1), (1, 0.9), (0.8, 0.2)$ as proposed in [Wang et al., IEEE Trans. Evol. Comput. 15, 55-66 (2011)].

Summary of Chapter 6

Section 6.2 Basic concepts

- Supervised learning deals with data having labels, and aims to identify a function approximation, which relates input $\mathbf{x}$ to output y, on the basis of hypothesizing a functional form, $\mathbf{y} = f_\theta(\mathbf{x})$. The functional ansatz should be tractable/efficient and possess flexibility and scalability.
- Kernel method provides a functional approximation that consists of a superposition of the kernel functions, and allows one to perform a nonlinear classification known as the support vector machine. Quantum computer may offer alternative way to define the kernel function from the overlap between different quantum states.
- Deep learning uses the multilayer feed-forward neural network as a functional ansatz. There exist efficient algorithms and many heuristics to optimize this function in a reasonable amount of time even for vastly large dataset.
- Unsupervised learning deals with data without labels, and aims to extract essential information about the probability distribution that generates the dataset. In the context of deep learning, one famous example is the autoencoder, which would allow one to compress data into lower dimensional vector space, but still keep the most relevant features in the data.
- Another example is the restricted Boltzman machine that attempts to approximate the whole probability distribution itself by using functional ansatz inspired by the Gibbs distribution.

Section 6.3 Black-box optimization

- Gradient-based optimization algorithms, such as the (stochastic) gradient descent, often fail to work due to the presence of local minima. In such a case, a heuristic, gradient-free optimization method called black-box optimization can be useful.
- In black-box optimizations, gradients or even the differentiability of the cost function are unnecessary, but the parameters are optimized in terms of the fitness function that provides a certain measure about the optimality of a solution.
- The simplest black-box optimization algorithm is the random search, which literally searches the whole parameter space randomly according to a certain distribution. Its refinement, called evolutionary strategy, would allow for a more efficient search.
- One of the most competitive approaches, called differential evolution, is similar to the genetic algorithm, but contains a number of heuristics that can expedite the search over the high-dimensional, nonconvex parameter space.

6.4. Exercises

Exercise 6.1 (Gaussian kernel method: 1 point). Given dataset $\{\mathbf{x}_i, y_i\}_{i=1}^n$, consider approximating function by

$$y = \sum_{i=1}^{n} \alpha_i k(\mathbf{x}, \mathbf{x}_i) \tag{6.4.1}$$

with the Gaussian kernel:

$$k(\mathbf{x}, \mathbf{x}') = \exp\left(-\beta \left|\mathbf{x} - \mathbf{x}'\right|^2\right). \tag{6.4.2}$$

As discussed in the main text, the training is performed by minimizing the following cost function

$$L(\alpha) = \frac{1}{n} \sum_{i=1}^{n} \left| y_i - \sum_{j=1}^{n} \alpha_j k(\mathbf{x}_i, \mathbf{x}_j) \right|^2 + \frac{\sigma^2}{n} \sum_{ij=1}^{n} \alpha_i k(\mathbf{x}_i, \mathbf{x}_j) \alpha_j. \tag{6.4.3}$$

Show that the optimal α^* is given by

$$\alpha_i^* = \sum_{j=1}^{n} \left(K + \sigma^2 I\right)_{ij}^{-1} y_j. \tag{6.4.4}$$

One can now use this α^* to predict the output $\hat{y}$ for an unknown input $\mathbf{x}$ from

$$\hat{y} = \sum_{i=1}^{n} \alpha_i^* k(\mathbf{x}, \mathbf{x}_i) = \sum_{ij=1}^{n} k(\mathbf{x}, \mathbf{x}_i) \left(K + \sigma^2 I\right)_{ij}^{-1} y_j. \tag{6.4.5}$$

However, this expression does not tell us about how good this estimation is. Explain how one can determine confidence level of the estimation by showing that the standard deviation of the estimated value $\hat{y}$ can be given by

$$\delta\hat{y} = \sqrt{\sigma^2 + 1 - \sum_{ij} k(\mathbf{x}, \mathbf{x}_i) \left(K + \sigma^2 I\right)_{ij}^{-1} k(\mathbf{x}_j, \mathbf{x})}. \tag{6.4.6}$$

Hint: consider Gaussian process regression for this estimation problem and calculate the conditional probability distribution from the Bayesian analysis.

Exercise 6.2 (Global optimization: 1 point). Consider and numerically demonstrate a concrete example of objective functions that is difficult to (globally) minimize by gradient-descent methods, but can be optimized by black-box optimizations. Discuss why that is the case by plotting the optimization landscape.

CHAPTER 7

Reinforcement learning

7.1. Introduction

As briefly mentioned in Chapter 1, the goal of reinforcement learning is to train machines solely from many repetitions of trials and errors for achieving a certain task whose performance can be quantified by the so-called "reward" function. In contrast to supervised/unsupervised learnings, reinforcement learning does this without given data or knowledge, but rather machine itself acquires information about data to find the best solution by interacting with an environment. We may say that reinforcement learning can acquire sort of creativity in the sense that a machine can behave in a new and unexpected way (at least from the point of view of human), which makes a sharp contrast to supervised learning where a machine can, at best, imitate the teacher.

In reinforcement learning (RL), an *agent* observes the *state* of the environment and decides how to *act* to maximize the *reward*. This *action* causes changes in state of the environment and thus there is a closed feedback loop between the agent and environment. A way of determining the action taken by an agent based on the state of the environment is often called *policy*. Importantly, there is no teacher who tells which action should be taken; instead, the agent must discover the optimal action that leads to the best reward by repeating trials an errors many times. The main goal of Chapter 7 is to help you to gain intuition/key ideas behind the reinforcement learning algorithms, rather than teaching specific techniques for numerical implementations, such as how to use existing libraries etc.

7.2. Motivating example

To illustrate these ideas (and another important concepts of RL) in a simple example, consider a single classical particle on 1D lattice whose position is labelled by $x \in \mathbb{Z}$. The particle at position x randomly hops to the right $x+1$ or left $x-1$ site at each discrete time $t \in \{0, 1, 2 \ldots\}$. The hopping is asymmetric, namely, the probabilities of hopping to the right $(+)$ or left $(-)$ directions are

$$p_\sigma^{(\pm)} = \frac{1 \pm \sigma \delta p}{2}, \quad \sigma \in \{+1, -1\}\,, \tag{7.2.1}$$

where $\delta p \in [0, 1)$ is a fixed asymmetric parameter. Now suppose that we want to guide this stochastic particle into the origin of 1D lattice, i.e., $x = 0$ site. To do so, we consider a situation that, at each time, an agent can change the sign of asymmetric hopping probabilities, $\sigma \in \{+1, -1\}$ depending on the position of the particle x. Building on this, each notion of RL framework in the present problem can be formulated as follows:

- Environment: stochastic particle on 1D lattice that randomly hops to right or left sites with probabilities $p_\sigma^{(\pm)}$.
- State: position x of the particle. State at time t is represented by $s_t = x_t$.
- Agent: external controller that continuously observes the state of the environment and uses this information to manipulate $\sigma \in \{+1, -1\}$ in $p_\sigma^{(\pm)}$ to guide the stochastic particle to the origin $x = 0$.
- Action: choice of the sign $\sigma \in \{+1, -1\}$ in $p_\sigma^{(\pm)}$. Action at time t is represented by $a_t = \sigma_t$.
- Policy: conditional probability distribution $\pi_\theta(\sigma|x)$ of choosing action σ given a state x. The distribution function is parameterized by a set of parameters θ.
- Reward: the (minus) distance $r_t = -|x_t|$ from the origin at each time.
- Return: the sum of subsequent reward (with *discount* factor γ) which is defined by[1]

$$R_t = \sum_{t'=0}^{\infty} \gamma^{t'} r_{t+t'}, \quad r_t = -|x_t|, \quad 0 \le \gamma \le 1. \tag{7.2.2}$$

- Quality function: the expectation value of the return for a given state s and action a at time t:

$$Q_\pi(s, a) = \mathbb{E}[R_t | s_t = s, a_t = a]. \tag{7.2.3}$$

  Note that the ensemble average $\mathbb{E}$ is taken over all the possible subsequent stochastic evolutions of the state conditioned on $s_t = s, a_t = a$. Their sequence is affected by the feedback loop determined by a given policy π. Thus, the quality function also depends on π as indicated by the subscript in $Q_\pi(s, a)$.
- Value: similarly, the expectation value of the return for a given state s at time t is called the value:

$$V_\pi(s) = \mathbb{E}[R_t | s_t = s]. \tag{7.2.4}$$

  Here, the ensemble average $\mathbb{E}$ is taken over all the possible subsequent stochastic evolutions conditioned on $s_t = s$.

The ultimate goal of RL then is to find the best policy π_{θ^*} with the optimized parameters θ^*, which maximizes the value V. If we identify the probabilities in π_θ themselves as the parameters θ, the optimal policy in the present example can simply be given by

$$\pi_{\theta^*}(\sigma|x) = \begin{cases} \frac{1+\sigma}{2} & x < 0 \\ \frac{1-\sigma}{2} & x > 0 \end{cases}. \tag{7.2.5}$$

In a more complex realistic problem, however, it is almost impossible to analytically find an exact, optimal policy. We thus need a systematic way to train the parameters θ to maximize the expected reward V_{π_θ}. To efficiently learn the optimal policy, the agent should tend to perform action that is found to be favorable for acquiring better reward (i.e., the agent needs to *exploit* the knowledge from experiences), but at the same

[1] Roughly speaking, the factor γ plays the role of effective cutoff for a number of future rewards that the agent takes into account; it represents the agent's ability of foreseeing. For instance, the agent with $\gamma = 0$ behaves in a greedy manner, i.e., it always tries to maximize the reward at next step, but does not think about a long-term return.

time it needs to try new possibilities to find action that leads to better reward in the future (i.e., the agent also needs to *explore* to discover a possibly better new solution). The RL algorithms explained below aim to find the optimal policy by balancing these exploitation and exploration in the search space.

7.3. Formalism: Markov decision process

Let us now introduce a general framework of RL on the basis of Markov decision process. Consider state space $\mathcal{S}$ and action space $\mathcal{A}$. The environment considered by the Markov decision process then satisfies the property that future dynamics only depends on the current state. In other words, its dynamics is fully characterized by the transition probability from $s_t \in \mathcal{S}$ to $s_{t+1} \in \mathcal{S}$ given action $a_t \in \mathcal{A}$:

$$p(s_{t+1}|s_t, a_t). \tag{7.3.1}$$

The Markov decision process also assigns the real number called the reward r_t for each pair (s_t, a_t) of state and action at time t. In other words, the reward r_t is a function $r_t(s_t, a_t)$ of the current state-action pair (s_t, a_t)[2].

The goal of the agent is to maximize the total reward accumulated over the whole evolution. As introduced above, we thus have to consider the return, which is the sum of subsequent reward with discount factor γ:

$$R_t = \sum_{t'=0}^{\infty} \gamma^{t'} r_{t+t'}, \quad 0 \leq \gamma \leq 1. \tag{7.3.2}$$

We also need to introduce the function, policy, to describe how the agent chooses the next action for a given current state. Specifically, a policy π is usually defined as a conditional probability distribution $\pi(a|s)$ for the agent selecting action a given current state s. To formulate the optimization problem, we then define the quality function and the value function by

$$Q_\pi(s, a) = \mathbb{E}[R_t|s_t = s, a_t = a] \tag{7.3.3}$$

$$V_\pi(s) = \mathbb{E}[R_t|s_t = s], \tag{7.3.4}$$

where the ensemble average $\mathbb{E}$ is taken over all the possible subsequent state evolutions generated by the policy π with initial conditions $s_t = s, a_t = a$ or $s_t = s$.

Summarizing, the RL problem on Markov decision process is defined by the optimization problem of finding the following π_* on a set $(\mathcal{S}, \mathcal{A}, r, p, \gamma)$:

$$V_{\pi_*}(s) \geq V_\pi(s), \quad \forall s, \pi, \tag{7.3.5}$$

or equivalently,

$$V_*(s) \equiv \max_\pi V_\pi(s). \tag{7.3.6}$$

[2]The reward can in general depend on the state s_{t+1} at the next step reached by $s_t \xrightarrow{a_t} s_{t+1}$, however, for the sake of simplicity we assume that r_t only depends on (s_t, a_t) as this situation is most commonly encountered in many practical problems.

This is obviously equivalent to the following optimization problems in terms of the quality functions:

$$Q_*(s,a) = \max_\pi Q_\pi(s,a), \tag{7.3.7}$$

where $V_*(s) = \max_a Q_*(s,a)$ is satisfied. Note that the optimal policy π_* achieves both optimal value and action-value functions.

There are basically two different types of approaches to tackle this optimization problem. The first one, called a *value-based* search, attempts to evaluate the quality function Q for possible state and action, and chooses the action $a_t = \operatorname{argmax}_a Q(s_t,a)$ that gives the maximum quality at each time step during the training process. While the policy π does not appear manifestly here, after the quality function converges to the optimal one Q_*, this strategy automatically defines the optimal policy π_* in which the action is (deterministically) chosen as $a_t = \operatorname{argmax}_a Q_*(s_t,a)$. The second strategy, called a *policy-based* search, aims to approximate the conditional probability distribution for policy π and directly optimize π by (typically) some iterative methods to maximize the value. Below we briefly review the main ideas and procedures in each of the two approaches.

7.4. Value-based search

7.4.1. Bellman equation. To formulate an empirical method for a value-based search, we start from the following recursive relation satisfied by the value function (often called Bellman equation):

$$V_\pi(s) = \sum_{a\in\mathcal{A}} \pi(a|s) \left[r(s,a) + \gamma \sum_{s'\in\mathcal{S}} p(s'|s,a) V_\pi(s') \right]. \tag{7.4.1}$$

This equation can readily be derived from the definition (7.3.4) of the value function. In particular, the optimal value function (7.3.6) satisfies

$$V_*(s) = \max_a \left[r(s,a) + \gamma \sum_{s'\in\mathcal{S}} p(s'|s,a) V_*(s') \right]. \tag{7.4.2}$$

For a given set of (π,p,r), these equations are ultimately linear problems for a vector $V_\pi(s)$ and the $S\times S$ matrix with S being the total number of states. However, in practice, it is almost intractable to exactly solve this problem because S is typically very large.

However, one may still iteratively solve this equation, called *value iteration*:

$$V(s) \leftarrow \max_a \left[r(s,a) + \gamma \sum_{s'\in\mathcal{S}} p(s'|s,a) V(s') \right]. \tag{7.4.3}$$

In this way, one could find the optimal value function $V_*(s)$ and thus obtains the optimal policy that chooses the action according to $\operatorname{argmax}_a \left[r(s,a) + \gamma \sum_{s'\in\mathcal{S}} p(s'|s,a) V_*(s') \right]$. A major difficulty in this iterative approach is that it contains the summation over all possible states s' at each iterative step. More importantly, this method requires the complete knowledge about the exact form of the conditional probability distribution $p(s'|s,a)$ in the first place, which is usually not available. We thus need to consider alternative approach.

Algorithm 5 Q-learning

Initialize: $Q(s,a)$ for $\forall s, a$
while till convergence of Q **do**
  Get: initial state s
  while till s is terminal **do**
    Take a from s and get next state s', based on ϵ-greedy policy of Q:
    $a = \begin{cases} \text{random action} & \text{with probability } \epsilon \\ \text{argmax}_{a'} Q(s,a') & \text{otherwise} \end{cases}$
    if s' is not terminal **then**
      $Q(s,a) \leftarrow Q(s,a) + \alpha\left[r(s,a) + \gamma \max_{a'} Q(s',a') - Q(s,a)\right]$
    else
      $Q(s,a) \leftarrow Q(s,a) + \alpha\left[r(s,a) - Q(s,a)\right]$
    $s \leftarrow s'$

7.4.2. Q learning. One possible way to circumvent these difficulties is to iteratively update the quality function $Q(s,a)$, rather than the value function itself, while using this function to approximate the optimal policy during the process of training. To this end, we first start from the similar recursive relation for the optimal quality function:

$$Q_*(s,a) = r(s,a) + \gamma \sum_{s' \in \mathcal{S}} p(s'|s,a) \max_{a'} Q_*(s',a'), \tag{7.4.4}$$

which can be obtained from Eq. (7.4.2) by noting the relation $V_*(s') = \max_{a'} Q_*(s',a')$. In the similar manner above, this recursive equation can ideally be solved by the iterative method as follows:

$$Q(s,a) \leftarrow Q(s,a) + \alpha \left[r(s,a) + \gamma \sum_{s' \in \mathcal{S}} p(s'|s,a) \max_{a'} Q(s',a') - Q(s,a) \right], \tag{7.4.5}$$

where α is a small positive number that acts as the learning rate. This method, however, still includes the intractable summation $\sum_{s' \in \mathcal{S}}$ over the whole state space.

The idea of *Q-learning* is to train the quality function iteratively from a sequence of states, actions, and rewards $\{s_t, a_t, r_t\}_{t=0,1,2\ldots}$ experienced by the agent, each of which is called an *episode*. Then, the expectation value $\sum_{s' \in \mathcal{S}} p(s'|s,a) \max_{a'} Q(s',a')$ may be replaced by the estimated value $\max_a Q(s_{t+1},a)$ at the state s_{t+1} arrived from s_t with action a_t. Specifically, we arrive at the iterative procedure

$$Q(s_t,a_t) \leftarrow Q(s_t,a_t) + \alpha_t \left[r(s_t,a_t) + \gamma \max_a Q(s_{t+1},a) - Q(s_t,a_t) \right], \tag{7.4.6}$$

where the residual term $r(s_t,a_t) + \gamma \max_a Q(s_{t+1},a) - Q(s_t,a_t)$ is often called the *temporal difference*. Note that now there is no need to know about the complete form of $p(s'|s,a)$, which significantly simplifies the iterative analysis. This approach, coined as Q-learning, can be effective especially when the state and action space is not very large, and thus one can prepare the whole table of Q function on the variable space $(s,a) \in \mathcal{S} \times \mathcal{A}$. In particular, under certain conditions, it is theoretically known that the Q-learning allows the quality function to converge to the optimal one, $Q \to Q_*$, after a sufficiently large number of iterations if the learning rate satisfies

$$\sum_{t=0}^{\infty} \alpha_t \to \infty, \quad \sum_{t=0}^{\infty} \alpha_t^2 < \infty. \tag{7.4.7}$$

One may wonder how one should choose action a_t in the middle of training process where the Q function is still suboptimal. In practice, there are several options for this, but one common approach is the so-called *ϵ-greedy algorithm* defined by

$$a = \begin{cases} \text{random action} & \text{with probability } \epsilon \\ \text{argmax}_{a'} Q(s, a') & \text{otherwise} \end{cases}, \tag{7.4.8}$$

where the action is set to be the one that maximizes the (suboptimal) Q function at the time with probability $1 - \epsilon$, while otherwise it is chosen in a completely random manner. In this way, one can balance the exploitation and exploration in the RL problem. The usual practice is to start with high ϵ, say $\epsilon = 1$, to expedite the exploration, while eventually decreases it to smaller value, say $\epsilon = 0.05$ at later stages of the training. To summarize, the Q-learning proceeds as described in the pseudocode of Algorithm 5.

7.4.3. Deep Q-learning. The dimension of the state-action space is often quite large in many realistic problems, and in practice it is often intractable to prepare the complete table of the Q function on the whole state-action space; this makes it challenging to apply the value iteration approach explained above. To overcome this difficulty, one can use a flexible and efficient functional ansatz to approximate the Q function. Given recent successes of deep neural networks, it is then natural to use neural network functions for the purpose of approximating the Q function and apply the RL algorithm to more complex problems that are otherwise challenging to solve by naive value iterations above.

We recall that the deep neural network is defined by the function

$$f_\theta(\mathbf{x}) = g(w_L \cdots g(w_2\, g(w_1 \mathbf{x}))), \tag{7.4.9}$$

where $\mathbf{x}$ is input, w_i are weight matrices at each layer i, and g is the nonlinear function which here we shall choose to be the ReLU function:

$$g(x) = \begin{cases} x & x \geq 0 \\ 0 & x < 0 \end{cases}. \tag{7.4.10}$$

Suppose that we have a single data $(\mathbf{x}, y)$ and define the loss function for this by

$$L(\theta) = \frac{1}{2} \left(y - f_\theta(\mathbf{x}) \right)^2. \tag{7.4.11}$$

To approximate the input-output relation $y \sim f_\theta(\mathbf{x})$, a standard way was to optimize the neural network parameters θ by the gradient descent

$$\theta \leftarrow \theta - \eta \nabla_\theta L. \tag{7.4.12}$$

Algorithm 6 Deep Q-learning with the fixed target network

Initialize: network parameters θ in $Q_\theta(s,a)$ and set $\tilde{Q} = Q_\theta$
while till convergence of θ **do**
  Get: initial state s
  while till s is terminal **do**
    Take a from s and get next state s', based on ϵ-greedy policy of Q_θ:
    $a = \begin{cases} \text{random action} & \text{with probability } \epsilon \\ \text{argmax}_{a'} Q_\theta(s,a') & \text{otherwise} \end{cases}$
    if s' is not terminal **then**
      $\theta \leftarrow \theta + \eta \left(r(s,a) + \gamma \max_{a'} \tilde{Q}(s',a') - Q_\theta(s,a) \right) \nabla_\theta Q_\theta(s,a)$
    else
      $\theta \leftarrow \theta + \eta \left(r(s,a) - Q_\theta(s,a) \right) \nabla_\theta Q_\theta(s,a)$
    $s \leftarrow s'$
    Every C steps set $\tilde{Q} = Q_\theta$

Fixed target network. Building on this, we may now consider applying the deep learning method to the present RL problem. To do so, we receive the observed state-action pair as input data and use f_θ to approximate the Q function, which is known as the *deep Q-network* (DQN). The goal is to minimize the temporal difference and approximate the optimal relation $r(s,a) + \gamma \max_{a'} \tilde{Q}(s',a') \sim Q_\theta(s,a)$, which corresponds to the target relation $y \sim f_\theta(\mathbf{x})$ above. Specifically, we get the correspondence as follows:

$$\mathbf{x} = (s,a), \quad f_\theta = Q_\theta, \tag{7.4.13}$$

$$y = r(s,a) + \gamma \max_{a'} \tilde{Q}(s',a'), \quad s \xrightarrow{a} s'. \tag{7.4.14}$$

Here, note that "data" y is obtained by using the so-called *fixed target network* $\tilde{Q}$, whose parameters are copied to those of Q_θ only at every C iterations. This use of a separate network to estimate the target data y is a heuristic method to improve the convergence and stability of training in the RL algorithm. The resulting loss function is

$$L(\theta_t) = \frac{1}{2} \left(y_t - f_{\theta_t}(\mathbf{x}_t) \right)^2 \tag{7.4.15}$$

$$= \frac{1}{2} \left(r(s_t,a_t) + \gamma \max_a \tilde{Q}(s_{t+1},a) - Q_{\theta_t}(s_t,a_t) \right)^2, \tag{7.4.16}$$

where s_{t+1} is chosen by some policy using Q_θ such as the ϵ-greedy method in the similar manner as done in the usual Q-learning. The neural network parameters are then updated as

$$\theta_{t+1} = \theta_t - \eta \nabla_{\theta_t} L(\theta_t) \tag{7.4.17}$$

$$= \theta_t + \eta \left(r(s_t,a_t) + \gamma \max_a \tilde{Q}(s_{t+1},a) - Q_{\theta_t}(s_t,a_t) \right) \nabla_{\theta_t} Q_{\theta_t}(s_t,a_t). \tag{7.4.18}$$

We summarize the algorithm of this deep Q-learning in the pseudocode of Algorithm 6.

Experience replay. Unfortunately, one has to keep in mind that this simple deep RL algorithm still rarely works as is in many real-life tasks or some physics problems. To overcome this issue, many heuristic schemes have been proposed in these years; the use of the fixed target network $\tilde{Q}$ above is one such an

Algorithm 7 Deep Q-learning with the fixed target network and experience replay

Initialize: network parameters θ in $Q_\theta(s,a)$ and set $\tilde{Q} = Q_\theta$
Initialize: replay memory $\mathcal{D}$
while till convergence of θ **do**
  Sample minibatch of N experiences $\{e_i\}_{i=1}^N$ randomly from $\mathcal{D}$
  for every experience $e_i = (s_i, a_i, r_i, s_i')$ **in** minibatch **do**
    if s' is not terminal **then**
      $y_i \leftarrow r_i + \gamma \max_{a'} \tilde{Q}(s_i', a')$
    else
      $y_i \leftarrow r_i$
  $\theta \leftarrow \theta + \eta \sum_{i=1}^N (y_i - Q_\theta(s_i, a_i)) \nabla_\theta Q_\theta(s_i, a_i)$
  Every C steps set $\tilde{Q} = Q_\theta$

example. The progress along this line is very rapid and it is impossible to cover all the heuristics here, but let us just introduce one commonly used RL technique known as *experience replay*.

In the deep RL algorithm above, we directly used a sequence of agent's experience in each episode to train the network. The difficulty here is that state-action pairs (s_t, a_t) in those sequences are in general highly correlated as they are generated sequentially in the environment, which often makes the training inefficient.

The basic idea behind experience replay is to break this correlation between different samples by shuffling the order of training data used. Specifically, before starting the training, we construct the replay memory $\mathcal{D}$ which is data set of random agent's experiences $e_t = (s_t, a_t, r(s_t, a_t), s_{t+1})$; this can be done by simply repeating simulations in the environment using, say, the ϵ-greedy method of some initialized Q function. During the training, we then randomly sample experiences from the memory $\mathcal{D}$, and use them to define the loss function and update the neural network parameters via the stochastic gradient descent. It is usually advantageous to construct and use minibatch of N experiences from $\mathcal{D}$ rather than using the whole replay memory. Specifically, together with the fixed target network technique above, we calculate the loss as follows:

$$L(\theta) = \frac{1}{2N} \sum_{i=1}^{N} \left(r_i + \gamma \max_{a'} \tilde{Q}(s_i', a') - Q_\theta(s_i, a_i) \right)^2, \tag{7.4.19}$$

which leads to the stochastic gradient descent

$$\theta \leftarrow \theta + \eta \sum_{i=1}^{N} \left(r_i + \gamma \max_{a'} \tilde{Q}(s_i', a') - Q_\theta(s_i, a_i) \right) \nabla_\theta Q_\theta(s_i, a_i). \tag{7.4.20}$$

The algorithm is summarized in Algorithm 7. For further reading about other heuristic methods to improve the DQN algorithms, see for example arXiv:1710.02298. Nevertheless, the basic techniques explained here, including ϵ-greedy method, fixed target network, and experience replay, constitute the key elements of most of more advanced algorithms; notably, these are the main techniques that have enabled DeepMind to successfully train DQN to demonstrate the human-level control of 49 Atari video games in [Nature 518, 529 (2015)], despite the common belief at the time.

7.4.4. Physics application: quantum control of continuously monitored systems. As one possible application of deep Q-learning to quantum science, here we briefly discuss the measurement-based feedback control of a quantum particle. Specifically, we assume that the particle feels certain potential V and is also subject to external force F that is appropriately controlled by feedback loop:

$$\hat{H} = \frac{\hat{p}^2}{2m} + V(\hat{x}) - F\hat{x}. \tag{7.4.21}$$

We then consider continuously monitoring the particle position; as we learned before, this measurement backaction makes the dynamics noisy and nonunitary. The time evolution equation is given by (cf. Eq. (3.6.50))

$$d|\psi\rangle = \left[1 - i\hat{H} - \frac{\kappa}{2}(\hat{x} - \langle\hat{x}\rangle)^2\right] dt|\psi\rangle + \sqrt{\kappa}(\hat{x} - \langle\hat{x}\rangle)dW|\psi\rangle. \tag{7.4.22}$$

To facilitate the deep Q-learning, it is in practice useful to discretize F into ~ 20 possible values within the interval $[-F_{\max}, F_{\max}]$.

The reward is chosen depending on the task the feedback controller aims to achieve. For instance, if the potential satisfies $V \to \infty$ as $|x| \to \infty$ and the goal is to prepare the ground state of the system, we may choose the reward to be the minus system energy $r = -\langle\hat{H}\rangle$. In contrast, if the potential is unbounded $V \to -\infty, |x| \to \infty$ and the goal is to stabilize (otherwise unstable) state, we may choose the reward in such a way that $r = 1$ if the wavepacket remains stable at final time $t = T$ while $r = 0$ if it fails to do so. The latter problem setting gives the quantum analogue of the common RL problem known as the CartPole problem.

Summarizing, the present quantum control problem can be formulated as the following RL task:

- State: quantum state $|\psi\rangle$.
- Action: external force $F \in [-F_{\max}, F_{\max}]$.
- Environment: the stochastic Schrödinger equation (7.4.22).
- Reward: the minus energy $r = -\langle\hat{H}\rangle$ (for the ground-state preparation) or $r = 1$ only if the wavepacket remains stable at $t = T$ (for the stabilization of an unstable state).

Note that, in realistic quantum systems, what is available to an observer is the measurement outcome (i.e., realization of a sequence of the Wiener process dW). Thus, to simulate experimentally relevant situations, one has to use this information as input to the Q function rather than a quantum state itself during the training. Nevertheless, if an observer has a good knowledge about the initial state, she/he may combine it with the measurement outcome to reconstruct the wavefunction by solving the time-evolution equation, and would use a quantum state itself or its distribution moments as the input. It is reported in [PRL 125, 100401 (2020)] that deep Q-learning can outperform the known control strategies, especially when V contains the nonquadratic terms and thus the problem becomes nonlinear.

7.5. Policy-based search

The DQN algorithms above would be a first choice to solve realistic RL problems if action space is discrete and limited in such a way that the search problem in $\max_{a'} \tilde{Q}(s', a')$ is still tractable. If not, especially when the action space is *continuous*, yet another approach called *policy-based search* is in

general more favorable. While we do not explain details about the policy-based approaches in this lecture, let us outline basic ideas below.

We first recall that the policy is defined by the conditional probability distribution of action a for a given state s:

$$\pi_\theta(a|s), \tag{7.5.1}$$

where θ is a set of parameters that define the policy. The goal of RL is to maximize the total expected reward

$$\mathbb{E}_{\pi_\theta}[R] = \sum_{\{(s_t,a_t)\}_{t=1}^T} p_\theta\left(\{(s_t,a_t)\}_{t=1}^T\right) R\left(\{(s_t,a_t)\}_{t=1}^T\right), \tag{7.5.2}$$

where $R = \sum_{i=1}^T \gamma^{i-1} r_i$ represents the accumulated total reward along the whole episode $\{(s_t,a_t)\}_{t=1}^T$ and the summation is taken over all the possible episodes. Due to the Markov property, we can represent the probability p_θ by the product of the conditional probabilities as

$$p_\theta\left(\{(s_t,a_t)\}_{t=1}^T\right) = \prod_{t=1}^T p(s_{t+1}|a_t,s_t)\pi_\theta(a_t|s_t). \tag{7.5.3}$$

This allows us to rewrite

$$\nabla_\theta \log p_\theta = \sum_{t=1}^T \nabla_\theta \log \pi_\theta(a_t|s_t). \tag{7.5.4}$$

The gradient of the expected reward is then given by

$$\nabla_\theta \mathbb{E}_{\pi_\theta}[R] = \sum_{\{(s_t,a_t)\}_{t=1}^T} R p_\theta \nabla_\theta \log p_\theta = \mathbb{E}_{\pi_\theta}\left[R\left(\sum_{t=1}^T \nabla_\theta \log \pi_\theta(a_t|s_t)\right)\right]. \tag{7.5.5}$$

We may then use this gradient to update the parameters θ

$$\theta \leftarrow \theta - \eta \nabla_\theta \mathbb{E}_{\pi_\theta}[R] = \theta - \eta \mathbb{E}_{\pi_\theta}\left[R\left(\sum_{t=1}^T \nabla_\theta \log \pi_\theta(a_t|s_t)\right)\right]. \tag{7.5.6}$$

In practice, one has to approximate the ensemble average $\mathbb{E}_{\pi_\theta}$ by using a certain subset of episodes and repeat this iterative procedure many times. Similar to the value-based search, it is possible to use deep neural networks to approximate the policy function π_θ. Many possible policy-based deep RL algorithms, such as the actor-critic methods, are proposed; see e.g. arXiv:1810.06339. That said, it would be important to keep in mind that it has been reported that policy-based RL algorithms tend to be less sample efficient and sensitive to choices of hyperparameters, network architectures, and reward functions, which often causes difficulties for reproducing numerical results; see arXiv:1709.06560. Generally speaking, policy-based methods would be a better option when (i) action space is continuous and (ii) simulation of the environment is fast and numerically cheap.

7.6. Black-box optimization in deep RL

Since the performance of many deep RL algorithms tends to be sensitive to choices of specific hyper-parameters and it is often this aspect that makes the application of deep RL methods to realistic problems not straightforward, it would be highly desirable to construct a more stable and versatile approach to deep RL[3]. One emerging candidate for solving this issue is to employ the black-box approaches we have reviewed in Chapter 6 to solve the RL problems without relying on specific RL-oriented algorithms, such as Q learning.

In the black-box approaches, many agents simulate different policies in parallel and, based on the rewards they obtain, one selects the policy that gives the most reward as the optimal policy. In practice, the use of the black-box optimization might also be of advantageous for physicists who may only have usual computational resources such as multicore CPU, since the calculations can be parallelized and no derivatives of neural networks are necessary (i.e., the advantage of using GPU is marginal).

As we explained in Chapter 6, black-box optimization algorithms prepare a set of individuals each of which has a set of parameters θ, and then train those individuals solely on the basis of the values of the fitness $F(\theta)$ at each iteration. In the deep RL problems, the parameters θ correspond to the network parameters in the deep neural network that represents either the state-action function $Q_\theta(s,a)$ in the value-based approaches (for which the policy is simply defined by $a = \mathrm{argmax}_{a'} Q_\theta(s,a')$) or the policy itself $\pi_\theta(a|s)$ in the policy-gradient methods. More specifically, the fitness in the value-based methods is given by the total reward accumulated over each episode $\{(s_t,a_t)\}_{t=1}^T$,

$$F(\theta) = R(Q_\theta) \equiv \sum_{t=1}^{T} r\left(s_t, a_t(\theta)\right), \quad a_t(\theta) = \mathrm{argmax}_a Q_\theta(s_t,a), \tag{7.6.1}$$

which depends on the parameters θ through the Q function Q_θ. Meanwhile, in the policy-based methods, the fitness corresponds to the total reward along an episode generated by the policy:

$$F(\theta) = R(\pi_\theta) = \sum_{t=1}^{T} r\left(s_t, a_t(\theta)\right), \quad a_t \sim \pi_\theta(a|s_t), \tag{7.6.2}$$

where θ dependence follows from the policy function π_θ. Given these identifications, one can directly apply the black-box optimization algorithms, such as the ones outlined in Algorithms 2,3,4 in Chapter 6, to the deep RL problems. For further details, see arXiv:1703.03864 or arXiv:1712.06567 for applications of evolutionary strategies or genetic algorithms to deep RL methods, respectively.

7.7. Some tips on implementation

While it is not mandatory requirement of this lecture for you to implement the RL algorithms in some simple problem, that would be a very good Exercise if you aim to apply RL methods to actual, more complex problems at your hand (see, e.g., Exercise 7.1). Here I shall only give a few remarks for that, which you might find helpful. Obviously, this section is far from complete and we refer the interested readers to the modern text book for practitioners (Deep Reinforcement Learning Hands-On)

[3]For further readings about the challenges in deep RL, you may refer to the following blogpost: "Deep Reinforcement Learning Doesn't Work Yet".

and the sample codes available in GitHub page of this book. As an introduction, PyTorch tutorial and Chapter 12 of arXiv:2009.05673 would also be useful. You can find some collection of useful sources and sample codes in GitHub page.

To be concrete, I assume PyTorch implementation here. First, it would be useful to install Anaconda from here, and choose appropriate installer for your OS and just follow the instruction (I assume Mac from now on, but the similar steps should be followed also in Windows). Once you have completed the installation, choose Anaconda-Navigator from the applications. For later use, you may install Jupyter Notebook in the Home. Then, you can create PyTorch environment by choosing "Environments" in the left bar and checking the Python package. Launch the environment by clicking the play button $\rightarrow$ Open Terminal.

You should now be able to install PyTorch by just doing "conda install pytorch torchvision -c pytorch" on the terminal (see this page). You can launch the Jupyter Notebook by choosing the "Open with Jupyter Notebook" in the Pytorch environment and may run a simple Python code to check whether or not the installation is successful; see Pytorch-tutorial, PyTorchZeroToAll, or Chapter 3 of Deep Reinforcement Learning Hands-On for further readings about PyTorch introduction.

To implement RL algorithms for solving some prototypical problems, you can use the useful toolkit called "OpenAI Gym". To install this, it is usually enough to do "pip install gym" on the terminal you launched above. To simulate Atari games, which are now known as benchmark problems for modern deep RL algorithms, you should install ROMS from here and do "python -m atari_py.import_roms <path to folder>". In general, to continuously monitor the training process, it is very useful to install TensorBoard; for details, see for instance Chapter 3 of Deep Reinforcement Learning Hands-On. Once you have installed this, you can monitor the training process by doing "tensorboard —logdir <file name>" and typically opening "http://localhost:6006/" in the browser. After these preparations, you should be ready to do Exercise 7.1.

7.8. Exercise

Exercise 7.1 (Mastering video game "Pong" via Black box optimization: 2 points). In 2015, DeepMind has demonstrated that the RL algorithm using DQN can achieve human-level control in different types of video games in Atari 2600 [Mnih et al., Nature 518, 529 (2015)]. You may reproduce this result by following the same approach, namely, Deep Q learning, but (since you have to calculate the derivatives of deep neural networks) it typically requires the GPU acceleration, which may not readily be available for physics students. Also, the results are often rather sensitive to choices of hyperparameters and may not be very stable.

Here let us follow another approach we discussed above, namely, black box optimization of DQN (see Sec. 7.6). An advantage here is that the GPU acceleration is no longer essential and you can parallelize the calculations over multicore CPU on usual computers. The number of hyperparameters is also much less than those in the other DRL algorithms.

To be concrete, in this Exercise, consider solving the video game named "Pong" among Atari games by using black-box optimization of DQN based on the genetic algorithm (cf. Algorithm 3). Then, plot

typical results of the evolutions of the mean and maximum values of the reward during the training process.

Hint: you may built your code on the basis of useful wrapper functions or sample codes available in GitHub page of Deep Reinforcement Learning Hands-On, especially those in Chpaters 6 and 20. You should get the results that should look like Fig. 7.8.1 below, where we choose the hyperparameters as

- Network structure of DQN: 3 convolutional layers with 32, 64, and 64 channels followed by a hidden layer with 512 units. They use 8×8, 4×4, and 3×3 filters with strides $4, 2$, and 1, respectively. The same as in [Mnih et al., Nature 518, 529 (2015)].
- Population size: $n = 800$
- Parents count: $m = 8$
- Noise standard deviation: $\sigma = 0.004$

To obtain the results in this figure, the calculations are distributed over 10 CPU cores on a single machine. To reach the maximum reward of the elite agent $r_{\max} = 20$, the learning roughly takes ~ 1 day. To achieve the maximum possible reward 21, you have to be a bit more patient; it typically takes another ~ 1 day to increment $r_{\max}$ from 20 to 21.

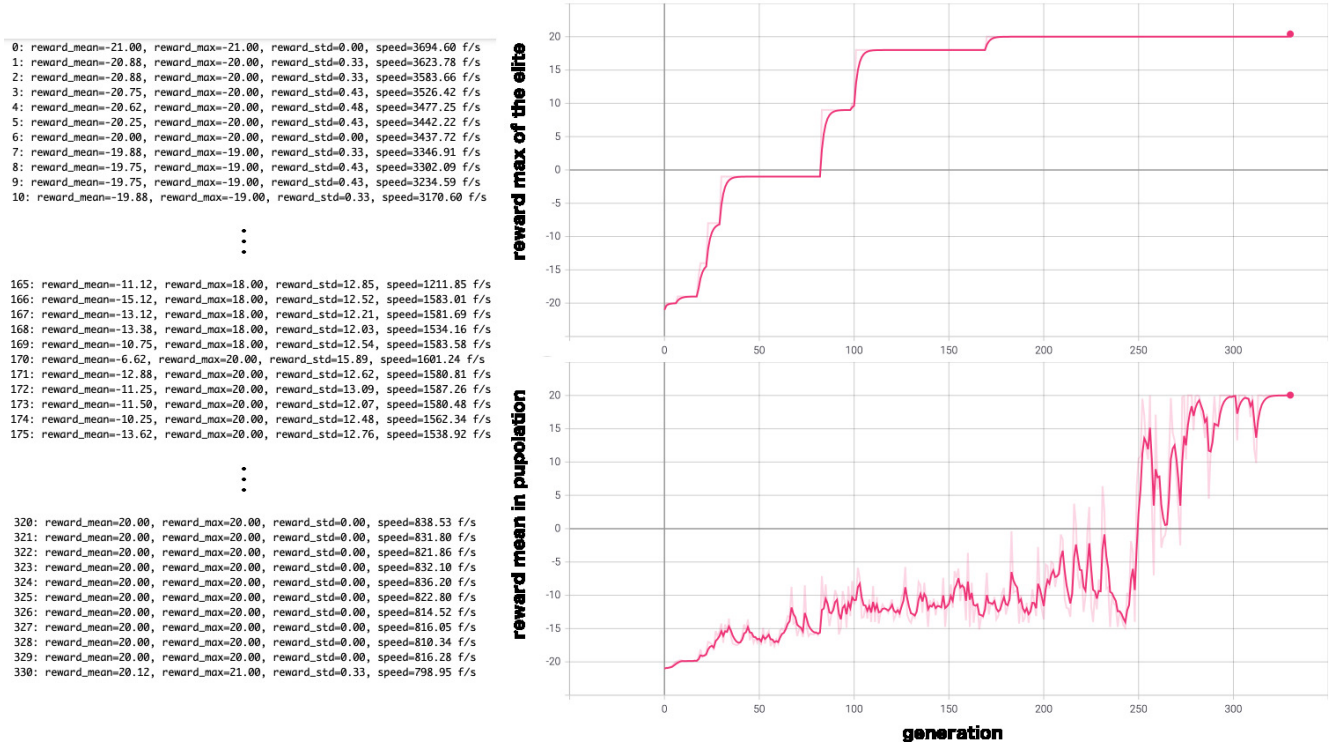

FIGURE 7.8.1. Typical learning process of Exercise 7.1 performed on my personal computer with 10 CPU cores.

Summary of Chapter 7

Sections 7.1-7.4 Reinforcement learning formalism and the value-based search

- In reinforcement learning (RL), a machine called agent acquires information about data by many repetitions of interactions with environment and, on the basis of this experience, it attempts to find the best solution that maximizes the objective function called reward. A state of the environment can change according to how the agent act on the environment.
- A way of determining the action a taken by an agent based on the state s of the environment is given by the conditional probability distribution called policy $\pi(s|a)$. In the framework of Markov decision process, the future dynamics only depends on the current state and the reward r_t can be defined as a function of the current state-action pair (s_t, a_t).
- The expectation value of the sum of subsequent reward with initial conditions $s_t = s, a_t = a$ and policy π is called the quality (Q) function and denoted by $Q_\pi(s, a)$. An iterative method to find the best policy by optimizing the Q function is known as Q learning.
- Deep Q-learning uses a deep neural network to approximate the Q function and optimizes it by the stochastic gradient descent. There exists a number of heuristic methods to improve the stability and efficiency of the training process.

Section 7.5 Policy-based search

- In a policy-based approach, the policy π_θ itself is approximated by using some functional ansatz, such as neural networks, and directly optimized to maximize the total expected reward along the whole episode.
- Compared to a value-based method, policy-based methods can be advantageous when action space is continuous and/or simulation of the environment is fast and cheap.

Section 7.6 Black-box optimization in deep RL

- Identifying the total reward as the fitness, one can apply black box optimizations to deep RL algorithms.
- This could be advantageous since the black box approaches typically require much less hyper-parameters than the other deep RL methods and can be parallelized on multicore CPU while GPU acceleration is only marginal.